SECONDARY RADIOACTIVE CONTAMINATION OF THE ATMOSPHERE IN INTERMEDIATE AND LATE PHASES OF A NUCLEAR EMERGENCY

EVGENI GARGER, ANATOLII NOSOVSKYI, MYKOLA TALERKO

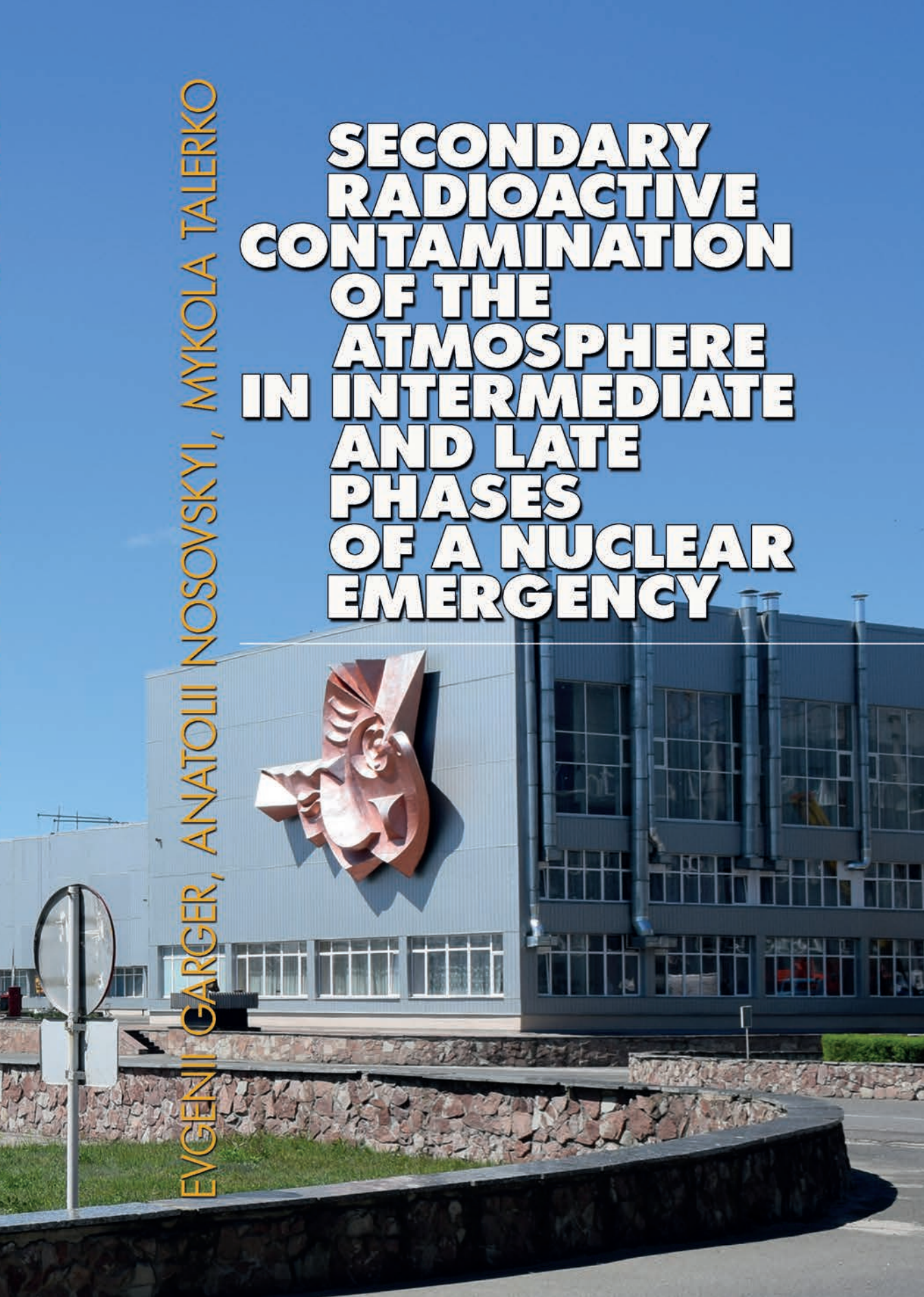

NATIONAL ACADEMY
OF SCIENCES OF UKRAINE

INSTITUTE FOR SAFETY PROBLEMS
OF NUCLEAR POWER PLANTS
OF THE NAS OF UKRAINE

НАЦІОНАЛЬНА АКАДЕМІЯ
НАУК УКРАЇНИ

ІНСТИТУТ ПРОБЛЕМ БЕЗПЕКИ
АТОМНИХ ЕЛЕКТРОСТАНЦІЙ
НАН УКРАЇНИ

ЄВГЕН ГАРГЕР, АНАТОЛІЙ НОСОВСЬКИЙ, МИКОЛА ТАЛЕРКО

ВТОРИННЕ РАДІОАКТИВНЕ ЗАБРУДНЕННЯ АТМОСФЕРИ НА ПРОМІЖНІЙ ТА ПІЗНІЙ ФАЗАХ РАДІАЦІЙНОЇ АВАРІЇ

ПРОЄКТ
«УКРАЇНСЬКА НАУКОВА КНИГА
ІНОЗЕМНОЮ МОВОЮ»

КИЇВ
АКАДЕМПЕРІОДИКА
2020

EVGENII GARGER, ANATOLII NOSOVSKYI, MYKOLA TALERKO

SECONDARY RADIOACTIVE CONTAMINATION OF THE ATMOSPHERE IN INTERMEDIATE AND LATE PHASES OF A NUCLEAR EMERGENCY

PROJECT
«UKRAINIAN SCIENTIFIC BOOK
IN A FOREIGN LANGUAGE»

KYIV
AKADEMPERIODYKA
2020

UDK 621.039.586:504.054
G 19
doi: http://org/10.15407/akademperiodyka.410.274

Reviewers:

M. ZHELEZNYAK
Project Professor, Ph. D. in Sciences (Physics and Mathematics),
Institute of Environmental Radioactivity, Fukushima University, Japan

S.A. PASKEVYCH
Deputy Director on Research, Ph. D. in Sciences (Biology),
Institute for Safety Problems of Nuclear Power Plants,
National Academy of Sciences of Ukraine

Approved for publication by Institute for Safety Problems of Nuclear Power Plants of the NAS of Ukraine (August, 12, 2019, Protocol No. 7)

Publication was funded in the frame of the Target Complex Program «Creation and Development of Scientific Publishing Complex of the National Academy of Sciences of Ukraine»

Garger Evgenii

G 19 Secondary Radioactive Contamination of the Atmosphere in Intermediate and Late Phases of a Nuclear Emergency / Evgenii Garger, Anatolii Nosovskyi, Mykola Talerko; Institute for Safety Problems of Nuclear Power Plants of the NAS of Ukraine. — Kyiv : Akademperiodyka, 2020. — 274 p.

ISBN 978-966-360-410-7

The book presents experimental data obtained in the Chernobyl exclusion zone since May 1986 up to now. The results of extensive experimental and theoretical studies of the processes of the radioactive aerosol re-entrainment into the atmosphere from the contaminated surfaces are presented, including natural wind resuspension, technogenic impact, agricultural activities, forest fires and dust storms.

The book is designed for specialists in the fields of radioecology, environmental protection, atmospheric physics, meteorology, radiation and environmental safety.

UDK 621.039.586:504.054

ISBN 978-966-360-410-7

PREFACE

Studies of processes of re-entrainment, dispersion, and deposition of dust contaminated with radioactive substances have become topical after tests of nuclear weapons and accidents at nuclear power plants. Numerous measurements of re-entrainment processes, both in wind tunnel experiments and in the natural environment, have been made by scientists of Ukraine, Russia, Western Europe, the USA and Japan during the 33 years since the Chernobyl accident and the eight years since the Fukushima accident. The present book does not claim to cover this problem completely. Predominantly, it presents extensive experimental results and theoretical estimations obtained under operational conditions connected with elimination of consequences of the Chernobyl accident, carried out generally in the 30-km exclusion zone of the Chernobyl nuclear power plant (ChNPP) since May 1986 up to the present day.

The analysis of the results of re-entrainment measurements is a rather complicated task on account of the Chernobyl zone features. First, the measured air activity concentration is determined by the land surface, which is a constant source of radioactive aerosol with time-dependent intensity depending on the season, the character of the underlying surface, and meteorological conditions. Second, radionuclide deposition after the accident consisted of radioactive aerosols of different sizes, nuclide composition, and chemical properties (including «hot» particles). Third, the activity concentrations of radionuclides in air within the zone were influenced not only by resuspension in a traditional sense, but also by mechanical disturbances enhanced by intensive human activity and by the constant emissions of radioactive substances into the atmosphere from the «Shelter» object above Unit 4 of the ChNPP. Since 2016, after the completion of the construction of the New Safe Confinement, the risk of additional

radioactive air pollution by emissions of radioactive aerosols from Unit 4 has significantly decreased. However, in general, the problem of a possible deterioration of the radiation situation in consequence of emissions from various industrial facilities located in the Chernobyl exclusion zone remains relevant.

Additionally, the mesoscale meteorological phenomena, such as the passage of cold fronts with squalls, have been important; during dry seasons there were also fires in contaminated forests and grass territories. Though these phenomena are short-term, but may cause considerable transport of radioactive substances over long distances above relatively clean territories.

In investigations under field conditions, primary attention was given to derivation of the integral characteristics of the resuspension process of radioactive particles used in practice, in particular, generalized data about the resuspension factor and the resuspension rate. The special feature of this book is the generalization of data about the distribution of the radionuclide activity concentration with respect to particle size under various conditions of aerosol resuspension in the atmospheric surface layer. Measurement with impactors has allowed estimation of the contribution of particles of various size ranges to the total activity concentration value. Additionally, results of measurements obtained near the Chernobyl NPP in the post-accidental period are presented for the number concentration of aerosol «hot» particles, the beta-activity distribution on «hot» particles sizes, and their contribution to the total beta-activity concentration. The estimation of the leaching rate and the size-dependent dissolution rate of «hot» particles in a simulator of lung fluid are also given.

The main approaches to modeling of radionuclide resuspension and consequent redistribution in space and over time are reviewed. These approaches are necessary for estimating human inhalation doses. They include resuspension factor models, a mass loading approach, and mathematical models of radionuclide atmospheric transport and dispersion on the basis of the semi-empirical equation of turbulent diffusion. The verification of several models used the resuspension factor approach was made on the grounds of measurement results within the Chernobyl exclusion zone. Besides wind resuspension, other processes in the environment that result in the emission of radionuclides over contaminated territories are briefly reviewed, including forest fires, dust storms, and tornadoes. Special attention is devoted to publications in Russian and Ukrainian authored by researchers from countries of the former USSR, which are not widely known in English-speaking countries.

INTRODUCTION. RE-ENTRAINMENT OF RADIOACTIVE AEROSOLS AS A PROCESS OF REDISTRIBUTION OF SURFACE CONTAMINATION

During the 19th and 20th centuries, the anthropogenic effect on the environment became evident. In particular, during the end of the 19th and the beginning of the 20th century, processes of wind erosion were sharply intensified due to the rapacious use of land in steppe and semi-arid zones of the terrestrial globe.

The importance of studying processes of re-entrainment and dispersion of dust contaminated with toxic substances was realized after nuclear weapons tests and especially after radiation accidents at nuclear power plants.

A variety of reviews were devoted to giving an idea of the basic concepts of mechanisms and models for estimating the characteristics of resuspension (Linsley 1978; Healy 1980; Sehmel 1984; Smith et al. 1982; Nicholson 1988; Makhonko 1992; Chamberlain 1991; Ziskind et al. 1995). According to Sehmel (1984), resuspension is understood as a process of lifting into the atmosphere of a substance deposited earlier. The lift-up of a substance can be an effect of the wind action and mechanical perturbation of soil particles. Aerosol particles with diameters from several micrometers up to several tens of micrometers are transported by wind over various distances, depending on the particle size, wind velocity and thermodynamic stability of the surface layer of the atmosphere.

The study of the resuspension phenomenon is of applied interest not only in ecological problems but also in technical ones. Resuspension of particles from surfaces in a turbulent flow became an object of many theoretical and experimental study cases in recent years. The removal of small particles from surfaces is important in many engineering problems, for example, in the production of semiconductors, where the particles influence the quality of chips. The analysis made by Ziskind et al.

(1995) has shown that models of particle resuspension should be based on two main factors, namely: the action of airflow on a particle and ways of contact formation between a particle and a surface. The flow of fluid near a surface is a result of mean fluctuating hydrodynamic forces. Resuspension of particles takes place when these forces are great enough to exceed the adhesive force between particles and surface, the adhesive force being a combination of physical attractions, chemical bonds, and mechanical stresses. Despite the advances in this area, Ziskind et al. (1995) noted that the real mechanisms of resuspension phenomena are still unclear.

Re-entrainment and resuspension in natural conditions, where the underlying surface is always heterogeneous, and meteorological conditions are highly variable, depends on many factors that influence its intensity and, strictly speaking, are irreproducible. Nevertheless, experimental investigations in laboratory and natural conditions are important for the best understanding of mechanisms of this event in practice.

Re-entrainment of radioactive substances deposited on the ground surface should be taken into account in the estimation of the radioactivity redistribution in space and time and estimation of human doses from radioactivity. Some special physical resuspension experiments in the field have been conducted, mainly in the USA (Healy 1980; Sehmel 1984). A large part of the data has been obtained in different conditions after industrial accidents and nuclear weapons testing. This book presents mainly empirical data on the resuspension of radioactive particles in the field after the Chernobyl accident. Specifically, many measurement data have been obtained in Ukraine, Russia, Belarus, and various European countries during the 30 years after the Chernobyl accident, and similarly, in Japan after the accident at the Fukushima-1 nuclear power plant. As a rule, these data were analyzed and generalized in frameworks of integrated empirical models. Thus, the emphasis was on the practical significance of the determination of characteristics that are necessary for the description of the redistribution of radioactive substances or estimation of the inhalation dose, as presented in Table.

Parameters necessary for calculating the consequences of resuspension

Redistribution of contamination:	Inhalation dose assessment:
Density of depositions	Activity concentration in the air
Resuspension rate	Density of depositions
Emission rate	*Resuspension factor*
Activity concentration in the air	*Activity median aerodynamic diameter (AMAD)*
Dry deposition velocity	Geometric standard deviation (GSD)
Activity distribution of aerosol size particles	Activity distribution of aerosol size particles
	Solubility class of nuclides

The parameters marked by italic type are often absent in practice, as their direct measurement is met with great difficulties for a variety of reasons. For example, the activity concentration in the air is quite often estimated as a measured deposition density multiplied by the resuspension factor taken from available models in the literature, assuming uniformity of the underlying surface and deposition density.

It should be noted that the resuspension factor enables evaluation of the activity concentration of a radionuclide at the point where it is necessary to assess the inhalation dose. The resuspension rate, which characterizes the emission intensity of radioactive substances, is needed to assess the activity concentration and deposition of radioactivity over space and time. This allows evaluating both an inhalation dose and an ingestion dose due to the consumption of contaminated food.

In the present book, the processes of radionuclide re-entrainment and atmospheric transport are considered at the local and meso- scales. It is known that particles of contamination are deposited on the soil and attach to large particles of soil. In this connection, the soil erosion becomes an important source of resuspension, especially when the soil loses its vegetative cover or is broken. These conditions are especially typical for arid and semi-arid regions, for example, for the southeastern and southern countries of Europe, Central Asia, and Africa, where a considerable amount of dust can be lifted and transported over a distance of several hundreds or thousands of kilometers (Smirnov and Novitski 1998). According to Kuznetsova et al. (2000), in 1995 in the Volgo-Vyatsk region and territory behind the Ural Mountains (Russia), the total background levels of beta activity were exceeded by a factor of 7-33, due to entry of air masses from Kazakhstan.

In middle latitudes with a wet climate and low wind velocities, soil erosion is rather seldom marked, and consequently, dust particles blown off from the surface layer of soil and other elements of an underlying surface contaminated with radioactive materials become one of the main mechanisms of secondary air contamination by radioactive particles, as the effect is practically permanent.

Thus, the underlying surface is a constant source of aerosol with a varying rate of emission of a substance, depending on the meteorological conditions and character of the underlying surface. The re-entrainment of radioactivity caused by wind in the middle latitudes in practice does not exceed one-tenth of one percent of deposited radioactivity on the underlying surface per year. But at the local scale, various anthropogenic activities sharply intensify the re-entrainment of a substance and its redistribution in space. In this connection, in practice, it is necessary to study the redistribution of the primary contamination after an accident in space and time due to its secondary lift up, transport, and deposition, and to estimate possible doses for the population.

In the case of a severe nuclear emergency, during its acute phase, the contribution of resuspension in the overall radioactive dose is usually significant, and its correct estimation is an important problem concerning for to protection of the

personnel participating in liquidation of the consequences of an accident and to the population living in the region of the emergency. Thus in examinations and practical calculations, the emphasis is on the measurement of aerosol particles in the respirable size range, which are determined mainly as particles with diameters ≤10 microns. In this connection, the first chapter of this book is devoted to a short overview of modern physical conceptions about resuspension and adhesion of aerosol particles and also methods of estimating resuspension characteristics in practice under field conditions in a polluted territory. The main theoretical conceptions of estimate secondary air contamination due to natural wind resuspension over radioactively polluted territories are considered, including the approaches of the resuspension factor, the resuspension rate, and mass loading. Additionally, other important mechanisms of radionuclide emission are discussed, such as forest fires, dust storms, and tornadoes in a radioactively contaminated territory.

This book mainly presents empirical data about the re-entrainment of radioactive particles under field conditions after the Chernobyl accident. These data are the results of studies that combined scientific investigation of radioactive aerosol resuspension with the need to give practical answers promptly regarding the implementation of countermeasures for protection of personnel who worked in the Chernobyl exclusion zone and the population who lived around it.

CHAPTER 1

BASIC DESCRIPTION OF RESUSPENSION PROCESSES OF AEROSOL PARTICLES

1.1. Aerosol emissions from soil

The academician V. A. Obruchev (1951) wrote: «In a warm season and dry weather in densely populated countries abundant in plowed fields, kitchen gardens, unpaved roads, some dust always occurs in the air. It represents the finest particles of organic and mineral substances, which even the weak wind lifts into the air and carries up to meet with some obstacle, or until a calm, when these particles, obeying gravity, are deposited. In dry steppes with scarce vegetation, all soil surfaces raise a cloud of dust which is strongly dried up in the summer and the autumn. Bare riverbeds of transient streams, alkaline lands, bare and weakly overgrown inclines of hills, rocks and cliffs of any composition raise dust, on which the processes of weathering create particles of dust». Further in this work, it is noted that «…in fact, generation of dust from a ground surface is easy to ensure, when you go out of the city on a hot summer day. Despite calm weather, it is possible to note that from time to time, now here now there, in different places, suddenly a column of dust occurs, which moves fast to any side, spirally turning upwards and broadening, capturing within itself dry twigs and leaflets. Suddenly it disappears, being diffused; litter elevated by it falls on the ground, but the dust remains in the air**.** In deserts and semi-deserts of Medial and Central Asia in the hot summer days, such vortexes appear at once in several places on the horizon, and they move far away, whirling and rising high in the air». The vortexes form dusty haze and mist, and they are observed under moderate, sometimes even weak winds. Strong winds create dusty storms. According to Obruchev (1951), «dust which is generated everywhere on the dry land surface, but especially in countries with a dry climate, in connection with processes

of weathering of any mountain rocks and soil and blowing them, and also due to activity of men, deposits everywhere». In Northern China in the winter and early spring, dusty winds blow up from the northwest, from the Gobi, Ordos, and Alashan deserts, and come to the Hwang Ho river valley, where, according to Obruchev, loess soils were formed in a huge territory. Similar processes occur for periods on a geological time scale.

For radioecology, the adducing citation shows the importance of accounting for temporal and spatial scales of processes of re-entrainment and subsequent transport of the pollutants in the atmosphere. It is especially important in studying the redistribution of artificial long-lived radionuclides.

The resuspension process describes the re-entrainment into the atmosphere of previously deposited material and includes the study of particle transfer in the respirable range of particle diameters. Pollutant particles are attached to larger host soil particles and take part in soil erosion. Thus soil erosion becomes important for resuspension when vegetated surfaces are disturbed. According to Sehmel (1971; 1984), soil movement can occur on several scales. On a small scale, many sand grains tend to move simultaneously in a series of intermittent bursts. As wind speed increases, particle bursts become more active until particles are suspended and transported into the air. Large-scale erosion has been described by three terms, which express continual soil movement as a function of surface stress (Sehmel 1971; 1984): saltation, surface creep, and suspension.

Differences in motion between these three are gradual and depend on the diameter of the particle and the wind speed or wind turbulence. Saltation describes particles ranging in diameter from about 100 to 500 μm (Sehmel 1971; Newman et al. 1976) which jump or bounce within a layer close to the air-surface interface. Particles transported by surface creep range in diameter from about 500-1,000 μm. These particles move by a sliding or rolling motion and are pushed along the ground by wind stresses and momentum exchange from the impact of smaller particles transported by saltation. Particles are smaller than about 100 μm in diameter move by a suspension.

Bagnold (1954) measured the soil flux under sandy desert conditions in the Sahara and found that the flux can be described using the equation:

$$J = C u_*^3 \frac{\rho}{g}, \tag{1.1}$$

where J is the substance flux; ρ is the air density; g is the acceleration of gravity; u_* is the friction velocity, and C is a constant which depends on the soil type and the form of erosion. The amount of soil eroded by saltation, surface creep, and suspension varies greatly for different soils (Newman et al. 1976; Chepil 1965): suspension moves from 3 to 40% by weight, saltation 50 to 75%, and surface creep 5 to 25%.

According to a review by Oksza-Chosimovski (1976), field measurements and wind tunnel simulations have shown that the ratio of sedimentation velocity to friction velocity at which aerosol particles were significantly affected by settling was larger than 0.12 and smaller than 0.68. The shapes of the size distributions of wind erosion soil aerosols (of radius $2 < r < 10$ μm) were fairly constant with wind speed. This result is evidence that the dominant mechanism of aerosol production by soil erosion is sandblasting of the soil surface. Oksza-Chosimovski (1976) noted that for low wind speeds of 2-3 m s^{-1}, corresponding to the usual weather conditions at middle latitudes, the smallest radioactive dust particles rise from the surface of the soil as a result of random breakthrough of turbulent eddies to the ground. For the indicated wind speed, this dust does not settle under the action of gravity. Such dust particles are mainly hundredths and tenths of a micron in size, but they can reach 1-2 μm in size. Larger particles of radioactive dust are too heavy to remain in the air for a long time.

According to Gillette et al. (1972), direct aerodynamic lift up of particles with $r < 10$ μm cannot be excluded. Air bursts always penetrate to a ground surface, especially above a rough surface. Turbulent vortexes can penetrate at the expense of a component of a wind burst, directed to the ground, or at small dust devils. In measuring a vertical turbulent flux of a substance with the help of gradient measuring (Gillette et al. 1972), significant quantities were recorded in days when saltation was observed. The values of the vertical substance flux under the conditions of the field experiments were in an interval from 0.6×10^{-6} to 1×10^{-4} μg cm^{-2} s^{-1}.

Fairchild and Tillery (1982) investigated the influence of saltation of spherical glass particles with sizes of 100 and 200 μm on the resuspension of monodisperse glass particles with sizes of 4, 7 and 10 μm. It was determined that the resuspension rate rises with the increasing size of the saltation particles and with the decrease in the size of the particles lifted in vertical airflow. The resuspension intensity grows with increasing mean flow speed as a degree function with an exponent from 1.8 to 2.3 in the presence of the saltation process and with an exponent of 1.3 in its absence.

Thus from this short review of published works it follows that resuspension of radioactive aerosols may occur due to wind erosion in a territory with poor vegetation, with a long-lasting surface wind at an average wind speed of 4-5 m s^{-1} at height 1 m. The resuspension intensity increases as a degree function of flow speed with an exponent between 1.8 and 2.3 for particle diameters in the range of 4 to 10 μm. In dry steppes and arid zones, this process can be observed much more often and with high intensity. As was noted above (Oksza-Chosimovski 1976; Gillette et al. 1972), the smallest radioactive dust particles ($d < 10$ μm) rise from the surface of the soil as a result of random breakthrough of turbulent eddies to the ground and may move over long distances.

1.2. Theoretical and experimental studies of resuspension mechanisms under laboratory and natural conditions

Process-level study of the removal of fine aerosol particles now appears important for many engineering problems, for example, for production of semiconductors, in various overpasses, and for estimation of the contribution of an aerosol component to changes in the Earth's climate. Therefore, experimental and theoretical investigations have been intensified for studying the resuspension of particles under laboratory conditions, in various technological installations, and in-field experiments, especially in arid conditions.

Sehmel (1984) showed that even particles less than 2 μm can resuspend in a turbulent flow created in a wind tunnel. Zimon (1980) and Ranade (1987) discuss the various features of the adhesion and removal of finely-dispersed particles on surfaces. Nicholson et al. (1989) investigated the effects of moving machinery concerning for to their impact on particle resuspension from roads.

It is apparent that at high airflow speed near a surface, strong hydrodynamic forces act on particles. This means that the airflow at high speed creates turbulence. The particles on a surface are the subject of friction stress in the viscous sublayer of the turbulent boundary layer. Thus the adhesive force is directed against the force of detachment of the adhered particle. According to Zimon (1980), at blow-off of a dusty horizontal surface by airflow, an adhesive force F_a, a particle gravity force P, an aerodynamic force (a frontal force) F_L, and a lifting force F_p all act on the adhered particle. The condition of particle detachment is set by the inequality

$$F_L \geq \alpha_f (F_a + \mathrm{P} + F_p), \tag{1.2}$$

where α_f is a friction coefficient (Zimon 1980).

For particles of small sizes, when $F_L >> P$ and the frontal force is more than the lifting force, i.e. $F_L >> F_p$, the detachment of the adhered particle will happen under the condition

$$F_L \geq \alpha F_a. \tag{1.3}$$

Under the flow of adhered particles that takes place in the boundary layer, the flow speed varies with a height from zero up to a certain value (Zimon 1980). This change implies significantly on the frontal force value according to the formula

$$F_L = 0.5\, c_x \rho\, S_m U_a^2, \tag{1.4}$$

where S_m is the particle midsection; c_x is the particle resistance coefficient; and U is the airflow velocity at the level of the particle center.

Thus the condition of particle liftoff occurring in the boundary turbulent layer depends on the ratio between the diameter of the particles and the thickness of the laminar sub-layer, a buffer layer, and a turbulent core. If the diameter of the particles

is less than or equal to the laminar sub-layer thickness, i.e. adhered particles are submerged into it, then the laminar airflow acts on the adhered particles. When particle sizes are comparable to the thicknesses of the laminar sub-layer and the buffer layer, then an action of the laminar-turbulent airflow on the adhering particles is observed. If the turbulent boundary layer thickness and the diameter of the particles are of one order of magnitude, and the laminar sub-layer thickness is, at least, less than the particle radius, then turbulent action of the flow on the adhered particles takes place.

The quasi-static approach assumes that when the airflow velocity is high enough, the hydrodynamic forces exceed counteracting surface forces and cause instantaneous resuspension. However, measurements of experimental resuspension have indicated that the particle does not move off a surface instantaneously, but leaves its place over some time. It is supposed that resuspension has a statistical nature, connected with the turbulent character of a flow. To explain a stochastic move of fluid close to a surface, the concept of coherent structures of a boundary layer, or «bursts» was offered.

One model of resuspension (Cleaver and Yates 1973) uses this concept for determination of the resuspension rate, using visual observations of the distribution of «bursts explosions» in space and time. The case of lifting force, which exceeds an adhesion, was associated with this distribution, thus combining the concept of a balance of forces with the statistical nature of the flow.

Braaten et al. (1986; 1988; 1990) use a Monte-Carlo model to describe particle resuspension based on a hypothesis that particle resuspension is associated with coherent structures (bursts) which vary in magnitude in space and time. The occurrence of bursts for a large stress shear near walls was assumed to be a cause of particle removal from a surface by analogy to the concept of a balance of forces.

Resuspension is frequently observed, despite the presence of rather large surface forces. Reeks et al. (1988) have developed a new approach to this problem. Using the concept of the presence of a fluctuating lifting force, they assume a balance of energy instead of a balance of forces. Their model of resuspension is based on the assumption that when a particle is in a turbulent flow, transport of turbulent energy to the particle takes place. A particle can be detached from a substrate when it accumulates enough energy to escape from the surface adhesive potential well. The results show that the resuspension rate is naturally divided between short-term initial resuspension and long-term resuspension. For periods after the beginning of a flow effect $t \leq 10^{-2}$ s, the resuspension rate is very high, due to a considerable fraction of large particles being only weakly retained by the adhesive force. For long-term resuspension, the rate varies almost in inverse proportion with the increase in time

$$\Lambda(t) = \zeta t^{-\varepsilon}, \tag{1.5}$$

where ζ is a constant, and $\varepsilon \sim 1$.

Evaluations have shown that the inverse relationship is clearly defined for considerable variations in flow, particle diameter, and surface roughness. It was noted that $\Lambda(t)$ for particles of radius 50 μm has appeared smaller than for particles of radius 25 μm. This results from an appropriately high initial value of particle resuspension for large sizes. Hence, fewer large particles of radius 50 μm are present for resuspension at longer periods.

The latest experimental studies have provided data for comparison with the results of theoretical models, which are usually presented in the form of the resuspension rate or the particle concentration as functions of time.

Turbulent motion results from fluctuations of hydrodynamic forces and moments. Existing models based on the approach of force balance, as well as models based on the concepts of energy accumulation (Reeks et al. 1988), do not take into account the effect of the force moments that affect a particle. As shown by Ziskind et al. (1995), resuspension models that take into account only the forces result in unrealistic resuspension values in many cases. Ziskind et al. (1995) have noted that special consideration should be given to turbulent vortexes and layers with flow speed shear. The interaction of these two structures near a surface forms a flow field, which causes resuspension of small particles and is important for saltation and surface creep development. It has been shown that comparisons of theoretical predictions and experimental results should be made after data representation in a dimensionless form. The size of a particle in the dimensionless form defines its place in a boundary flow and, hence, values of hydrodynamic forces and moments. To obtain conditions for secondary lift up, these quantities should be compared to quantities of surface reactions, which are calculated using available adhesion models based on properties of a particle and its substratum. Only then is it possible to conclude the importance of conditions for the secondary lift up. Analysis of particle adhesion shows that it is insufficient to take into account the separation force value only, outside the context of adhesion models. Rather, a particle's material, shape, and size should be taken into account to estimate its behavior under the effects of various hydrodynamic forces in combination with a surface reaction. On the other hand, a surface reaction different from a normal (perpendicular) to a surface, does not necessarily establish a separation. The knowledge of these reactions is essential in the development of resuspension models. Also, it is important to study the influence of surface roughness on an adhesion. The roughness not only considerably reduces a separation force, but also results in various mechanisms of resuspension.

It follows from the aforesaid, that the experimental data on resuspension should be analyzed taking into account the particle size, the flow characteristics, and the surface roughness. As particle size and flow parameters are usually known, the analysis of surface roughness appears to be more complicated.

To describe the effect of surface roughness on particle detachment, the conditions of particle detachment could be taken according to Ziskind et al. (1995):

$$M_d/M_a = 7.14\,(\mu\dot{\gamma}/\sigma_s)(R^3/r\cdot a) > 1, \tag{1.6}$$

where M_d is the hydrodynamic moment of force, M_a is the moment of surface force, μ is the dynamic coefficient of viscosity, $\dot{\gamma} = \frac{du}{dz}$ is the vertical shear of a flow acting on the particle; σ_s is the surface energy, R is the radius of a spherical particle; r is the radius of surface irregularity, and a is the distance between surface irregularities.

Because we assume that $a > r$, it is possible to neglect the moment of the adhesive force. In this case, the condition $M_d/M_a > 1$ results in $r/a < 10^{-12}$.

According to Ziskind et al. (1995; 1997), the dimensionless mean hydrodynamic moment is equal to

$$M_d^{\pm} = 3\left(d_p^{\pm}\right)^3, \tag{1.7}$$

where $d_p^{+} = \frac{d_p u_*}{\nu}$, d_p is the particle diameter, ν is the kinematical coefficient of viscosity; u_* is the friction velocity.

The moment caused by fluctuations of the flow in a viscous underlayer is equal to

$$m_{d1}^{\pm} \approx \left(d_p^{\pm}\right)^3. \tag{1.8}$$

The moment caused by lateral oscillations of the flow velocity is approximately equal to

$$m_{d1}^{\pm} \approx 0.21\left(d_p^{\pm}\right)^3. \tag{1.9}$$

The dimensionless moment of surface forces can be presented as

$$M_a = \frac{0.39}{u_*}\left(d_p^{\pm}\right)^2. \tag{1.10}$$

The condition for particle detachment from a rough surface $M_d/M_a = C/(r\cdot a) > 1$ is defined above, where $C = 10^{-12}$ m^2. If a particle is in contact with a surface irregularity, for which the curvature and spatial distribution satisfy the condition $r \cdot a < C$, it will leave its initial site.

The following analysis shows that the leading role in particle detachment belongs to the hydrodynamic moment. This moment exceeds the surface moment, while the lift force is usually much smaller than the adhesion force.

The process of resuspension has two stages. In the first stage, the particle is detached from the surface by the hydrodynamic moment derived from the drag force. Typically, the force moment causes rotation of the particle relative to its initial position. Then, the particle is resuspended by the hydrodynamic lift force, which overcomes the force of gravity. The detachment under the influence of the hydrodynamic movement is the basis for particle resuspension from surfaces in a turbulent flow. When the flow rises, a large number of particles are immediately detached

under the impact of the mean moment. The condition of detachment (Eq. (1.6)) is satisfied for these particles which initially occupied sites within a certain configuration of surface irregularities under a given moment direction. Since the flow moment fluctuations have arbitrary directions, later on they result in detachment of particles from sites with other configurations of surface irregularities.

1.3. Study of submicron aerosol generation (emission or release)

For a description of radioactive particle redistribution in space and time or estimation of inhalation doses formed by the particles, it is very important to obtain information about the activity concentration, the distribution of radioactivity by particle size, and their specific activity. For these tasks information for particles in the respirable (10 μm - 2 μm), and inhalation (< 2 μm) aerosol ranges are important. In this connection, it is necessary to know what kinds of fine aerosol emission sources are possible to encounter in practice.

Different processes of submicron aerosol formation were investigated by Kozlov et al. (2000). It was shown that with sand, interspersing particles of 0.4 μm in size are formed and that this occurs constantly in desert territories under the influence of wind.

Another possible emission mechanism for fine aerosols is possible because of particle static electricity (Yablokov and Andronova 1997) when the relative humidity is less than 50-70%. This process is effective only in daytime when the relative humidity is low and the surface layer temperature is high.

Chkhetiani et al. (2012) conducted measurements in the desert of Kalmykia (Russia) in 2007, 2009 and 2010 under conditions of weak wind, strong heating of the soil surface and near-absence of a saltation process. Results of measurements have shown that deviations of the mass concentration of fine mineral aerosols (0.15-0.5 μm) measured at heights 0.5 m and 2.0 m from their background values are related to a temperature drop in the thermal layer at the surface and the values of friction velocity. For small and moderate values of the friction velocity ($u_* < 0.2$-0.3 m s^{-1}), the mass concentration increases proportionally to the temperature drop with an exponent of about 0.5. For high friction velocities, this exponent becomes negative ($\cong -0.5$), which implies a decrease in the concentration with an increase in a temperature drop.

It is known that large quantities of aerosols enter the atmosphere from earth surfaces with a low resistance to erosion. For example, this occurs in deserts and steppes at wind speeds above the threshold speed value, and during the development of dangerous phenomena on these lands such as dust storms and tornadoes. These phenomena, despite their huge intensity, may last only a short time, and as follows from Chkhetiani et al. (2012), fine aerosol emission takes place with very weak winds existing over a quite long time.

At mid-latitudes, the above-stated mechanisms of aerosol emission are much more poorly revealed, due to their rather large moisture or to extensive vegetation cover of the surface. Nevertheless, the emission of aerosols occurs constantly due to wind and technogenic activity. This is well evident from the results of radioactive particle emission measurement in the contaminated areas. Long-lived radionuclides (^{137}Cs, for example) have appeared to be a good marker of processes of atmospheric transport of contamination for various distances and redistributions in space. It is important to know both the possible sources of radionuclide emissions and the radioactive loading of particles of different sizes.

Thus, the time-dependent detachment process is determined by the statistical parameters of the surface and the flow. They include general parameters and characteristics of the turbulent flow near a surface — the friction velocity u_* and the surface roughness height z_0; characteristics of the surface sublayer (landscape, soil, vegetation, etc.); the parameters of particle size distribution (mean diameter $\overline{d}$, median diameter d_m, standard geometric deviation σ_g), and the form, density and toxic loading of the particles.

CHAPTER 2

SOURCES OF SECONDARY CONTAMINATION, MEASUREMENT CONDITIONS, AND SAMPLER INSTALLATIONS IN THE CONTAMINATED TERRITORY AFTER THE CHERNOBYL ACCIDENT

2.1. General description of resuspension conditions in the Chernobyl exclusion zone

In April 1986, the accident at the Chernobyl nuclear power plant (ChNPP) resulted in a widespread contamination episode, the effects of which could be easily measured throughout Europe. A large range of radionuclides was released into the atmosphere, primarily in particulate form. The radionuclides originated either from fuel fragments or by condensation of more volatile species onto environmental aerosols.

Shortly after the accident, the 30 km exclusion zone around the ChNPP was set up, from which the population was evacuated. The zone remains uninhabited, except several scientists that are accommodated there, temporarily, to conduct work related to the accident and on the nuclear power plant.

The total radionuclide inventory in the territory of the exclusion zone was estimated to be 4,100-5,600 TBq of ^{137}Cs, 2,600-3,700 TBq of ^{90}Sr, and 30 TBq of $^{239+240}$Pu, apart from the radioactivity located at the ChNPP site and in waste burials (Kashparov 2001). A map of the ^{137}Cs contamination density due to the Chernobyl accident is presented in Fig. 2.1.

The 30-km exclusion zone is located in an agricultural region containing mixed (i.e. deciduous and coniferous) forests. The forests occupy 30-35% of the area within the zone, with most of the remainder comprising agricultural land that was used to grow grass and cereal crops (and since left fallow). The soil type in the region is primarily a sod-podzol (94%), sod with low humus soil (5%) and swampy peat soil (1%). The topography of the 30-km zone is generally flat. Throughout the 30-km zone, there is extensive vegetation, and the soil is generally moist.

After the end of the initial phase of the Chernobyl accident, the contaminated ground surface immediately became a source of radioactive aerosol in many countries of Europe (USSR 1986). The consequences of the accident have been used to evaluate parameters related to resuspension (Nicholson 1988, Garland and Pomeroy 1994) in Western Europe.

Garger et al. (1990) and Garger (1987) reported a preliminary assessment of the effects of resuspension in the 30-km Chernobyl exclusion zone. In these studies, the atmospheric activity concentrations and the soil contamination levels were reported for the period August/September 1986, and the results are used to determine possible levels of resuspension intensity and their variability depending on time and location. The results are applicable in general for the evaluation of inhalation doses and in the assessment of the potential for the transport of contamination due to resuspension. During the period of the reported measurements, there were major decontamination activities in the vicinity of the ChNPP, which could have significantly contributed to resuspension, and the effects of this technogenic (i.e. mechanical) resuspension were considered.

Contamination due to dust lift from polluted roads and construction sites both in the Chernobyl exclusion zone and outside it took place on local or mesoscales. During dry summers forest fires occurred in areas of forests and peat bogs of Ukrainian and Belorussian Polesye contaminated by the accident at the

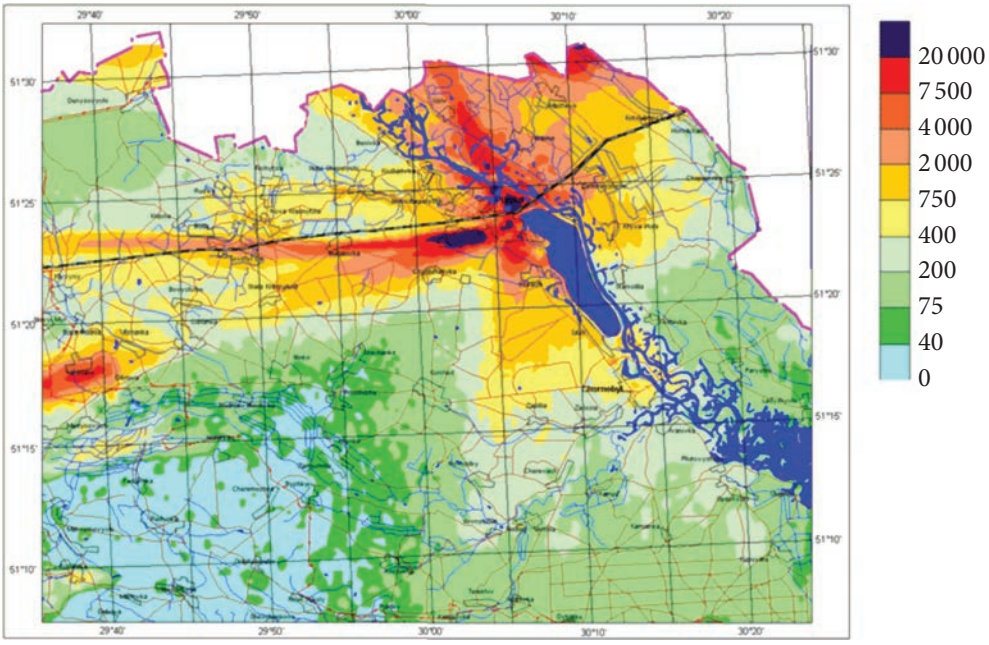

Fig. 2.1. Density of ^{137}Cs contamination (kBq m^{-2}) within the Chernobyl exclusion zone (from Kashparov 2016)

ChNPP. The spatial scales of these fires may amount to several tens of kilometers and more. An additional contribution in the exclusion zone is caused by stable unorganized emission of radioactivity into the atmosphere from the object «Shelter» above the destroyed 4th unit of the ChNPP.

Processes of saltation and movement of the soil surface layer caused by rolling of large soil particles (Sehmel 1980) can be observed at winds exceeding 12 m s^{-1} at the height of a wind vane, more often on plowed lands, an area of about several hundred hectares in Polesye.

As a whole, Polesye is characterized as a region with light winds, and consequently, the processes of saltation and surface soil movement are rare here, while for steppe and semiarid regions of Ukraine and Russia, the input of these processes into particle lift from soil increases sharply. An example related to the lifting of radioactivity in the atmosphere is presented by Kuznetsova et al. (2000), who studied radioactivity measurement data in the surface layer of the atmosphere over Russian territory in 1996-1999. Against a rather homogeneous background, a jump in total beta activity occurs from time to time, exceeding background levels by one order of magnitude or more, and these jumps are not always related to seasonal oscillations of radioactivity. Such cases were registered 130, 99, 221 and 175 times per year from 1996-1999. Their greatest occurrence takes place in the cold season, with maximums in January and November, and minimums in June and July. Some of the jumps were related to anthropogenic radionuclides, which were released into the atmosphere as a result of wind-driven resuspension and spread over large distances, for example, from East Kazakhstan to the middle and lower parts of the Volga River basin and Zauralye, Tomsk region (Russia).

In Polesye the scale of wind-driven resuspension and movement of substances in the polluted territory is mainly local, and mesoscale movement is rare. However, regional transport of radioactive dust particles from the contaminated regions of Ukraine, Belarus and Russia toward Central Europe by moderate east winds in the surface and the boundary layers of the atmosphere can occasionally be observed for a long period (7-10 days). This may happen in spring (April-May) when a steady anticyclone has set in over Eastern Europe, and the soil is not yet protected by a green cover. The resuspension and atmospheric transport of an aerosol may last up to ten or more days, as occurred in the spring of 1993.

2.2. Combustion of contaminated wood

The analysis of data on atmospheric activity concentrations in the forest and open terrain in Sweden (Vintersved et al. 1994) has led to the assumption that wood-burning increased the atmospheric activity concentration of ^{137}Cs. The atmospheric activity concentrations of ^{137}Cs were measured in Northern Sweden at two sites, in a forest and an open field placed 1 km apart. There

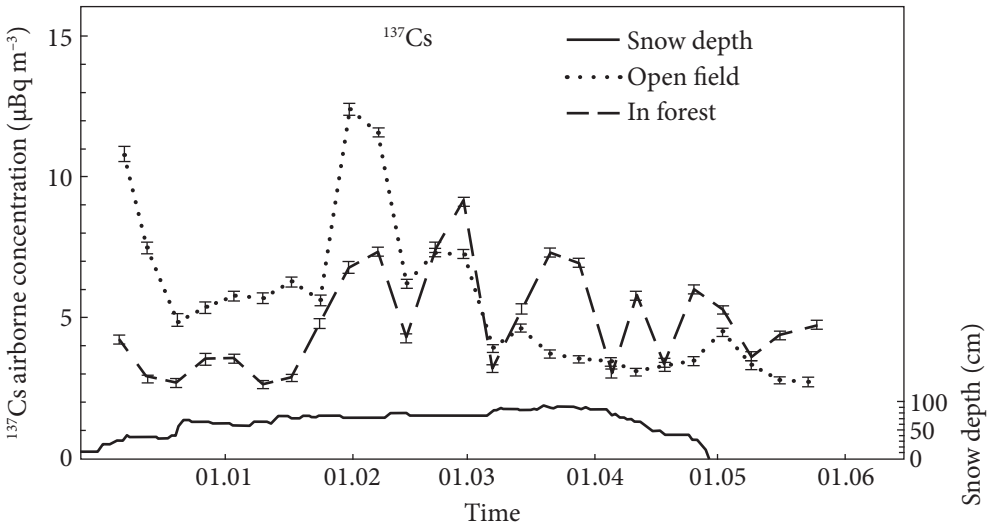

Fig. 2.2. ^{137}Cs atmospheric activity concentrations in a forest and an open field in Vindeln, Sweden

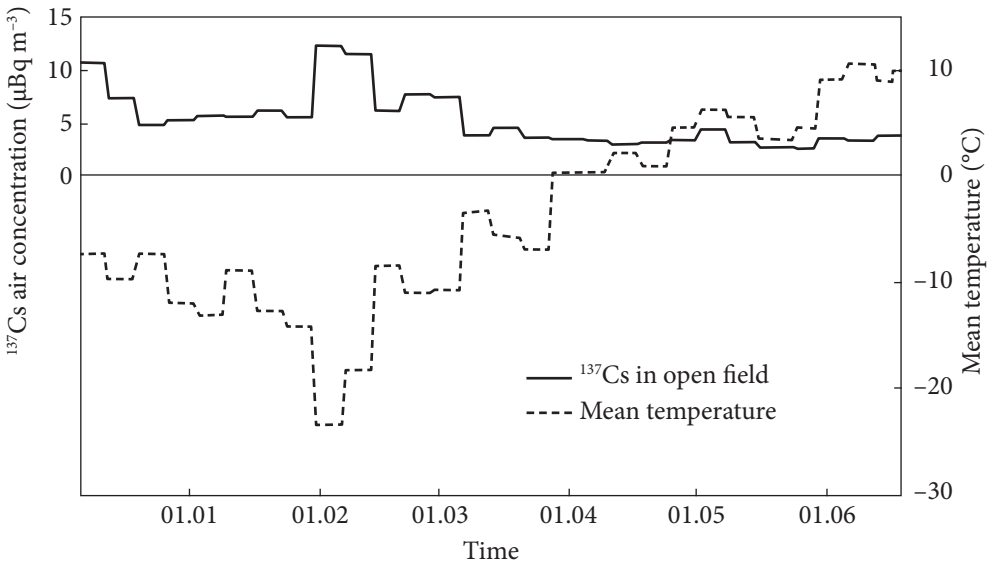

Fig. 2.3. ^{137}Cs air activity concentration in an open field in Vindeln, Sweden, and the mean temperature during the sampling periods

were 20 kBq m^{-2} of wet-deposited ^{137}Cs after the Chernobyl accident in region Vindeln, where the research was carried out. The sampling started at the end of December 1993, when the ground was covered with snow, and ended in mid-June 1994. These data and the snow depth are shown in Fig. 2.2.

The measurements showed that during the cold season, until the beginning of March, the atmospheric activity concentrations of ^{137}Cs in an open field exceeded those within the forest. From April to June the opposite situation was observed. The possible explanation of this is that in the cold months, the ^{137}Cs activity concentration in the air is elevated by particulate material from wood-burning heating systems in the area. In the warm months, the radioactive materials, precipitated on the trees, become a considerable source of ^{137}Cs. The hypothesis of heating systems acting as a source of ^{137}Cs is supported by the inversely proportional relationship of ^{137}Cs concentrations and mean temperatures (Fig. 2.3).

The snow cover remained until the end of April, but during its melting, no changes in the atmospheric ^{137}Cs activity concentrations were revealed. This shows that the influence of local resuspension of ^{137}Cs on the total atmospheric activity concentration was insignificant.

The influence of anthropogenic activity, especially at large-scale decontamination and construction works which were carried out around the ChNPP in the summer of 1986, was observed in terms of a sharp increase of the atmospheric activity concentration (by two orders of magnitude) measured at a distance of 14 km to the south from the NPP during a northern wind (Garger et al. 1990).

2.3. Re-entrainment by traffic

The influence of transport on resuspension processes has been studied in a series of works (Nicholson et al. 1989; Aarkrog et al. 1988; Johnson et al. 1992; Gilles et al. 2005; Garger 2001).

Sehmel (1980) noted that the traffic on a road immediately after its contamination results in the resuspension of 10^{-1}-10^{-2} of the deposited material per each vehicle pass. With time the resuspension rate decreases, and in 30 days it becomes less than two to three orders of magnitude. Nicholson et al. (1989; 1993) made measurements of the resuspension of particles (4.5-19.5 μm in diameter) by a car driving on a highway. The largest particles were removed the most rapidly. After two passes of the vehicle with a speed of 56 km h^{-1}, about 80% of the material was involved in the resuspension process. However, after a phase of rapid particle loss in the first two to three passes, there was little change in the fraction of material remaining on the road surface up to twelve passes. A maximum of fifty percent of the particles could be removed after seven passes of a vehicle traveling at 56 km h^{-1}. If the road surface was moistened, the amount of the lifted particles was decreased twice.

These studies considered the loss of material from a restricted part of the road. At the same time, the total amount of material removed from the whole road surface can be less because of repeated deposition on other parts of the road. There may also be deposition on areas contiguous to the road. This may have an

important influence on inhabitants who grow agricultural products on land close to roads, which frequently happens in Ukraine, Belarus and Russian Polesye.

Aarkrog et al. (1988) reported measurements of ^{137}Cs in the air in Risø (Denmark) that were carried out after the accident. A clearly defined weekly cycle in the atmospheric activity concentrations of ^{137}Cs in July and August 1986, was discovered. The higher activity concentrations were observed during weekdays, the lower, during days off. Later this dependence disappeared. The week periodicity has been attributed to the resuspension of radioactive material from the ChNPP accident caused by traffic; the traffic is usually heavier during working days than on the weekends. With time the deposited material presumably was lifted by traffic and scattered by the wind, and also partially has been bound to surfaces. These effects have considerably has lowered its concentration in the local air.

Johnson et al. (1992), with the help of lidar, an impactor, and micrometeorological measurements, researched the deposition of road dust with time after the passing of an automobile on an unpaved road. It was shown that during the initial period, the dust plume from perturbation of a surface due to car traffic on an unpaved road is the result of a suspension in a turbulent wake with particles from 0.5 up to >50 μm. The particles diffused and settled with a speed of about 6 $cm \cdot s^{-1}$ at small wind velocities and about 8 $cm \cdot s^{-1}$ at high wind velocities. The lower part of the wake contained 20-30% of the dust mass. During the first 40 s (with 10 s at high wind speed) the dust concentration decreased by approximately one-third of the initial concentration, losing mainly particles with sizes more than 10 μm. The concentration of particles with sizes less than 10 μm decreased by ***e*** times during 60-240 seconds in the early stage of dust plume existence.

In field experiments, Gillies et al. (2005) estimated the value of a coefficient of dust mass emission, which is equal to the mass of dust in grams deposited in an impactor PM10 multiplied by a transport speed in km h^{-1}. The coefficient of emission appears to be linearly related to the speed and weight of a vehicle. So, for a light vehicle (~1,200 kg) this coefficient was equal to 0.8 g of dust PM10 × km h^{-1}, and for a heavy army lorry (18,000 kg), 48 g of dust PM10 × km h^{-1}.

Bondarenko et al. (1993) carried out measurements of resuspension under the influence of traffic near roads in the 30-km Chernobyl zone. Values of the resuspension factor measured in advection conditions were obtained within the limits of 10^{-7}-10^{-6} m^{-1} in July-August, 1986. Measured resuspension factors were three orders of magnitude lower in Chernobyl town itself (10^{-6}-10^{-4} m^{-1}), where in that time a high level of traffic was observed. In ECP1 (1996), estimation of the emission rate of radioactive cesium was carried out for traffic of heavy lorries on a country road with a density of contamination of about 0.6 MBq m^{-2}. The rate of ^{137}Cs emission changed from 2.7×10^{-8} up to 2.0×10^{-6} s^{-1} for particles with an aerodynamic diameter from one up to several tens of micrometers, which exceeds the value of the wind-driven resuspension rate by three to four orders of magnitude for the

Fig. 2.4. Harrowing of the experimental ^{137}Cs contaminated strip with a T-150 tractor

Fig. 2.5. Harrowing of soil by a light tractor in Zapolie in 1993

same conditions in this area. The value of radioactive particle emission under these conditions is equal to about 1 Bq $m^{-2} s^{-1}$; the spatial scale of the source is equal to a lorry path length on a country road. The atmospheric activity concentration and the deposition velocity of ^{137}Cs, depending on conditions, has increased by several thousand times in comparison with background for distances of 20-30 m from the dust source and by 10-100 times for distances of 100 m and more.

Any anthropogenic activity on the contaminated surface of soil is a certain source of radioactive aerosol in the surface layer of the atmosphere. The dust emission in the atmosphere arises both at direct impact of vehicles and mechanisms (motor vehicles, tractors, combines etc.) and at harvesting or mowing. So, at cultivation of soil the dust concentration in the air may reach values of 500 mg m^{-3} (Figs. 2.4 and 2.5).

At harvesting, with a combine, the dust concentration may reach 300 mg m^{-3} (Noren 1985). Clausnitzer and Singer (1997) examined the influence of 29 agricultural works on dust generation and showed that during the preparation of soil (67% of all works), 82% of the dust produced has sizes less than 4 μm. The dimensions of

the dust plume are small, and the people who work near moving aggregates are the ones most exposed to the danger. When works are performed close to a settlement with the wind blowing toward the settlement, this source may be significant also.

The measuring that has been carried out in 1993-1994 in the 30-km Chernobyl zone, in Bragin district of Gomel region (Belarus) and Novozybkov district of Bryansk region (Russia) (ECP1 1996) has shown that agricultural works raise the activity concentration of ^{137}Cs in the air by several hundred to several thousand times in comparison with background, depending on distance from the source, soil humidity and other meteorological features of the surface layer of the atmosphere. For harrowing of soil in Zapolie (30-km Chernobyl zone) with a T-150 tractor, at a density of soil contamination by ^{137}Cs of about 0.5-1.0 MBq·m^{-2}, the value of radioactive dust emission reached 1-2 Bq · m^{-2} s^{-1}. An example of measurements of the number concentration of «hot» particles in air samples and on planchettes is given in Fig. 2.6.

Based on measurements, the dependence of «hot» particle number on the distance from a dusty stripe from a moving tractor could be described as $c \sim x^{-n}$, where c is the density of particle number on the soil surface; x is the distance, and n is an empirical exponent.

The influence of anthropogenic activity, especially at large-scale decontamination and construction works which were carried out around the ChNPP in the summer of 1986, was observed in terms of a sharp increase of the atmospheric activity concentration (by two orders of magnitude) measured at a distance of 14 km to the south from the NPP during a northern wind (Garger et al. 1990).

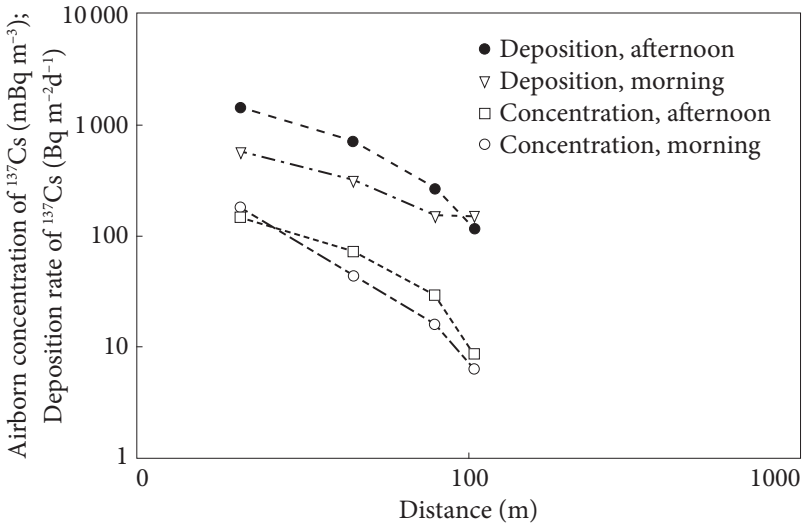

Fig. 2.6. Air activity concentration and deposition rate of ^{137}Cs as a function of distance

2.4. Radioactivity entrainment during forest fires

As a result of the Chernobyl accident, large forest areas in Ukrainian, Belarusian and Russian Polesye were polluted. The main polluted regions are located to the west, northwest, and northeast of the ChNPP. The total forest area in these regions is 32.5×10^3 ha. About 40% of the area of the 10-km zone around the ChNPP is covered with forests. The main tree species are pine, fir, oak, and birch. A large fraction of the radionuclides is located under a forest canopy and increases with proximity to the ChNPP (Table 2.1) (Tikhomirov et al. 1989).

Measurements of ^{137}Cs in different forest components were made by Garger and Kashpur (1995) at an experimental site near the village of Dityatki, situated a few kilometers outside of the Chernobyl exclusion zone border. Values of the ^{137}Cs specific activity were obtained for litter — 11.9 kBq kg^{-1}, bark — 0.78 kBq kg^{-1}, needles — 0.49 kBq kg^{-1}, branches — 0.14 kBq kg^{-1}, and wood — 0.11 kBq kg^{-1}. Accordingly, values of the ^{137}Cs inventory of forest combustible materials for the site were estimated as 252.3 MBq ha^{-1} in the litter, 32.4 MBq ha^{-1} in the wood, 16.2 MBq ha^{-1} in the bark, 11.6 MBq ha^{-1} in the needles, and 6.1 MBq ha^{-1} in branches.

Forest fires happened in the Chernobyl exclusion zone and contaminated regions around it almost every year after 1986. The largest ones took place during hot, dry summers in 1992, 2001-2002 and 2015. A review of the influence of forest fires on the radiation situation on local and mesoscale is presented in Chapter 14.

2.5. Radioactive pollen

The soil-to-plant transfer factors of some radionuclides, for example ^{137}Cs, are relatively high. Therefore, radionuclides will be transferred to plant parts from the reservoir in the soil. Plants are sources of atmospheric aerosols, and Matthias-Maser and Jaenicke (1994) have estimated that approximately 30% of total atmospheric aerosol (>4 μm in diameter, number concentration) is associated with biological particles. Part of this contribution will be from pollen.

Table 2.1. **Relative content of radionuclides in various parts of forest terrain in 1988**

Distance	Leaves and needles	Branches	Bark	Wood	Forest litter (0-3 cm)	Soil (3-10 cm)
Remote from Chernobyl 10-30 km area	0.5	1.9	4.4	0.7	81.7	10.8
Nearby to Chernobyl 7-10 km area	0.02	0.02	0.12	0.04	87.8	12.0

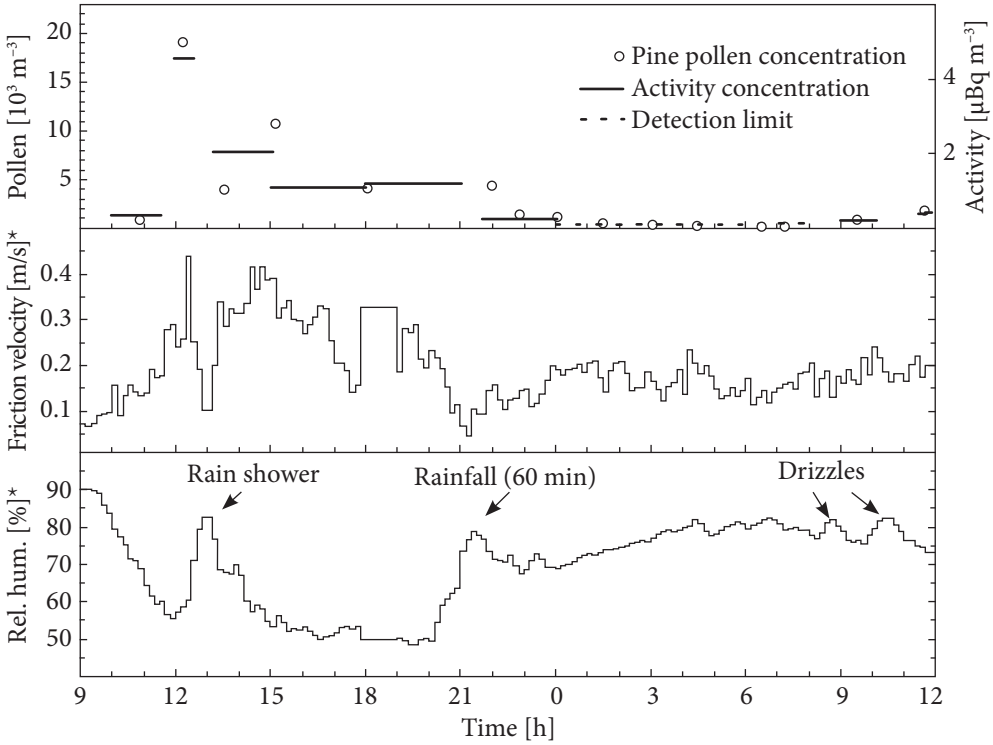

Fig. 2.7. Pine pollen concentration and ^{137}Cs activity concentration as measured by the rotating arm impactor on May 21/22 in Novozybkov. Both time series agree very well and can be understood from the meteorological conditions. *Note:* * meteorological data measured by AEA Technology

After the Chernobyl accident, the radionuclide contamination of flower pollen was measured in Bavaria, and an enrichment of ^{137}Cs was observed in pollen. Bunzl, Hötzl, and Wincler (1993) identified spruce pollen as a contributor to the ^{137}Cs air activity concentration in Munich, but noted that pine pollen was much less of a contributor. They explained this difference by the rooting depth of the two trees; pine roots are found mainly below the contaminated soil layer.

An assessment of the contribution of pine pollen to the radioactivity concentration in the air was made at one of the field measurement sites in Novozybkov, Russia (Fig. 2.7). The ^{137}Cs activity in samples of pollen from trees was relatively high, at 1.6 Bq g^{-1}. Assuming that all measured radioactivity originates from the pollen, a single pine pollen grain has an activity of 240 nBq. Straka (1975) has estimated that 1.5×10^9 pollen grains are produced in one flowering season per m^2 of forest floor, and this implies an emission rate of 360 Bq m^{-2} year^{-1} from this forest.

2.6. Radioactive aerosol from the object «Shelter»

Immediately after construction of the object «Shelter» above the destroyed 4th unit of the ChNPP at the end of 1986, studies of processes in the inside and characteristics of the radioactive aerosol released into the atmosphere were started (Borovoy 1990; 2000; Bogatov et al. 1990; Bogatov 2000). It was noticed during these efforts that all varieties of aerosols from the object «Shelter» may be divided into two classes: aerosol which contains fine-dispersed particles of fuel matrix depleted with volatile radionuclides, and aerosol with radioactivity due to adsorption of fission-fragment radionuclides. Bogatov (2000) showed that contaminated air forms in the space under the roof of the object «Shelter» due to large particles with AMAD about 5 μm. Also in that work, he estimated the value of particles AMAD equal to 6-9 μm, which are capable of resuspension under the intensive mechanical impact. The total amount of fuel dust was estimated to be about 5 t, from which about 100 kg could be a source of potential contamination due to resuspension.

The conditions of the object «Shelter» construction did not allow the creation of a completely pressure-tight structure. Technological and structural apertures have been constructed to provide for the release of radioactive aerosol into the environment. RSC Kurchatov Institute (1990) gives measurement data for radioactive aerosol deposition on vertical and horizontal plane tables near main gaps on the roof of the object «Shelter». Early studies showed that during observations in 1990-1993, the radioactive releases from gaps with a total area of about 206 m^2 were not more than 1.11×10^{10} Bq y^{-1} (the share of plutonium was 0.4-1.2%).

Measurements of the radioactive particles which have been released into the atmosphere from unorganized gaps of the object «Shelter» (Fig. 2.8) with a total area of 200 m^2 were carried out in 1996-2000 (Garger et al. 2002; 2004). Estimates of the average contribution of ^{137}Cs, ^{90}Sr, and $^{239+240}$Pu in the releases were 78.8, 21.16 and 0.04% respectively. The total release intensity of these nuclides from unorganized gaps equals 274.1 Bq s^{-1} or 8.64×10^9 Bq y^{-1}.

2.7. Sampling locations

Soon after the Chernobyl accident, measurements of the radioactive aerosol characteristics and the study of wind-driven resuspension in the 30-km exclusion zone of the Chernobyl NPP were launched by the Hydrometeorological Committee of the former USSR. These studies included measurements of resuspension characteristics and the temporal behavior of the activity concentration in the atmospheric surface layer.

At the time of the measurements, there was little knowledge about the spatial variability of the radionuclide deposition field in the 30-km zone. However, γ-radiation measurements demonstrated significant spatial variations. The part of the zone where

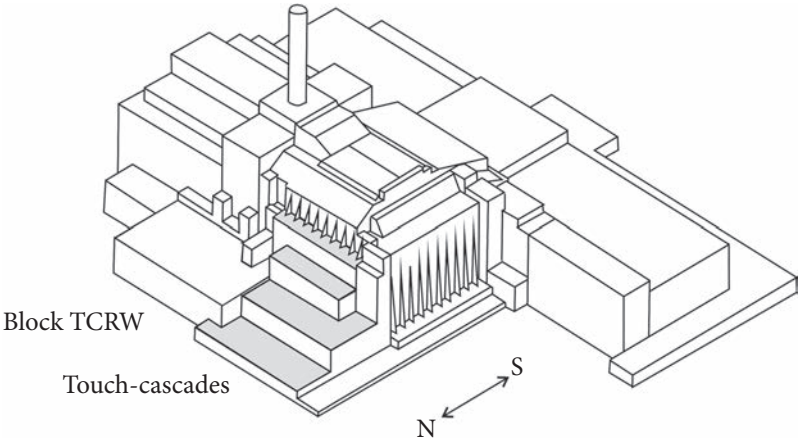

Fig. 2.8. The object «Shelter» and large horizontal and vertical gaps where measurements were made

intensive soil activity measurements were made is shown in Fig. 2.9. Additionally, the sites where aerosol measurements were performed since 1986 are shown. It was decided to set up a permanent field site, at which various types of samplers could be used and where it would be possible to measure the air activity concentration depending on the height above the ground. This site is located close to the village of Zapolie, about 14 km south of the Chernobyl NPP. The Zapolie site is located in the largest open place (a grass field of approximately 1,800 m by 600 m). The Zapolie site was selected because of relatively homogeneous surface contamination within 200 m of the sampling location (see Fig. 2.9). The site area is sufficient for the formation of the local surface boundary layer, in which the resuspended radioactive material is representative of the sampling location (Byzova et al. 1989). The activity variation (sigma/mean) of 20 soil samples taken at the site ranges from 22% (^{137}Cs) to 10% (^{103}Ru) (Garger 1987). This is a relatively high homogeneity for the 30-km exclusion zone. The surface roughness for this grass-covered site is approximately 0.1 m. Meteorological data collected in the 30-km zone indicate that wind direction frequency varies between 9 and 16% over the eight primary wind directions, with the highest frequency for south-western winds. The months with the highest wind velocities are February-April. The city of Pripyat was selected as a second permanent site in the summer of 1987. Episodic measurements were carried out at the sites Beach-Pripyat and Kopachi in 1986-1993. In August-September 1986 observations were made each 10 days at the following sites: Pripyat, Kopachi, Lelev, Zapolie (village), Zalesie, Korogod, Opachihi, Yampol, Zimovitshe, Chernobyl and Novoselki (Garger 1994).

After the accident, the high-volume sampler in the Chernobyl meteorological station (16 km from the NPP) provided daily filter sampling. In the period from the end of May to December 1986, size-segregated aerosol measurements in

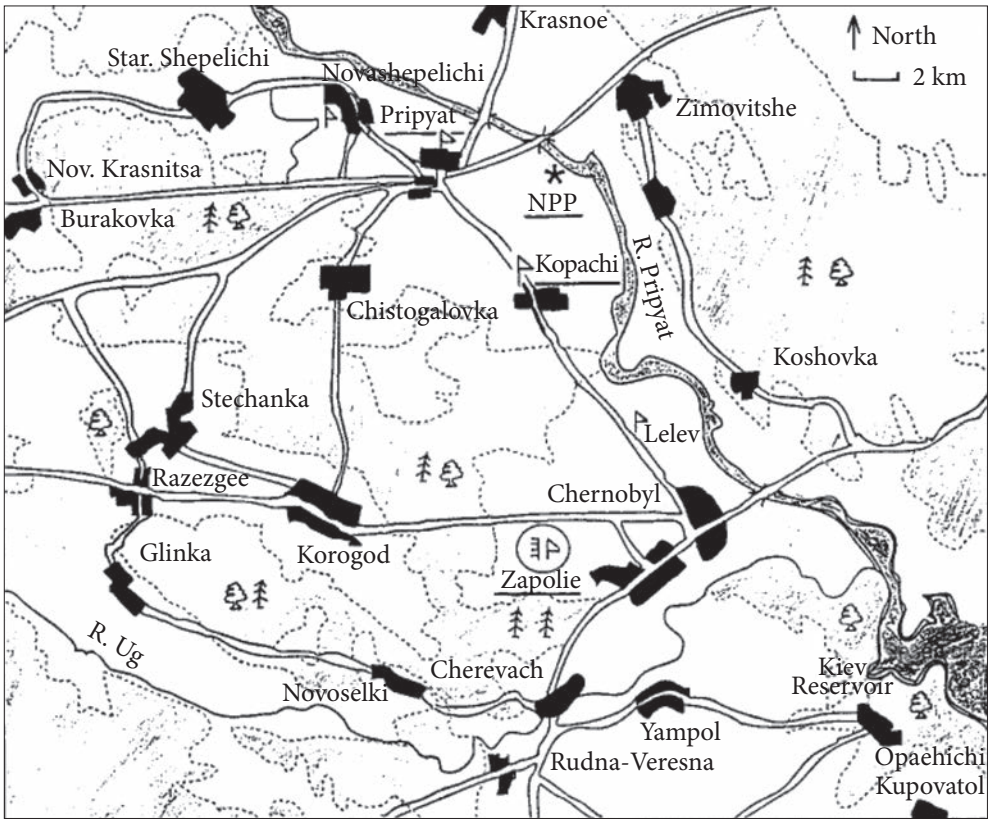

Fig. 2.9. Sampling locations in the 30-km exclusion zone (⋿ – main field measurement site; ⊧ – air activity concentration measurement site; NPP – location of the Nuclear Power Plant)

the radioactive plume from Unit 4 of the ChNPP were made by helicopter at different distances and heights. These measurements enabled the estimation of the emission rate from Unit 4 and the size distribution of particles (Gaziev et al. 1993; Gaziev and Kabanov 1993; Skitovich et al. 1993).

In 1992 and 1993 special aerosol measurements were conducted at Zapolie (field), Beach-Pripyat and Kopachi. Beach-Pripyat is a plateau of hydraulic fill sand of artificial origin. The azimuth of the measurement site is 315°, and the distance from Unit 4 of the ChNPP is 3.8 km. Vegetation is sparse; only separate spots of wild grass and lichens are observed. The soil is pure friable sand. The site Kopachi is a grass field located about 3 km to the south of Unit 4. The surface roughness in this site is about 0.02 m. At a distance of 250-300 m from this measurement site, highly contaminated vehicle installations, armatures, and reinforced concrete are put together.

Airborne particle material was collected using passive «cone» air samplers. They consist of a gauze placed on a conical-shaped (19 cm base radius and approximately 80 cm in length) wire frame. These frames rotate so that the open end

faces into the wind and the particulate material is collected by filtration of the air passing through the gauze. The volume of aspirated air is estimated as the product of the cone base area with the wind speed measured alongside the sampler. The efficiency of the cone samplers has been evaluated based on special experiments. The efficiency factor obtained for a cone sampler was compared with the results of Belyaev et al. (1967). This factor is based on empirical data, but it does not consider particle size. According to this work, under fine weather, the cone efficiency increases with increasing wind speed and decreases with increasing exposure time.

Efforts have been made to increase the efficiency of these cone samplers and to include the effects of particle size. They are, in any event, likely to be most efficient at collecting large (>several μm in diameter) particles, and most resuspended material will likely fall within this particle diameter range since resuspended material is usually associated with host particles (Sehmel 1980). Air samples were collected at eight heights, between 0.25 and 15 m, to evaluate vertical air concentration profiles. Whilst there was currently little validation data for the calibration of the cone sampler, it was considered that the results gained by its use would be reasonable indicators of the real air concentration.

In addition to air and soil samples, dry deposition samples have been collected at a height of 1 m. The samples were collected on planchettes, which are gauze-covered flat plates.

Estimation of the thermal stratification of the atmospheric surface layer was carried out based on gradient measuring data of wind velocity and air temperature in a layer of 0.5-30 m using a «Sosna» gradient device (Garger 1994). For the rest of the measuring points (see Table 2.2) for aerosol sample selection to deter-

Table 2.2. **Surface contamination in measurement sites**

Place	Distance from source (km)	Surface contamination (MBq m^{-2})							
		^{144}Ce	^{141}Ce	^{103}Ru	^{106}Ru	^{137}Cs	^{134}Cs	^{95}Zr	^{95}Nb
Pripyat	4	55.5	4.4	4.9	14.4	5.2	2.0	28.7	53.7
Kopachi	4	17.4	1.5	2.2	4.4	1.6	0.7	8.7	12.6
Lelev	10	4.8	0.5	0.8	1.7	0.7	0.3	2.6	3.9
Zapolie (village)	14	2.8	0.2	0.4	1.2	0.3	0.2	1.3	2.0
Zapolie (site)	14	6.9	1.2	1.2	–	0.5	0.2	3.3	5.8
Zalesie	16	3.0	0.3	0.4	0.9	0.4	0.2	0.2	2.2
Korogod	14	0.5	< 0.1	0.1	0.2	0.5	0.2	0.2	3.4
Opachichi	25	1.7	0.2	0.3	0.6	0.2	0.1	0.8	1.3
Yampol	21	2.1	0.2	0.4	0.9	0.3	0.1	1.3	1.9
Zimovitshe	7	70.3	9.7	6.8	7.5	2.4	0.3	–	–
Chernobyl	16	4.8	0.4	0.9	1.9	0.5	0.2	2.4	3.4
Novoselki	20	2.0	–	0.6	< 0.1	0.3	0.1	1.6	–

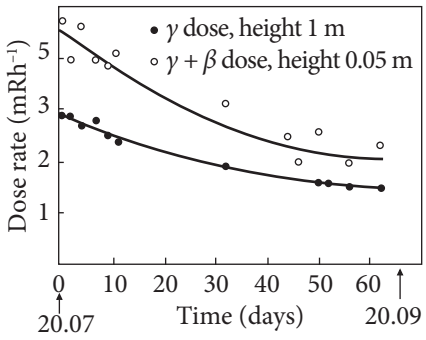

Fig. 2.10. Time course of the dose rate above a contaminated surface at Zapolie site during July-September 1986

Table 2.3. **Density of soil contamination at points of measurements in Kyiv**

Place of soil samples takeoff	Density of soil contamination (kBq m^{-2})		
	^{137}Cs	^{90}Sr	$^{239+240}$Pu
Center (14, Tolstoy str.)	43.3	6.7	0.30
Moscow square	36.3	10.0	0.33
Darnica	17.0	4.1	0.10
Vinogradar	16.3	1.2	< 0.01
Troeschina	28.1	7.8	0.15
Bagrinova Hora	11.1	4.4	0.05

mine the radionuclide activity concentration in the air, gauze cones were chosen, set on support at 1 m height and paired with a horizontal planchette on which a Petryanov filter was exposed. A gauze cone was chosen in the summer of 1986 because of its availability and simplicity of manufacturing in large quantities, and also its complete autonomy from power supplies. The cone was provided with a mechanical M-92 anemometer. This enables measurement of the atmospheric activity concentration and its vertical profile with large exposure time up to 2-3 days, with a corresponding high reliability of the spectrometer analysis data.

The contamination of the underlying surface was measured at various sites in the 30-km exclusion zone using a 15-cm diameter ring, and samples were taken to a depth of 5 cm. Twelve sites were chosen in the southern part of the zone (see Table 2.2 and Fig. 2.9), and a minimum of three samples were taken at each site. Samples were collected at various times during August and September 1986; for consistency, all results have been decay corrected to 25 September 1986.

From Fig. 2.10 it is evident that the density of surface contamination in the site territory for the measurement period of 2 months decreased with time. This decrease was due to natural decay of the short-lived radionuclides ^{141}Ce, ^{103}Ru, ^{95}Nb, and ^{95}Zr and part of the ^{144}Ce and ^{106}Ru.

Soil sampling was carried out by an envelope method, with subsequent analysis using a gamma-spectrometer. The estimation of the vertical distribution of depositions has shown that the main part of the radionuclides was contained in the upper 0.5-1.0 cm soil layer.

In November-December, 1991, special aerosol measurements were carried out in Kyiv to obtain information for estimating the inhalational radiation dose for the city population. For this purpose, air sampling with the help of a mobile sampler «Typhoon», sampling of dry deposition with the help of a planchette, and sampling of soil and near curb-stone dust in five points of Kyiv with massive traffic and in a point located in a park area were carried out. Radiochemical analysis

has enabled the determination of the ^{90}Sr, $^{239+240}Pu$, and ^{137}Cs activity concentrations in samples of soil, dust, fallout, and air. Table 2.3 presents the values of the soil contamination density in 1991 at six points in Kyiv.

2.8. Sampler installations

After the accident, the high-volume sampler in the Chernobyl meteorological station (16 km from the NPP) provided daily filter samples. In June 1987, measurements were started with high-volume samplers in the town of Pripyat (4 km from the NPP in the northwest direction). In both Chernobyl and Pripyat, high-volume samplers designed by SPA «Typhoon», Russia, operated at a flow rate of 100,000 $m^3\ day^{-1}$ (1.16 $m^3\ s^{-1}$) at a sampling height of about 1.5 m. The Russian type Petryanov cloth FPP-15-1.5 with an area of 1.05 m^2 was used in the filter. Later several similar high-volume sites were set up at other places in the exclusion zone. Permanent meteorological observations were carried out by the Chernobyl meteorological station.

For estimation of the wind-driven resuspension rate, only tests were taken into account with vertical profiles of the radionuclide activity concentrations and the average wind velocity close to logarithmic, i.e. the measurement conditions approximately corresponded to a horizontally homogeneous pollutant source. In total, 22 experiments with exposure time about 3 days were carried out during the period from August 1986 till September 1987.

In 1992 the ECP1 project was started, with the operational experimental period finished in 1994. Various joint field operations on the study of the radionuclide activity concentration flows and deposition were carried out. A principal advantage of field joint experiments was the simultaneous use of a great number of various measurement devices. It was necessary to perform their inter-calibration to receive comparable results. No standardized aerosol samplers are covering the complete particle size range. Only for the sampling of particle diameters up to 10 μm was there standard equipment available with well-defined collection characteristics (PM10). For a quantitative sampling of large aerosol particles, which are of special interest in the case of resuspension, devices of the special design were developed and deployed in the project. Most aerosol samplers which are widely in use in Ukraine, Russia, and Belarus have not been characterized in western literature. Nevertheless, in order to use and to interpret correctly all results obtained in the experiments, it was necessary to compare the sampling instruments which were operated in the experiments.

In the field experiments of ECP1, size-integrating samplers, as well as samplers that separate different size ranges, were used. Table 2.4 provides specifications of the integrating instruments. All devices separate the particles by filtration. The designs of the inlet and the flow rates are different, and anisokinetic sampling errors are likely to exist.

The Cone sampler is like a winding cone made from gauze with a certain inlet base diameter and length. The FOA, «Grad», «Typhoon» and WRAC samplers suck the aerosol through a filter medium at a constant flow rate. Isokinetic samplers IPA and IPSN adjust the air flow in an attempt to match the inlet velocity to the wind velocity. The measured entity is therefore not the air activity concentration but rather the radioactive particle flux.

Table 2.5 provides specifications of all samplers used in the field experiments that segregate the particles according to their size. The Andersen PM10 has an upper size limit, but the deposition in the inlet was used to indicate the large particle fraction. Two different cascade impactors were fitted to the PM10 in the field campaigns. The IBP cascade impactor was characterized in laboratory experiments (Frank et al. 1996). It was used for aerosol sampling inside a tractor cabin. The Rotating Arm Impactor (RAI) (Wagenpfeil et al. 1994) and the Wind Tunnel sampler collect particles larger than a certain size, each size fraction with a different flow rate (Frank et al. 1996). The WRAC parallel impactors (Hollander et al. 1989) collect particles smaller than a certain size on a filter. For details, see the quoted literature. The impactors IK, UP, and PK were widely used for observations in the 30-km zone, especially the IK impactor in Zapolie from September 1986 and the UP impactor in the city of Pripyat from September 1987. The flow rate of the well-characterized Berner impactor (Berner and Lurzer 1980) was too small to detect the nuclide size distribution, but the mass size distribution was determined. The Aerodynamical Particle Sizer (Blackford et al. 1987) was used

Table 2.4. **Integrating aerosol samplers used in the field experiments**

Sampler name	Reference	Flow rate ($m^3\ h^{-1}$)	Filter size	Filter material	Remarks
Cone	[1]	Dependent on wind velocity	19 cm base radius, 80–100 cm length	Gauze	Wind driven
FOA[a]	[2]	300	0.56 m × 0.56 m	Glass fiber (FOA)	
Grad	[3]	400	0.77 m × 0.34 m	Petryanov	
IPA[b]	[3]	Dependent on wind velocity (7.2 at 1 m s^{-1})	0.045 m^2	Petryanov	Isokinetic sampler, wind driven
IPSN[a]	[4]	Dependent on wind velocity	0.52 m × 0.6 m	Cellulose (Delbag)	Isokinetic sampler
Typhoon	[3]	4167	1.55 m × 0.34 m	Petryanov	
WRAC[c]	[5]	100	0.20 m × 0.25 m	Glass fiber (Binzer)	

Note: [a] Abbreviation of operating institute; [b] Isokineticheskiy Probootbornik Aerozoley (isokinetic aerosol sampler); [c] Wide Range Aerosol Classifier. * — [1] — Garger (1987), [2] — Vintersved (1994), [3] — ECP1 (1996), [4] — ECP1 (1996), [5] — Garger et al. (1994).

to measure the particle number concentration with a high time resolution (1-20 min) in the size range 0.6-30 μm.

In the field experiments, which lasted typically 3 weeks, ten institutes from eight countries participated. Resuspension measurements began during wind-driven conditions. The Andersen PM10, IK, PK, and IP IEM impactors, which segregate the particles according to their size, were the main measurement instruments. It was the general understanding that it is necessary to compare all methods of measurement of the atmospheric activity concentration, the deposition and the size distribution of radioactive particles at the same time. The first comparison was made at the sites Beach-Pripyat and Zapolie in 1992. Devices were placed in the limited area of 10 × 15 m at Beach-Pripyat and 30 × 20 m at Zapolie. Care was taken that the devices did not influence each other. During a special period in 1993, observations of the activity concentration in the air and the deposition density for inter-comparison were repeated because some divergence was observed, e.g. for the IPA sampler. Good characterization of the performance of this device is very important, because ten IPA samplers were used for the measurement of the concentration at different distances from a line source of dust. The samplers Andersen PM10, UP impactor, rotating impactors, FOA sampler, IPSN sampler, and «Grad» sampler were situated close to one another. The PK impactor, «Grad» sampler, and WRAC had their inlet at heights between 3.2 and 3.6 m and were placed 20 m apart from each other. The experimental area at the Kopachi site was about the same scale. Altogether, 10 experiments were conducted in 1992 and 19 experiments in 1993.

Table 2.5. **Size separated aerosol samplers used in the field experiments**

Sampler name	Reference	Flow rate ($m^3 h^{-1}$)	Size range cut point (μm)	Remarks
Andersen PM10	[1]	67.8	7.2, 3.0,1.5,0.95, 0.49, <0.49	Impactor (1992)
	[2]		4.9, 2.3, 1.4, 0.8, <0.8	Circular five stage impactor (1993/94)
Berner impactor	[3]	1.73	16, 8, 4, 2, 1, 0.5, 0.25, 0.13, 0.06	Mass size distribution
IBP impactor	[4]	1.05	29, 14, 5.4, 1.6, 0.56, <0.56	Inside tractor cabin
IK impactor	[5]	40	22, 10, 5, 3.2, 1.5,<1.5	
PK impactor	[5]	190	20, 12, 7, 4, 2, <2	
RAI	[6]	8.8, 35, 18	10, 20, 28	Parallel impaction
UP impactor	[5]	400	13, 4.5, 2.0, 0.65,<0.65	
Wind Tunnel	[4]	100, 47, 18	15, 24, 35	Parallel impaction
WRAC	[7]	100	9.2, 20.4, 48.6, 60.2	Parallel impaction

* — [1] — Garger et al. (1997), [2] — Marple and Liu (1974), [3] — Berner and Lurzer (1980), [4] — Frank et al. (1996), [5] — ECP1 (1996), [6] — Wagenpfeil et al. (1994), [7] — Hollander et al. (1989).

2.9. Inter-comparison of integrating aerosol samplers

The installation «Grad», which consists of four identical high-volume samplers with inlets at the heights 1.0 m, 1.8 m, 2.5 m, and 3.5 m, was chosen as a reference instrument for the measurements without size resolution. The sampler had been operated since 1990 at the site and showed consistent results in comparison with the «Typhoon» sampler (at the same sampling height). The design of the FOA and the «Typhoon» samplers is similar to the design of the «Grad» sampler, but the «Grad» sampler provides results at different sampling heights. In all comparisons with other instruments, the «Grad» sampler of similar inlet height to a given instrument was taken as the reference.

In 1992 a comparison was performed between the ^{137}Cs air activity concentration values measured using the samplers «Typhoon» and «Grad» and the integral activity concentrations over all cascades of the impactor PK. Table 2.6 gives the ratios of the measured activity from the «Typhoon» and PK samplers to the measured activity from the «Grad» sampler. The first four measurements in Table 2.6 were made for wind-driven resuspension, the following ones for experiments during agricultural work (imitation of cultivation). The PK concentration values are systematically less than the «Grad» values. The ratio between individual samples differs a little. The mean ratio equals 0.82 ± 0.13. The total individual error is determined generally by the accuracy of the gamma-spectrometric analysis which amounts to an error of not more than 10-15% of the measured activities. This value does not exceed the statistical variance of 16% of the total ensemble. The mean ratio of the samplers «Typhoon»/«Grad» is 0.91 ± 0.34; the scatter is larger, but it is never more than a factor of two.

For comparison of the instruments, the results of the joint measurement campaign in May 1993 at Zapolie are chosen. During this period all instruments operated close together, allowing a most complete comparison. The data from the isokinetic sampler IPA, the FOA sampler, the isokinetic sampler IPSN, the Rotating impactor, and WRAC are compared with data from the «Grad» sampler (see Table 2.7).

Table 2.6. **Comparison of the measured atmospheric ^{137}Cs activity concentrations for the samplers «Typhoon», «Grad» and «PK» at the site Zapolie in 1992**

Date	Typhoon / Grad	PK / Grad
14–17.04.1992	0.79	0.88
13–16.05.1992	1.40	0.82
10–13.06.1992	1.04	0.88
05–08.07.1992	1.11	0.94
10.07.1992, 11^{00}–13^{00}	0.64	0.85
10.07.1992, 16^{00}–17^{30}	0.48	0.56
Mean	0.91 ± 0.34	0.82 ± 0.13

The samplers were selected such that their heights were the same and the observation periods were equal. The FOA sampler construction is similar to the «Grad» design, and it differs mainly by the kind of filter material used.

«Grad» and FOA samplers «cut off» the aerosol particles with sizes near 25-30 μm. The isokinetic sampler IPA aspirates a wider spectrum of particle sizes than the «Grad» and FOA samplers but has the less aerosol capacity, which can easily be seen in periods of very high concentration during enhanced resuspension due to anthropogenic activity. The IPSN sampler is adjusted according to the wind velocity and wind direction to match isokinetic conditions and has two separate filters (a vertical filter for small particles and a horizontal filter for large particles). The rotating arm impactor (RAI) only samples particles larger than 10 μm, and therefore the measured activity concentration must be less than the FOA or «Grad» data. The aerosol samples of the WRAC were taken isokinetically from a 60-cm diameter duct with an average flow of 2.4 m s^{-1}. The samplers were operated using the individual routine filter material. The ratios between the WRAC data and the «Grad» data were systematically less than unity. In Table 2.7 the mean values of the relative atmospheric activity concentrations for ^{137}Cs and ^{7}Be of the different instruments are given.

In Fig. 2.11 the activity concentration of ^{137}Cs, as determined by the active (pump operated) integral instruments, is given for the whole experimental period. Results of «Grad» samplers with two different inlet heights are shown, together with samplers FOA and IPSN.

Results of the RAI (sampling only particles larger 10 μm) are included in Fig. 2.11 for comparison (see inter-comparison of size differentiating aerosol samplers in the next section). In general, the measured concentrations are in good agreement within a factor of two. Of special interest are the experiments on May 13 (experiments number 7 and 8), with a very high emission of large particles. Whereas for the «Grad» and FOA samplers, an upper cut-off of 25-30 μm is estimated, the isokinetic IPSN sampler collects larger particles effectively as well. Therefore this sampler detects higher concentrations during periods with a high portion of large particles.

Table 2.7. **Mean ratio of the measured atmospheric ^{137}Cs and ^{7}Be activity concentrations according to different samplers**

Mean ratio	^{137}Cs		^{7}Be	
	Wind resuspension	Anthropogenic resuspension	Wind resuspension	Anthropogenic resuspension
FOA / Grad	0.73 ± 0.09	0.71 ± 0.16	0.92 ± 0.10	0.67 ± 0.10
IPSN / Grad	1.38 ± 0.06	1.29 ± 0.55	0.79 ± 0.04	0.56 ± 0.14
WRAC / Grad	—	0.60 ± 0.01	0.65 ± 0.02	0.61 ± 0.04
IPA / Grad	1.80 ± 0.21	0.50 ± 0.51	0.22 ± 0.02	0.40 ± 0.18
RAI / Grad	0.76	0.39 ± 0.15	—	—

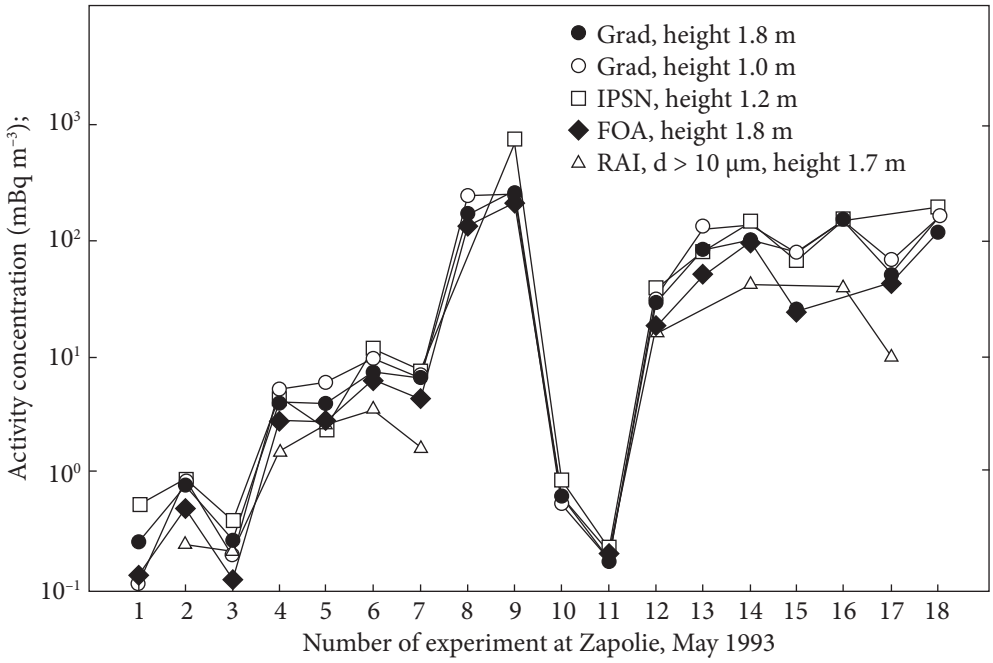

Fig. 2.11. Comparison of the ^{137}Cs activity concentration according to measurements with integrating samplers («Grad», IPSN, FOA) during wind resuspension (experiments 1, 3, 10 and 11) and different anthropogenic enhanced resuspension (all other experiments) at the site Zapolie, May 1993. The sampler RAI, collecting only particles larger than 10 μm aerodynamic diameter, generally shows about 40% of the activity of the integrating instruments

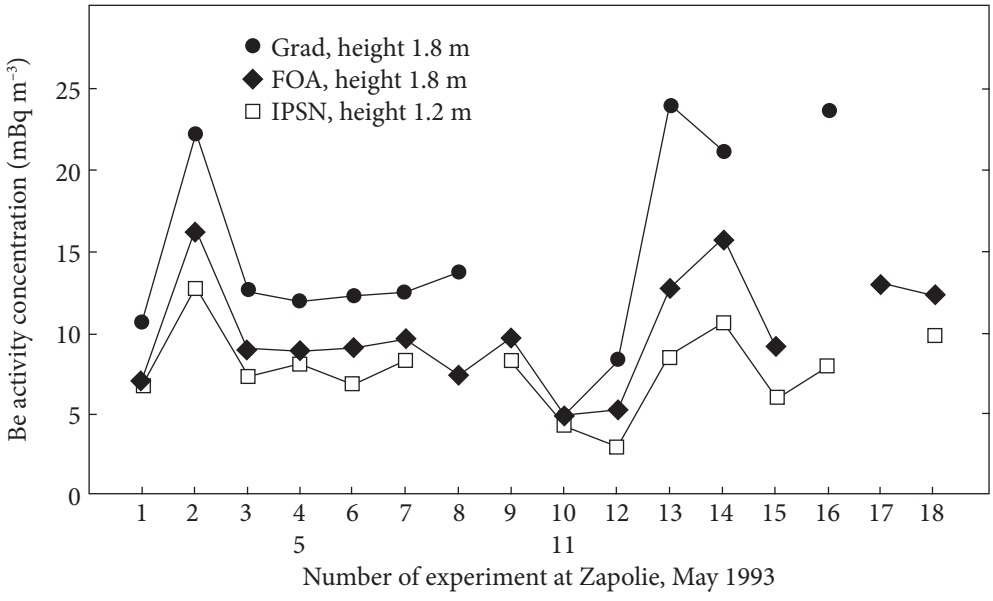

Fig. 2.12. Air activity concentration of ^{7}Be for three integrating samplers

The ^{7}Be atmospheric activity concentration (due to the stratospheric origin) is uniform at a given sampling site and is generally associated with smaller particles, which are unlikely to be prone to anisokinetic sampling errors. Several samplers are compared based on this nuclide in Fig. 2.12. Again the agreement is, in general, within a factor of two.

2.10. Inter-comparison of size differentiating aerosol samplers

Size distribution measurements of radionuclides by the impactors PK, UP and PM10 «Andersen» were compared for wind-driven conditions. Table 2.8 shows the results of the measurements of the ^{137}Cs activity concentration during five days in the absence of any other work at the observation site. The measurements by the PK impactor and PM10 agree satisfactorily. The UP impactor data for the integral total activity were within a factor of two of the PM10 results.

Another task was to estimate the share of large particles contributing to resuspension in different conditions. The rotating arm impactor (RAI) was designed to answer that question. Table 2.7 and Fig. 2.11 demonstrate comparisons of RAI data with the integrating samplers.

Fig. 2.11 unfolds in time this comparison for «Grad», IPSN, and FOA. It can be seen that the RAI concentration values were always less than the «Grad» and the IPSN values for both the wind-driven and anthropogenically enhanced resuspension. During the anthropogenic activity, on average 39% of the total activity concentration of ^{137}Cs in the air (as measured by «Grad») is connected to particles with diameter ≥10 μm. Fig. 2.13 shows a comparison of the ratio of the respirable fraction (d ≤ 10 μm) to the total concentration as measured by the PK impactor,

Table 2.8. **^{137}Cs activity concentrations of different aerosol particle size fractions according to the Andersen PM10, PK and UP samplers during simultaneous sampling**

Andersen PM10 Impactor (h = 1.8 m, V = 3832 m^3, sampling period 7185 min)		PK Impactor (h = 3.2 m, V = 13264 m^3, sampling period 7335 min)		UP Impactor (h = 1.5 m, V = 11845 m^3, sampling period 6855 min)	
Range (μm)	Concentration (mBq m^{-3})	Range (μm)	Concentration (mBq m^{-3})	Range (μm)	Concentration (mBq m^{-3})
>10	0.044	>12	0.036	>13	0.014
4.9-10.0	0.019	4.0-12.0	0.050	2.0-13.0	0.032
2.3-4.9	0.027	2.0-4.0	0.020		
0.8-2.3	0.045	<2.0	0.059	0.65-2.0	0.014
<0.8	0.011	—	—	<0.65	0.014
Total	0.146	Total	0.165	Total	0.074

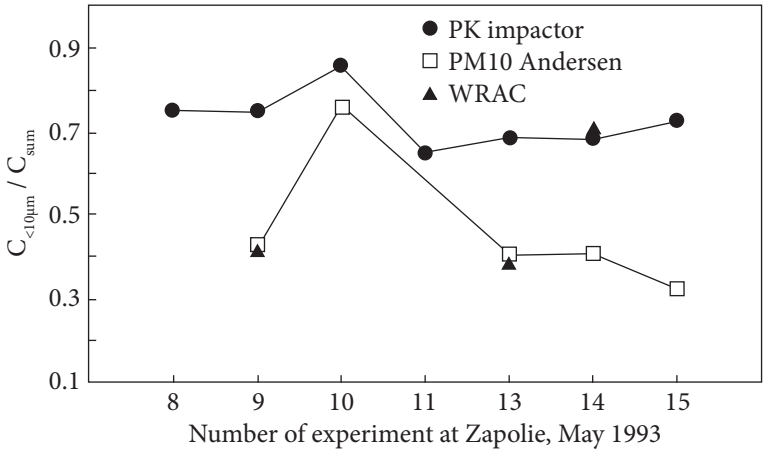

Fig. 2.13. The ratio of the ^{137}Cs activity concentration for the respirable fraction (<10 μm aerodynamic diameter) to the total concentration for several samplers

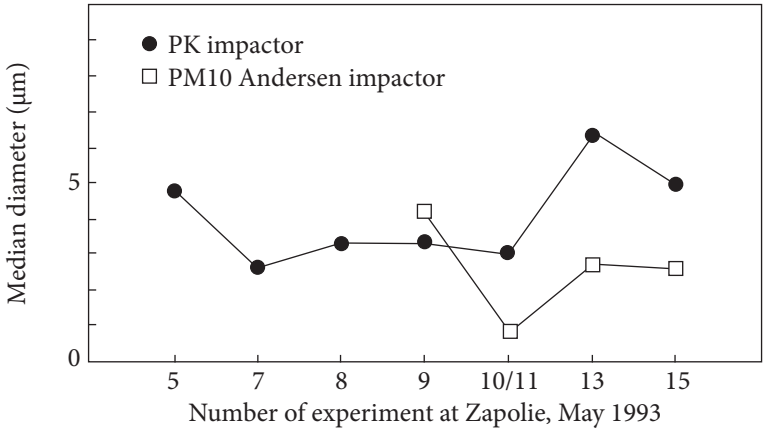

Fig. 2.14. ^{137}Cs activity median aerodynamic diameter according to the measurements by the PK and PM10 Andersen impactors

the Andersen impactor, and the WRAC during the field resuspension-diffusion experiments. Mostly, lower concentrations are found by the Andersen sampler and in two of three experiments by the WRAC. The PM10 inlet allows a quantitative sampling only for particles smaller than 10 μm. In general, according to these measurements, no overestimation is expected if the deposit in the inlet is added to the integral concentration. It is interesting to note that the contribution of the respirable fraction to the total concentration is near 70% of the PK concentrations and near 50% of the PM10 and WRAC concentrations.

Fig. 2.14 demonstrates a time dependence of the aerosol median diameter in the presented experiments. The median diameter according to the PK impactor measurements changes between 2.8 and 5.8 μm with a mean value of 4.3 ± 1.2 μm; the median diameter according to the measurements by the PM10 impactor was equal 2.6 ± 1.2 μm, and the median diameter of the WRAC data was 11.6 ± 6.0 μm. A special study for the comparison of the IBP impactor (which was used for measurements inside a tractor cabin) with the Berner impactor was performed (Frank et al. 1996). In general, the agreement was good, but a reduction of the cut-off diameters of the IBP impactor to smaller values was proposed.

Thus, a comparison of the integrating samplers shows that the samplers, in general, agree within a factor of two for ^{137}Cs and ^{7}Be activity concentration measurements. Larger discrepancies were found for the IPA sampler, and an additional investigation of its characteristics is demanded. The WRAC sampler detected systematically lower ^{137}Cs and ^{7}Be activity concentrations; because of the good characterization of the device based on gravimetry, a recalibration of the γ-spectrometry system is recommended. The isokinetic sampler IPSN has shown that ordinary integrating samplers may have about a 30% loss of the ^{137}Cs activity connected with large particles due to anisokinetic sampling. This sampler is very useful for the investigation of anthropogenic resuspension, for example, decontamination work, when a lot of radioactive dust with a wide size distribution is lifted into the air. The mean ratio of the ^{137}Cs activity concentration between RAI (sampling only particles larger than 10 μm) and «Grad» is 0.39 ± 0.15 during enhanced resuspension due to anthropogenic activity, which supports the results of the IPSN sampler. The importance of giant particles in the case of resuspension is clearly proved. Samplers with a similar design as the «Typhoon», «Grad», and FOA samplers have found concentration values that are very close. These data can be interpreted jointly for the analysis of different tasks of monitoring of radioactivity and radiation protection.

CHAPTER 3

EXPERIMENTAL ESTIMATIONS OF THE RESUSPENSION FACTOR

3.1. Definition of the resuspension factor

Several different reviews have been devoted to the description of the general concepts, mechanisms, and models for obtaining quantitative assessment of resuspension of radioactive particulates from the surface layer of soil (Linsley 1978, Healy 1980, Sehmel 1984, Smith, Whicler and Meyer 1982, Nicholson 1988, Makhonko 1992, Garger, Zhukov and Sedunov 1990, Garland, Pattenden and Playford 1992). One of the general results of these efforts is that the resuspension factor is used most frequently for environmental assessments of exposure to humans.

The resuspension factor K (m^{-1}) is defined as

$$K = \frac{q}{D}, \tag{3.1}$$

where q is the mean atmospheric activity concentration at the breathing height over a radioactively contaminated surface (Bq m^{-3}) and D is the initial surface deposit (Bq m^{-2}).

This factor is useful in localized situations for characterization of the relationship between surface and airborne contamination, and its use implies equilibrium between the resuspended and deposited aerosol (Sehmel 1984). In practice, however, there are no homogeneously contaminated surfaces, and the airborne concentration is a sum of the local resuspended contamination and contamination advected from upwind resuspension (Makhonko 1992, Garger, Zhukov and Sedunov 1990, Garger 1994). One deficiency in the concept of the resuspension factor is that the airborne concentration assumed to be «related to the surface concentration on the soil at a person's feet rather than upwind. Another deficiency is that resuspen-

sion factors are applicable only for which they were determined» (Sehmel 1984). As it is noted in Healy (1980) it is not inherent to this empirical approach inclusion of many variables, and modern estimations are based on short-term experiments with small attempts to find the factor applied to long-term averaging (for example, one year).

Nevertheless, several different models for K have been derived. Although the resuspension factor has a limited physical definition it is used as the universal parameter of the resuspension process.

The first attempt to estimate the temporal dependence of the resuspension factor $K(t)$ after the Chernobyl accident was described by Garland, Pattenden and Playford (1992); this work was continued by Garland and Pomeroy (1994) for empirical models of $K(t)$ based on experimental material obtained in different western countries after Chernobyl accident.

The uncertainty of K has been reported to have a range of 2-3 orders of magnitude even in a common field experiment (Garger, Hoffman and Thiessen 1997).

3.2. Uncertainty of the resuspension factor measurements

A stricter definition of K under spatial-temporal analyses is given in Healy (1980)

$$K = \frac{1/T \int q(x, y, z; R, t)\, dt}{1/S \int D(x, y, d_s; R, t)\, dt}, \tag{3.2}$$

where T is the averaging period of the air concentration; S is the averaging area of soil samples; x, y, z are coordinate axes; d_s is the soil depth, and R is the radius of aerosol particles. The functions q and D describe the airborne concentration and surface contamination, respectively; $D(x, y, d_s; R, t)$ represents the contaminant inventory in the soil layer at depth d_s.

For experimental measuring, the time T is either the «internal» averaging period of a sampler ($T = T'$) or a selected averaging period for a specific task (in this case $T' < T$; for example, this estimate may be made for a day, a week, ten days and more, or several hours, depending on the needs of the health physicists).

Essentially, T' represents the averaging time of the raw data depending on sampling specifics; T represents the averaging time of interest for the analysis of K, which might not be equal to T'.

Ideally, the values of time averaging and spatial averaging should be compatible. In practice, the period for measuring radioactivity lasts over many hours or several days. The surface concentration is usually averaged over the space in the vicinity of the air sampler. The air path (trajectory) for typical values of the air sampling period (1-3 days) may be hundreds of kilometers long. Therefore, the

magnitude of the uncertainty of an empirical resuspension factor will be dependent on the spatial heterogeneity of surface contamination. Garger (1994) have shown that the advection effect from a highly contaminated upwind area may increase K values by two to three orders of magnitude for distances up to about 14 km from the contaminated area center.

The function $q(x, y, z; R, t)$ for the airborne concentration is highly variable in time due to the great mobility of the atmosphere and the high variability of the vertical turbulent flux of radioactivity. Besides, the function is influenced by the change of synoptic processes over this area and the change of meteorological processes with seasons. Knowledge about the aerosol characteristics of the airborne samplers is also important, as the value of K depends directly on the integrated airborne concentrations both over time and over the distribution of particle sizes. Strictly speaking, only a portion of the full distribution of aerosol particles will be sampled by typical sampling equipment. In practice, the upper bound on the size of particles is not well known, and absence of this information may lead to different results of $q(x, y, z; R, t)$ measured in the same time and place by a factor of two to three.

The time dependence of the contaminant inventory in soil $D(x, y, d_s; R, t)$ is weaker than that of the airborne concentration. However, this function has several typical time periods resulting from the interaction of the surface deposit with soil and subsequent processes affecting the migration of this material. These processes are important for the long-term estimation of K (Sehmel 1984, Makhonko 1992).

In practice, the radioactivity in the soil is usually measured in terms of the total inventory. In the first period (0-1 month) after an accident, this practice does not cause problems for the estimation of the resuspension factor, as the majority of the deposited material is on the soil surface. After this initial period, it is necessary to determine $D(x, y, d_s; R, t)$ for the upper-most layer of soil, because an estimate of K based on the total inventory may be biased low. This bias will be most pronounced for light or dusty soil, for which determination of the total inventory may require measurement to a greater soil depth (e.g. 30-40 cm).

From the examination of the various experimental measurements, and noting conditions for which there are a lack of measurements, the uncertainty in K is expected to vary a factor of 2-3 up to 2-3 orders of magnitude.

3.3. The evaluation of the resuspension factor for homogeneous and stationary conditions

To examine the physical basis for evaluation of the resuspension factor, it is sufficient to consider two idealized conditions: that is, (i) a homogeneous and stable turbulent flow over an infinite plane source of the deposited material, and (ii) a constant point surface source for the stationary surface layer of the atmosphere (Garger, Hoffman and Thiessen 1997).

The first case includes conditions corresponding to a very large spot of contamination or global depositions. Then the equation can be written using the Monin-Obukhov theory (Monin and Yaglom 1970, Byzova, Garger and Ivanov 1991)

$$\overline{q}(z_2) - \overline{q}(z_1) = -\frac{J_A}{\kappa u_*}\left[\ln\frac{z_2}{z_1} + F\left(\frac{z_2 - z_1}{L}\right)\right], \tag{3.3}$$

where J_A is the nongravitational vertical flux of the deposited material, κ is the von Karman constant ($\kappa \approx 0.4$), z_2 and z_1 refer to different measurement heights, L is the Monin-Obukhov length, and F is the universal function of similarity in the Monin and Obukhov theory. For simplicity, the character of the turbulent transport of matter is considered to be no different from the character of the turbulent transport of the momentum.

From Eq. (3.3), the difference between concentrations is seen to be a function of two groups of integral parameters: (a) pure micro-meteorological parameters (u_* and L) and (b) the vertical turbulent flux of the surface deposit J; the latter is the result of the interaction of the surface adhesive forces and the different lift forces induced by turbulent flow. The assumption of constancy of these sources is correct only within the limits of time comparable to the integral of the scale of small-scale turbulence in the atmospheric surface layer. The values of the friction velocity and the Monin-Obukhov length have clear diurnal variations; the value of the friction velocity depends on the seasonal (one-half year period) variations of the roughness length of the ground surface. The short temporal scale of the variations for the first period (ten days to two weeks) after an accident should be considered. A short temporal scale must also be considered in the case of very high contamination, when it is necessary to obtain a high temporal resolution to determine the fluctuation in the air concentration; the fluctuation may have large amplitudes and periods.

Quantification of the vertical flux of deposit matter J_A is complicated, as J_A is a function of several parameters of the soil which must be examined separately. Dividing Eq. (3.3) by the value of the surface contamination, we obtain

$$\frac{\overline{q}(z_2)}{\overline{D}(d)} - \frac{\overline{q}(z_1)}{\overline{D}(d)} = K(z_2) - K(z_1) = -\frac{\Lambda}{\kappa u_*}\left[\ln\frac{z_2}{z_1} + F\left(\frac{z_2 - z_1}{L}\right)\right], \tag{3.4}$$

where $\Lambda = J_A / \overline{D}$ is the resuspension rate (see Chapter 7) and the terms on the left-hand side of the equation formally represent the resuspension factors at different heights. In other words, the difference $[K(z_2) - K(z_1)]$ may be a universal function only in the case of an idealized situation of a uniformly contaminated plane surface. From Eq. (3.4) it follows that for a constant friction velocity and Monin-Obukhov length, the resuspension factor will be directly connected only

with the temporal function of the resuspension rate. From Eq. (3.4) it is easy to determine the ratio between Λ and K (for this idealized situation)

$$\frac{\Lambda}{K} = \kappa u_* \left[\ln \frac{z_2}{z_1} + F\left(\frac{z_2 - z_1}{L}\right)\right]^{-1} \left[1 - \frac{\overline{q}(z_2)}{\overline{q}(z_1)}\right], \tag{3.5}$$

where $K = \overline{q}(z_1) / \overline{D}$ and $[1 - \overline{q}(z_2) / \overline{q}(z_1)] < 1$ for wind-driven resuspension. For neutral conditions when $L = \pm\infty$ m, and for selection of z_1 or z_2 equal to the roughness length z_0, the ratio Λ/K will have a magnitude near $0.1u_*$. The expression

$$v_\alpha = \frac{\Lambda}{K} = \kappa u_* \left[\ln \frac{z_1}{z_2} + F\left(\frac{z_1 - z_0}{L}\right)\right]^{-1} \tag{3.6}$$

for that case is the turbulent vertical resuspension velocity of the deposited material for this idealized situation.

This analysis shows that the dispersion part of the resuspension process has only one factor of long-term variation namely seasonal variability, which controls the long-term dependence of the resuspension rate.

The second case, a contaminated point source (or a small spot), could be considered for neutral thermal stratification and a receptor that is far removed from the source. In this case, the simple asymptotic expression for the air contamination at ground level (Byzova, Garger and Ivanov 1991, Garger 1982) could be used:

$$\overline{q}(x, 0, 0) \approx \frac{Q}{u_*^3 \tau^3 \ln (c_1 \cdot u_* \tau / z_0)}, \tag{3.7}$$

where Q is the emission rate of radioactivity from the point source, τ is the diffusion time, and c_1 is an empirical universal constant equal to 0.2 (Garger 1982). In this equation, τ must be determined through the abscissa of the center of gravity of the particle cloud $\overline{x}$

$$\overline{x} = \frac{u_* \tau}{\kappa} \left(\ln \frac{c_1 u_* \tau}{z_0} - 1\right). \tag{3.8}$$

For non-neutral thermal stratification a more complicated function is used based on the dimensionless argument $\overline{z} / L$, where $\overline{z}$ is the height of the center of gravity of the particle cloud.

As opposed to the first case, the air concentration is dependent on the diffusion time, or the distance from the center of gravity of the particle cloud to the point source. The ratio J/D (x, y, d) will be a function of distance or diffusion time for this simple case.

Thus, if the conditions differ from the idealized case of a uniformly contaminated plane surface, an uncertainty for K of several orders of magnitude may be expected (Garger 1994). Large uncertainties also exist for cases with contami-

nated spots, where the ratio of the horizontal scale of a spot X to the characteristic height of the atmospheric surface layer h (where there is equilibrium between concentrations in the atmosphere and the underlying surface) is small. That is, the necessary condition (Vozhennikov and Nesterov 1988)

$$\frac{X}{h} \geq \frac{T_x}{\max\left(\frac{h}{u_*}, \frac{h}{v_d}\right)} >> 1 \qquad (3.9)$$

will not be met. T_x is the characteristic time of the horizontal transport of the surface deposited material, v_d is the dry deposition velocity, h/v_d is the characteristic time of the establishment of equilibrium between the atmosphere and the underlying surface, and h/u_* is the characteristic time of the vertical mixing.

3.4. Resuspension factor in the Chernobyl exclusion zone

There is considerable variation in the levels of radionuclides deposition density in the 30 km Chernobyl exclusion zone (see Table 2.2). There is also a rapid decline in a deposition with increasing distance from the ChNPP. Consequently, any interpretation of atmospheric activity concentrations that arise from resuspension should consider the possible effects of the advection from upwind surfaces.

The atmospheric activity concentrations of radionuclides measured on 14-17 September 1986 are shown in Table 3.1. During this period the wind direction varied from the west to northwest and the advection of resuspended aerosol from highly contaminated areas to the measurement sites would have been small. The wind speed, however, was quite low, between 1.0 and 1.5 m s^{-1} for the greater part of the period. The air activity concentrations in Table 3.1 can be seen to be generally higher at the most contaminated sites (Pripyat, Kopachi, and Zimovitshe). Calculations of the resuspension factor (Table 3.2) give values in the range 6×10^{-9} to 3×10^{-6} m^{-1} for the same period. The values at Pripyat town, a highly contaminated site, are similar to most other sites, indicating a relationship between the atmospheric activity concentration and the surface contamination of the underlying ground.

The quite high variability of the resuspension factor shown in Table 3.2 is likely to reflect several influences. Firstly, the type of surface has an important effect on resuspension, with the presence of vegetation significantly reducing the occurrence of saltation (i.e. skipping of particles across a surface) which is important in the resuspension process. Secondly, a contaminant vertical migration within the surface layer of soil will be important in determining the amount available for resuspension. Although for consistency, the top 5 cm of soil were taken for radionuclide analysis, it is unlikely that a material near the bottom of this sample would be normally available for resuspension (Nicholson 1988). Thirdly, there were the ef-

fects of mechanical actions which could greatly influence resuspension. The third effect is likely to be important at Kopachi, where the resuspension factor was the order of 10^{-7} m^{-1} for all nuclides, since intensive decontamination activities around the Chernobyl nuclear power plant during the period of study would have resulted in resuspension and advection into the sampling area. The passage of vehicles

Table 3.1. **Activity concentration of the radionuclides in the air at 1.0 m: 14-17 September 1986**

Place	Air activity concentration (Bq m^{-3})							
	^{144}Ce	^{141}Ce	^{103}Ru	^{106}Ru	^{137}Cs	^{134}Cs	^{95}Zr	^{95}Nb
Pripyat	5.40	0.44	0.56	1.11	0.41	0.02	2.52	4.59
Kopachi	14.70	1.07	1.33	2.59	0.96	0.41	5.59	11.00
Lelev	0.78	0.10	0.11	0.44	0.04	0.14	0.24	0.68
Zapolie	0.30	0.02	0.01	0.01	0.02	0.02	0.08	0.13
Zalesie	0.31	0.03	0.04	0.18	0.02	0.03	0.09	0.21
Korogod	0.04	0.01	0.01	0.05	0.02	0.02	0.03	0.03
Opachichi	0.15	0.01	0.01	0.12	0.03	0.02	0.03	0.09
Yampol	0.07	0.01	0.02	0.24	0.02	0.02	0.06	0.06
Zimovitshe	12.60	1.00	1.48	2.29	1.00	0.37	5.55	10.40
Chernobyl	0.74	0.07	0.17	0.20	0.10	0.03	0.41	0.78
Novoshepelichi	0.22	0.18	0.03	1.00	0.04	0.01	0.05	0.18
Chistogalovka	0.81	0.07	0.09	0.48	0.07	0.02	0.30	0.63
Tolsty Les	0.48	0.03	0.07	0.19	0.07	0.01	0.22	0.37

Table 3.2. **Resuspension factor: 14-17 September 1986**

Place	Resuspension factor $\times 10^{-8}$ (m^{-1})							
	^{144}Ce	^{141}Ce	^{103}Ru	^{106}Ru	^{137}Cs	^{134}Cs	^{95}Zr	^{95}Nb
Pripyat	9.7	10.0	11.0	7.6	7.7	0.9	8.7	8.5
Kopachi	85.0	72.0	60.0	59.0	59.0	58.0	64.0	88.0
Lelev	16.0	322.0	15.0	26.0	5.2	42.0	9.0	18.0
Zapolie	11.0	9.0	3.0	0.6	5.3	10.0	6.0	6.5
Zalesie	10.0	11.0	10.0	21.0	6.8	17.0	55.0	9.2
Korogod	10.0	23.0	10.0	28.0	4.2	11.0	11.0	9.90
Opachichi	9.0	7.0	5.6	21.0	13.0	21.0	4.0	6.7
Yampol	3.3	7.5	5.5	26.0	5.9	16.0	4.1	2.8
Zimovitshe	18.0	10.0	22.0	30.0	42.0	120.0	—	—
Chernobyl	15.0	18.0	19.0	10.0	20.0	15.0	17.0	23.0

has also been shown to be an effective influence on resuspension (Nicholson and Branson 1990) although this is difficult to quantify for the measurement period.

The mean resuspension factor calculated over August and September 1986 for the main measurement site in Zapolie is shown in Table 3.3. A much lower variation of the resuspension factor depending on radionuclide is evident as compared with measurements presented in Table 3.2. It is important to note that the values of about 5×10^{-8} m^{-1} are within the large range of reported resuspension factors (see Sehmel 1980) and that they were obtained for 3-4 months after deposition. The time dependence of resuspension has been widely noted and has been considered as either decreasing as a reciprocal function of time after deposition (Garland 1979, Nicholson 1993, Bondarenko, Garger and Giriy 1993) or as a negative exponential function.

The importance of advection from upwind sources is illustrated in Table 3.4. A comparison of the air activity concentration measurements during the north winds, when the wind was passing across the most contaminated part of the region in which decontamination activities were taking place, with the air activity concentration during the south winds shows significantly lower values for the latter. These results relate to measurements made at an agricultural site and may be considered to be typical for the Chernobyl exclusion zone. It is also shown in Table 3.4 that the atmospheric activity concentrations are significantly lower during rainfall and the occurrence of a moist surface.

Surface contamination and atmospheric activity concentration in the 30-km Chernobyl exclusion zone varied significantly in space during 1986. The

Table 3.3. **Mean resuspension factors at Zapolie during August/September 1986**

Resuspension factor $\times 10^{-8}$ (m^{-1})						
^{144}Ce	^{141}Ce	^{103}Ru	^{134}Cs	^{137}Cs	^{95}Zr	^{95}Nb
7.7 ± 3.9	4.4 ± 2.1	9.9 ± 7.5	6.3 ± 1.3	7.7 ± 2.1	5.4 ± 3.6	5.5 ± 3.7

Table 3.4. **Comparison of the air activity concentrations for north and south winds at the Zapolie site**

Period of air sample	Surface conditions	Wind direction	Wind speed at 1 m ($m\ s^{-1}$)	Air activity concentration ($Bq\ m^{-3}$)					
				^{144}Ce	^{141}Ce	^{103}Ru	^{137}Cs	^{134}Cs	^{95}Zr
6-9 Aug 86	Dry	North	0.8	9,400	1,600	2,000	700	250	7,700
9-12 Aug 86	Wet	»	1.0	850	78	220	92	37	740
12-13 Aug 86	Dry	South	2.9	67	9.2	5.2	3.2	1.5	28
27-29 Aug 86	»	»	1.7	100	3.7	4.8	5.9	2.6	6.7
2-3 Sep 86	»	»	1.0	25	7.8	2.6	9.6	7.0	8.5

atmospheric activity concentration was dependent on resuspension, as well as the radionuclide advection was an important factor in many cases. The effects of decontamination activities around the Chernobyl NPP were also found to be important in determining the downwind air activity concentration. During 1986 the resuspension factor was found to be mostly in the range from 10^{-8} to 10^{-7} m^{-1} depending on radionuclide.

3.5. Dependence of the resuspension factor from fractional composition of soil particles

In 1993 in Zapolie six series of measuring with the help of PK impactor (designed by SPA «Typhoon», Russia) were carried out with the purpose to estimate the ^{137}Cs resuspension factor depending on the aerosol particle size (Table 3.5).

Table.3.5 shows that the maximal value of the resuspension factor corresponds to the range of inhalational particles with an aerodynamic diameter less than 2 μm. It is seen that the resuspension factor for respiratory particles with diameters less than 12 μm is equal 3.6×10^{-10} m^{-1} and exceeds the resuspension factor for particles >12 μm more than twice.

In the period from July 23 till August 15, 1992, it was investigated resuspension of radioactive particulates near village Vertebu, Novozybkov district (Bryansk region, Russia) on a cultivated field with the total area about 276 hectares (Lukoyanov, Naydenov and Mashkova 1994). In the surface layer of the atmosphere, a considerable concentration of dust was observed. In some days it exceeded the maximum permissible mass concentration equal to 15×10^{-5} g m^{-3}. The measurements of concentration have shown that the share of respiratory particles (d < 10 μm) was 46% of all particle mass and the share of inhalation particles (<1.0 μm) was on the average 14%. At that 87% of ^{137}Cs activities fell on respiratory particles (£ 10 μm). Experimental data of that work have enabled to estimate a relation of the activity concentration of ^{137}Cs bound to the particles with their sizes, and to calculate the dependence of the resuspension factor on the particle size. In Table 3.6 values of the resuspension factor K_1 for the density of contamination in 1 cm layer and K_2 for the density of contamination which correspond the inventory of ^{137}Cs in soil depending on the soil particle size are given (Lukoyanov, Naydenov and Mashkova 1994).

In that work, the mass particles concentrations measured and calculated using data of the number concentration considering a measured soil density 2.6 g m^{-3} have been compared. It turned out that the average value of the experimental mass concentration exceeds calculation one by 1.4 times. According to Table 3.6 with increasing particle size the resuspension factor value decreases. Lukoyanov, Naydenov, and Mashkova (1994) proposed the empirical dependence

for the ^{137}Cs resuspension factor on a particle size

$$K = A \cdot d^{-1.61}, \tag{3.10}$$

where K is the resuspension factor (m^{-1}); $A = 6.2 \times 10^{-7}$ and 8.5×10^{-8} accordingly for calculations of K_1 and K_2; d is the mean diameter of particles size interval (μm). The dependence (3.10) was obtained for respiratory particles of soil at the wind velocity at a level of 1 m not exceeding 3 m s^{-1} for weak unstable conditions of thermal stratification of the atmosphere.

Generalized data of the resuspension factor estimations for ^{137}Cs and $^{239+240}$Pu at six measuring sites in Belarus, Russia, and Ukraine under the project ECP-1 are presented in Table 3.7 (Hollander and Garger 1996). The highest values of the resuspension factor have been obtained in Novozybkov where the soil was the most eroded. Despite the different environmental conditions at six sites, the differences between the minimum and maximal values of the resuspension factor do not exceed four times. Rather low values were obtained for the Pripyat-beach site though there was the largest radionuclide deposition density in this place. It's probably due to a character of beach surface which consist of coarse hydraulic fill sand where the radioactivity easily penetrate deeply during the rains period. It seems that the resuspension factor for $^{239+240}$Pu is the same order of magnitude as for ^{137}Cs.

Measurements of the atmospheric activity concentration of radioactivity after the Chernobyl accident were made in many countries. According to Swedish data (Vintersved et al. 1991), there are at least three sources that contribute to the atmospheric activity. The first one is natural wind resuspension, i.e., wind-blown dust of soil and plant origin from the ground in the areas surrounding the mea-

Table 3.5. **The resuspension factor obtained to the PK impactor data**

Aerosol particle size range, μm	<2	2-4	4-7	7-12	12-20	>20
Resuspension factor, m^{-1}	1.5×10^{-10}	0.85×10^{-10}	0.51×10^{-10}	0.71×10^{-10}	0.71×10^{-10}	0.77×10^{-10}

Table 3.6. **Resuspension factors for various fractions of soil particles**

Dust fraction of soil (μm)	Number concentration of particles (l^{-1})	Calculated concentration of ^{137}Cs $\times 10^{-4}$ (Bq m^{-3})	$K_1 \times 10^{-8}$ (m^{-1})	$K_2 \times 10^{-8}$ (m^{-1})
0.5-1.0	11631	1.22	110.0	6.25
1.0-5.0	1274	8.79	52.7	2.99
5.0-10.0	20	3.78	6.7	0.38
10.0-25.0	5	1.79	1.9	0.11

surement sites. The second source is radioactivity transported over large distances from heavily contaminated areas like the Chernobyl zone, and this activity could originate from resuspension too. The third source may be the local combustion of contaminated wood. Mean annual atmospheric activity concentrations of ^{137}Cs have been measured at a variety of Swedish sampling stations (Fig. 3.1). The atmospheric activity concentration of ^{137}Cs declined until 1991 but has remained approximately constant after this. The resuspension factors have been derived for each site using mean values of the atmospheric activity concentration of ^{137}Cs from

Table 3.7. **Average values resuspension factors of ^{137}Cs and $^{239+240}$Pu during 1992-1994**

Site	Soil surface	Direction and distance in km from ChNPP	^{137}Cs soil contamination (Bq m^{-2})	^{137}Cs resuspension factor × 10^{-10} (m^{-1})	$^{239+240}$Pu soil contamination (Bq m^{-2})	$^{239+240}$Pu resuspension factor ×10^{-10} (m^{-1})
Pripyat-beach	>90% sand	West, 4	3.3×10^{6}	2.2 ± 1.9	5.0×10^{4}	1.1
Zapolie (1993)	Grass	South, 4	5.9×10^{5}	4.4 ± 2.3	5.7×10^{3}	1.8
Kopachi	Grass	South , 2	2.3×10^{6}	2.0 ± 1.4	3.9×10^{4}	0.24
Novozybkov	Fallow	North-East, 150	1.1×10^{6}	7.7 ± 3.5	—	—
Mikulichi	Rye field	North, 45	4.2×10^{5}	3.1 ± 3.1	—	—
Kovali	Barley field	North, 45	5.3×10^{5}	6.3 ± 7.2	3.4×10^{2}	11.0

Table 3.8. **Resuspension factors at sites in Sweden (1990-1991)**

Site	^{137}Cs activity concentration in the air decay corrected to May 1, 1986 (μBq m^{-3})	^{137}Cs deposition after the Chernobyl accident (Bq m^{-2})	^{137}Cs deposition from nuclear weapons fallout (Bq m^{-2})	Total deposition of ^{137}Cs (Bq m^{-2})	Resuspension factor (m^{-1})
Kiruna	0.7	250	1,250	1,500	4.7×10^{-10}
Umeå	14.0	40,000	1,750	41,750	3.3×10^{-10}
Őestersund	2.3	2,000	1,700	3,700	6.3×10^{-10}
Ursvik	2.3	600	2,000	2,600	9.0×10^{-10}
Grindsön	1.8	1,300	2,000	3,300	5.5×10^{-10}
Visby	2.2	2,100	2,000	4,100	5.4×10^{-10}
Geteborg	1.4	2,500	2,600	5,100	2.7×10^{-10}
Ljungbyhed	1.6	1,100	2,750	3,850	4.2×10^{-10}

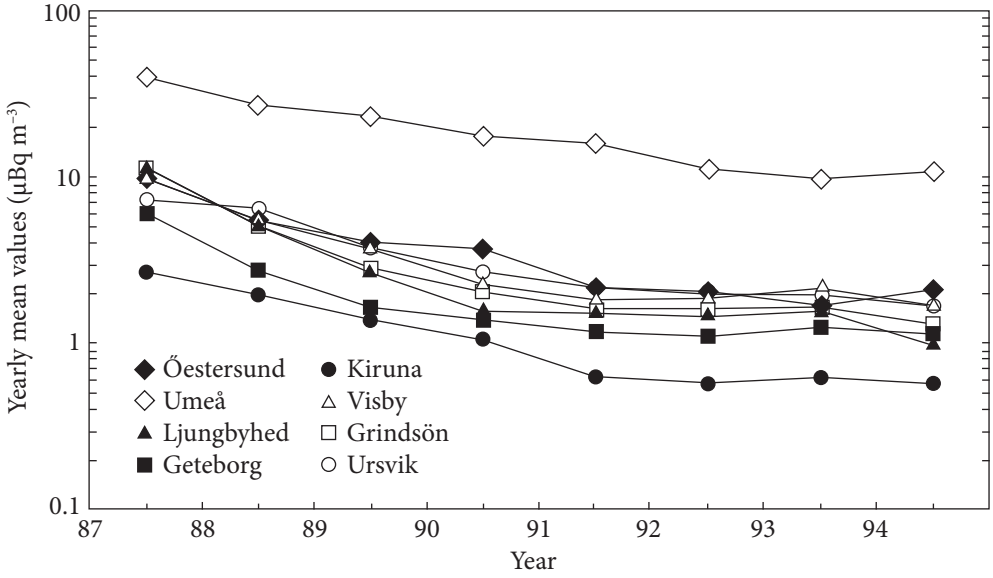

Fig. 3.1. Yearly mean values of the ^{137}Cs air activity concentration for the sampling stations in Sweden

January 1991 to December 1991, divided by the total deposition of ^{137}Cs (Table 3.8). It is interesting to note that the resuspension factor is similar at all sites and shows little dependence on the value of Cs deposition due to the Chernobyl accident. A value of 5×10^{-10} m^{-1} was chosen as the resuspension factor value and was multiplied by the total deposition that provided a good approximation of an atmospheric ^{137}Cs activity concentration in six-eight years after the initial deposition.

3.6. Time variability of resuspension factor

In Fig. 3.2 the monthly averaged values of the resuspension factor are presented according to measurement data in Chernobyl and Baryshevka (Garger, Hoffman and Thiessen 1997). Despite the different distance of these settlements from the Chernobyl NPP (18 and 150 km accordingly) and different soil contamination values in these places, the time dependence of the resuspension factor is similar. The greatest difference is seen mainly only in the part of the measurement period when anthropogenic activity was taking place in Chernobyl. Thus, it is possible to conclude that high-frequency oscillations of the resuspension factor and the radionuclides air activity concentration were well smoothed by their monthly averaging, and it is evidence that the character of resuspension process in the northern part of Ukraine is similar.

Garger, Zhukov, and Sedunov (1990) showed that for short periods after the accident (about 10 days) the resuspension factor exceeded value of 10^{-5} m^{-1}; for

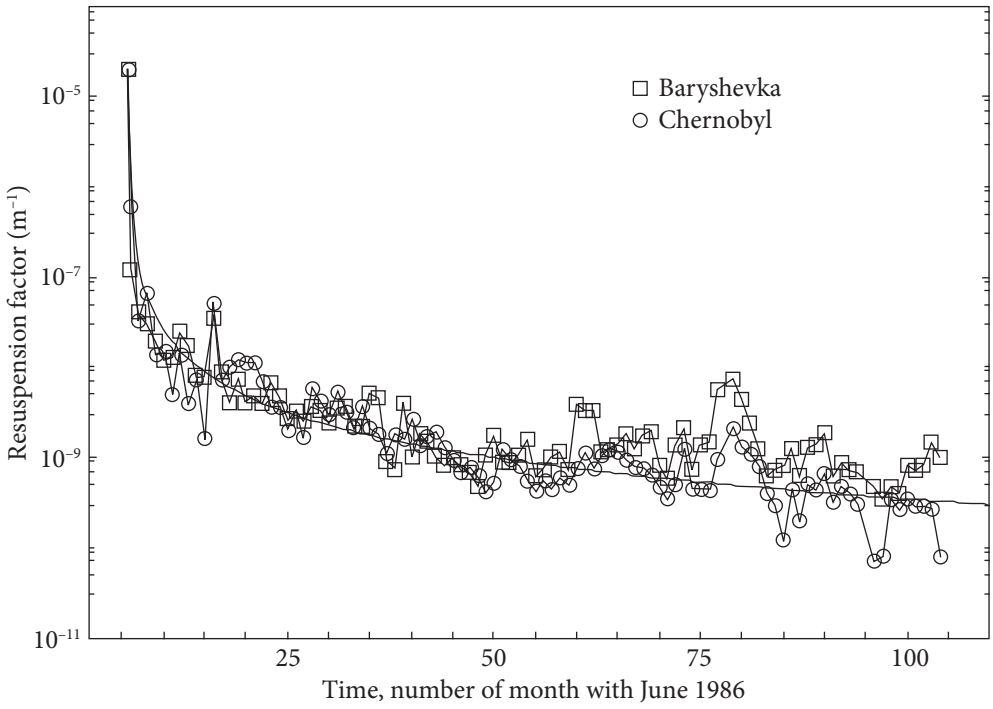

Fig. 3.2. Time dependence of the resuspension factor in Chernobyl and Baryshevka

the subsequent days the value of the resuspension factor was about 10^{-6} m^{-1} in Chernobyl and after three months it was about 10^{-8} m^{-1}. In this later period the exceptional high values of resuspension factor equals to 10^{-6}-10^{-7} m^{-1} were obtained in places with high anthropogenic activity near the ChNPP and near main roads with intensive traffic (Bondarenko, Garger and Giriy 1993). Eight years after the accident the resuspension factor value was equal to about 10^{-10} m^{-1}.

3.7. Comparison of the resuspension factor values

Finally, the integral measurements of wind resuspension are used to determine the resuspension factor for comparison with the resuspension factors measured after the Chernobyl accident in different European countries.

The resuspension factor is defined for a given location as the ratio of the mean air activity concentration to the mean surface contamination. This general characteristic of the local process responsible for the activity concentration of ^{137}Cs in the atmospheric surface layer was determined for our measurements from 1986 to 1993 at the different sites in Ukraine, Belarus, and Russia. We have used the paper (Garland and Pomeroy 1994) as a database (Fig. 3.3). Additionally, we pres-

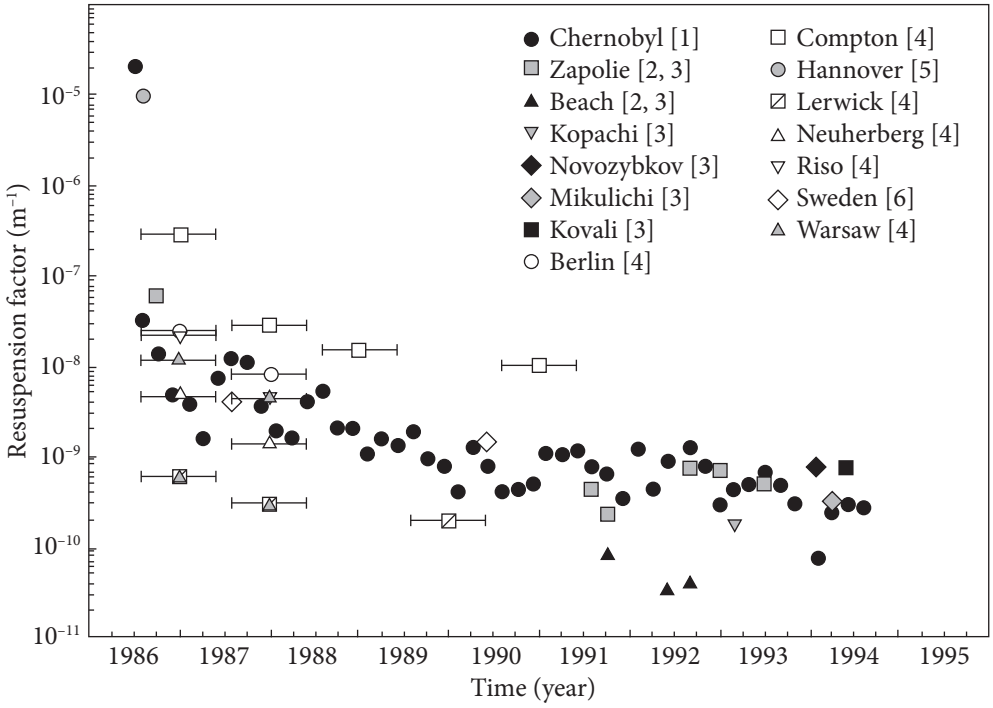

Fig. 3.3. Summary of available data of measured resuspension factors in Europe. The bars show the sampling periods. [1] — (Garger, Hoffman and Thiessen 1997), [2] — (Garger 1994), [3] — (Hollander and Garger 1996), [4] — (Garland and Pomeroy 1994), [5] — (Hollander 1994), [6] — (Vintersved et al. 1991)

ent data of measurement started after the Chernobyl accident in 1986: measurements at the sites Zapolie, Beach-Pripyat, Kopachi (Ukraine) (Garger, Zhukov and Sedunov 1990), (Hollander and Garger 1996); Mikulichi, Kovali (Belarus), Novozybkov (Russia) (Hollander and Garger 1996) and information from Great Britain (Compton, Lerwick), Germany (Berlin, Neuherberg, Hannover), Poland (Warsaw) (Garland and Pomeroy 1994), and Sweden (Vintersved et al. 1991).

Despite of a different distance of the Chernobyl NPP and different contamination levels at these measuring points, one may note a similar time dependence of the resuspension factors for these places. The greatest differences were observed in Chernobyl until the moment of an end of anthropogenic activity in the town (Nicholson 1988).

The data from Compton and Lerwik have shown the range of variability. One may note that the resuspension factor depending on the underlying surface character mainly varies in the range of two factors of magnitude. It shows the similar character of wind resuspension over enough moist soil at moderate latitudes of Europe.

CHAPTER 4

EMPIRICAL MODELS OF THE RESUSPENSION FACTOR

4.1. Time-variable models of the resuspension factor

The process of resuspension depends on micro-scale features of the particle-surface interface, such as the local water content and chemistry, as well as the large-scale fluid mechanical removal forces. There currently exists no robust mechanistic model that applies to small and large fluxes at short and long times after deposition. Instead, modelers rely on simple models, such as those for the resuspension factor K (see Chapter 3). The resuspension factor approach has the advantage that both the concentration of a contaminant and the surface deposition are directly measurable in the field, so this quantity appears in numerous data sets. The simplest available models for the resuspension factor are based on empirical formulas.

However, the choice of the proper values of K is usually not a simple task, being quite site-specific and related to the meteorological, geomorphologic and environmental characteristics of the area to be studied. (Magnoni 2012). The main problems of the interpretation of the measurement data are great variability in the values of the resuspension factor, as well as its significant dependence on the time after the moment of deposition. This quantity is difficult to interpret when there is the potential for upwind contamination, when the surface deposition is inhomogeneous, and when there is variability in meteorological conditions (Nicholson 1988). The selection of the parameterization for the resuspension factor is complicated by the fact that the parameters are highly dependent on the location of the site and can not easily be related to some physical quantity (Magnoni 2012). Besides, measurement of K may be complicated since the concentration in the air may include important contributions from processes other than resuspension. The resuspension factor K is likely to be strongly dependent

on such details of measurement technique as the height of air sampling above the surface. In evaluating the deposition density D (Eq. (3.1)) a decision must be made regarding the depth of surface to be included, and it is not straightforward to decide what depth of soil may contribute to airborne radioactivity. In practice, for prediction of resuspension from an accidental dispersion, it is convenient to use the total amount initially deposited, without allowance for vertical mixing into the soil or for removal by weathering (Garland, Pattenden and Playford 1992).

So the simplest parameterizations for the resuspension factor are widespread in the form $K(t) = K_0 f(t)$, where K_0 is the resuspension factor at the initial deposition time $t = 0$, and $f(t)$ is a dependence of the resuspension factor on time.

A variety of mathematical models exist for K, however, the models show great variability and uncertainty even when applied to longer-term data sets (Garger, Hoffman and Miller 1996; Garger, Hoffman and Thiessen 1997). Garger et al. (1999) pointed out in detail the problems in existing models, including sensitivity to the choice of initial resuspension factor; these authors indicate that these models work at best for predicting the annual air concentration in homogeneous conditions. The applicability of the existing models to short-term resuspension (occurring within the first hours to days of an event) has not been tested (Loosmore 2003).

The early parameterizations of the resuspension factor dependence on time were obtained on the base of observations data of plutonium resuspension at the Nevada Test Site (NTS), including data of specially organized experiments of the plutonium dispersal. According to Lem, Behar, and Buck (1977) and Oksza-Chocimovski (1977), Kathren in 1968 and then Langham in 1969 first formulated a time dependency of K in the form of the **one exponential model**

$$K(t) = K_0 \exp\left(-\frac{\ln 2}{T_1} t\right), \tag{4.1}$$

where t is measured in days.

The value of the half-time T_1 has been estimated by Kathren equals to 45 days. Then Langham in 1969 estimated half-time equal to 35 days under conditions of «extensive vehicular traffic», it means «disturbed NTS conditions». For «prevailing NTS conditions» Langham estimated T_1 equals 40 days. The value of K_0 was chosen 10^{-4} m^{-1} for the Kathren model and 10^{-6} m^{-1} for the Langham model.

As the results of the model (4.1) application to the analysis of time series of the radionuclide activity concentration measurements due to resuspension have shown, it gives reasonably good results for periods up to several weeks. However, many studies of the early 70-ies showed a decrease in the accuracy of the model for large periods (Oksza-Chocimovski, 1977). Within the model of the exponential dependence (4.1), this meant an increase in the «effective» value of half-time with an increase in observation time after the time of deposition. The obtained results of long-term measurements of time dependence of the resuspension factor gave grounds for Anspaugh et al. (1975) to suggest a «time-dependent» model of

the resuspension factor. The following grounds were laid into the model: «1) The apparent half-time of decrease during the first 10 weeks should approximate a value of 5 weeks and should approximately double over the next 30 weeks; 2) The initial resuspension factor should be 10^{-4} m^{-1}, and 3) The resuspension factor 17 years after the contamination event should approximate 10^{-9} m^{-1}.»

The most important feature of this model was the assumption that for long periods the resuspension factor tends to the asymptotic value K_∞ for $t \to \infty$. Its value in 1974 was chosen according to the measurements for 17 years, which at that time was «the longest period post deposition for which measurements been reported».

The Anspaugh model (Anspaugh et al., 1975) has the following form:

$$K(t) = K_0 \exp(-\lambda\sqrt{t}) + K_\infty, \tag{4.2}$$

where $K_0 = 10^{-4}$ m^{-1}, $\lambda = 0.15$ (days)$^{-1/2}$, $K_\infty = 10^{-9}$ m^{-1}.

The Anspaugh formula (Eq. (4.2)) can be interpreted as the one exponential model (4.1), but with the «residual» resuspension factor K_∞ when $t \to \infty$, as well as the «effective» value of half-time T_1, increases with time after the deposition as $T_1(t) = \frac{\ln 2}{\lambda}\sqrt{t} \approx 4.62\sqrt{t}$.

Subsequent observations at the sites of the «old» depositions confirmed the validity of the choice of the value of K_∞. Therefore, in the later variants, the one exponential model of resuspension is represented as

$$K(t) = K_0 \exp\left(-\frac{\ln 2}{T_1} t\right) + K_\infty, \tag{4.3}$$

where t is time after deposition in days and K is in m^{-1}.

Thus, within the one exponential model, the resuspension factor is determined by 3 parameters K_0, K_∞, T_1 (or λ). Their values obtained by different authors based on processing the experimental observations are presented in Table 4.1.

Table 4.1. **The parameters of the one exponential model of the resuspension factor according different studies**

K_0, m^{-1}	K_∞, m^{-1}	T_1, d	Half-time $\lambda = \ln 2 / T_1$, d^{-1}	Study	Comments
10^{-5}	10^{-9}	50	0.0139	USAEC (1974)	
10^{-5}	10^{-9}	374	0.00185	USAEC (1975)	
10^{-6}	10^{-9}	70	0.01	Linsley (1978)	
10^{-5}	10^{-9}	70	0.01	Linsley (1978)	For periods of «regular disturbance by vehicular or pedestrian traffic.»
$5.0'10^{-8}$	10^{-9}	231	0.003	Tschiersch et al. (1995)	Used in the decision support system RODOS (Bartzis et al., 2013)

Oksza-Chocimovski (1977) proposed the empirical model with time-dependent half-time. The model presents half-time value as a function of time and local conditions, represented by «initial» and «final» resuspension factors, respectively.

It's formulated in the general form of

$$T_1(t) = A \ln(1 + B + Ct^D) + \frac{\ln(2)}{\ln(K_0 / K_\infty)} t. \quad (4.4)$$

The second term in the proposed analytical expression (4.4) provides asymptotic attainment of the half-time to the final value of the resuspension factor K_∞ for any given value of the initial resuspension factor K_0. In the initial period after the deposition (up to 100 days) the rate of the resuspension factor $K(t)$ decrease over time is determined mainly by values of the constants A (days), B (dimensionless), C (day^{-D}) and D (dimensionless) (1st term in Eq. (4.4)) and is virtually independent of the ratio K_0 / K_∞ in the second term. Thus, the proposed formula for the resuspension factor contains 5 empirically determined parameters instead of 3 ones in the ordinary one exponential model (4.3). According to the author, the choice of the values of the constants A, B, C, and D makes it possible to take into account the impact of local conditions of the territory on the resuspension factor value. Values of A, B, C and D constants may be adapted to fit existing empirical observation data. Oksza-Chocimovski proposed values $A = 28$ days, $B = 4 \times 10^{-2}$, $C = 1$ days$^{-1/3}$, $D = 1/3$ using available data of Sehmel and Orgill (1974) measurements in 1971 and 1972 at an area contaminated with plutonium at Rocky Flats.

Another approach to take into account the increase in the «effective» half-time with time after deposition, which is found at large observation time (about several years), is the parameterization of the resuspension factor in the form of a **double exponential model**

$$K(t) = K_0 \exp\left(-\frac{\ln 2}{T_1} t\right) + K_1 \exp\left(-\frac{\ln 2}{T_2} t\right) + K_\infty. \quad (4.5)$$

The first (faster) component can be the result of the higher initial mobility of the surface contamination in the first months which was substantially diminished by the gradual fixation of the deposited radionuclides by the end of the first vegetation season. After this period the activity concentration of airborne radiocaesium decreases slowly with time, with some fluctuations especially during winters. This slow decrease is due to the migration of ^{137}Cs into the deeper layers of the soil (Tschiersch et al. 1995).

The values of 5 parameters K_0, T_1, K_1, T_2, K_∞ that determine the resuspension factor value according to data from experimental observations of some authors are shown in Table 4.2.

In Eqs. (4.3) and (4.5) the first general uncertainty is the selection of the initial value of the resuspension factor which can vary from 9×10^{-5} to 5×10^{-8} m^{-1} (Tables 4.1 and 4.2) during the first ten days, producing a difference among model estimates of

Table 4.2. **The parameters of the double exponential model of the resuspension factor according different studies**

K_0, m^{-1}	T_1, day	λ_1, d^{-1}	K_1, m^{-1}	T_2, day	λ_2, d^{-1}	K_∞, m^{-1}	Source
10^{-5}	55	1.26×10^{-2}	10^{-9}	36 500	3.0×10^{-5}	0	NRPB/CEA model (Makhonko, 1992)
8.1×10^{-8} 1.04×10^{-7}	95 95	7.3×10^{-3} 7.3×10^{-3}	1.30×10^{-8} 6.50×10^{-9}	2 000 1 500	3.47×10^{-4} 4.62×10^{-4}	0 0	Feher and Zombori (1993), Tschiersch et al. (1995) (2 versions of the model)
9.0×10^{-5}	44	1.58×10^{-2}	10^{-5}	374	1.85×10^{-3}	10^{-9}	Lassey (1980)
3.4×10^{-6}	4.6	0.152	18.4×10^{-9}	231	0.003	0	Hoetzl, Rosner and Wincler (1989)
10^{-5}	10	6.93×10^{-2}	6×10^{-9}	231	0.003	10^{-9}	Anspaugh at al. (2002)
10^{-5}	10	6.93×10^{-2}	7×10^{-9}	347	0.002	10^{-9}	Maxwell and Anspaugh (2011)

K of three orders of magnitude. The second general source of the uncertainty is connected with the rate of decrease of K with time; the half-times $\lambda = \ln 2 / T_1$ in Eqs. (4.3) and (4.5) may change by 2-3 orders of magnitude. The background term K_∞ causes errors in the estimates of K for a very long time after the initial starting point.

The models of Anspaugh et al. (2002) was derived on the base of analysis the data a large (about 300 individual values) historical dataset of radionuclide resuspension factors obtained for different sites, climatic conditions, radionuclides and time scales, including the short-term measurements at the Nevada Test Site and the longer-term measurements following the Chernobyl accident. It was used for reconstruction of internal doses of the Nevada Test Site workers in 1963-1992. The values of K_0, T_1, K_1, T_2, K_∞ were estimated by «eyeball» fitting to the preliminary form of the observational set. Later Maxwell and Anspaugh (2011) refitted the K_1 and T_2 parameter values in the long-term component (Table 4.2) on the base of the supplemented set of observation data.

Garland (1982, 1983) analyzed the measurement data of resuspension of tracer materials with radioactive labels in a wind tunnel. The results gave reason to conclude that for available data length ranges from several tens of days to about 3 years the resuspension factor is better approximated by a power function than exponential functions. For describing the resuspension factor diminishing with time he proposed the **inverse power law model**

$$K(t) = 1.2\times\frac{10^{-6}}{t}, \tag{4.6}$$

where t is the time in days.

The proposed time dependence of K is agreed with the formula theoretically derived by Reeks, Reed, and Hall (1988). In a study aiming at shorter time scales (several hours to several days), they have obtained the following equation for the resuspension factor

$$K(t) = \xi t^{-\varepsilon},$$

where ξ is a constant and $\varepsilon \cong 1$ for $10^{-2} \le t \le 10^{5}$ s.

Lately, the Garland model was modified to account for long-term resuspension (Walsh, 2002):

$$K(t) = \frac{K_0}{t} + K_\infty, \tag{4.7}$$

where $K_0 = 1.2 \times 10^{-6}$ m^{-1} day, $K_\infty = 10^{-9}$ m^{-1}.

This model was recommended by UK NRPB for the calculation of resuspension doses for the emergency response. Using this model it was recommended to assume a resuspension factor during the first day of 1.2×10^{-6} m^{-1} (Walsh, 2002).

The modified Garland model (Eq. (4.7)) is used in the methodology for evaluating the radiological consequences of routine releases called CREAM (Consequences of Releases to the Environment: Assessment Methodology) which was applied in the computer system PC-CREAM 08 (Smith and Simmonds 2009).

These empirical resuspension models are very simple to represent the complex processes involved. They are considered to be sufficiently robust for use in assessing individual and collective doses due to routine releases of radionuclides to the environment. For such assessments, annual or long-term integrated exposures are required and so the averaging implicit in the models is appropriate. However, care should be used in applying such models in considering the accidental releases of radionuclides (Smith and Simmonds 2009).

U.S. National Council on Radiation Protection and Measurements (NCRP, 1999) recommended a similar model for use under calculation of screening limits for contaminated soil:

$$K(t) = \begin{cases} 10^{-6}, & t < 1\,d; \\ \dfrac{10^{-6}}{t}, & 1\,d < t < 1000\,d; \\ 10^{-9}, & t > 1000\,d. \end{cases} \tag{4.8}$$

The empirical equations that account for changes of the ^{137}Cs activity concentration in the air with time have been described for Neuherberg, Germany from mid-May 1986 to the end 1988 (Garland, Pattenden and Playford 1992) and from June 1986 to the end of 1990 (Hoetzl, Rosner and Wincler 1989). Normalizing these equations for the density of contamination of ^{137}Cs in the 0-1 cm soil layer Hoetzl, Rosner and Wincler (1989) gave the following

$$K(t) = 2.67 \times 10^{-6}\, t^{-1.07}, \tag{4.9}$$

where t is the time in days.

Earlier Hoetzl concluded that for the relatively short period from mid-1986 to the end of 1988 the decrease of the ^{137}Cs activity concentration in the air could also be described by an exponential decay curve (Table 4.2) (Hoetzl, Rosner and Wincler 1989). However, the resulting half-time of –250 days no longer held for the longer observation period to the end of 1990. Five years after the reactor accident an effective half-time of –1000 days can be estimated, if obtained data for the ^{137}Cs air activity concentration and deposition are fitted with an exponential function.

Garger, Hoffman, Tiessen (1997) analyzed the atmospheric activity concentration measured around Chernobyl some years after the accident using the inverse dependence of the resuspension factor with time. They found the power of an inverse function to be about 1.4. Using these data on the scale invariability of the fluctuation of the measured atmospheric activity concentration Hatano and Hatano (2003) proposed a model of the time dependence of the resuspension factor. They assumed the wind velocity to have the autocorrelation in time, and obtained the formula of K in the form:

$$K(t) = Bt^{-4/3}. \tag{4.10}$$

They tested the model Eq. (4.10) using data of several wind-tunnel experiments with short time scales from a few seconds to an hour (Nicholson, 1993) and from several hours to two weeks (Garland, 1979). For longer periods they tested the model on the data of the post-Chernobyl measurements in Ukraine (Garger et al., 1999). They concluded that the model fits quite well with experimental data ranging from several seconds to 10 years. As it is based on the scale-free power-law (Eq. (4.10)), it indicates that the resuspension appears to be a fractal (self-similar) phenomenon. Despite some theoretical grounds of the model compared with previous empirical resuspension factor models, it also doesn't link the resuspension characteristics with observed environmental and nuclide parameters.

Using the dataset of radionuclide resuspension factors Maxwell and Anspaugh (2011) fitted the parameters of the double exponential (see Table 4.2) and power functions (Eq. (4.6)). For Eq. (4.7) they obtained $K_0 = 4.47 \times 10^{-5}$ m^{-1} and $K_\infty = 10^{-9}$ m^{-1}. Four models have been compared with the observation data: 2 versions of the double exponential model (Anspaugh et al., 2002; Maxwell and Anspaugh, 2011) and 2 versions of the inverse power-law model (Maxwell and Anspaugh, 2011, NCRP, 1999). They concluded that the modified model (Maxwell and Anspaugh, 2011) overpredicts resuspension early in the process and then underpredicts during the period around 10 days. The double exponential model (Maxwell and Anspaugh, 2011) underestimates during early times and then performs better during the period beyond 10 d. The NRCP model underestimates resuspension until very late periods of about 1000 d. On the base of intercomparison, they concluded that the power-law and modified models (Maxwell and Anspaugh, 2011) appear to be more reasonable representations of the measured resuspension process during the first

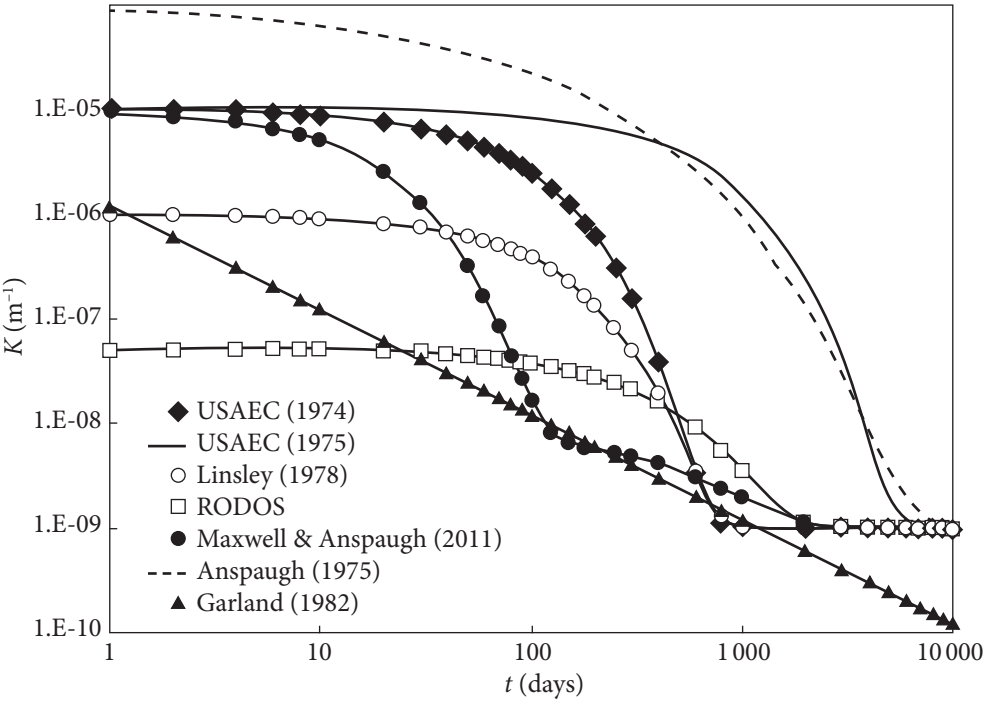

Fig. 4.1. The resuspension factor K as a function of time for seven models of resuspension

100 days. Of these two forms, they recommended using the double exponential form as it appears to be a more accurate predictor at early times $t < \sim 100$ d.

In Fig. 4.1 seven most used models for the resuspension factor are shown. Variability of the resuspension factor values for the initial period after the fallout caused by the choice of the initial value K_0 is greater than 3 orders of magnitude. Over time, the same difference in values of $K(t)$ according to the presented models remains for about first 10 years after the deposition. Only in 15-20 years, the resuspension factor value for all exponential models tends to generally accepted value $K_\infty = 10^{-9}$ m^{-1}. The inverse power-law model of Garland can be matched to the long-term trend of K dependence of time under its modification according to Eq. (4.7).

IAEA (2010) recommended several models to use for different environmental conditions. For rural conditions, the model of Garland was suggested for use in the form of Eq. (4.7) and $K_0 = 10^{-6}$ m^{-1}, $K_\infty = 0$. For urban environments (IAEA 2010) stated that the Linsley model provides the best results in the intercomparison exercises. It yields a resuspension factor that lies within the range of those estimated in situ experiments.

For rural conditions, Garger et al. (1995) tested some resuspension factor models using the airborne activity concentration measurement data from 1986 to 1991 in Chernobyl and Baryshevka cities that are 16 km and 150 km, respectively, from the

Chernobyl NPP. It was concluded that the model of Hoetzl, Rosner, and Wincler (Eq. 4.9)) agrees best with data. The model of Garland (Eq. (4.6)) agrees well with data, but it systematically underpredicts the experimental values. The calculated values of K according to the Linsley model (Table 4.1) are conservative, especially for the first two years. If the calculated values are compared with the upper limits of the measured resuspension factor (monthly averaged), the data of the Garland model and the Hoetzl model are lower than the upper limits of K by a factor of two or three.

For arid and desert conditions IAEA (2010) recommends the Anspaugh model (Eq. (4.2)) to be used, but $K_0 = 10^{-4}$ m^{-1} was proposed instead of $K_0 = 10^{-6}$ m^{-1} in the original formulation of the model. This model gives values that are intermediate between those observed for urban and rural environments in the long term.

Takahara et al. (2014) estimated the resuspension factor using the air activity concentration trend in Fukushima city measured from March 2011 to July 2013 after the radiation accident at the Fukushima NPP. The averaged surface activity concentration of ^{137}Cs in Fukushima city was 0.95 MBq m^{-2} (decay corrected to 15 March, 2011). Measurement data of the air activity concentration was fitted to three main formulas for the time dependence of the resuspension factor. For the one exponential model (Eq. (4.3)) they assessed parameters as $K_0 = 9.9 \times 10^{-4}$ m^{-1}, $T_1 = 13.5$ days, $K_\infty = 10^{-9}$ m^{-1}. Application of the two exponential model (Eq. (4.5)) for these measurements resulted in the following values of its parameters $K_0 = 2.2 \times 10^{-3}$ m^{-1}, $T_1 = 11.4$ days, $K_1 = 6.9 \times 10^{-9}$ m^{-1}, $T_1 = 145$ days, and $K_\infty = 10^{-9}$ m^{-1}. Parameters of the inverse power low model (Eq. (4.7)) were obtained eqals to $K_0 = 1.0 \times 10^{-6}$ m^{-1} day and $K_\infty = 10^{-9}$ m^{-1}.

Some authors proposed **combined models** for the resuspension factor.

In the testing of resuspension models within the BIOMOVS program (Garger et al., 1999) the Makhonko/Garland/Kryshev model was used. It yields superposition of an exponential and a power function:

$$K(t) = A(u)\,(e^{-at} + bt^{-1}), \tag{4.11}$$

where t is time in years, u is the wind velocity (m/sec), $A(u)$ is the function of the wind velocity

$$A(u) = 5 \cdot 10^{-15} \times (2620u^3 + u^8), \tag{4.12}$$

and $a = 0.9$, $b = 0.1$ are constants.

Kumazawa (2014) proposed a hybrid scale (HS) model, combining two main analytical approximations for the resuspension factor K - power and exponential. Based on the statistical analysis of experimental observations reported by Maxwell and Anspaugh (2011), he proposed the dependence of K on time in the form of a non-linear equation

$$hyb\left[\nu\frac{(K-a)}{(b-K)}\right] = \alpha + \beta \cdot hyb\,(\tau t), \tag{4.13}$$

where $hyb\,(x) = x + \ln(x)$.

The parameters a and b are determined by the limiting values of the resuspension factor immediately after the fallout $t \to 0$ and in the remote period $t \to \infty$, respectively. In accordance with the available observational data, the limiting value of K equal to 1.5×10^{-10} m^{-1} was selected for the remote period. Since the available data of K for times t <10 d is a few, so the dependence of the upper limit b in the denominator of Eq. (4.13) can be neglected for the moderate constraint. The HS model with 5 parameters $\nu = -6.65 \times 10^4$, $a = 1.5 \times 10^{-10}$, $\alpha = -8.36$, $\beta = -1.40$, $\tau = 0.001$ was found to fit well to the data of K over the whole observation times.

4.2. Dependence of the resuspension factor on soil characteristics and meteorological parameters

Makhonko (1984) obtained an expression for the dependence of the resuspension factor on time after a single contamination of the earth's surface with radionuclides. As the main mechanism of decreasing the resuspension factor on time was assumed a natural radionuclide migration from the surface into the depth of soil, which leads to a decrease of its concentration in the surface dusting layer. Under the assumption of linear dependence of the radionuclide effective diffusion coefficient in the soil (which is met in the surface layer of 20-30 cm depth to a high degree of accuracy), Makhonko proposed an equation

$$K(t) = \frac{Ce^{-\lambda_R t}}{\rho_S \Gamma(1+\nu)(V_D t)^{1+\nu} l} \int_0^l x^\nu e^{-x/V_D t} dx, \qquad (4.14)$$

where t is the time, $\nu = V/V_D$ is the ratio of the linear convective velocity of the downward transfer of radionuclides to its diffusion velocity, λ_R is the radioactive decay constant, Γ is the gamma function, l is the thickness of the surface soil layer available for resuspension, C is the mass concentration of soil dust in the air, ρ_s is the density of the surface layer of soil.

In special cases $\nu = 0$ (heavy soils or lack of precipitation) and $\nu = 1$ (light soils, washing mode) the resuspension factor is expressed as:

$$K(t) = \frac{Ce^{-\lambda_R t}}{\rho_S l}\left(1 - e^{-l/V_D t}\right), \qquad \nu = 0, \qquad (4.15)$$

$$K(t) = \frac{Ce^{-\lambda_R t}}{\rho_S l}\left[1 - \left(1 + \frac{l}{V_D t}\right) e^{-l/V_D t}\right], \qquad \nu = 1. \qquad (4.16)$$

From Eqs. (4.15) and (4.16) it follows that for large values of the diffusion velocity ($V_D \geq V$) the dependence of $K(t)$ can be approximated by a simple exponential function of the form $k(t) = at^{-b}$ where $b = 1$ for $\nu = 0$ according to Eq. (4.15) and $b = 2$ for $\nu = 1$ according to Eq. (4.16).

In the case of a prolonged period of accumulation of radionuclides on the surface of the earth at a constant rate $D \sim t$ (deposition of radionuclides released from a source of constant intensity) Makhonko obtained a similar expression for the dependence of the re-suspension factor on time in the form

$$K(t) = \frac{C}{\rho_S \nu\, G(\nu) V_D^{1+\nu}\, lt} \int_0^t \frac{e^{-\lambda_R \theta}}{\theta^{1+\nu}} \int_0^l x^{\nu} e^{-x/V_D\theta} d\theta\, dx. \tag{4.17}$$

Magnoni (2012) proposed a similar model to relate a time dependency of a resuspension factor with parameters of radionuclide migration in soil. He obtained the general expression of the resuspension factor $K(t)$ in the form

$$K(t) = K_0 \frac{\left(1 + \frac{\nu l}{2D_S}\right) \cdot l}{2\sqrt{\pi D_S t}} e^{-\nu^2 t/4D_S}, \tag{4.18}$$

where D_s is the diffusion coefficient of radioactivity vertical migration in soil.

Basing on the comparison with available experimental data Magnoni concluded that his model fits better than the single exponential models. The model seems also to describe better a long-term behavior that, in this case, seems to be overestimated and underestimated, respectively, in the Garland (Eq. (4.6)) and Hatano (Eq. (4.10)) models.

Ishizuka et al. (2016) developed one-dimensional resuspension scheme that considers the particle-size distribution of the ground surface soil to estimate the size spectrum of atmospheric radioactivity associated with particles resuspended by the wind from flat, bare ground. The validation process was conducted with four different representative soil textures (soil fractions according to particle size ranges): sand, loamy sand, sandy loam, and silt loam. The particle-size distribution for each type of surface soil is expressed as the sum of three log-normal distribution functions with parameters taken from Shao (2008). The dust flux was calculated by the equation for free dust emission (see Eq. (8.95)) proposed by Loosmore and Hunt (2002).

The results were compared with observational data of continuously sampled radioactive aerosols at the Tsushima District school ground in Namie Town, Futaba County, Fukushima Prefecture, which was heavily contaminated by the Fukushima Daiichi NPP accident. The calculated results for sandy loam and silty loam were in good agreement with the observed concentrations of atmospheric radioactivity when friction velocity was assumed to be 0.4 m s^{-1}. The goodness of fit with the observational data depended on the amount of silt and illustrated the importance of taking into consideration the texture of surface soil in calculating the influence of secondary emissions of dust particles. Authors marked that this scheme can be applied to the regional atmospheric transport model for evaluation of the influence of secondary emissions from the ground and for the assessment of future risk for a wide area around the Fukushima Daiichi NPP. Additionally, the results of the work

explain the effect of enrichment of radioactive aerosol particles in the »mass loading» method (see Chapter 6) and underline the importance of the account of the granule-metric structure of the top soil layer under resuspension estimation.

An approach based on the use of the resuspension factor is mainly used to assess the time-averaged activity concentrations of radionuclides in the air. Accordingly, the resuspension factor values calculated by processing the observation data are obtained for different meteorological conditions, averaged over the measurement period. Experimental data on the effect of short-term changes in individual meteorological factors are scarce in the literature. As a result, virtually there are no models of the resuspension factor, which take into account the influence of meteorological factors on the resuspension.

In the HotSpot HealthPhysics Codes, or HotSpot program, which provides a first-order approximation of the radiation effects associated with the atmospheric release of radioactive materials (Homann and Aluzzi 2013), for wind speeds, more than 3 m/s the resuspension factor is adjusted as follows

$$K(U) = K \cdot (U/3)^2, \quad \text{for } U > 3 \text{ m/s}, \tag{4.19}$$

where K is determined according to one of 3 standard resuspension factor models Maxwell and Anspaugh (2011), NCRP (1999), and USAEC (1975). The increase in the resuspension factor with the intensification of the wind speed represents the strengthening effect of wind soil erosion (see Chapter 8.3).

Thus models, based on the use of the resuspension factor are a simple and convenient tool for rapid assessment of radioactive pollution as a result of secondary wind rise after the formation of the radioactive fallout field, including for the first assessments of inhalation intake of radioactive aerosols into the human body in the acute phase of a radiation accident. After the field formation, but before widespread measurements of the activity concentration in the air, this approach makes it possible to calculate the inhalation dose, which is particularly important when making decisions on countermeasures to protect the public.

The major source of uncertainty for all models is the choice of the initial conditions, i.e. the K_0 values. Because of it the uncertainty in the activity concentration estimation using this approach can reach one order or more. Significant differences in the K_0 value may be related to differences in physical and chemical properties of depositions, the properties of the underlying surface (soil type, type of vegetation, etc.), as well as climatic and meteorological characteristics of conditions of resuspension (season of the year, wind speed, precipitations, soil moisture). However, typically, the resuspension factor models don't take into account and don't use such detailed information. A partial solution of this problem is to carry out conservative estimates of the atmospheric activity concentration based on the maximum K_0 values, obtained in experiments and field observations. If obtained estimations of the activity concentration and the associated radiation

doses due to inhalation under the actual values of the deposition density do not exceed the established limits, so this approach makes it possible to conclude about the compliance of the radiation safety standards. However, if the values obtained conservatively are equal to or exceed the radiation standards, then it is difficult to make definite conclusions, and additional research is needed to clarify the K_0 values for the territory in question, taking into account its features. As a result, the main advantages of this approach –simplicity and efficiency — are lost.

According to all the most common models, the resuspension factor decreases rapidly during the first days and weeks after the deposition event. The contribution of the time-integrated activity concentration during the first week after deposition in the integrated activity concentration over 70 years is 32% according to the Maxwell-Anspaugh model and 10% by the Garland model, for the first month — 73% and 34%, and in the first year — 85 and 58%, respectively. So, the differences in the mathematical form of the expressions after the first year after the deposition are of minor importance. On the other hand, information about the time course of the resuspension factor can be used for reconstruction of the doses due to inhalation using the available data about its values during the late stage after the deposition.

Thus, to improve the predictive capabilities of empirical models of the resuspension factor, it is first necessary to find a better description of the model parameters in the initial period (during the first month) after deposition. Preventively (before the deposition) the resuspension model for the selected site can be adapted first of all by taking into account the influence of the underlying surface properties. In particular, it is expedient to parameterize the resuspension factor dependence on the soil properties, especially by considering the particle-size distribution of parent surface soil (soil texture).

CHAPTER 5

TEST OF EXISTING EMPIRICAL MODELS OF THE RESUSPENSION FACTOR AND ESTIMATION OF THEIR UNCERTAINTY

5.1. Introduction

Atmospheric resuspension of radionuclides can be a secondary source of contamination after a release has stopped, as well as a source of contamination for people and areas not exposed to the original release. This process is very complicated, and the acquisition of experimental data and improvements of their theoretical understandings are continuing. Models using the resuspension factor K approach (see Chapter 4) are the most applicable for practical purposes, including estimations of human exposure doses due to radionuclides resuspension. The resuspension factor is useful in localized situations for characterizing the relationship between surface and airborne contamination; however, its use implies equilibrium between the resuspended and deposited aerosol. In practice, the contamination on the surface is not homogenous and the airborne activity concentration is a sum of the local resuspended contamination and the contamination advected from upwind sources of resuspension (Smith, Whicker and Meyer 1982).

The present chapter focuses particularly on testing the widely applied models for K based on data obtained in the vicinity of the Chernobyl NPP, estimating the uncertainty of the resuspension factor using common physical reasoning and experimental data obtained inside and outside the 30-km Chernobyl exclusion zone, and estimating the limits of their applications.

For these reasons, the resuspension scenario (Garger et al. 1996) was developed within BIOMOVS II. BIOMOVS (BIOspheric Model Validation Study) was an international cooperative study to test models designed to quantify the transfer and bioaccumulation of radionuclides and other trace substances in the environment. The objective of the scenario was

to test existing mathematical models of contaminant resuspension. This scenario offered a unique opportunity to examine data and test models for atmospheric resuspension of radionuclides, to understand resuspension processes on both local and regional scales, and to investigate the importance of seasonal variations of these processes. The results of the models were compared with the measurements to investigate and explain the discrepancies among model predictions and between model predictions and observations and thus to evaluate the predictive capabilities and drawbacks of commonly used generic resuspension models.

This specifics scenario examined three sets of circumstances in which different levels of inhalation exposure from resuspended contamination could occur. The first situation involved the city of Kyiv, located approximately 120 km southeast of the Chernobyl nuclear power station and inhabited by approximately 3 million residents. The contamination at Kyiv was significantly lower than at the other locations studied and, due to the distance from the source, relatively homogeneous. Vehicular traffic is believed to be the dominant mechanism for the resuspension of contaminants in this region (see detailed data in (Garger et al. 1996)).

The second situation covered the agricultural district and settlement of Polesskoe (population about 14,000), located 40-60 km west of the Chernobyl power plant. The contamination in this area was quite heterogeneous, and exposures in this district were influenced both by resuspension of locally deposited radioactive materials and by the advection of material from upwind sources, e.g. the heavily contaminated 30-km zone and large highly radioactive deposits («hot spots») within the Polesskiy district (Kyiv region) in particular (Garger et al. 1996). The settlement of Polesskoe is situated between the western, southern and northeastern hot spots with contamination densities of 0.2 to 3.7 MBq m^{-2}. About 25-30% of the district is forested; the remainder includes agricultural areas, settlements, villages, and roads.

The third situation represented an intermediate case and involved data for two locations (Pripyat and Zapolie) within the highly contaminated 30-km zone, where exposures to resuspended material were probably dominated by local processes. Decontamination activities took place through 1989, after which essentially no traffic existed in these areas. The modelers were provided with measured activity concentrations of various contaminants in the summer of 1986 in Pripyat, Zapolie, and other locations within the 30-km zone. The measured densities of ^{137}Cs contamination in the soil were 5.22 and 0.35 MBq m^{-2} at Pripyat and Zapolie, respectively. A contour map representing the activity concentration of ^{137}Cs on the soil surface during the summer of 1990 was also provided (Garger et al. 1996).

Participants in the test exercise were provided with detailed information on air sampling and measurements, regional climatology (wind speeds and directions, air temperatures, precipitation, dust storms, snow cover), and levels of surface contamination at the test sites (Garger et al. 1996, BIOMOVS II 1996). Par-

ticipants were requested to make the following endpoint predictions at Pripyat, Kyiv, and Polesskoe:

• Monthly average air activity concentrations of ^{137}Cs due to resuspension for January, April, August, and October, beginning in 1987 and continuing through 1992; and

• Annual average air activity concentrations of ^{137}Cs due to resuspension for each year from 1987 through 1992.

For Zapolie, the modelers were requested to estimate the annual average resuspension factor (m^{-1}) for 1986 and for 1992. For Kyiv, the modelers were also requested to estimate the resuspension factors for ^{137}Cs, ^{90}Sr, and $^{239+240}$Pu in December 1991. A full description of the scenario, the modeling results, and the field data is given in (BIOMOVS II 1996).

5.2. Participating modelers

Fifteen modelers took part in this test exercise: C. Miller and S. Nair from the US, D. Galeriu from Romania, M. Talerko and T. Lev from Ukraine, A. Kryshev from Moscow State University in Russia; and 9 students from the Institute of Atomic Power Engineering (Department of Ecology), Obninsk, Russia. The students from Obninsk included A. Abramenkov, I. Antoshkina, S. Galata, D. Kondratyuk, L. Malyutyak, L. Mokrova, L. Priymak, Y. Romanova, T. Semenova, and O. Skorkina.

5.3. Types of models used

In general, the participants used classic empirical models (e.g., Anspaugh et al. 1975; Linsley 1978; Garland 1982; Makhonko 1992; Garland, Pattenden and Playford 1992) or modifications or these models. The analyses show that nine distinct models or adaptations were used for the calculation of the airborne activity concentrations. These models differed primarily in the empirical parameterizations used for the resuspension factor or the resuspension rate as described below. Detailed model descriptions are provided in the BIOMOVS II final report (BIOMOVS II 1996). A summary of the models used in the test exercise is provided below.

Most of the models were based on the following expression for the calculation of the airborne radionuclide activity concentration:

$$c(t) = K(t) \cdot D(0), \tag{5.1}$$

where c is the activity concentration of the radionuclide in the air (Bq m^{-3}); K is the resuspension factor (m^{-1}), calculated with the help of different models of $K(t)$; and D is the density of the radionuclide in the soil (Bq m^{-2}) at time $t = 0$. Lev and Talerko calculated $C(t)$ using the resuspension rate and the density of contamina-

tion. Nair calculated the decrease of soil density with time by

$$D(t) = D(0)\exp[-(\lambda_R + k)t], \tag{5.2}$$

where λ_R is the radioactive decay constant of the radionuclide (d^{-1}); and k is the first-order rate constant accounting for loss processes (d^{-1}), calibrated for the site (Nair et al. 1997).

The approach using Eq. (5.1) is based on the assumption of spatially homogeneous contamination and an equilibrium situation with long term stability. However, a value for this time was not defined by any of the modelers except Galeriu. Modelers who used an exponential approach included Nair, Miller, Mokrova, Antoshkina, Galata, Abramenkov, Skorkina, Priymak, Malyutyak, Kondratyuk and Romanova.

Mokrova and Antoshkina used a model from (Anspaugh et al. 1975) (see Eq. (4.2)) but with a value of 10^{-6} instead of 10^{-4} for the initial resuspension factor K_0. Galata used a model from (Linsley 1978) (Table 4.1). Abramenkov used Linsley's model with different values for the half-time λ and the initial resuspension factor K_0 (Table 4.1).

Miller and Galeriu each used the one exponential model Eq. (4.1). Galeriu used point estimates for $K_0 = 10^{-8}$ m^{-1} and $\lambda = 3 \times 10^{-3}$ d^{-1}, while Miller used a log-uniform distribution of K_0 (3.6×10^{-9} to 4.9×10^{-8} m^{-1}) and a uniform distribution of λ (8.7×10^{-4} to 4.1×10^{-3} d^{-1}).

The assumption of equilibrium conditions also holds for other models that have an exponential form, e.g. the NRPB/CEA model (Table 4.2). This equation was used by Priymak, Malyutyak, Kondratyuk, and Romanova.

Semenova used the Garland formula (Eq. (4.6)) for K as an inverse function of time. Nair also used this dependence on time for the first 1,000 days and set $K(t) = 10^{-9}$ m^{-1} for $t >$ 1,000 days.

Kryshev built an approximation for K as a superposition of an exponential and a power function (Eq. (4.11)), and the initial value of the resuspension factor is a function of the wind velocity (Eq. (4.12)).

Galeriu tried to take into account both local processes and an advection process:

$$c = C_{local} + C_{adv}, \tag{5.3}$$

where C_{local} is calculated by Eq. (4.1) and C_{adv} is represented by a standard Gaussian model for the virtual point source, for a square area source of 1,000 m × 1,000 m:

$$C_{adv}(x, y, z = 0) = \frac{Q\exp\left(-\frac{y^2}{2\sigma_{y^2}}\right)}{\pi\sigma_y\sigma_z U} \tag{5.4}$$

where x and y are the coordinates of a receptor relative to the center of the source, σ_y and σ_z are the horizontal and vertical dispersions of the pollutant particle coordinates accordingly.

Lev and Talerko made calculations only for Polesskoye; they had available to them more detailed information on the contamination of the area and the character of the underlying surface than was available to the other participants. Lev and Talerko made calculations using Eq. (5.4) for a large area around the receptor, taking into account the whole set of climatological information about wind speed and direction from distances of about 16 km to the receptor. The calculations used a variable step (1,000-100 m) that allowed them to use their detailed data.

The source intensity Q in Eq. (5.4) is a product of the contamination density, an area source and the resuspension rate Λ (s^{-1}).

Galeriu, Kryshev, and Lev and Talerko used the resuspension rate in their calculations for the heterogeneously contaminated Polesskiy district. Galeriu and Kryshev calculated the resuspension rate from the general equation

$$\Lambda = Kv_d, \tag{5.5}$$

where v_d is the dry deposition velocity. Galeriu used a value of 4.3 cm s^{-1} for v_d based on the surface roughness height z_0=0.05 m and the annual average wind speed U_{10}=4.0 m s^{-1}. Kryshev used a literature value of 2 cm s^{-1} for v_d.

Lev and Talerko used the mean value of the resuspension rate Λ from (Makhonko 1992) to calculate the source intensity from Eq. (5.4). From measurements of the ^{137}Cs airborne activity concentrations taken from 1987 to 1992 by the State Hydrometeorological Committee, they obtained the averaged curve of the monthly concentrations reflecting the seasonal change of the concentration. Lev and Talerko assumed that the monthly average resuspension rates have the same temporal course, which they represented by a fourth-order polynomial for the Polesskiy district.

5.4. Comparison of model predictions with empirical data

The validation of a model must take into account the specific application of the model: namely, the evaluation of a model must consider the intended purpose and the time and spatial scales for which it was developed. As this scenario is concerned with a temporal process, models must have a satisfactory definition of the time characteristics considered.

5.4.1. Annual data

When model predictions are compared with empirical data, the question arises about the correspondence of the external conditions and the time averaging of the calculated and experimentally estimated values of K. All of the models except for the model of Makhonko/Garland/Kryshev are idealized, in that they assume homogeneity of external area conditions (soil, contamination, character of the underlying surface) and stationary meteorological conditions for the

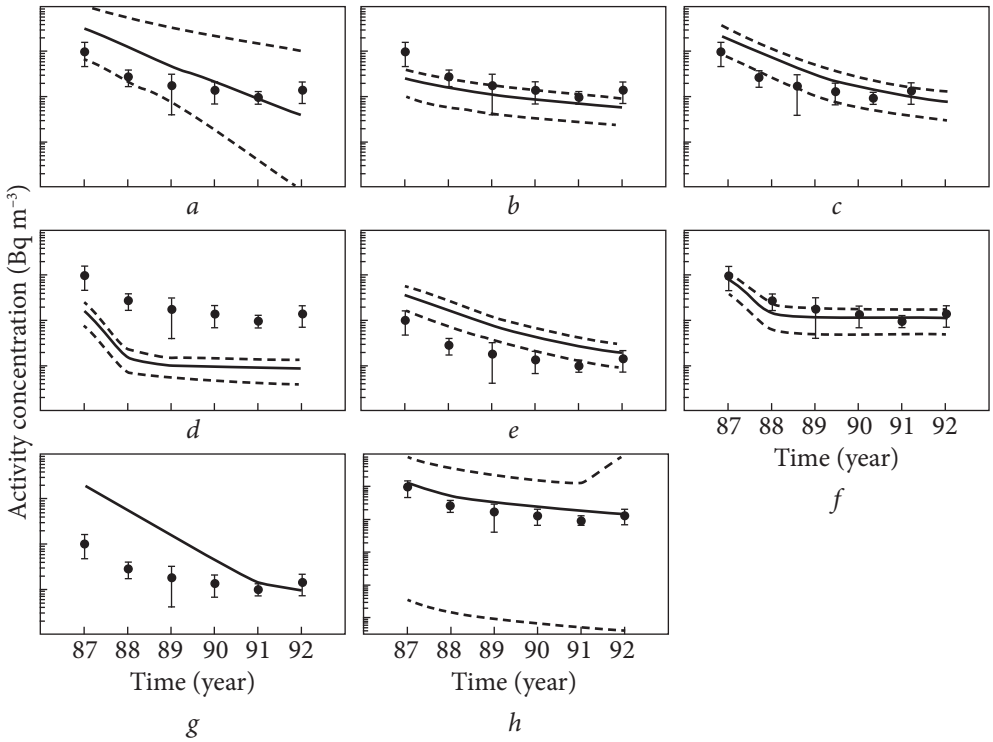

Fig. 5.1. Comparison of selected model predictions (solid line) with observations (dark circles) for annual average air activity concentrations of ^{137}Cs in Kyiv (homogeneous conditions, with stabilization occurring after about 2 years): *a* — IAEA/Miller, *b* — Garland/Semenova, *c* — Makhonko/Garland/Kryshev, *d* — NRPB/CEA/Malyutyak, *e* — Anspaugh/Antoshkina, *f* — Linsley/Galata, *g* — Galeriu, *h* — Nair. The dashed lines represent 95% subjective confidence intervals on the model predictions. The vertical lines represent the 95% confidence intervals about the observations

measuring period. Therefore, it was decided to use empirical data averaged over the whole year rather than averaged for the month. The comparison of the annual data is presented in three parts according to the sites of the measurements.

5.4.1.1. Kyiv (homogeneous case). A comparison of model predictions with the annual average data is provided in Fig. 5.1 for selected examples of the general models (IAEA-Miller, NRPB/CEA, Anspaugh, Garland-Linsley, Makhonko/Garland/Kryshev). The full set of comparisons is provided in the summary report BIOMOVS II (BIOMOVS II 1996). The empirical data are represented by points with the standard deviations indicated. The main peculiarity of the temporal course of the Kyiv data is the existence of two temporal regimes: the first when the derivative of the airborne activity concentration $\frac{dc(t)}{dt}$ in the period of 1987—1988 is large, and the second when the derivative is near zero, within the confidence intervals

of the measurements (for example, see Galata-Linsley in Fig. 5.1). In other words, for quasi-homogeneous conditions such as the large city of Kyiv, the models that take into account the stabilization of a situation after two to three years are valid in practice if the parameters have been selected correctly (see, for example, the original Linsley model in Fig. 5.1, which has the best fit to the observations).

If we selected the NRPB/CEA model as interpreted by Malyutyak (Fig. 5.1), we again have two regimes for the decrease in the air activity concentrations, but the discrepancy between calculations and observations is larger than the confidence intervals of both the measurements and the calculations, implying that the parameter values for that model were not selected appropriately. The models that use the inverse relation between $K(t)$ and time describe this situation satisfactorily (e.g., the calculations by Nair, Semenova, and Kryshev in Fig. 5.1).

Miller's calculations using the model from (Garland, Pattenden, Playford 1992) agree with the observed data within the levels of the calculation errors. However, it is clear from Fig. 5.1 that the simple exponential model does not describe the real process of the decrease of the resuspension factor for this large city with its extensive traffic. Galeriu used the same IAEA model; in this case, the differences between predictions and observations are very significant (Fig. 5.1). The author noted some difficulty in the accurate estimation of K_0; however, the general discrepancy is the difference in the rate of decrease in the resuspension process in the large city.

Of the eight models presented in Fig. 5.1, two show underpredictions and five show overpredictions. For estimating the inhalation dose, the first period after the accident is very important. When the predicted and empirical annual average activity concentrations were compared for 1987 and 1992, the majority of the models were found to give conservative values (overestimates) of the annual airborne concentrations for 1987 and underestimates of the airborne concentrations for 1992. This underestimation may reach a factor of 2 to 3, which is significant given the approximately three million residents in Kyiv.

5.4.1.2. Pripyat (intermediate case). In contrast to Kyiv, stabilization of the resuspension process in Pripyat began about one year later, with the major decontamination work in the 30-km zone being finished in 1990. Predicted and observed annual average activity concentrations of ^{137}Cs in Pripyat are compared in Fig. 5.2 for the same selected set of models.

Of eight predictions, five are overestimated, one shows good agreement (NRPB/CEA model with parameter values selected by Malyutyak), and two show agreement within the confidence intervals (Kryshev and Nair). The largest overestimate (two orders of magnitude) was by Antoshkina, who used the Anspaugh model with the original resuspension factor. That model was developed for a desert area and does not suit the damp climate of central Europe. The Linsley model (Galata), which was elaborated for the damp climate of Great Britain, provided the best fit for Kyiv but not for the uninhabited city of Pripyat. This model as-

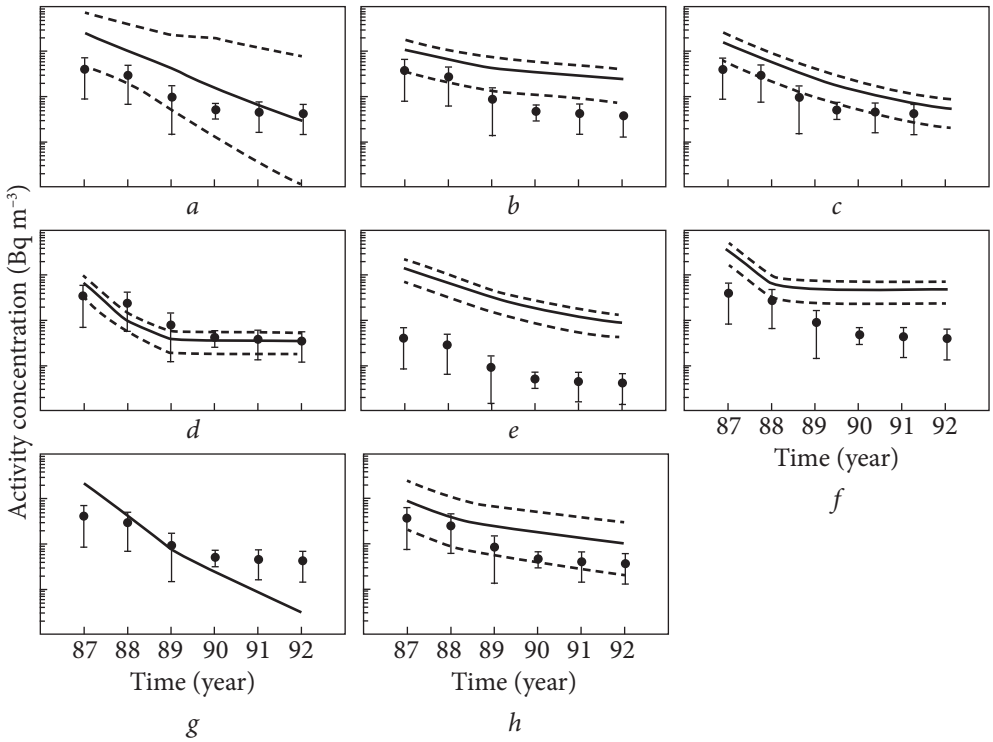

Fig. 5.2. Comparison of selected model predictions (solid line) with observations (dark circles) for annual average air activity concentrations of ^{137}Cs in Pripyat (homogeneous conditions, with stabilization occurring after about 3 1/2 years): *a* — IAEA/Miller, *b* — Garland/Semenova, *c* — Makhonko/Garland/Kryshev, *d* — NRPB/CEA/Malyutyak, *e* — Anspaugh/Antoshkina, *f* — Linsley/Galata, *g* — Galeriu, *h* — Nair. The dashed lines represent 95% subjective confidence intervals on the model predictions. The vertical lines represent the 95% confidence intervals about the observations

sumes that the stabilization period lasts two years, while in Pripyat this period was approximately 3.5 years because decontamination work in the 30-km zone continued until 1989.

5.4.1.3. Polesskoe (heterogeneous case). Comparisons of predicted and observed air activity concentrations in Polesskoe are provided for the same selected set of models as before, plus the results of the Lev/Talerko predictions (Fig. 5.3). Significant differences are observed for four models. The best fit was by the NRPB/CEA model (Malyutyak), and the worst fits were by the Anspaugh model (Antoshkina) and Galeriu's model.

Galeriu, Kryshev, Lev, and Talerko tried to take into account the effect of advection from the hot spots around the settlement of Polesskoe by using various solutions of the diffusion equation. For the estimation of the resuspension rate, Galeriu and Kryshev used equation $\Lambda = Kv_d$, where v_d is values of the deposition velocity taken

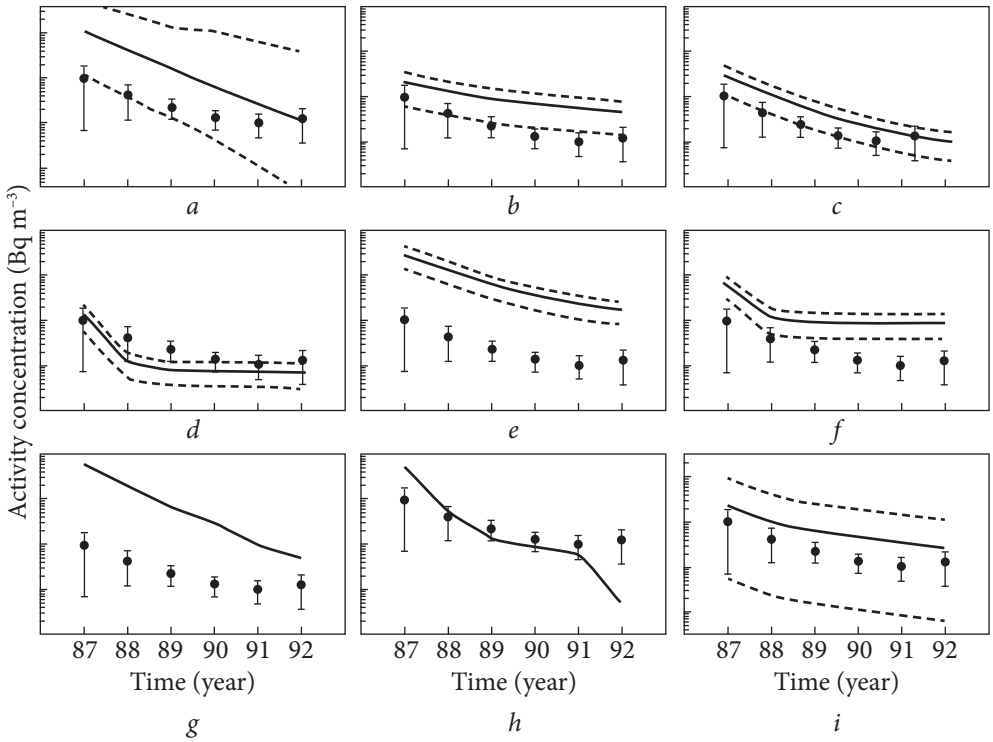

Fig. 5.3. Comparison of selected model predictions (solid line) with observations (dark circles) for annual average air activity concentrations of ^{137}Cs in Polesskoe (heterogeneous conditions): *a* — IAEA/Miller, *b* — Garland/Semenova, *c* — Makhonko/Garland/Kryshev, *d* — NRPB/CEA/Malyutyak, *e* — Anspaugh/Antoshkina, *f* — Linsley/Galata, *g* — Galeriu, *h* — Lev/Talerko, *i* — Nair. The dashed lines represent 95% subjective confidence intervals on the model predictions. The vertical lines represent the 95% confidence intervals about the observations

from the literature. The resuspension factor was calculated accordingly using formulas for $K(t)$, with climatic data about the wind velocity taken into account by the Makhonko formula (Kryshev) or the simple expression of the IAEA model (Galeriu).

Galeriu used a very conservative approach for the selection of the density of the contamination around the Polesskoe area and increased the resuspension factor by a factor of 3 to account for the traffic. This approach is very subjective. Kryshev`s calculation is preferable in that it is more objective.

Lev and Talerko used *a priori* information about the resuspension rate from the literature, together with a fourth-order polynomial. Good agreement of the predictive and empirical data is observed for the period 1989 to 1991 (Fig. 5.3). For the first and last years, however, there are differences that exceed the confidence intervals. The NRPB/CEA and Makhonko/Garland/Kryshev models performed best for rural territories and may be recommended for use in practice.

5.4.2. Monthly data

Predictions by the general eight models for the monthly average airborne activity concentrations (for January, April, August, and October) of ^{137}Cs in Kyiv are compared with the observations (Garger et al. 1999). The values of the winter minimum airborne activity concentrations of ^{137}Cs are not greatly different than summer values. This fact reflects that for the big city, winter differences are less important due to the presence of traffic. Models that predicted a stabilization period agree better with observations than models that did not. The differences in this case ranged over 4 to 5 orders of magnitude. The Linsley model (Galata) showed the best agreement of all models. The models using an inverse dependence between $K(t)$ and time (Garland, Makhonko/Garland/Kryshev) may be used in practice.

For Pripyat, the monthly values of the airborne activity concentrations give the same picture as the annual data. Greater distinctions are evident for seasonal variations than in Kyiv. The best agreement is seen for the NRPB/CEA model (Malyutyak). With the Nair predictions for Pripyat, one can see the same character as for Kyiv for the winter months, although Pripyat is a dead city with no traffic. Perhaps there are other sources of radioactivity in winter in that area. The radioactive aerosol may come from the large, very highly contaminated (almost ten times higher) forest and roads around the ChNPP.

For Polesskoe, the best agreement was observed for the Makhonko/Garland/Kryshev model, although it showed significant differences for the first period of the comparison. All models overpredicted, except for the NRPB/CEA model (Malyutyak), which underestimated for the later periods. This results from an underestimation of the influence of the very highly contaminated forest area surrounding the settlement Polesskoe on three sides. The Lev/Talerko data, based on detailed characteristics of this district, gave good agreement only from January 1988 to January 1992. Before and after that period their results diverge from the empirical data.

5.4.3. SIngle period of measurements in Kyiv and Zapolie

In December 1991, the air activity concentrations of ^{137}Cs, ^{90}Sr, and $^{239+240}$Pu were measured over 3-day periods at six locations in Kyiv, five in typical urban squares near pedestrian and vehicular traffic and one in an urban park location (~300 m from the avenue). Predicted values for the resuspension factor in Kyiv at this time point are compared to the observed resuspension factors for the radionuclides (Fig. 5.4). Within the limits of errors, the empirical values of the resuspension factors for the three nuclides are the same. For this episodic measurement period, the best agreements were by the modified Anspaugh model (Antoshkina) and Nair`s model. The results of Miller, Makhonko/Garland/Kryshev and NRPB/CEA models have the biggest distinctions, in that their models did not take into account the stabilization situation in Kyiv. This

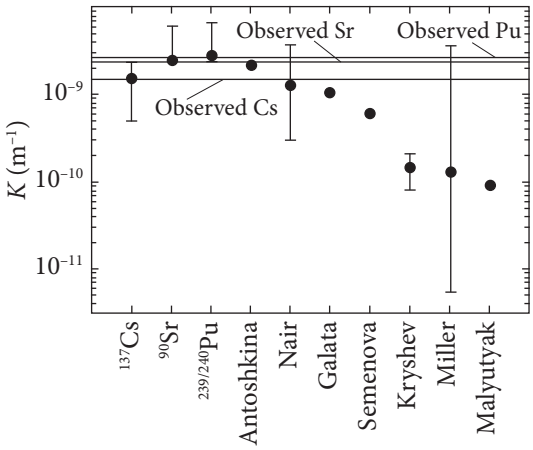

Fig. 5.4. Comparison of selected model predictions (dark circles labeled with name of participant) with observations (horizontal lines, dark circles labeled with radionuclide) for resuspension factor *K* in Kyiv in December 1991. The vertical lines represent 95% confidence intervals on the predictions or observations. For ^{90}Sr and $^{239+240}$Pu, the lower 95% confidence limit was 0

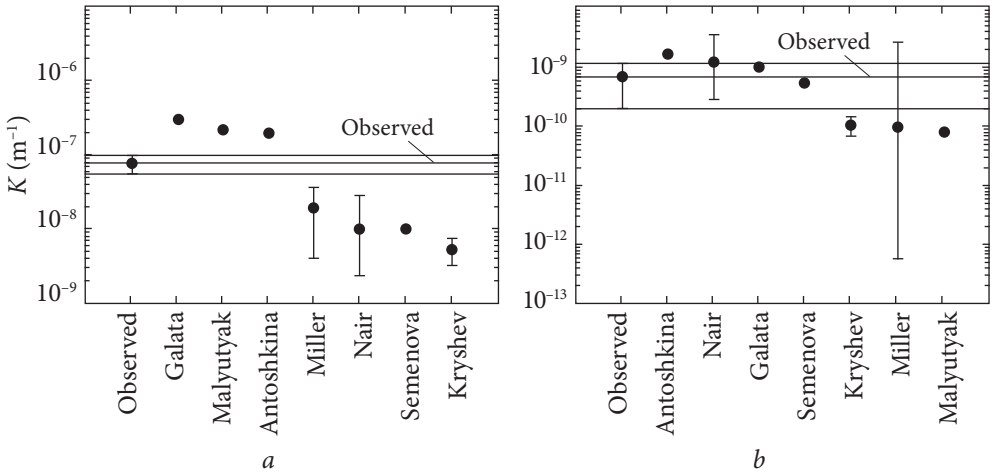

Fig. 5.5. Comparison of selected model predictions with observations for the resuspension factor K in Zapolie in 1986 (*a*) and 1992 (*b*). The vertical lines represent 95% confidence intervals on the predictions or observations

means that calculations by these models will give an underestimate of the collective inhalation dose for the residents of Kyiv.

The Zapolie data enable the comparison of the calculated resuspension factor with the empirical value for 1986, after the Chernobyl accident. It can be seen that the Linsley model (Galata), NRPB/CEA (Malyutyak), and the modified Anspaugh (Antoshkina) models are more conservative; they overestimated the empirical value by a factor of 2 to 3 (Fig. 5.5). The Miller, Nair, Garland (Semenova) and Makhonko/Garland/Kryshev models underestimated the resuspension factor by factors of 4 to 16. For 1992, all predictions were better, and the maximum differences were less than one order of magnitude.

5.5. Discussion

Simple exponential models for resuspension can provide good predictions of the annual air activity concentrations only for homogeneous conditions. If there is a heterogeneous situation as in the Polesskiy district, one can see discrepancies of more than one order of magnitude. The development of more complicated models that can account for heterogeneous conditions is important. Accounting for snow cover in winter gave worse predictions for seasonal values because it did not allow for the existence of sources of radioactive aerosols in winter. The nature of these sources is not clear and requires additional investigation.

5.6. Additional data for the testing the resuspension factor models

Additional post-Chernobyl data for the testing of models for K was presented by (Garger et al. 1995), who described data from the stationary air samplers operated at Chernobyl and Baryshevka (cities that are 16 km and 150 km, respectively, from the Chernobyl nuclear power plant) and provided a comparison of models for K with experimental data obtained in different points of the 30-km zone in 1986.

The model values of K assume homogeneity of external conditions (soil contamination, the character of the underlying surface) and stable average meteorological conditions for the measuring period. It is known that averaging for a large period considerably smoothes small-scale fluctuations of the different nature, therefore empirical data averaged for a year better correspond to above noted conditions. The annual means of the resuspension factor, determined experimentally and calculated by models, are shown in Table 5.1 (Garger, Hoffman and Thiessen 1997).

Table 5.1 also presents the lower and upper limits of K from 1986 to 1991 and the ratio of the calculated values of K to the experimental values. The model of Hoetzl et al. (1992) agrees best with the data. This model was derived from empirical data measured in Munich, Germany, after the Chernobyl accident.

The model of Garland, Pattenden and Playford (1992) agrees well, but this model systematically underpredicted the experimental values. The calculated values of K from the Linsley model (Linsley 1978) are very conservative for the first two years and much closer to the observations for later years. If the calculated values are compared with the upper limits of the measured values, the predictions of the models by Garland and Hoetzl are lower than the upper limits of K by a factor of two to three. It is important to note that the lower and upper limits are obtained on the monthly mean resuspension factors.

The high range of the resuspension factors is due to different underlying surface, soil, and effects of anthropogenic actions in the 30-km zone. Anthro-

pogenic activities were especially important for places which were situated near the NPP or main roads. For specific locations, however, the K values may be higher than estimated by the models of Garland and Hoetzl by two to three orders of magnitude.

The models for K were compared with experimental monthly data and with each other in the form of the normalized resuspension factor $K(t)/K_0$ as a function of time (Fig. 5.6). The Chernobyl and Baryshevka data are shown, along with five equations and a new equation derived from the experimental data $K(t)/K_0 = t^{-1.4}$. This equation was selected after a study of the value of the power function for the entire time series of measurements at Chernobyl (Fig. 5.7). It provides the best fit to the experimental data and shows that the process of stabilization is going more rapidly, with stabilization of the experiment occurring near 1,200 d. The processes of migration in the soil are probably appreciable by this time. Presentation of the model predictions as $K(t)$ normalized for K_0 enables comparison of the dependence of K on time without the effect of differences in the initial value of K. The value K_0 is dependent on a substantial amount of subjective estimation.

The similar character of the inverse curves with powers from 1.0 to 1.4 is easily seen (Fig. 5.6). The results of Linsley (1978) and Anspaugh et al. (1975) models exceed the experimental data in the first 1,000 days by two to three orders of magnitude. The curve by Makhonko (1992), developed for long-term resuspension after the deposition of radionuclides from the stratosphere for stationary atmospheric conditions in the midland of Russia, describes the resuspension factor

Table 5.1. **Annual mean resuspension factors K for ^{137}Cs measured at Chernobyl city in 1986 (after 20 May 1986) and in 1987—1991, compared with model calculations** [a]

Year	Lower limit of K $\times 10^{-7}$ (m^{-1})	Mean value of K $\times 10^{-7}$ (m^{-1})	Upper limit of K $\times 10^{-7}$ (m^{-1})	K_{Gar} $\times 10^{-7}$ (m^{-1})	K_{Hoet} $\times 10^{-7}$ (m^{-1})	K_{Lin} $\times 10^{-7}$ (m^{-1})	$\frac{K_{Gar}}{K_{exp}}$	$\frac{K_{Hoet}}{K_{exp}}$	$\frac{K_{Lin}}{K_{exp}}$
1986	0.053	0.330	0.830	0.270	0.510	3.90	0.82	1.54	11.8
1987	0.013	0.082	0.170	0.030	0.042	0.27	0.36	0.51	3.30
1988	0.004	0.032	0.070	0.014	0.021	0.016	0.44	0.66	0.50
1989	0.002	0.014	0.034	0.010	0.014	0.010	0.71	1.00	0.71
1990	0.0008	0.006	0.015	0.008	0.010	0.010	1.33	1.66	1.66
1991	0.001	0.008	0.018	0.006	0.008	0.010	0.75	1.00	1.25

Note: K_{Gar} — calculated according to the model (Garland, Pattenden and Playford 1992); K_{Hoet} — calculated according to the model (Hoetzl, Rosner and Wincler 1992); K_{Lin} — calculated according to the Linsley model (Linsley 1978); K_{exp} — derived from experimental measurements.

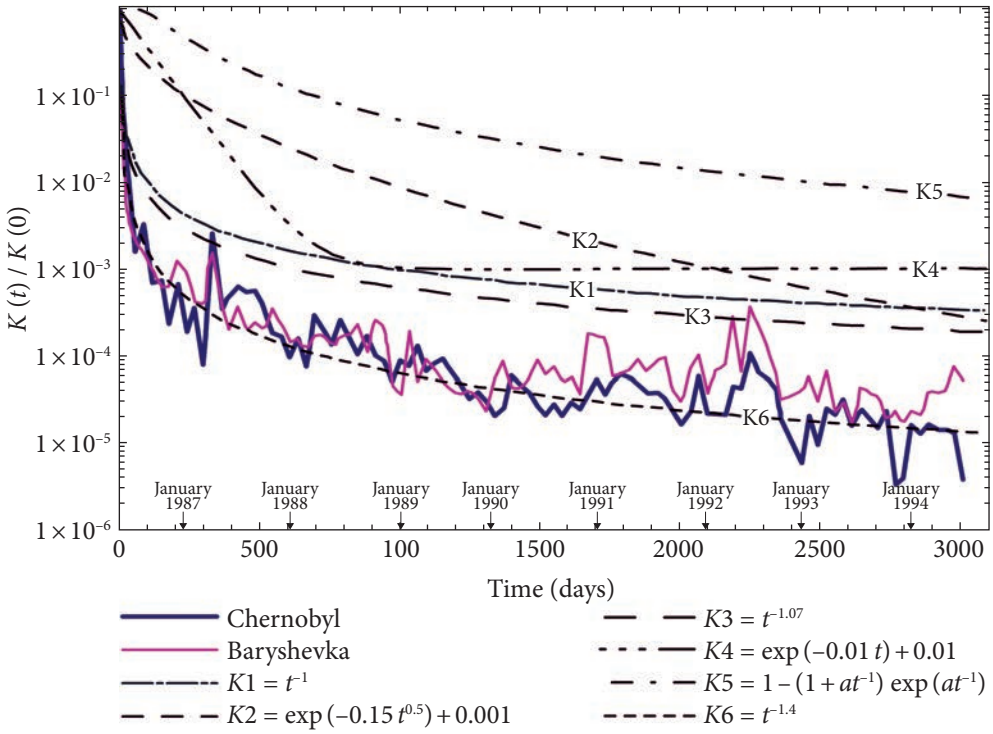

Fig. 5.6. Comparison of observed and predicted resuspension factors over time, normalized for the initial resuspension factor K_0. *K*1, model of Garland; *K*2, model of Anspaugh; *K*3, model of Hoetzl; *K*4, model of Linsley; *K*5, model of Makhonko; *K*6, empirical dependence described in this Chapter. For all equations, *t* is the time in days

controlled by the process of soil migration (Makhonko 1984): it differs sharply in value from the other curves in Fig. 5.6. In spite of the inverse dependence with a predicted power near 1.1 (Hall and Reed 1989), the decrease of the resuspension («the decrease in the power of the spring and capacity of the well») is more rapid than predicted. This is explained by the downward migration processes of radiocesium initially deposited on the soil surface.

Certainly, the material presented in this Chapter does not exhaust all possible models and approaches. The data presented are concentrated on the estimation of *K* by models that are widely used in practice, all of which are empirical models. This is a reflection of the low level of our knowledge about the resuspension process. Thus, it is important to validate these models against real observations data obtained after the Chernobyl accident.

Most of the modelers used the assumption that the relative decrease of the resuspension factor $\left(\frac{1}{K}\cdot\frac{dK}{dt}\right)$ has a constant value that defines the exponential time-dependence of *K*. The real process is more complicated, and this has led to

the use of several exponents (for instance, the formula of NRPB/CEA) with new temporal scales, but without a full comprehension of what physical processes the equations represent. Several modelers used an inverse empirical time-dependence for K; this requires selection or fitting of only one parameter, K_0, and does not agree badly for the long-term period. However, the selection of the initial value of the resuspension factor is currently subjective, rather than being based on physical or geographical considerations. This uncertainty, which applies for all the models presented here, can vary by two orders of magnitude.

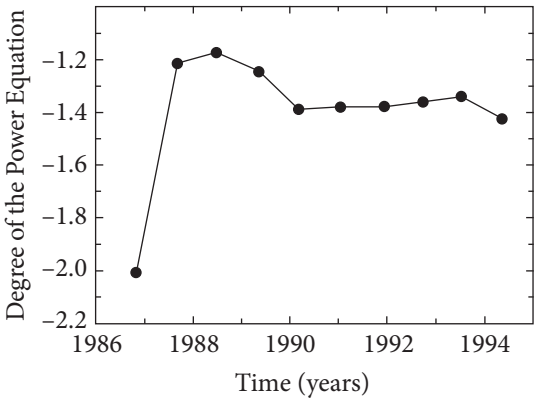

Fig. 5.7. Estimated values of the degree a in the power function $K(t)/K_0 = t^{-a}$, based on measurements of K made in Chernobyl

The second important source of uncertainty is the rate of decrease of K over time. The time-scales in the models used may vary by two to three orders of magnitude, and the background term may cause errors in the estimates of K long after the initial starting point. To avoid the problems associated with the estimation of K, the approaches using the resuspension rate and transport model could be extended to describe heterogeneous situations when there are highly contaminated spots in the neighborhood of settlements.

5.7. Limits of model applications

There are several limitations to the application of the empirical models described here:

(1) The use of one of these models for a new situation can lead to significant errors (up to 3 to 4 orders of magnitude) if the modeler does not have *a priori* information about the resuspension process in the new conditions.

(2) These models do not account for the fact that the real processes have both a deterministic and a stochastic component, nor do the models give a basis for the selection of the averaging time for comparison or for understanding the time limits of use and application of the models in practice.

(3) The generic models do not account for seasonal aspects of meteorological conditions.

These considerations put definite limitations on the application of K in practice and demand a new elaboration on a more physical basis. This does not mean that the validation of the models presented here is not needed. On the contrary,

this type of exercise is necessary to better understand our present capabilities and make use of this understanding in future applications.

Thus, the resuspension factor could be used as one of the key parameters necessary for the calculation of the inhalation dose to humans; therefore, accurate estimation is necessary to perform reliable post-accident evaluations of health risk. Uncertainty in K may reach 2-3 orders of magnitude if the definition of K as a function of its controlling variables is disregarded. The value of K averaged over large regions may differ from calculated values by more than one order of magnitude; however, uncertainties in the estimates of K are decreased to within one order of magnitude if annual averaging of the experimental data is used and K is determined as a function of time and predominant regional conditions of vegetative cover and climate.

A comparison of empirical data for long-term K factors with model estimates shows that models based on the inverse power function best reflect reality. These models have a clearer physical basis for territories with damp climates and moderate conditions of wind. Continued progress in this area is expected, based on new experimental and theoretical data.

CHAPTER 6

MASS LOADING

6.1. General information

Anspaugh and Phelps (1974), Anspaugh et al. (1975) noted that observations of many authors (Beck 1966, Krey and Hardy 1970) showed that radionuclides deposited on the earth's surface in the form of a solution or in the particulate form penetrate to depths more than 10 mm within a few months. Its distribution implies that a close bond with a host soil is formed quickly. Therefore, a method of predicting the average airborne radioactivity concentration c (Bq m^{-3}) over a contaminated area due to resuspension of soils several years after the contamination event is to simply multiply the measured activity of the contaminant per unit weight of soil C_s (Bq g^{-1}) taken from the top soil layer by the concentration of particulate matter in the atmosphere, i.e. the average mass loading of the atmosphere M (g m^{-3})

$$c = MC_S. \tag{6.1}$$

The use of this value avoids the need to decide what depth of soil to include in the resuspension calculation (Garland, Pattenden and Playford 1992)).

Authors bring several experimental results are available to check the accuracy of this simple prediction method (Anspaugh and Phelps 1974, Gudiksen et al. 1972, Hamilton 1970) which presented in Table 6.1. The predicted values were calculated by multiplying the average values of the soil concentration by an assumed mass loading of 100 μg m^{-3}. Measured values of the air activity concentration are averages of many individual measurements (Anspaugh and Phelps 1974, Anspaugh et al. 1975, Beck 1966, Gudiksen et al. 1972, Silver et al. 1974, Hamilton 1970). As authors noted an agreement between the predicted values is generally good.

According to Smith, Whicker and Meyer (1982) the mass loading approach is perhaps the simplest method of estimating airborne radioactivity originating from the radioactive contamination of surface soil. It was proposed originally as an estimator of the resuspension of fallout particles from nuclear weapons testing. Assuming continual entrainment and depletion of particles in the airstream, the dust loading of the air at a given point is indicative of the gross balance between the two processes. The airborne dust is assumed to originate from the suspendable fraction of the upwind surface soil. The radioactivity associated with the suspendable fraction of the surface soil C_s must be measured.

Measurements of the atmospheric dust loading M are commonly time-averaged. They may be averaged over space as well and may provide particle-size distribution information. When particle-size data are available for both the dust loading and the radioactivity in suspendable soil, Eq. 6.1 may be rewritten as

$$c = \sum_{i=1}^{n} c_i = \sum_{i=1}^{n} M_i C_{si}, \tag{6.2}$$

where the subscript i represents the n particle-size classes.

Two important assumptions underlie this formulation. First, the requirement that the contaminated area should be large is fundamental, because the available mass loading data represent the average condition for areas large enough that suspension and depletion of dust in the airstream can equilibrate (Anspaugh et al. 1975; Smith, Whicker and Meyer 1982). Second, estimation of the radioactivity associated with the suspendable soil fraction requires reasonable uniformity of the contaminant in the contaminated area.

The mass loading approach is useful in situations for which suitable dust loading measurements are available. Because no environmental parameters such as soil moisture content or wind speed are incorporated into this model, care must be taken that the conditions at a given site are properly represented by the average conditions during the measurement of M. The calculated air activity concentration c is an estimate of suspended particulates (Smith, Whicker and Meyer 1982). The height of the dust loading measurement specifies the height for the estimated air activity concentration c.

Healy (1980) notes in his review that if the quantity of particulates in the air is known from other data, one need, theoretically, only measure the soils in the region to provide an estimate of the air concentration of the contaminant.

In the absence of data for a specific site, Anspaugh et al. (1975) have suggested the use of 100 μg m^{-3} for predictive purposes. This default value was based on particulate concentrations in 30 nonurban locations where annual arithmetic averages varied from 9 to 79 μg m^{-3} with a mean for all 30 locations of 33 μg m^{-3}. This same approach was adopted by the NRC in NUREG/CR-5512 for the residential scenario for exposure outdoors, using a mass loading value of 100 μg m^{-3} (Beyeler et al., 1999).

The U.S. Environmental Protection Agency (1977) examined the data from the nonurban stations from the National Air Surveillance Network (NASN) for the years of 1964 and 1965. In general, annual mean mass concentrations of airborne particulate material are in the range of 5-59 μg m^{-3}; the mean arithmetic average for 1966 of all 30 nonurban NASN stations was 38 μg m^{-3}. The prevalence of high values in the east would indicate the possible inclusion of industrial particulates in these samples. The U.S. Environmental Protection Agency used a value of 100 μg m^{-3} in the calculation of their screening level.

As it is noted in (Healy 1980), several uncertainties appear in the data from the National Air Surveillance Network. The first was pointed out above in that the particulates that are collected can include a portion of those generated by industrial operations; so the values could be high. The second problem arises from the fact that the samplers are frequently in positions, such as on top of buildings; so they do not measure the air breathed by people. Associated with the question of the concentration of soil particles in the air is the question of the origin of the particles. Once airborne, the smaller particles can travel very long distances.

Table 6.1. **A comparison of the observed and predicted air activity concentrations based upon a simple mass loading model**

Location, etc.	Radionuclide	Air activity concentration		
		Predicted	Measured	Ratio Pr/Mes
GMX site, USAEC Nevada Test Site [1, 2]				
NE, 1971-1972	^{239}Pu	7200 aCi m^{-3}	6600 aCi m^{-3}	1.09
GZ, 1972, 2 weeks	^{239}Pu	120 fCi m^{-3}	23 fCi m^{-3}	5.22
Lawrence Livermore Laboratory [3-5]				
1971 [3]	^{238}U	150 pg m^{-3}	52 pg m^{-3}	2.88
1972 [4]	^{238}U	150 pg m^{-3}	100 pg m^{-3}	1.50
1973 [5]	^{238}U	150 pg m^{-3}	86 pg m^{-3}	1.74
1974 [5]	^{40}K	1000 aCi m^{-3}	980 aCi m^{-3}	1.02
Argonne National Laboratory [6]				
1972	^{232}Th	320 pg m^{-3}	240 pg m^{-3}	1.33
1972	^{nat}U	215 pg m^{-3}	170 pg m^{-3}	1.26
Sutton, England				
1967-1968	^{nat}U	110 pg m^{-3}	62 pg m^{-3}	1.77
Mean				1.98 ± 1.34

* — [1] — (Anspaugh and Phelps 1974), [2] — (Anspaugh et al. 1975), [3] — (Gudiksen et al. 1972), [4] — (Gudiksen et al. 1973), [5] — (Silver et al. 1974), [6] — (Sedlet, Golchert and Duffy 1973).

Since most contaminated areas are relatively small in area, one would expect that only a fraction of dust in the air would expect that only a fraction of the dust in the air would originate from the area. Because of preferential deposition of the larger particles from sources some distance away, this «background dust» would contain a higher percentage of the smaller particles that are more readily deposited in the lung than the dust originating from the local, contaminated area. Thus Anspaugh and Phelps (1974) report that measurements at the GMX Area in Nevada with Anderson high-volume cascade impactors for about 1 month indicate that the mass distribution of sizes is about 1.6 μm a mass median aerodynamic diameter-with a geometric standard deviation σ_g of about 15, and the distribution for the plutonium and ^{241}Am had an activity median aerodynamic diameter of about 3 μm with a σ_g of about 7. It was also noted that the average activity of the soil was about one-third that found in the soil close to the sampler. It is noted that even higher activity was upwind.

From this data they concluded that a direct comparison of the size distribution of contaminated particles in the air with those in the soil is probably valid only for very large areas. The second question, that of the appropriate concentration of the contaminant in the soil, more subtle. As it was discussed earlier, soil particles that are carried in suspension are the smaller ones because the large ones will settle rapidly. Thus, if the concentration of the contaminant in the soil fraction containing the small particles is greatly different from that in the other particle sizes, it would appear that the concentration predicted by the mass-loading approach using the total soil concentration would theoretically be low.

In Mauro et al. (2015) the mass-loading approach was used for reconstructing inhalation doses from the resuspension process for individuals employed at the Nevada Test Site during the period from 1951 through 1992, as opposed to the use of the resuspension-factor approach. The calculations were made with an arbitrary mass loading of 1 mg m^{-3}. The authors made conclusions that (1) mass loading is a reasonable approach, (2) a mass loading of 0.168 mg m^{-3} gives the same dose as the resuspension method, and (3) the value of 1 mg m^{-3} is reasonable and would be more favorable.

The measurements of mass loadings were made in Amargosa Valley, Nevada (Bechtel SAIC 2006). The scenario «Inactive Outdoor Environment» was considered which would be similar to the locations where the Nevada Test Site environmental surveillance air samplers were located. Mass loading in this scenario was described by a triangular distribution with a mode of 0.060 mg m^{-3}, a minimum of 0.025 mg m^{-3}, and a maximum of 0.100 mg m^{-3}. The second scenario «Active Outdoor Environment» was also considered, and would include activities such as driving bulldozers, tractors, heavy construction machinery, etc. Mass loading in this scenario was again described by a triangular distribution, but now with a mode of 3 mg m^{-3}, a minimum of 1 mg m^{-3}, and a maximum of 10 mg m^{-3}.

For rural areas in Ukraine with different agricultural activities, the concentration of dust in air ranged from 0.3 to 203 mg m^{-3} for a soil moisture content of 3 to 20% (Loshchilov et al. 1991). The maximum concentration of dust in samples collected from air stirred up by agricultural machinery in Ukraine was 4,000 mg m^{-3} during potato planting (Anokhova and Krivtsova 1991).

6.2. Enhancement factor

Measurements in the Chernobyl exclusion zone showed that in the topsoil layer, radionuclides were attached mostly to small soil particles less than 1 μm in diameter (Loshchilov et al. 1991). Therefore, the specific activity of small soil particles exceeds that for the largest particles (0.1 to 1 mm). According to measurements in Ukraine after the Chernobyl accident for different radionuclides, the specific activity of small particles for ^{134}Cs exceeds that of large particles by a factor of 12.7, for ^{137}Cs by a factor of 9.1, for ^{90}Sr by a factor of 7.4, and for $^{238+239+240}Pu$ by a factor of 19.2 (Anokhova and Krivtsova 1991).

Considered these effects, the subsequent development of the above approach was made by Shinn (1992). He proposed to improve estimations calculated with the Eq. (6.1) by introducing into consideration the enhancement factor *EF* for resuspended aerosol to include disturbance effects on the soil:

$$c = MC_S \cdot EF, \tag{6.3}$$

where *EF* is the ratio of the specific activity in the aerosol to the specific activity in the underlying surface of contaminated soil. The author considers that the enhancement factors are useful for assessment of worst-case expose scenarios and transport conditions and the *EF* values should be entirely satisfactory considering the possible alternatives of theoretical prediction and site-specific monitoring data.

Garger, Paretzke, and Tschiersch (2008) estimated the enhancement factor of the different size ranges for anthropogenically enhanced resuspension experiments in the Chernobyl exclusion zone (see details of the experiments in Chapter 11). Comparing the enhancement factor of the different size ranges (Table 6.2), the highest factor is found for large particles (7-16 μm) and the lowest for fine particles (<2 μm). The enrichment of radioactivity on particles during agricultural

Table 6.2. **Enhancement factor according to the measurement results in the Chernobyl exclusion zone and two other sites**

Experiment	< 2.0 μm	2-4 μm	4-7 μm	7-16 μm
May 1993 Zapolie	3.8 ± 2.2	9.5 ± 4.9	8.6 ± 5.0	28.8 ± 15.7
Nevada Test Site (Shinn 1992)	3.6			
Bikini Atoll	3.9			

activity discriminates against fine particles, which tend to adhere to large host ones. In the fine and coarse particle size ranges the enrichment is about a factor of 4-9 especially for little distances from sources. This is in agreement with the results of resuspension measurements at nuclear weapon test sites (Shinn 1992) where enhancement factors of ^{239}Pu were determined in the particle range <10 μm during the mechanical disturbance of soil (Table 6.2).

Methods of mass loading and the resuspension factor, therefore, are the express methods, which enable to assess the atmospheric activity concentration and the inhalation dose in the acute phase of a radiation accident almost immediately after the formation of deposition field. These two methods are not mutually exclusive; they can be used as alternative approaches to the assessment of the secondary air contamination as a result of resuspension. These methods can be improved thanks to a priori knowledge of the composition of soil particle size by weight (or activity). The size distribution of radioactive particles in the initial phase of a radiation accident is usually unknown, so estimates of radioactivity particles enrichment must be used, especially for the fine fraction of aerosols. Also, it's necessary to consider the meteorological parameters — the speed of the wind, soil moisture, and others.

CHAPTER 7

RESUSPENSION RATE

7.1. Definition of the resuspension rate

For calculation of transport of radionuclides from a surface, it is necessary to know its emission ability equal to a vertical turbulent flux of radionuclides at a ground surface J (Bq m^{-2} s^{-1}) normalized to a ground surface contamination density, or in other words, the resuspension rate.

According to (Healy and Fuquay 1958, Healy 1974), the resuspension rate is defined as a share of contamination on the ground, which rises in the air in a unit of time caused by wind or mechanical perturbation. According to this definition, the resuspension rate Λ (s^{-1}) expresses as

$$\Lambda = \frac{J}{D}, \tag{7.1}$$

where D is the mean density of surface contamination by radionuclides (Bq m^{-2}).

The total resuspension rate as a function depending on various mechanisms of particles lift of in air could be represented in the form (Chepil 1951)

$$\Lambda = f(\Lambda_{air}, \Lambda_{salt}, \Lambda_{sc}, \Lambda_{w}, \Lambda_{m}), \tag{7.2}$$

where Λ_{air} is the resuspension rate of particles (<100 microns) moving actually as air suspension; Λ_{salt} is the resuspension rate for saltation particles (50-500 μm); Λ_{sc} is the resuspension rate of particles due to large particles (>1000 μm) motion on a surface by creep. The author considered that these three functions should be taken into account though one of them can dominate; Λ_{w} is the wind resuspension rate also should be considered in absent for three surveyed types of transport observed at strong winds and soil erosion; Λ_{m} is the resuspension rate caused by the mechanical reasons of lift up.

As it was already mentioned in Chapter 1, at middle latitudes with a wet climate and low wind speed a soil erosion is

observed many fewer and then of a dust particles blow-off from the surface layer of ground and other elements of surface polluted with radioactive materials or others toxics, and their lift up becomes the important mechanism of the further transport over different distances.

In this case, an estimation of Λ_m is necessary, as despite of a little resuspension intensity in these conditions, the process of secondary lift up takes place within extensive polluted territories and for a long time, continuing many years. On a local scale various anthropogenous activity strengthens a substance lift up and its redistribution in space sharply. In this connection in practice, experimental estimations of Λ_m are necessary at calculations of contamination redistribution after an accident in space and time caused by a mechanical lift up, atmospheric transport and deposition of radioactive dust and, in the end, estimation of possible dose loadings on the population.

Generally, for an area source with a non-uniform surface and a surface contamination density, the intensity of wind uplift of radionuclides can depend on the physical characteristics of a surface and radionuclides, and also on spatial coordinates and time. The knowledge of the resuspension rate as functions of coordinates and time enables to describe a field of concentration in any point around the polluted territory with the help of the equation of eddy diffusion for a point or area source. It was illustrated in (Healy 1974) in the territory, polluted with plutonium. (Garger, Gavrilov and Zhukov 1992) solved the inverse task of Λ determination using data on a field of the ^{137}Cs activity concentration in the ground soil. In (Anspaugh 1975) this approach was used widely for an estimation of fields of the ^{137}Cs activity concentration in the air at the extensive territory contaminated after the Chernobyl accident in Kyiv region (Ukraine), Gomel and Mogilev regions (Belarus) using the experimental estimation of the Λ value in 1986 (Garger 2008).

The uncertainties in the estimation of the resuspension rate appear the same as at the resuspension factor estimation. The vertical turbulent flow of substance due to resuspension should vary in time caused by daily and seasonal variability of meteorological parameters, and by depletion of ground surface contamination, wash off, erosion and penetration of contamination into the ground. The estimation of the resuspension rate depends also on methods of air sampling. The estimation of Λ can be carried out by several methods:

1) direct measurements of vertical turbulent flow of radionuclides above a flat source;

2) gradient measurements of mean wind speed, mean air temperature and mean activity concentration of radionuclides in the surface layer of the atmosphere that enables estimating the vertical turbulent flow of radionuclides from homogeneous and stationary source;

3) measurements of the radionuclide activity concentration in air at fixed height outside of a finite source or directly above a source.

7.2. Theoretical basis of methods of matter vertical flow measurement

The scientific basis of measurement methods of matter vertical flows is given below. The technical realization of these methods is described in details in original works according to given references.

Gillette, Blifford, and Fencer (1972) and Gillette (1976) described measuring dust vertical and horizontal flows during saltation. The vertical flow was calculated using the measurement data of the aerosol concentration (with diameters < 20 μm) at two heights according to the equation

$$J_N = -K_A \rho \frac{\partial n}{\partial z}, \tag{7.3}$$

where J_N is the aerosol number flux (number of particles / area / time); K_A is the coefficient of the turbulent exchange for an aerosol; n is the number of particles in the unity of air mass.

The assumption has been made that K_A is equal to the coefficient of eddy diffusivity k_z which was determined by the formula

$$k_z = \kappa u_* z, \tag{7.4}$$

where $\kappa = 0.4$ is von Karman constant, u_* is the friction velocity.

Shinn et al. (1976) used this approach introducing the following simplification with the help of the equation

$$J = -k_z \frac{\partial \overline{q}}{\partial z}, \tag{7.5}$$

where J is the aerosol mass flux (kg m^{-2} s^{-1}); $\overline{q}$ is the average aerosol concentration at height z (kg m^{-3}).

Shinn et al. (1976), Chepil and Woodruff (1957) showed that the aerosol concentration at height z, normalized by the aerosol concentration at height of 1 m at neutral thermal stratification appears to be the function of height z according to the power law

$$\frac{\partial \overline{q}}{\partial z} = -p \frac{\overline{q}}{z}. \tag{7.6}$$

Values for p were reported to fall typically between 0.25 and 0.35 (Anspaugh et al. 1975) and between 0.05 and 0.5 with a median value of 0.18 (Shinn 2002). Loosmore (2003) used a value of 0.25.

Combining Eq. (7.4), (7.5), and (7.6), the expression for aerosol flow was obtained

$$J = p \kappa u_* \overline{q} \tag{7.7}$$

and the relation between resuspension rate and the resuspension factor in the form

$$\Lambda = p \kappa u_* K, \tag{7.8}$$

by dividing Eq. (7.7) on the contamination density D. The method is practically convenient as it requires a minimum of input data, hence a minimum of the micrometeorological measurements: wind velocity depending a height in the surface layer of the atmosphere and the average activity concentration of radionuclides at a fixed height ($z = 1.5$ m). The authors of these works have received estimations of radioactive plutonium resuspension at the various US sites and these generalized data are used below at comparison of values Λ.

7.3. Models of the resuspension rate

Makhonko (1992) used a relation between the resuspension rate Λ (he named it as «wind pickup coefficient») and the wind speed U (m/s), determined at a height of 2.1 m from Healy (1980), which was obtained in experiments on deflation of submicron calcium molybdate particles above a vegetation cover with roughness height $z_0 = 3.4$ cm

$$\Lambda = 0.96 \cdot 10^{-13} U^{4.8}. \tag{7.9}$$

As the averaging interval increased, the power of the wind speed decreased from 4.8 to 1. Makhonko (1992) noted that since the method of averaging the wind speed is not indicated in Healy (1980) and the turbulent characteristics of the atmosphere were not measured, it is difficult to use the formula (7.9) in practice.

Besides the wind speed, the state of the underlying surface also affects dust resuspension. Empirical formulas, obtained under conditions of a plain in the middle band of the country (wooded-steppe foothills of the southern Urals) are presented in Makhonko (1986). These formulas relate the resuspension rate to the roughness height z_0 of the ground, the height of the grass h, and the phytomass m stored in the air-dried form:

$$\Lambda = \frac{2 \cdot 10^{-10}}{z_0^{1.4}}; \quad \Lambda = \frac{2.5 \cdot 10^{-9}}{h^{1.4}}; \quad \Lambda = \frac{2.5 \cdot 10^{-8}}{m^{1.4}}, \tag{7.10}$$

where Λ is expressed in s^{-1}; z_0 and h are expressed in cm; and m is expressed in g cm^{-2}.

Reducing the resuspension intensity Λ with increasing the roughness height z_0 of the surface covered with vegetation, because an increase in height of the cover occurs. The rise of the dust particles from the soil is mainly due to the breakthrough of turbulent eddies of different scales to the soil surface. Increasing grass height reduces the likelihood of the breakthrough of turbulent eddies to the soil surface (at the same time, perhaps, reducing the scale of these eddies), so the upward flow of dust from the soil decreases. The remaining two dependencies in Eq. (7.10) are obtained based on empirical relationships between z_0, the height of the grass h, and the phytomass m, obtained by the author.

Loosmore (2003) developed an empirical model for the resuspension rate appropriate to short-time resuspension. Three data sets for wind tunnel studies

of short-time resuspension were taken from the literature and used to develop a model. The resuspension rate (s^{-1}) was assumed to be a function of five parameters: the friction velocity u_* (m s^{-1}), time after deposition t (s^{-1}), the particle diameter d (μm), the particle density ρ (kg m^{-3}) and the roughness z_0. The resuspension rate was assumed to vary either in power-law relationships or exponential relationships with the parameters, and a variety of models were examined. The best model fits to these data were the following, named «empl» and «emp3»*:*

$$\Lambda = 0.42 \frac{u_*^{2.13} d^{0.17}}{t^{0.92} z_0^{0.32} \rho^{0.76}}, \quad \text{(model empl)} \tag{7.11}$$

$$\Lambda = 0.01 \frac{u_*^{1.43}}{t^{1.03}}. \quad \text{(model emp3)} \tag{7.12}$$

According to (7.11) and (7.12) the resuspension rate increases with u_* and particle diameter and decreases with time, surface roughness, and particle density. Loosmore noted that these trends are consistent with intuition and observations: resuspension increases with velocity but falls in time; larger surface roughness provides more shielding; heavier particles are harder to move; larger particles stick up higher into the boundary layer and thus experience higher removal forces.

Loosmore tested these two models the same as 4 other known models for the resuspension factor against two independent data sets. He concluded that the empirical model «emp1» that includes all parameters performed the best throughout the study. The models «emp3» and the rest tested models cannot take into account the effects of the surface and particle characteristics, but where these values are uncertain, the Loosmore model «emp3» and model NCRP (1999), which is used by early responders to emergency scenarios, may be more appropriate.

7.4. The estimation of the resuspension rate in the 30-km Chernobyl zone based on Monin-Obukhov theory

In (Garger, Zhukov and Sedunov 1990, Garger 1994) the resuspension rate by the wind was determined with the help of gradient measuring of average radionuclides concentration, wind velocity, and air temperature, provided that conditions appropriate to the case of a flat homogeneous constant source are valid:

$$-\frac{d}{dz} k_z \frac{d\overline{q}}{dz} = 0. \tag{7.13}$$

Eq. (7.13) after integration results in

$$J_A = -k_z \frac{d\overline{q}}{dz} = \text{const}, \tag{7.14}$$

where k_z is the vertical coefficient of turbulent diffusion.

From Eq. (7.14) it follows that the no gravitational vertical flux of the deposited material J_A in the surface layer of the atmosphere is constant.

According to the Monin and Obukhov theory (Zilitinkevich 1979) in the surface layer of the atmosphere, the similarity is observed for the vertical gradient of the radionuclide concentration

$$\frac{d\overline{q}}{dz} = -\frac{J_A}{\kappa u_* L} q_a\left(\frac{z}{L}\right), \tag{7.15}$$

where q_a (z/L) is the universal function of similarity in the Monin and Obukhov theory; L is the Monin-Obukhov length equals to

$$L = \frac{u_*^3}{g/T_a \times P_0/c_p\rho},$$

where P_0 is the heat flux density in the air; c_p is the specific heat of the air at constant pressure; ρ is the air density.

After the integration of Eq. (7.15) over z we obtain

$$\overline{q}(z_2) - \overline{q}(z_1) = -\frac{J_A}{\kappa u_*}\left[f_a\left(\frac{z_2}{L}\right) - f_a\left(\frac{z_1}{L}\right)\right], \tag{7.16}$$

where f_a (z/L) is an antiderivative of q_a (z/L).

For the case when $L \to 0$, i.e. for conditions of neutral stratification

$$\frac{d\overline{q}}{dz} = -\frac{J_A}{\kappa u_* z}. \tag{7.17}$$

After integration we have

$$\overline{q}(z_2) - \overline{q}(z_1) = -\frac{J_A}{\kappa u_*} \ln\frac{z_2}{z_1}. \tag{7.18}$$

At small values of z/L we have approximately (Byzova, Garger and Ivanov 1991)

$$\overline{q}(z_2) - \overline{q}(z_1) \cong -\frac{J_A}{\kappa u_*}\left(\ln\frac{z_2}{z_1} + \beta_a \frac{z_2 - z_1}{L}\right), \tag{7.19}$$

where β_a is an empirical constant. For simplicity, it is considered that the character of turbulent transport of substance does not differ from the character of turbulent momentum transfer. Dividing Eq. (7.19) by a density of contamination (Garger, Zhukov and Sedunov 1990, Garger 1994) we have a final expression for the radionuclides resuspension rate by the wind at small values of z/L:

$$\Lambda = \frac{[\overline{q}(z_1) - \overline{q}(z_2)]\kappa u_*}{D\left(\ln\frac{z_2}{z_1} + \beta_a \frac{z_2 - z_1}{L}\right)}, \tag{7.20}$$

where according to (Byzova, Garger and Ivanov 1991) $\beta_a = 1.45$ for $-0.16 < z/L \le 0$ and $\beta_a = 9.9$ for $z/L > 0$.

Eq. (7.20) can be used at the study of the wind resuspension rate dependence on time of day. If Λ is determined for the period more one day, when ther-

mal conditions at the average almost always could be considered as equilibrium, Eq. (7.20) becomes simpler

$$\Lambda = \frac{\kappa u_* [\overline{q}(z_1) - \overline{q}(z_2)]}{D \ln \frac{z_2}{z_1}}. \tag{7.21}$$

The difference between Eq. (7.20), (7.21) and (7.7) is that gradient measurements of the activity concentration in the air or other characteristics of contamination gives the information about a sign of the flux in the surface layer and allow to determine the occurrence of radionuclide advection from the more intensive distant surface source of an admixture.

From Eq. (7.20) the relation between Λ and K (for this idealized situation) could be easily determined:

$$\frac{\Lambda}{K} = \kappa u_* \left[\ln \frac{z_2}{z_1} + \beta_a \left(\frac{z_2 - z_1}{L}\right)\right]^{-1} \left[1 - \frac{\overline{q}(z_2)}{q(z_1)}\right], \tag{7.22}$$

where $K = \frac{\overline{q(z_1)}}{D}$ and $[1 - \overline{q}(z_2)/\overline{q}(z_1)] < 1$ for wind-driven resuspension. For neutral thermal conditions when $L = \pm \infty$ m, and for selection of z_1 or z_2 equal to the roughness height z_0, the ratio Λ/K will have a magnitude of $0.1u_*$. The expression

$$v_\alpha = K/\Lambda \approx \kappa u_* \{\ln z_1/z_2 + \beta_a [(z_1 - z_0)/L]\}^{-1} \tag{7.23}$$

for that case is the turbulent vertical resuspension velocity v_α of the deposited material for this idealized situation.

Vertical air activity concentration profiles of ^{137}Cs, ^{103}Ru, and ^{144}Ce are shown in Fig. 7.1, along with a measured wind speed profile, for an individual experiment on 13-14 September 1986. The decrease in the atmospheric concentration with height is consistent with upward diffusion and indicates a distant source of resuspension. However, data have to be carefully chosen so that the effects of upwind advection are minimized. Fig. 7.2a shows the ^{144}Ce activity concentration profiles, taken over 3 h intervals on 1 August 1986. These profiles illustrate the change in gradients which can occur throughout a day. In particular, an increase in concentration with increasing height can occur under certain conditions which imply deposition of material originating from an upwind source. Fig. 7.2b shows the average of these profiles.

Table 7.1 illustrates some calculated values of the resuspension rate for various surface types. These results are considered appropriate for conditions when the advection of material from upwind sources was considered negligible (i.e. by choosing results when the upwind fetch was relatively uncontaminated). The three experimental sites include an agricultural field, a forest and an area of sand without vegetation that had been prepared for building work immediately before the Chernobyl accident. All the resuspension rate values relate to similar conditions (i.e. a dry surface with a moderate wind of about 2 m s^{-1} at 1 m above

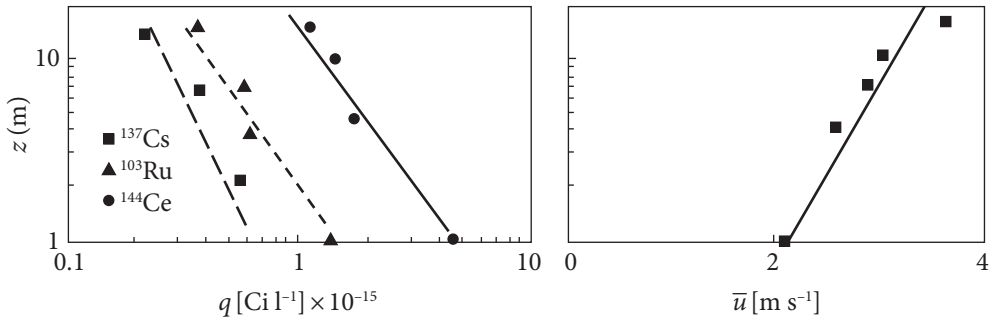

Fig. 7.1. Vertical air activity concentration profiles of ^{137}Cs, ^{103}Ru and ^{144}Ce and wind speed profile measured on 13-14 September 1986 at Zapolie (1 Ci l^{-1} = 37 TBq m^{-3})

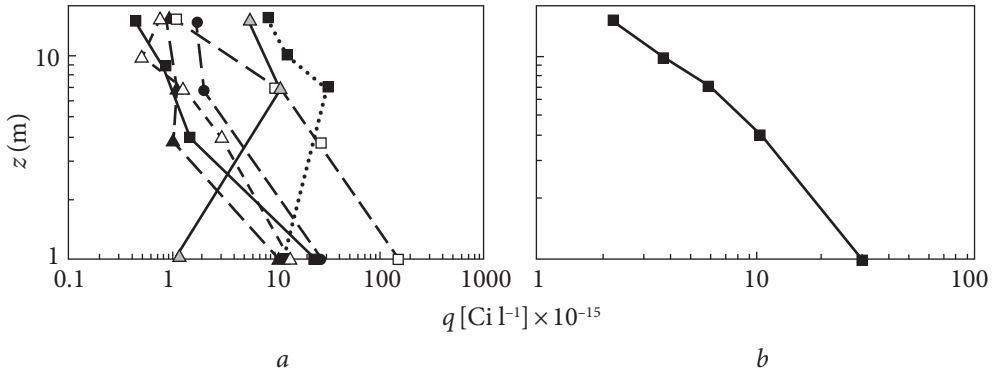

Fig. 7.2. *a* — ^{144}Ce activity concentration profiles taken over 3-hr intervals on 1 August 1986. *b* — ^{144}Ce activity concentration profile averaged over ones presented in (*a*) (1 Ci l^{-1} = 37 TBq m^{-3})

ground level at the field site). It would be seen from Table 7.1 that similar resuspension rates were obtained for the forest and the sandy sites equals to about 2×10^{-9} s^{-1}, whilst values several times lower were found at the agricultural site. Although there is little information to suggest a difference in the resuspension rate according to radionuclide in Table 7.1, the time dependence of resuspension must be remembered and this may differ according to the physical and chemical characteristics of the deposited material.

The systematic difference in values of wind resuspension intensity between a forest and a field for all radionuclides is could be seen well. These data have allowed estimating a dust-forming power of the underlying surface and a radioactivity transport from the 30-km zone to the surrounding regions in the first two years after the accident. It has appeared that the transport of radioactive dust within one year did not exceed several tenths of a percent of the density of contamination.

In Belyaev and Surnin (1991) a dust concentration at heights from 0.6 up to 34 m in June, 1986 in the Chernobyl zone with the help of samplers with three-layer

filters AFA-HA was measured. The upper layer of a filter was imbued with NaOH solution and the third one was covered by a layer of activated carbon. The samplers are fastened to a rope anchored to a mast of high voltage line at a height of 36 m. The vertical profiles of gamma-radiating radionuclides activity concentration were obtained. The estimations of the resuspension rate were carried out only at the east wind during observations with the help of the formula (Garger, Zhukov and Sedunov 1990). The estimations have shown that in June, 1986 the resuspension rate was about 2×10^{-8} s^{-1} for ^{144}Ce, ^{95}Zr, ^{95}Nb, what was related by the authors with large-dispersed dust; 4×10^{-8} s^{-1} for ^{103}Ru, ^{137}Cs, what was related to low dispersed dust; and for ^{131}I the wind resuspension rate was obtained about 4×10^{-6} s^{-1}.

Naydenov and Lukoyanov (1994) studied experimentally parameters of wind-driven resuspension radioactive dust above a ^{137}Cs contaminated cultivated field in Novozybkov district of Bryansk region (Russia). The measuring was carried out in July-August, 1992 with the help of gradient device by the method of Naydenov and Lukoyanov (1994).

As a result of measuring of the ^{137}Cs activity concentration vertical profile for 3 days under absence of noticeable advection flow of a radioactivity the values of resuspension rate were calculated in the range of 1.2×10^{-9}-1.5×10^{-9} s^{-1} for a surface density of contamination taken within 1 cm soil layer and in the range of 7×10^{-11}-9×10^{-11} s^{-1} for an inventory of ^{137}Cs within 20 cm of arable soil layer.

Table 7.2 summaries the resuspension rate estimations obtained for different underlying surfaces in the polluted territory as a result of the Chernobyl accident in the 30-km exclusion zone in Ukraine (in brackets a distance of measurement sites from the 4th unit of the CNPP is indicated) and in Bryansk region are represented.

Table 7.2 also contains data obtained in Bavaria (Rosner and Winkler 2001) at use of Slinn's assumption (Slinn 1978) that on average during the year radionuclide losses from the underlying surface are equal to a radionuclide deposition. Also, American researcher's data on the study of radioactive plutonium resuspension for different places of the USA which differ sharply by the character of the underlying surface and in particular by soil are presented.

Table 7.1. **Resuspension rate for different surface types (Garger et al. 1990)**

Surface type	Resuspension rate × 10^{-9} (s^{-1})		
	^{144}Ce	^{137}Cs	^{95}Zr + ^{95}Nb
Field	0.3 ± 0.1	1.0 ± 0.7	0.4 ± 0.2
Forest	2.1 ± 0.9	2.1 ± 0.8	3.7 ± 0.9
Sand beach without vegetation	2.2	3.7	2.4

From Table 7.2 it follows that the weakening of the resuspension process with time occurs in the surface layer of the atmosphere by one-two orders of magnitude during four months considering the character of the underlying surface. In 1986 the resuspension rate values differed noticeably depending on a distance from the source and the type of underlying surface. It is clear that during eight incomplete years after the accident the values of resuspension rate in Zapolie on a grass field have decreased by one order of magnitude, and on the beach Pripyat, consisting of coarse sand hydraulic fill before the accident, they have decreased by three orders of magnitude, apparently, due to more intensive radionuclide ver-

Table 7.2. **Resuspension rate (year^{-1}) for various underlying surfaces**

Surface type	Place and time of measuring	Resuspension rate (year^{-1})		
		^{144}Ce	^{137}Cs	^{95}Zr + ^{95}Nb
Urban area (Belyaev and Surnin 1991)	Chernobyl, June 1986	6.3×10^{-1}	1.3×10^{0}	6.3×10^{-1}
Grass field(Garger 1994)	Zapolie (14 km), September 1986	9.4×10^{-3}	3.2×10^{-2}	1×10^{-2}
Forest (Garger 1994)	Forest (14-15 km), September 1986	6.6×10^{-2}	6.6×10^{-2}	1.2×10^{-1}
Sand beach (Garger 1994)	Pripiat town (2 km), Ukraine, September 1986	6.3×10^{-2}	1.2×10^{-1}	8×10^{-2}
Field, sand beach (Holander and Garger 1996)	Pripiat town, 1993	—	2.5×10^{-3} 2×10^{-4}	—
Cultivated field (Naydenov and Lukoyanov 1994)	Novozybkov district, Briansk region, Russia, 1992	—	4.7×10^{-2} a) 2.8×10^{-3} b)	—
Surface type	Place and time of measuring	Resuspension rate (year^{-1})		
		^{90}Sr	^{137}Cs	$^{239+240}$Pu
Half rural area (Rosner and Winkler 2001)	Bavaria, Germany, 1987 1997	 2.5×10^{-4} 1.0×10^{-4}	 4.3×10^{-3} 2.0×10^{-4}	 1.8×10^{-4} 0.4×10^{-4}
Cultivated field (Shinn, Homan and Don 1982)	South Carolina, USA, old deposit	—	—	1.4×10^{-4}
Desert (Shinn, Homan and Don 1982)	Nevada, USA, old deposit	—	—	0.8×10^{-4} - 1.5×10^{-2}
Forest-steppe (Makhonko and Robotnova 1982)	Southern Ural, Russia, polluted soils from 1957 up to 1960	1.4×10^{-4} - 0.4×10^{-1}	—	—

Note: a) Resuspension rate at ^{137}Cs density in 1 cm of soil layer; б) At the inventory of ^{137}Cs in 20 cm of arable soil layer.

tical migration into the soil. The data which was obtained in Novozybkov district of Bryansk region well illustrates a dependence of the resuspension rate value on a form of normalization of vertical turbulent flux of radioactive aerosols. According to these data, the normalization of a total inventory of radionuclide in soil underestimated the resuspension rate value by an order of magnitude. Measurement data of old radionuclide deposits with age from 8 up to 20 years result in the resuspension rate is of the order of 10^{-4}-10^{-3} year^{-1} regardless of radionuclide type. In other words, only one-thousandth or one ten-thousandth share of deposition in the surface layer of soil resuspends in the air within one year.

7.5. Use of the semi-empirical equation of turbulent diffusion for estimations of the resuspension characteristics

Makhonko (1981) made a theoretical calculation of the effective velocity of wind resuspension of dust from the underlying surface based on the solution of the semiempirical equation of the turbulent diffusion in the surface layer of the atmosphere above an infinite horizontal homogeneous plane (more details in Chapter 8.2.3). The effective wind resuspension velocity was estimated equal to 1.9-2.8 cm s^{-1} for typical meteorological parameters in summer in Ukraine (Makhonko 2008).

Makhonko (1993) estimated the change of the ^{137}Cs wind resuspension intensity from the ground surface after the Chernobyl accident. For this purpose, the solution of the equation of the turbulent diffusion for the ground quasi-stationary point source which is the center of the elementary square was used according to Eq. (8.68). The data of the concentration calculation were averaged considering a wind rose during the period of deposition sampling. The resuspension rate value was calculated as the deposition value divided by the calculated concentration and multiplied by the effective velocity of turbulent sedimentation. The effective sedimentation velocity was determined on a restricted series of simultaneous measurement of depositions and concentrations. The stratification of the atmosphere was considered neutral. The calculations were carried out for a height of 1 m at following typical values of a vertical coefficient of a turbulent exchange 0.1 m^2 s^{-1}, a wind velocity of 2.3 m s^{-1}, a roughness height of 3 cm. According to the calculations, the maximal value of the resuspension rate was observed in May 1986 during intensive works on liquidation of the accident consequences when the vegetation cover was not completely formed. By August the resuspension rate was declined by two orders of magnitude ~10^{-9} s^{-1}.

Buikov (1993) has obtained an expression for the resuspension rate from the solution of the equation of turbulent diffusion for a flat homogeneous infinite

source of contamination with initial and boundary conditions:

$$D(x, y, 0) = D_0(x, y); \quad q(x, y, z, 0) = q_0(x, y, z), \tag{7.24}$$

where D is the density of contamination, Bq m^{-2}; q is the activity concentration in the air, Bq m^{-3}.

$$k_z(z)\frac{\partial q}{\partial z} + wq = \frac{\partial D}{\partial t} \quad \text{at } z = z_0, \tag{7.25}$$

$$K_z(z)\frac{\partial q}{\partial z} + wq = 0 \qquad \text{at } z = H, \tag{7.26}$$

where H is the height of the upper boundary of the boundary layer; w is the velocity of gravitational sedimentation, $z_0 = z_* + \Delta z$; z_* is the height of roughness; Δz is the thickness of saltation layer; $k_z(z)$ is the coefficient of turbulent diffusion.

The author use the Slinn equation (Slinn 1976), which defines a time dependence of the contamination surface density D due to resuspension and dry deposition:

$$\frac{\partial D}{\partial t} = -J_A = v_d q(x, y, z_0, t) - \Lambda \cdot D(x, y, t), \tag{7.27}$$

where v_d is the dry deposition velocity; Λ is the resuspension rate; J_A is the vertical flux of contamination.

For the neutrally stratified surface layer of the atmosphere the solution of the diffusion equation for the activity concentration in the air results in the formula for resuspension rate estimation:

$$\Lambda = \left(1 + \frac{v_d}{w}(\varsigma - 1)\right) \ln\left(1 - \frac{J_\uparrow - \Lambda Q_0}{q_1(t) v_d\, \varsigma}\right) \cdot t^{-1}, \tag{7.28}$$

where $\varsigma = \left(\frac{z_1}{z_0}\right)^{\lambda}$, $\lambda = \frac{w}{\kappa u_*}$.

This transcendental equation for Λ can be solved by a method of iterations if there are measurement data of the vertical flux of contamination J_A, and also parameters u_*, v_d, z_0, Q_0, w, and data about particles size.

It can be seen from this chapter the estimations of the resuspension rate or velocity could not be obtained without measuring of the vertical turbulent flux of substance. The measuring of Λ is connected with great difficulties.

Wen and Kasper (1989) proposed a kinetic model of particle re-entrainment from surfaces that enable calculation of the particle concentration in the air generated by resuspension as a function of time. The equation for the particle concentration was obtained in the form

$$n(t) = \frac{N_t}{(F^* - F_0)Qt}\left[1 - e^{-t(1/\tau_1 - 1/\tau_2)}\right] e^{-t/\tau_2}, \tag{7.29}$$

where $n(t)$ is the concentration of particles in a flux which are generated by resuspension from a unit surface element; N_t is an initial total particle number on the surface; Q is the volume flow rate; $F = adhesion\ force\ /\ removal\ force$ is a dimensionless variable combining adhesion forces and removal forces for a given particle on a given surface under given local flow conditions; $\tau_1 = e^{F_0}/A$, $\tau_2 = \tau_1 e^{(F^*-F_0)}$; F_0 corresponds to initial and, as a rule, to great number of the deposited particles on a surface; F^* corresponds to situation when the particle reservoir on the surface is exhausted due to resuspension.

In this model, the resuspension rate is parameterized as a function of F in the form $\Lambda(F) = A \cdot \exp(-F)$. The process of resuspension begins from the moment of $t = 0$ with resuspension rate $\Lambda(F=0) = A$, when most of the weakly bounded particles lift off a surface and the process continues up to the moment of depletion of particles number on the surface. To calculate the concentration of the particles it is necessary to know the model parameters N_t, A, F_0 and F^*, which are unknown a priori. But they can be derived from a measurement of $n(t)$ over a sufficient long time using estimations of the particle concentration for $t = 1$ (Wen and Kasper 1989)

$$n(t=1) = \frac{N_t}{(F^* - F_0)Q}, \tag{7.30}$$

and at $t = 0$

$$n(t=0) = \frac{N_t A e^{-F_0}}{(F^* - F_0)Q}. \tag{7.31}$$

According to the model, the time dependence of the particle concentration for short times $t \le 4\tau_1$ is given by

$$n(t) \propto \frac{1 - e^{-t/\tau_1}}{t}, \tag{7.32}$$

and also, for periods longer than $t \ge 4\tau_2$

$$n(t) \propto \frac{e^{-t/\tau_2}}{t}. \tag{7.33}$$

The important advantage of this model is that it takes into account a relation between adhesive forces and aerodynamic forces which effects on particles for a long time. Unfortunately, it does not provide expressions of these forces in an explicit form. It is possible to use this model for the description of the time dependence of the activity concentration in the air. The empirical data about a time dependence of the activity concentration after the Chernobyl accident in different parts of Europe with distinct soils and meteorological conditions are accumulated for obtaining integrated estimations of the resuspension intensity in an initial period, when $\Lambda = A$, and $\Lambda(F^*)$ for large periods of observations.

7.6. Emission of the radioactive dust from the polluted territory during anthropogenic activities

Resuspension of contamination deposited on an underlying surface is the important process that should be considered at the estimation of the dose of human exposure. Considering this the analysis and understanding of a radioactive aerosol behavior in the surface layer of the atmosphere is one of the priority problems in case of future accidents for a choice of an efficient strategy on damage minimization. As a rule, the anthropogenic influence on a soil surface layer leads to a dust resuspension in the surface layer of the atmosphere. It may result in a redistribution of soil contaminants to adjacent territories. In some cases, this anthropogenic resuspension process may result in rapidly increasing the dust concentration in the air and its deposition. In the countryside it may create a negative situation as these radioactively contaminated areas can be located near settlements, gardens, fields, and others. Considering this it is necessary to estimate the intensity of contamination emission to the air from these areas and to calculate radionuclide atmospheric transport and deposition on the surface layer of soil, vegetation, building, etc.

The vertical flux of pollutants practically could not be measured by direct methods. As a rule, the various indirect ways of measuring and various physical assumptions about processes that occur during the resuspension of particles are used. In the Chernobyl exclusion zone, in main, the average activity concentration of ^{137}Cs was measured by various air samplers (ESP1 1996, Garger et al. 1997), located on different distances from a dust source and at different heights. But these samplers were not of identical construction and characteristics (Garger et al. 1997). The first estimations of the emission intensity were made with using of isokinetic IPA aerosol samplers located on four distances from a source, and multicascade impactor PK. The detailed analysis of the quality of all these measurements could be found in Garger et al. (1997). Additionally, for estimation of emission intensity, the powerful samplers «Grad» were used located practically at the same distances but at various heights. It has enabled to test the quality of obtained data using results of the concentration vertical profile measurements.

The model of a constant surface source of resuspended dust in the form of an infinite strip (Onikul and Khurshudyan 1983) (for details see Chapter 8.2.2) was taken as a basis of estimation of a radioactive dust emission which rises at agricultural works. The analysis of the model solution for the pollutant air concentration (Eq. (8.31)) which have been carried out in Garger et al. (1996) showed that for distances $x/L \geq 4$, where L is the strip width, and a change of the dimensionless particle sedimentation velocity ω from 0.1 up to 0.9, it is practically possible to

use more simple expression

$$c(x, z) = \frac{A_0 \sin \pi \omega}{k_1 (1+n) \pi\omega \, (1+\omega) \left(\frac{x}{L}\right)^{\omega} \left(1 + \frac{x}{L}\right)} \cdot \exp\left[-\frac{u_1 z^{1+n}}{(1+n)^2 k_1 x}\right]. \qquad (7.34)$$

where A_0 is the admixture vertical turbulent flux from the underlying surface. Other symbols could be seen in Chapter 8.2.2.

The large particles ($\omega > 0.5$) fall down near the strip, small particles ($\omega > 0.2$) can be transported over considerable distances.

An imitation of agricultural works and car traffic were carried out in a field with the help of various tractors and trucked vehicles in Zapolie in May, 1993. The sources as a strip of radioactive dust were created with the help of light and heavy tractors (MTP-82 and T-150 accordingly) and also with large army trucked vehicles ZIL-131 and ZIL-130. Approximately half of the experiments were planned for physical modeling of agricultural activity (harrowing) while another part modeled lorries traffic on dirt roads. The strip sources were prepared around a side with measuring devices considering possible various wind directions. Data of only those experiments were analyzed which meet the following requirements:

1. The wind was directed across of dusting strips in a direction of measuring side.
2. The wind velocity was high enough to provide a steady well-intermixed plume.
3. A type of the lorry and its velocity during the experiment had to be constant.
4. The meteorological conditions should be similar for all experiments. In particular, a soil condition and average wind direction have to be maintained during the experiment.

The activity concentration, the mass dust concentration and the number concentration of dust particles were measured by isokinetic samplers, «Grad» samplers at heights of 1.0, 1.8, 2.5, 3.5 m, PK impactor with effective aerodynamic cut-off diameters of 2.0, 4.0, 7.0, 12, 20, 30 μm, Berner-impactor and Aerodynamic Particle Sizer (APS). The size distribution of «hot» particles was measured by the autoradiography method at different distances from a dust source.

On Fig. 2.4 one may see that the dust rises upwards, moves behind the tractor and was blown away by the wind. For imitation of a stationary dust source, the tractors or lorries moved along the line there and back. Dust activity and mass concentration were measured during the whole period of tractors and lorries motion along the line, therefore they can be interpreted as average concentrations for this period (see Fig. 11.3). The dust lifts height reached 1-3 m depending on a vehicle type. Taking into account these results, the model (Onikul and Khurshudyan 1983) was improved to consider this effect introducing a virtual surface source of larger width with the same effective height on the strip internal boundary (Garger 2001):

$$l = l_0 + \Delta l, \qquad (7.35)$$

Table 7.3. **Experimental conditions at Zapolie in May 1993, total ^{137}Cs activity concentration due to resuspension and parameters of ^{137}Cs activity size distribution as measured with the PK impactor**

Date and time	Kind of activity	Mean wind and friction velocity (m s^{-1})	Monin-Obukhov length L (m)	Soil humidity H (%)	^{137}Cs activity concentration (mBq m^{-3})	Mean diameter (μm)	Median diameter (μm)
07.05.93–08.05.93 10^{00}–15^{20}	Arrangement of equipment	4.3 , 0.40	–	–	0.81	13.8	11.0
08.05.93 10^{00}–17^{00}	Grass cutting	5.6 , 0.55	–	6.2	1.7	5.5	0.83
11.05.93 12^{20}–14^{10} 16^{15}–17^{25}	Harrowing by small tractor	3.5 , 0.31 3.5 , 0.32	–43 –63	6.1 7.4	4.6	7.7	4.8
12.05.93 11^{45}–13^{45} 16^{30}–18^{30}	Harrowing by small tractor	4.6 , 0.42 5.0 , 0.44	–38 –96	5.2 4.9	6.7	5.6	2.6
13.05.93 11^{30}–16^{30} 17^{15}–18^{40}	Harrowing by large tractor	6.7 , 0.60 6.8 , 0.61	–92 700	– 3.7	68.1	6.8	3.3
14.05.93–20.05.93 12^{00}–10^{00}	Wind resuspension	2.2 , 0.20	± ∞	5.7 7.0 7.1	0.54	5.6	3.0
21.05.93 15^{00}–16^{40}	Driving of truck ZIL131	3.1 , 0.30	–42	4.0	39.3	8.1	5.3
22.05.93 10^{50}–12^{15} 15^{06}–16^{06}	Driving of truck ZIL131	4.6 , 0.45 4.8 , 0.46	–48 –71	2.6 2.1	78.1	8.2	6.4
23.05.93 10^{40}–12^{50}	Harrowing by small tractor	4.7 , 0.47	–36	1.9	41.7	7.1	5.0
24.05.93 15^{30}–18^{30}	Driving of trucks ZIL130 and ZIL131	3.1 , 0.31	–28	1.4	96.7	6.6	3.6
25.05.93 11^{15}–13^{05}	Harrowing by small tractor	5.0 , 0.48	–56	3.5	28.1	8.7	6.8
25.05.93 16^{00}–17^{10}	Driving of truck ZIL131	4.7 , 0.42	–84	3.5	169	6.5	3.0

Table 7.4. **Distribution of the ratio of the sedimentation velocity to the turbulent vertical velocity ω for various particles sizes and micrometeorological conditions**

Diameter of impactor cascades cutoff (μm)	Average diameter of cascade range (μm)	ω 13.05 $u_* = 0.60$ m s^{-1}, $n = 0.27$ morning and noon[a]	ω 12.05 $u_* = 0.42$ m s^{-1}, $n = 0.24$ morning	ω 22.05 $u_* = 0.45$ m s^{-1}, $n = 0.24$ morning	ω 24.05 $u_* = 0.31$ m s^{-1}, $n = 0.24$
30		0.22	0.32	0.30	0.44
	25	0.16	0.24	0.21	0.31
20		0.10	0.14	0.13	0.20
	16	0.07	0.09	0.09	0.13
12		0.04	0.05	0.05	0.07
	9.5	0.03	0.03	0.03	0.04
7		0.01	0.02	0.02	0.02
	5.5	0.008	0.011	0.010	0.015
4		0.004	0.006	0.005	0.008
	3.0	0.003	0.003	0.003	0.004
2		0.001	0.001	0.001	0.002
	1.05	0.0004	0.0005	0.0005	0.0007
0.1		3×10^{-6}	3.3×10^{-6}	3.1×10^{-6}	4.5×10^{-6}

[a]Calculation has been made under assumptions of a power-law dependence of the wind speed on the height with exponent *n*.

Table 7.5. **Emission rate of a radioactive dust Λ**

Date	Vehicle type	Emission rate $\times 10^{-6}$ (s^{-1})	Emission rate for $d \leq 12$ μm $\times 10^{-6}$ (s^{-1})
12.05.93 morning	MTP-82	0.027	0.004
13.05.93 morning	T-150	1.5	0.16
13.05.93 noon	T-150	2.0	0.20
22.05.93 morning	ZIL-131	1.0	0.09
22.05.93 noon	ZIL-131	1.4	0.13
24.05.93 noon	ZIL-131 and ZIL-130	0.48	0.09

where Δl could be calculated with using of consequences of the similarity hypothesis of Lagrange turbulence characteristics of the surface layer of the atmosphere

$$\Delta l = \kappa^{-1} u_* \tau \ln \frac{b_z u_* \tau}{e z_0}, \tag{7.36}$$

where τ is the diffusion time which could be calculated according to the formula

$$h = b_z u_* \tau. \tag{7.37}$$

Here h is the effective height of a dust cloud, which is measured in the experiment. It linearly depends on diffusion time for conditions close to neutral thermal stratification of the surface layer of the atmosphere. In Eq. (7.36) z_0 is the roughness length; e is a logarithmic base; b_z is the universal empirical constant equals to 0.8 (Garger 1982).

In Table 7.3 data of the experiments which have been carried out in Zapolie in May, 1993 are presented. From Table 7.3 it can be seen that the experiments were carried out at moderate wind velocity and conditions which are close to neutral stratification (experiments 13.05.93) and weak thermal instability during other days.

According to data from Table 7.4, almost all particles with diameters smaller 25-30 μm correspond to the criteria of nonsettling particles (Barenblatt 1953).

The evaluations were made using Eq. (7.34). The obtained values of a vertical turbulent flux of ^{137}Cs were normalized by the contamination density of a southwest strip 0.56 ± 0.06 MBq m^{-2}, and northeast strip 0.31 ± 0.05 MBq m^{-2}. All this made it possible to estimate the emission rate according to Eq. (7.1).

In Table 7.5 the results of estimations of the emission rate for various types of vehicles and meteorological conditions are presented. In calculations, the measuring data of the ^{137}Cs activity concentration in the air up to distances about 130 m from a dusting strip and measuring data with the help of cascade impactor were used.

At calculations, the stationary source in the form of an infinite dust strip assumed to exist. Actually, the source was of the limited time of release and finite length. So far as experiments last within one hour and more and the measuring devices were located in the center of the dusting strip at a short distance from it, the edge effects to a first approximation could be neglected. The periods of observations were sufficient the average characteristics of the measured field of the activity concentration were stable. From Table 7.5 one may see that the emission rate reached high values which exceeded the background values (Garger 2001) by four orders of magnitude for the whole fixed particles range and by three orders of magnitude for respiration and inhalation ranges of particles size.

CHAPTER 8

MODELING OF ATMOSPHERIC TRANSPORT OF RESUSPENDED MATERIAL

8.1. General classification of resuspension-diffusion-deposition models

The models of atmospheric dispersion of radioactive substances could be classified according to the following main features determining the properties of the pollution source:

1) release duration (instantaneous, short-term, continuous);

2) geometric dimensions (point, area, line, and volume sources);

3) effective source height;

4) physical and chemical characteristics of the pollutant material.

From this standpoint, the problem of calculating the atmospheric pollution due to resuspension comes to using models of a ground source of aerosol particles with prolonged release duration. The geometrical dimensions of the source (and, accordingly, the model type) may be different depending on the specific problem to be solved: local, linear (infinite or finite size) or area (infinite or finite size) source.

Further, each of these types of resuspension models is subdivided depending on account of the spatial and temporal characteristics of the source. In the former case, a stationary or variable resuspension intensity source can be considered, in the latter - horizontal homogeneous or non-uniform surface contamination density area source.

Selecting the type of resuspension model is justified by a specific problem that has to study. Table 8.1 presents the main ones.

In the case where the contaminated area can be considered as a horizontally homogeneous infinite area source, the methodology for the calculation of airborne radionuclide activity from particulate surface contamination has been ex-

pressed using a resuspension factor (Sehmel 1980). Empirical parameterization of resuspension factors for radionuclides has been discussed in Chapters 3 and 4. As an alternative, a mass loading approach has been applied (Linsley 1978, Anspaugh et al. 1975) in which the concentration of soil in the air is used along with the assumption that the particulate in soil and air contains the same proportion of contaminant (Chapter 6). If the surface contamination density field is substantially nonuniform then a ground source of resuspended aerosol particles should be considered as a source of the finite area or as a combination of such sources. In this case, the air activity concentration can be calculated from atmospheric diffusion and transport models which include the low boundary condition for nuclide transfer across the air-surface interface (Chapter 8.2). Parameterization of an upward aerosol flux from the ground due to resuspension could be made

Table 8.1. **Types of models suitable for some problems of atmospheric contamination and people health caused by radionuclide resuspension**

No	Problem	Source	Model type
1	Assessment, prediction and reconstruction of internal exposure doses of the population living in areas of radioactive contamination as a result of large radiation accidents at nuclear power plants (Chernobyl, Fukushima-1) due to inhalation of radionuclides under their resuspension.	(Jacob et al. 1996, Harada et al. 2014)	Model of an infinite area surface source
2	Assessment, prediction and reconstruction of internal exposure doses of personnel in the territories of the former nuclear weapons tests (in particular, Nevada, USA and Semipalatinsk, Kazakhstan) due to inhalation of radionuclides under their resuspension.	(Mauro et al. 2015, Algazin et al. 1995)	
3	Assessment of horizontal flux of radionuclides due to the resuspension from areas of intensive radioactive contamination onto relatively clean territories (the removal from the Chernobyl exclusion zone, the evacuation zone around the Fukushima-1 NPP).	(Garland, Pattenden and Playford 1992, Yamauchi 2012, Garger and Gavrilov 1992)	Model of a finite area surface source
4	Assessment of the impact of man-made resuspension of radioactive particles due to traffic or agricultural work (plowing, harrowing) in the contaminated area.	(Lebedeff and Hameed 1975)	Model of a ground line source or strip
5	Assessment of a long-range transport of radionuclides due to the resuspension from radioactive contaminated territories	(Vintersved et al. 1994)	Model of a surface point source

on the base of the resuspension rate approach. Some empirical parameterizations for the resuspension rate for radionuclides obtained after measurements within contaminated territories are presented in Chapter 7. But the number of such contaminated sites is limited (nuclear weapon test sites, territories contaminated after large radiation accidents), so these data are limited in scope and linked to specific environmental conditions of their location and the specific characteristics of radioactive contamination. On the other hand, there is a very large amount of bulk soil erosion measurement data. The results of their theoretical analysis, including models to parameterize the eroding soil flux quantity into the atmosphere, could be applied to the radionuclide resuspension problem. Appropriate results of agricultural erosion research are presented in Chapter 8.3.

8.2. Modeling of resuspension from an area surface source

This approach can be used to calculate the atmospheric activity concentration and the density of radioactive deposition on the underlying surface for radionuclides rising from the territory of a finite area. At that, this calculation can be performed for both a territory outside a source and over a source. The main issues, in this case, are: 1) the definition of a resuspended aerosol particles surface source size and the distribution of radioactive contamination density within it; 2) a parameterization of intensity of radionuclides resuspension from a contaminated surface source, and 3) a description of the processes following dispersion of radionuclides in the atmosphere and their redeposition on the underlying surface.

In general, the atmospheric transport of radioactive particles is described by the semi-empirical 3-dimensional equation of turbulent diffusion in the atmospheric boundary layer with appropriate initial and boundary conditions, which describe the specifics of the pollutant source (Csanady 1973):

$$\frac{\partial c}{\partial t} + U\frac{\partial c}{\partial x} + V\frac{\partial c}{\partial y} + (W - w)\frac{\partial c}{\partial z} = \frac{\partial}{\partial x} k_x \frac{\partial c}{\partial x} + \frac{\partial}{\partial y} k_y \frac{\partial c}{\partial y} + \frac{\partial}{\partial z} k_z \frac{\partial c}{\partial z}, \qquad (8.1)$$

where c (t, x, y, z) is the air activity concentration, $\vec{U} = (U, V, W)$ is the wind velocity, w is the particle gravitational sedimentation velocity, k_x, k_y, and k_z are the coefficients of eddy diffusivity.

For the problem of radionuclides resuspension from the contaminated area, the boundary condition on the ground includes data on the spatial distribution of deposition density. In the case of contamination of large areas (for example, in the case of severe radiation accidents) radionuclides deposit in a highly inhomogeneous way (Izrael et al. 1996). The spots of radioactive fallout could be formed of the characteristic scales varied within several orders of magnitude (from a few meters to tens of kilometers).

Therefore, the method of parameterization of radioactive pollutant surface source for a specific resuspension task should be determined by the ratio between the characteristic length scales: linear dimension of the surface contamination area L_s, the characteristic scale of inhomogeneities of radioactive deposition density field within this region L_d, and the distance L_x from the surface contamination area to the point at which the atmospheric concentration activity of resuspended aerosol is calculated. If $L_x >> L_s$, then the size of the surface contamination area and features of the radioactive fallout field within it can be neglected. In this case, the resuspension source can be parameterized as a point surface one with release intensity, defined by the integral stock of radionuclides in it. This problem arises when the long-range transport of resuspended radionuclides estimations (for example, for estimation of radioactivity removal from contaminated sites into relatively clean areas).

In the case where the ratio $L_d \geq L_s \geq L_x$ is satisfied, the source may be described as a surface area one with a constant deposition density within it. Besides, if the shape of such a source is close to the regular shape, the problem can be reduced to the calculation of resuspension from a surface source in the form of a circle, a rectangle, etc.

In other cases (in particular, if the source geometric dimension L_s is comparable or exceed the deposition field inhomogeneity scale L_d, while estimations of the atmospheric activity concentration of radionuclides are carried out either within the contaminated area or in its immediate vicinity, it is expedient to represent this non-uniform source as a sum of the individual rectangular surface sources and to calculate the contribution of each to the total contamination of the atmosphere. Then the problem is actually reduced to the previous case, i.e. calculation of resuspension from a surface source of regular shape.

8.2.1. Modifications of the plume model for calculation of atmospheric transport of resuspended material

For the assessment of resuspended radionuclides diffusion in the atmosphere, the Gaussian plume model is used the most widely (Slade 1968). In its original form, the model was formulated for calculating emissions from the elevated point source (for example, the NPP stack) of constant intensity in stationary meteorological conditions. However, the simplicity of the mathematical formulation of the Gaussian plume model makes it easy to adapt it for the case of a surface source, including area one.

According to the model, the value of the pollutant activity concentration c (Bq m^{-3}) for a stationary point source of an intensity Q (Bq s^{-1}) located on the earth's surface, defined by the formula

$$c(x, y, z) = \frac{QF(x)}{\pi \sigma_y \sigma_z U} \cdot \exp\left[-\frac{y^2}{2\sigma_y^2}\right] \cdot \exp\left[-\frac{z^2}{2\sigma_z^2}\right], \qquad (8.2)$$

where x, y, z are the point coordinates, U is the wind speed (m s^{-1}), σ_y, σ_z are the horizontal and vertical dispersion of the pollutant particle coordinates (m), $F(x)$ is a function of the source depletion.

The emission source is located at the origin of coordinates, and the Ox-axis is directed along the wind velocity.

The source depletion function $F(x) = f_R f_F f_W$ is a part of resuspended radionuclides remaining in the air as a function of downwind distance. The factors f_R, f_F and f_W represent a correction for radioactive decay, loss of material from the plume due to its dry and wet deposition on the underlying surface, respectively. The result of the latter two processes is the formation of pollutant deposition flux on the earth surface.

Input meteorological information for the model is data of standard observations at the meteorological station, including the speed and direction of surface wind, the atmospheric stability class, and the precipitation intensity.

The most widely used schemes to estimate σ_y and σ_z were developed by Pasquill (1961) and Briggs (1973). Briggs' formulas apply from a distance of 0.1 km to approximately 10 km and are extendible to 20 or 30 km, although Briggs does not recommend this extension. However, for lack of any other validation schemes, these formulas are commonly used out to a distance of 100 km (Homann and Aluzzi 2013).

In the case of an area source, a modification of the Gaussian plume model can be made in several different ways.

The first one is the introduction of an upwind virtual source. For area source in the form of a circle with a radius R, the virtual-term point source is positioned at an upwind distance dx, which is obtained from the condition $\sigma_y(dx) = R/2$ (Homann and Aluzzi 2013). In the case of an irregularly shaped area source, the value of R can be regarded as the effective radius of the site.

The second way is a correction of the formulas for calculating of the horizontal dispersion $\sigma_y(x)$ taking into account the horizontal dimensions of an area source. This approach was used by Garger, Gavrilov, and Zhukov (1992) for estimations of the secondary contamination due to resuspension within the 30-km Chernobyl exclusion zone within the period from 1986 to 1988. The activity concentration of ^{137}Cs in the air has been calculated using Eq. (8.2) for the non-deposited pollutant $F(x) = 1$. The equations for the dispersion of the pollutant particles coordinates from the i-th elementary source were the following:

$$\sigma_{zi}^2 = b^2 (x - x_i)^2, \tag{8.3}$$

$$\sigma_{yi}^2 = l_{0i}^2 = a^2 (x - x_i)^2, \tag{8.4}$$

where $a = 0.08$, $b = 0.05$, x_i, y_i are the coordinates of the elementary source center, l_{0i} is the side length of the square elementary source.

The third way is obtaining the equation of the air concentration for an area source by integrating the equation for a point source over the source area. Nimmatoori and Kumar (2013) developed a ground-level area source analytical dispersion model taking into account dry deposition v_d and gravitational settling w velocities of the particle. An area source of width X and length Y is divided into n number of strips of equal width dX and length Y.

$$c(x,y,z)=\frac{Q}{2\sqrt{2\pi}}\sum_{i=1}^{n}\frac{1}{\sigma_{zi}}\exp\left(-\frac{wz}{2K}-\frac{w^2\sigma_{zi}^2}{8K^2}\right)\times$$

$$\times\left[2\exp\left(-\frac{z^2}{2\sigma_{zi}^2}\right)-\sqrt{2\pi}\,\frac{v_1\sigma_{zi}}{K}\exp\left(\frac{v_1 z}{K}+\frac{v_1^2\sigma_{zi}^2}{2K^2}\right)\times\right.$$

$$\left.\times\operatorname{erfc}\left(\frac{v_1\sigma_{zi}}{\sqrt{2}K}+\frac{z}{\sqrt{2}\sigma_{zi}}\right)\right]\cdot 2\operatorname{erf}\left(\frac{Y/2}{\sqrt{2}\sigma_{yi}}\right)\delta X, \tag{8.5}$$

where σ_{yi} is the horizontal dispersion coefficient of the i-th strip (m), σ_{zi} is the vertical dispersion coefficient of the i-th strip (m), U is the wind speed (m s^{-1}), $v_1=v_d-w/2$, $K=\frac{\sigma_z^2 U}{2x}$ is the eddy diffusivity (m^2 s^{-1}).

The equations for the horizontal and vertical dispersion coefficients were taken from Smith (1993):

$$\sigma_y=0.84678x\tan(a-b\ln x); \tag{8.6}$$

$$\sigma_z=cx^d. \tag{8.7}$$

The values of the parameters a, b, c, and d were also taken from Smith (1993).

In all three cases, the intensity of the area source Q (Bq s^{-1}) in Eqs. (8.2) and (8.5) can be parameterized using the resuspension rate Λ (s^{-1}) (see Chapter 7):

$$Q=\Lambda DS, \tag{8.8}$$

where D is the deposition density (Bq m^{-2}) and S is the source area (m^2).

For the upwind virtual source approach Homann and Aluzzi (2013) used an alternative formula for Q on the base of the resuspension factor K (m^{-1}):

$$Q=K(U)\cdot D\cdot\pi\cdot\sigma_{y,\,origin}\cdot\sigma_{z,\,origin}\cdot U, \tag{8.9}$$

where U is the wind speed (m s^{-1}), $K(U)$ is the resuspension factor adjusted for wind speed according to Eq. (4.19), $\sigma_{y,\,origin}$ and $\sigma_{z,\,origin}$ are the Gaussian standard deviations evaluated at a distance equal to the distance from the origin to the upwind virtual source position (m).

8.2.2. Modeling of Atmospheric Transport and Deposition of Resuspended Material using Analytic Solutions of the Turbulent Diffusion Equation

Some resuspension models use analytical solutions of the turbulent diffusion equation for a ground surface point or an area source of regular form, in which the dependencies of the vertical profiles of wind and the eddy diffusion coefficient in the atmospheric boundary layer are parameterized in the form of simple functions.

In most models, presented below, the source intensity is specified by the resuspension flux (Bq m^{-2} s^{-1}) value in the lower boundary condition of the turbulent diffusion equation. This value can be calculated through the resuspension rate (see Chapter 7) or is set using special models for fluxes of aerosols presented (see Chapter 8.3).

Models of a semi-infinite area source. In steady conditions transport of resuspended aerosol pollutant in the atmosphere over uniform area source extending from $x=0$ to $x=\infty$ may be described by the 2-dimensional diffusion equation

$$U(z)\,\frac{\partial c}{\partial x} - w\frac{\partial c}{\partial z} = \frac{\partial}{\partial z}\left(k_z \frac{\partial c}{z}\right) \tag{8.10}$$

with the boundary condition

$$-\left(k_z \frac{\partial c}{\partial z} + wc\right) = A_0 > 0, \quad z = 0, \tag{8.11}$$

where A_0 is the flux from the source (the pollutant flux from the underlying surface to the atmosphere, averaged over the dusty surface).

In Eq. (8.10) U is the turbulent-mean wind, assumed to be in the x direction, w is the velocity of particles gravitational settling, k_z is the coefficient of eddy diffusivity in the vertical direction, and $c\,(x, z)$ is the concentration of the transported substance.

The boundary condition at the upwind edge of the source is

$$c\,(x, z) = 0, \quad x = 0, \tag{8.12}$$

and for large values of z

$$c\,(x, z) = 0, \quad z \to \infty. \tag{8.13}$$

The z dependence of the wind and the diffusivity is represented by empirically determined power laws:

$$U(z) = u_1 z^m,\ k_z(z) = k_1 z^n, \tag{8.14}$$

where m and n are constants depending on the roughness height of the underlying surface and the atmospheric stability class.

Lebedeff and Hameed (1975) found a solution of the problem represented by Eqs. (8.10)-(8.14) for the concentration of a weightless and non-depositing ($w = v_d = 0$) substance as:

$$c(x, z) = \frac{A_0}{k_1} \frac{z^{1-n}}{(2+m-n)\,\Gamma(1-\nu)} \Gamma\left[-\nu, \frac{u_1 z^{2+m-n}}{k_1(2+m-n)^2 x}\right] \tag{8.15}$$

where $\Gamma(t)$ is the gamma function, $\Gamma(p,\ t) = \int_t^\infty e^{-x} x^{p-1} dx$ is the upper incomplete gamma function, and

$$\nu = \frac{1-n}{2+m-n}. \tag{8.16}$$

For $n < 1$ the near-ground concentration is

$$c(x, z=0) = \frac{A_0}{k_1} \frac{(2+m-n)^{2\nu-1}}{\nu\Gamma(1-\nu)} \left(\frac{k_1 x}{u_1}\right)^{\nu}, \quad n < 1. \tag{8.17}$$

For $n \geq 1$ the concentration at z=0 is infinite.

Gavrilov and Gormatyuk (1989) studied a similar problem on the pollutant diffusion from the dusty surface in the case of a more general description the interaction of the aerosol particles with the underlying surface. In the case of ***a weightless pollutant (w = 0)*** the boundary conditions for Eq. (8.10) were given in the form of

$$c(x, z) = c_a, \quad x < 1, \tag{8.18}$$

$$c(x, z) = c_a, \quad z \to \infty, \tag{8.19}$$

$$-k_z \frac{\partial c}{\partial z} + v_d c = A_0, \quad z = 0, \tag{8.20}$$

where c_a is the background pollutant concentration in the atmosphere, v_d is the particle dry deposition velocity on the underlying surface.

The wind speed and the vertical eddy diffusion coefficient were given by Eq. (8.14).

The solution for a semi-infinite uniformly dusty surface has been found in the form of an infinite series in terms of the dry deposition velocity v_d. Since this series converges quickly enough, so for practical calculations the zeroth-order approximation can be used, which corresponds to the first term of the series in terms of v_d

$$c(\xi, \zeta) = c_a + \alpha\left(c_a + \frac{A_0}{v_d}\right) \frac{\nu}{\Gamma(1-\nu)} \left\{\zeta\Gamma\left(-\nu, \frac{\nu^2\zeta^{1/\nu}}{2\xi}\right) -\right.$$

$$\left. -\,\alpha \frac{\nu^{2(1-\nu)}\Gamma(\nu)\Gamma(\nu-1)}{\Gamma(1-\nu)\Gamma(1+\nu)} \zeta^{(\nu-1)/2\nu} \exp\left(-\frac{\nu^2\zeta^{1/\nu}}{2\xi}\right) \times W_{-(3\nu+1)/2,\,\nu/2}\left(\frac{\nu^2\zeta^{1/\nu}}{2\xi}\right)\right\}, \tag{8.21}$$

where $\xi = \frac{x}{\tilde{L}}$; $\zeta = \left(\frac{u_1}{k_1 \tilde{L}}\right)^{\nu} \frac{z^{1-n}}{(1-n)^{2\nu}}$ are the dimensionless coordinates, $\tilde{L}$ is the characteristic scale of the problem, $\Gamma(\nu, x)$ is the incomplete gamma function, $W_{\mu,\nu}(z)$ is the Whittaker function, parameter ν is defined according to Eq. (8.16), and

$$\alpha = \frac{v_d}{k_1} \left(\frac{k_1 \tilde{L}}{u_1}\right)^{\nu} (1-n)^{2\nu-1}. \tag{8.22}$$

The former term in braces in Eq. (8.21) describes the pollutant dispersion due to advection and diffusion, and the latter — the pollutant depletion in the plume due to the deposition on the underlying surface.

At zero background concentration $c_a = 0$ and non-deposited pollutant ($v_d = 0$), the first term in the braces of (8.21) coincides with the solution of Lebedeff and Hameed (1975) according to Eq. (8.15).

From Eq. (8.21) in the zeroth-order approximation, the near-ground concentration from a uniformly dusting surface is

$$c(\xi, \zeta = 0) = c_a + \alpha \left(c_a + \frac{A_0}{v_d}\right) \frac{\nu}{\Gamma(1-\nu)} \times$$

$$\times \left\{\nu^{1-2\nu}\, \xi^{\nu} - \alpha \frac{\nu^{3(1-\nu)} \Gamma^2(\nu)\, \Gamma(\nu-1)}{\Gamma(1-\nu)\, \Gamma(1+\nu) \Gamma(2\nu)}\, \xi^{2\nu}\right\}, \tag{8.23}$$

In the case of the diffusion of sedimented pollutant ($w \neq 0$) Gavrilov and Gormatyuk (1989) obtained an analytical solution of the problem Eq. (8.10), (8.18)-(8.20), (8.14) for neutral stratification, i.e., $n = 1$. It was shown that in this case, the solution of the problem reduces to the solution of the previous one by proposed substitution for parameters m, n, ν, and ζ. In the special case of a uniformly dusting surface when $q_a = v_d = 0$ the obtained solution for the pollutant concentration field comes to:

$$c_w(x, z) = \frac{A_0 z^{w/k_1}}{k_1(1+m)\, \Gamma\left[1 - \frac{w}{k_1(1+m)}\right]} \Gamma\left[1 - \frac{w}{k_1(1+m)}, \frac{u_1 z^{1+m}}{k_1(1+m)^2 x}\right]. \tag{8.24}$$

The surface concentration can be represented as

$$c_w(x, z = 0) = \frac{A_0}{w} \left[\frac{(1+m) k_1 x}{u_1}\right]^{w/k_1(1+m)} \frac{1}{\Gamma\left[1 - \frac{w}{k_1(1+m)}\right]}. \tag{8.25}$$

Models of an infinite strip. The model describes the pollutant diffusion from a stationary ground area source in the form of the strip of infinite length ($0 \le x \le L'$, $-\infty < y < \infty$). The same as for the semi-infinite source, the problem is represented by Eqs. (8.10)-(8.14). Besides, in all models described below a tur-

bulent flux outside the strip ($x > L'$) was assumed to be zero

$$k_z \frac{\partial c}{\partial z} = 0, \quad z = 0, \tag{8.26}$$

According to the model of Lebedeff and Hameed (1975) for the source in the form of a strip $0 < x < L$ the near-ground concentration of weightless and undeposited pollutant outside is

$$c(x, z=0) = \frac{A_0}{k_1} \frac{(2+m-n)^{2\nu-1}}{\nu\Gamma(1-\nu)} \left(\frac{k_1}{u_1}\right)^{\nu} [x^{\nu} - (x-L')^{\nu}], \quad x > L'. \tag{8.27}$$

Onikul and Khurshudyan (1983) generalized a model of «dusting strip» on the case of distribution of settling pollutant. At that, the wind speed and the vertical eddy diffusion coefficient were set by Eq. (8.14), but the problem was solved only for the linear profile of k_z, i.e. $n = 1$ was assumed in Eq. (8.14).

The solution of the turbulent diffusion equation with these boundary conditions gives the following expression for the pollutant concentration in the air over the strip ($0 \le x \le L'$)

$$c(x, z) = \frac{A_0}{(1+m)k_1 \Gamma\left[1 - \frac{w}{k_1(1+m)}\right]} \Gamma\left[-\frac{w}{k_1(1+m)}, \frac{u_1 z^{1+m}}{k_1(1+m)^2 x}\right]. \tag{8.28}$$

The resulting solution is different from the similar solution of Gavrilov and Gormatyuk (1989) (Eq. (8.24)). The difference between Eqs. (8.24) and (8.28) is due to the use of various forms of the boundary condition on the underlying surface. The ground-level concentration according to Eq. (8.28) diverges, and for the solution of Gavrilov and Gormatyuk (1989) (Eq. (8.24)), it is a finite value, increasing with distance.

The distribution of the pollutant concentration in the air beyond the source ($x > L'$) can be expressed by the formula

$$c(x, z) = \frac{A_0 \left(\frac{x}{L'}\right)^{-\omega} e^{-u_1 z^{1+m}/(1+m)^2 k_1 x} {}_2F_1\left(1; 1; 2+\omega; \frac{L'}{L+x}\right)}{k_1(1+m)\,\Gamma(1-\omega)\,\Gamma(1+\omega)\,(1+\omega)\,(1+x/L')}, \tag{8.29}$$

where $\omega = \frac{w}{k_1(1+m)}$, and ${}_2F_1(c_1; c_2; c_3; t)$ is the hypergeometric function.

The ground-level concentration is determined by the following expression:

$$c(x, 0) = \frac{A_0^{-\omega} {}_2F_1\left(1; 1; 2+\omega; \frac{L'}{L+x}\right)}{k_1(1+m)\,\Gamma(1-\omega)\,\Gamma(1+\omega)\,(1+\omega)\,(1+x/L')}. \tag{8.30}$$

When $\omega < 1$ the expression (8.30) can be reduced to the form

$$c(x, z) = \frac{A_0 \sin(\pi\omega) \int_1^{1+L'/x} \frac{(t-1)^{\omega}}{t} dt}{k_1(1+m)\pi\omega} \cdot \exp\left(-\frac{u_1 z^{1+m}}{k_1(1+m)^2 x}\right). \quad (8.31)$$

For weightless pollutant ($\omega = 0$) the ground-level concentration is determined according to

$$c_s(x, 0) = \frac{A_0}{k_1(1+m)} \ln \frac{x+L'}{x}. \quad (8.32)$$

In the case of a dusty strip of width L Gavrilov and Gormatyuk (1989) have got the solution for the weightless non-deposited pollutant ($w = v_d = 0$) outside:

$$c^{out}(x, z) = c_a + \frac{A_0 z^{1-n}}{k_1(2+m-n)\Gamma(1-\nu)} \times$$

$$\times \left\{\Gamma\left[-\nu, \frac{u_1 z^{2+m-n}}{k_1(2+m-n)^2 x}\right] - \Gamma\left[-\nu, \frac{u_1 z^{2+m-n}}{k_1(2+m-n)^2 (x-L')}\right]\right\}. \quad (8.33)$$

In the case of a dusty strip of width L' the solution for the *settled non-deposited pollutant* ($w \neq 0$, $v_d = 0$) outside is:

$$c_w^{out}(x, z) = c_a + \frac{A_0 z^{w/k_1}}{k_1(1+m)\Gamma\left[1-\frac{w}{k_1(1+m)}\right]} \times$$

$$\times \left\{\Gamma\left[1-\frac{w}{k_1(1+m)}, \frac{u_1 z^{1+m}}{k_1(1+m)^2 x}\right] - \Gamma\left[-\frac{w}{k_1(1+m)}, \frac{u_1 z^{1+m}}{k_1(1+m)^2 (x-L')}\right]\right\}. \quad (8.34)$$

Model of a rectangle source. Garger, Gavrilov and Zhukov (1992) used the model of resuspension from the rectangular surface source with sides of L_x and L_y, described by the following boundary conditions:

$$k_z \frac{\partial c}{\partial z} - wc\Big|_{z=z_0} = \begin{cases} -\Lambda D & \text{for } 0 < x < L_x, \ |y| \le \frac{L_y}{2}, \\ 0 & \text{for } x > L_x \text{ or } |y| \le \frac{L_y}{2}. \end{cases} \quad (8.35)$$

The wind speed and vertical eddy diffusion coefficient were set in the form of power function according to Eq. (8.14), and the horizontal eddy diffusion coefficient was equals to

$$k_z = \frac{1}{2} U \frac{d\sigma_y^2(x)}{dx}, \quad (8.36)$$

The solution of the semiempirical equation of turbulent diffusion with the boundary condition (8.35) in (Garger, Gavrilov and Zhukov 1992) has the form

$$c(x, y, z) = \frac{\Lambda D z^{1-n} \exp(-y^2/2\sigma_y^2)}{\sqrt{2\pi}\,\sigma_y k_1 (2+m-n)\ \Gamma(1-\nu)} \times$$

$$\times \left\{ \Gamma\left[-\nu, \frac{a z^{2+m-n}}{k_1 (2+m-n)^2 x}\right] - \Gamma\left[-\nu, \frac{a z^{2+m-n}}{k_1 (2+m-n)^2 (x-L_x)}\right] \right\}. \qquad (8.37)$$

Models of a point ground source. The problem of pollutant diffusion from a surface point source was investigated by Slinn (1976). He has found analytic solutions of equations describing the radioactive contaminants diffusion-deposition-resuspension problem. He used equations for the pollutant air concentration C, integrated over z

$$C(x, y, t) = \int_0^\infty c(x, y, z, t)\, dz \qquad (8.38)$$

and for the deposition density D under the assumption $U(z) = \overline{u} = const$.

The set of the equation has been obtained in the form

$$\frac{\partial C}{\partial t} + \overline{u}\frac{\partial C}{\partial x} = \Lambda D - \Omega C, \qquad (8.39)$$

$$\frac{\partial D}{\partial t} = \Omega C - (\Lambda + \alpha) D, \qquad (8.40)$$

where a is the rate at which D becomes fixed to the surface and thereby unavailable for resuspension. In Eqs. (8.39)-(8.40) in analogy with the resuspension rate Λ, a deposition rate Ω has been defined. This value must be understood as some «effective» intensity of the radionuclides removal from the atmosphere due to the dry deposition process.

In the case of a ground source, given with initial conditions

$$C(x, t=0) = 0;\ \ C(x=0, t) = 0;\ \ D(x, t=0) \equiv D_0 = Q_0 \delta(x - x_0) \qquad (8.41)$$

the solution of Eqs. (8.39)-(8.40) for the value C is:

$$C(x, t) = \frac{\Lambda Q_0}{u} \exp\{-\Omega\tau - (\Lambda + \alpha)(t-\tau)\} \times I_0\left[2\{\Omega\Lambda\tau(t-\tau)\}^{1/2}\right], \qquad (8.42)$$

where $\tau = (x - x_0)/\overline{u} \le t$, I_0 is the zeroth order modified Bessel function.

The solution of the system for the deposition density

$$D(x, t) = D_0(x) \exp[-(\Lambda + \alpha)\, t] +$$

$$+ \frac{\Lambda Q_0}{2\overline{u}} \frac{e^{-\Omega\tau}}{\Omega\tau} \times \exp\{-(\Lambda + \alpha)(t-\tau)\} \times \xi^{1/2} \times I_1(\xi^{1/2}), \qquad (8.43)$$

where $\xi = 4\Omega\Lambda\tau(t-\tau)$.

Using the obtained formula, Slinn gave a first estimate of the air concentration downwind of a point source taking into account diffusion of radionuclide in the y- and z-directions:

$$c(x, y, z, t) \cong \frac{\Lambda Q_0}{\pi \overline{u}\, \sigma_y \sigma_z} \exp\left\{-\Omega \frac{(x-x_0)}{\overline{u}} - (\Lambda+\alpha)\left[t - \frac{(x-x_0)}{\overline{u}}\right]\right\} \times$$

$$\times I_0\left[2\left\{\Omega\Lambda \frac{(x-x_0)}{\overline{u}}\left[t - \frac{(x-x_0)}{\overline{u}}\right]\right\}^{1/2}\right] \times \exp\left[-\left(\frac{y^2}{2\sigma_y^2} + \frac{z^2}{2\sigma_z^2}\right)\right]. \quad (8.44)$$

The resulting solution describes the dependence of the radionuclide concentration in the atmosphere in space and time, which is determined by resuspension from a point source located at the point $x = x_0$, taking into account the radionuclides deposition and their repeated resuspension downwind (for $x_0 \le x \le \infty$).

The solution (8.42) is the Green's function for the problem, so it can be used to determine the concentration field for an arbitrary initial distribution of a ground source $D(x, t=0)$.

In the model of Slinn, the radionuclide concentration in the air depends on the deposition rate Ω. Slinn did not lead its rigorous definition, made a note that for a pollutant with an approximately uniform concentration in the atmospheric mixed layer of height H this value $\Omega = v_d/H$. It is obvious that the relationship Ω with dry deposition velocity v_d is ambiguous since it is determined not only by pollutant properties, the underlying surface, meteorological parameters, but also depends on the specific height distribution of radionuclide concentration within the mixing layer formed at this time. However, as can be seen from Eq. (8.44), this value is used for calculations assuming a Gaussian distribution of the concentration in the air with height, resulting in an internal contradiction in the model. In general, to obtain a self-consistent solution within the Slinn model the system of equations should include one more equation to calculate the value of Ω.

Zhuang (1998) obtained a generalized solution of the Slinn equations system of Eqs. (8.39) and (8.40). In the Slinn task for a given initial ground source, Zhuang included an effect of a gradual redistribution of deposited contamination with time. According to the model, the continuously deposited contamination becomes an additional source for downwind air and ground concentrations. This effect is included in the last term on the right-hand side of Eq. (8.39) and resulted to a solution in the form

$$C(x, t) = C(x - \overline{u}\, t, 0) \exp(-\Omega t) + \frac{\Lambda}{\overline{u}} \int_0^x D\left(x_0, t - \frac{x-x_0}{\overline{u}}\right) \exp\left(-\frac{x-x_0}{\overline{u}}\Omega\right) dx_0 \quad (8.45)$$

$$D(x, t) = D(x, 0) \exp[-(\Lambda+\alpha)\, t] + \Omega \int_0^t C(x, t-\tau) \exp[-(\Lambda+\alpha)\, \tau]\, d\tau \quad (8.46)$$

In Eq. (8.45) $C(x-x_0-Ut,\ 0)=0$, when $x-x_0<Ut$ and $D\left(x_0,\ t-\frac{x-x_0}{U}\right)=0$, when $t<\frac{x-x_0}{U}$.

Equation (8.45) indicates that the air concentration at any location is due either to the advection of an upstream air concentration (the first term) or to the resuspension of the ground concentration from the upstream source at an earlier time (the second term). Equation (8.46) reveals that the ground concentration decreases exponentially as a result of resuspension and soil fixation and increases due to deposition.

The system of Eqs. (8.45)-(8.46) can be solved by successive approximations. The air and ground concentrations at any downwind location and at any time can be calculated in such a way.

Gavrilov and Gormatyuk (1989) have got the solution for the problem of calculating the concentration field from the stationary point ground pollutant source. Assuming that the diffusion coefficient k_y depends only on the distance from the source x, the concentration field can be represented as a Gaussian form

$$q(x, y, z)=\frac{\exp\left[-\frac{y^2}{2\sigma_y^2(x)}\right]}{\sqrt{2\pi}\,\sigma_y(x)}\,c(x, z), \tag{8.47}$$

where $k_y=\frac{1}{2}\,U\frac{d\sigma_y^2(x)}{dx}$, $\sigma_y(x)$ is the lateral dispersion.

The semi-empirical turbulent diffusion equation for the two-dimensional problem was used in the form

$$U(z)\,\frac{\partial c}{\partial x}-w\frac{\partial c}{\partial z}=\frac{\partial}{\partial z}\left(k_z\frac{\partial c}{\partial z}\right)+s(x, z), \tag{8.48}$$

where the function $s(x, z)$ was set as a

$$s(x, z)=Q\delta(x)\,\delta(z), \tag{8.49}$$

which corresponds to a point source of an intensity Q, located at the origin.

Parameterizations for the wind speed and the vertical turbulent diffusion coefficient were given by Eq. (8.14).

The solution of Eqs. (8.48)-(8.49) with the boundary conditions (8.18)-(8.19) and the lower boundary condition

$$k_z\frac{\partial c}{\partial z}+wc=0,\quad z=0, \tag{8.50}$$

for the weightless pollutant ($w=0$) was obtained in the form of an infinite series in terms of the dry deposition velocity v_d. The same as for a **model of a semi-**

infinite area source (Eq. (8.23)) the obtained expression for the concentration field can be used in the zeroth-order approximation as

$$c(\xi,\zeta)=c_a+\frac{Q}{Q_0}\frac{\nu^{1-2\nu}\exp\left(-\frac{\nu^2\zeta^{1/\nu}}{\xi}\right)}{\Gamma(1-\nu)\xi^{1-\nu}}-$$

$$-\alpha\frac{Q}{Q_0}\frac{\nu^{3(1-\nu)}\Gamma(\nu-1)\,\Gamma(\nu)\,\xi^{(3\nu-1)/2}}{\Gamma^2(1-\nu)\,\Gamma(1+\nu)}\exp\left(-\frac{\nu^2\zeta^{1/\nu}}{2\xi}\right)\times W_{(3\nu-1)/2,\,\nu/2}\left(\frac{\nu^2\zeta^{1/\nu}}{\xi}\right), \qquad (8.51)$$

where

$$Q_0=\tilde{L}u_1\left(\frac{k_1\tilde{L}}{u_1}\right)^{1-\nu}(1-n)^{1-2\nu}, \qquad (8.52)$$

and the other values are specified in the notation to Eq. (8.21).

For *non-deposited pollutant* ($v_d=0$) and a zero background concentration, the weightless pollutant concentration distribution from a ground point source was obtained the same as in (Berlyand 1975, Huang 1979).

$$c(\xi,\zeta)=\frac{Q}{Q_0}\frac{\nu^{1-2\nu}\exp\left(-\frac{\nu^2\zeta^{1/\nu}}{\xi}\right)}{\Gamma(1-\nu)\xi^{1-\nu}}=Q\frac{\exp\left[-\frac{u_1 z^{2+m-n}}{k_1(2+m-n)^2x}\right]}{u_1^{\nu}k_1^{1+\nu}(2+m-n)^{1-2\nu}\Gamma(1-\nu)x^{1-\nu}}. \qquad (8.53)$$

The expression for the near-ground concentration in the zeroth-order approximation is

$$c(\xi,\zeta=0)=c_a+\frac{Q}{Q_0}\frac{\nu^{1-2\nu}}{\Gamma(1-\nu)\xi^{1-\nu}}-\alpha\frac{Q}{Q_0}\frac{\nu^{3(1-\nu)}\Gamma^2(\nu)\Gamma(\nu-1)}{\Gamma^2(1-\nu)\Gamma(1+\nu)\Gamma(2\nu)}\xi^{2\nu-1}. \qquad (8.54)$$

The former term in Eq. (8.54) describes the decrease of the near-ground concentration with the distance from the source, proportional to $x^{\nu-1}$, while the latter describes the distribution of the deposited pollutant on the underlying surface, proportional to $x^{2\nu-1}$.

In the case of the *settled pollutant* ($w\neq 0$) diffusion from a continuous ground point source for the neutral stratification ($n=1$) Gavrilov and Gormatyuk (1989) have obtained a general solution for the field of concentration of settled particles taking into account their dry deposition.

In the special case of non-deposited ($v_d=0$) pollutant at $q_a=0$ this solution for the concentration field from a continuous ground point source is

$$c_w(x,z)=Q\frac{(1+m)^{2w/k_1(1+m)-1}\,e^{-(u_1z^{1+m})/k_1(1+m)^2x}}{u_1^{\,w/k_1(1-m)}\,k_1^{\,1-w/k_1(1+m)}\,\Gamma\left[1-\frac{w}{k_1(1+m)}\right]x^{1-w/k_1(1+m)}}. \qquad (8.55)$$

8.2.3. Low boundary condition for the equation of turbulent diffusion of resuspended material

Selecting the lower boundary condition at the height $z = 0$ gives rise to many problems with the interpretation of obtained solutions and the comparison them with data of experimental observations. Buikov (1990) highlighted the major uncertainties associated with this condition. Exact analytical solution Eq. (8.28) of the turbulent diffusion equation becomes infinite at $z = 0$. However, the divergence of the solution for concentration $c(x, y, 0)$ in a thin near-ground layer of the air is physically untenable. It is a consequence of the parameterization of vertical turbulent diffusion coefficient as an exponential or linear function increasing with height at which $k_z(z \to 0) \to 0$. Makhonko (2008) noted that this choice of vertical profile k_z can not explain the rise of the dust particles in the air from the soil surface due to the turbulent diffusion mechanism. In this regard, in some studies, the modified lower boundary condition has been suggested.

Buikov (1990) proposed to set it at a certain height $z = z^*$. In the layer $z < z^*$ a turbulent transport is considered to be negligible, so the pollutant concentration is assumed a constant over height within it. The pollutant exchange in this layer with the rest of the turbulent flow will be due to vortices, whose dimensions are comparable to z^*. Theoretical evaluations made in this study showed that the choice of the value of z^* can have a significant impact on the surface concentration in the case of the microscale spottiness of the original deposition field. When establishing a quasi-uniform balance between the near-surface layer and the rest of the flow a specification of the boundary conditions will be negligible. At that, the theoretical estimations for selecting the value of z^*, obtained in (Buikov 1990), proved to be much too high, so the author proposed to conduct special experiments to determine the thickness of the near-surface layer.

Kind (1992) analyzed the theoretical solution for the concentration profile of suspended particles above an infinite surface source. A one-dimensional turbulent diffusion equation could be applied in this task in the form

$$\frac{d}{dz}\left(k_z \frac{dc}{dz}\right) + w\frac{dc}{dz} = 0, \tag{8.56}$$

where $k_z = \kappa u_* z$ was assumed.

For particles with non-zero settling velocity w integration of Eq. (8.56) yields

$$\kappa u_* z \frac{dc}{z} + wc = -\Phi, \tag{8.57}$$

where the constant of integration Φ represents the net vertical flux of particles at any height z. It determines the balance between the upward transport mechanism due to turbulent diffusion and gravitation settling. If Eq. (8.57) is treated as the boundary condition at a certain height z_r above the ground, then in the case

$\Phi = 0$ when $z = z_r$ the solution of Eq. (8.56) is

$$c(z) = c(z_r)\left(\frac{z}{z_r}\right)^{-w/\kappa u_*}, \tag{8.58}$$

where $c(z_r)$ is the concentration at a reference height z_r. Kind (1972) noted that the reference height should be chosen such that it is outside the saltation later.

Thus, if the underlying surface is not a source or a sink for the particles in the air (the flux of depositing particles is balanced by the flux of resuspended particles), the solution of Eq. (8.56) gives an exponential decrease of the concentration with height. The vertical gradient of the particle concentration is determined by their gravitational sedimentation velocity. For very fine particles the settling velocity tends to zero and according to Eq. (8.56) concentration profile tends to be uniform that is contradicting the expected logarithmic profile (Monin 1970).

In general case of the non-zero net vertical flux of particles Φ at the low boundary height z_r Kind obtained the solution of Eq. (8.56) in the form

$$c(z) = \left[\frac{\Phi}{w} + c(z_r)\right]\left(\frac{z}{z_r}\right)^{-w/\kappa u_*} - \frac{\Phi}{w}. \tag{8.59}$$

For very fine particles $w \to 0$ the logarithmic concentration profile could be obtained from Eq. (8.57) as

$$c(z) = c(z_r) - \frac{\Phi}{\kappa u_*}\ln\left(\frac{z}{z_r}\right). \tag{8.60}$$

According Eqs. (8.59) and (8.60) with an increase in the height the concentration approaches zero and becomes negative, so solutions of one-dimensional equation (8.56) become unrealistic. Kind showed that above some height over particle covered surface the problems must be treated as two-dimensional. Above this height, there is a net downwind convective flux of particles which balances the vertical flux Φ and effectively acts as a sink for the upcoming particles. As a result, the concentration gradient at these heights is less steep than that predicted by Eq. (8.59) and the concentration doesn't become negative.

Similar arguments were used by Makhonko (1984, 2008). To solve the problem of raising dust above the uniformly contaminated site the lower boundary condition was set at the height $z = 0$, however, to correct the problem of the solution divergence $c(z \to 0)$ the vertical profile of the vertical turbulent diffusion coefficient was set different from zero at $z = 0$:

$$\begin{aligned} k_z &= k_0 + \frac{k_1}{z_1}z, \qquad z \le H, \\ k_z &= k_0 + \frac{k_1}{z_1}H, \quad z > H. \end{aligned} \tag{8.61}$$

In Eq. (8.61) $k_0 = D + k_{0z}$ is the sum of the coefficient of Brownian diffusion of aerosol particles (or the coefficient of molecular diffusion of gaseous pollutant) in the air, and $k_{0z} = p\overline{k_z}$ characterizes the turbulent flux at the height of the dust particles lying on the ground, which results in its separation from the earth surface. This value is determined by the likelihood of turbulent eddies breakthrough to the surface p and the average value of $\overline{k_z}$ characterizing these vortices.

Also, it was assumed that the coefficient of vertical turbulent diffusion increases linearly with height only to the atmospheric surface layer height H. Therefore, the turbulent diffusion equation was solved separately for the two layers ($0 < z < H$ and $z > H$). In the approximation of a weightless pollutant and provided its full reflection from the underlying surface Makhonko used it as follows:

$$\frac{d}{dz}\left(k_z \frac{dc}{dz}\right) = \Lambda c, \tag{8.62}$$

where $\Lambda = \frac{v_{eff}}{H}$, v_{eff} is the effective rate of dust removal from the atmosphere as a result of it's self-cleaning by different mechanisms.

Equation (8.62) has been solved with the boundary conditions (8.13),

$$k_z \frac{dc}{dz} = -\Lambda D \qquad \text{at } z = 0, \tag{8.63}$$

$$c(H - \varepsilon) = c(H + \varepsilon) \qquad \text{at } \varepsilon \to 0, \tag{8.64}$$

$$k_z(H - \varepsilon)\frac{dc(H - \varepsilon)}{dz} = k_z(H + \varepsilon)\frac{dc(H + \varepsilon)}{dz} \qquad \text{at } \varepsilon \to 0. \tag{8.65}$$

The last two formulas are the conditions of solutions joining at $z = H$.

The solution of the problem (8.62), (8.13), (8.63)-(8.65) for $z \le H$ is:

$$c(z) = \frac{\Lambda D}{\sqrt{\Lambda k_0}} \frac{I_0(\xi) + \mu K_0(\xi)}{-I_0(\xi_0) + \mu K_1(\xi_0)}, \tag{8.66}$$

where Λ is the resuspension rate, D is the density of soil contamination, I_0, I_1 are the zeroth and first order modified Bessel functions, respectively, K_0, K_1 are the zeroth and first order Macdonald functions, $\xi = \frac{2z_1}{k_0}\sqrt{\Lambda\left(k_0 + \frac{k_1}{z_1}z\right)}$, $\xi_0 = \frac{2z_1}{k_0}\sqrt{\Lambda k_0}$, $\mu = \frac{I_0(\xi_H) - I_1(\xi_H)}{K_1(\xi_H) - K_0(\xi_H)}$, $\xi_H = \frac{2z_1}{k_1}\sqrt{\Lambda\left(k_0 + \frac{k_1}{z_1}H\right)}$.

Makhonko (1979) has solved the problem of divergence of the turbulent diffusion equation solution for a point ground source in a different way. He set a ground source of resuspended dust not at the earth's surface $z = 0$, but the roughness height z_0 of the underlying surface. At that the wind speed was taken to increase with height as a power law (8.14), the turbulent diffusion coefficient k_z was taken linearly increasing with height ($n = 1$ in Eq. (8.14)), and the lateral

turbulent diffusion coefficient was set as

$$k_y = b_y^2 x u_1 \left(\frac{z}{z_1}\right)^m, \tag{8.67}$$

where $b_y = 0.08$ is an empirical constant.

As the boundary conditions, the pollutant flux to the surface was assumed equal to zero and $c \to 0$ when $x = y = z \to 0$.

As a result, Makhonko (1979) derived an expression for the pollutant concentration $c(x, y, z)$, determined by dust resuspension from a point source located at a height z_0, as

$$c(x, z) = \frac{\Lambda A_0}{\sqrt{2\pi}\,(1+m)\,k_1 b_y x^2} \times$$

$$\times \exp\left[-\frac{y^2}{2b_y^2 x^2} - \frac{u_1 (z^{1+m} + z_0^{1+m})}{k_1 (1+m)^2 x}\right] I_0\left[\frac{2u_1 (z z_0)^{(1+m)/2}}{k_1 (1+m)^2 x}\right]. \tag{8.68}$$

8.3. Models for horizontal and vertical fluxes of aerosols

Soil erosion by the wind is an important mechanism for aerosol production above an eroding field. At the radioactively contaminated territories, wind erosion of soil is the main cause of the radionuclides resuspension. The average annual soil erosion in Ukraine from 1987 to 1990 resulting from spring winds was 1 t ha^{-1} (Prister et al. 1991). For topsoil with a density of 1.3×10^3 kg m^{-3}, this corresponds to soil loss of 0.008 cm per year. Erosion led to the total (spring and fall) annual removal of 0.7×10^5 Bq ha^{-1} of ^{137}Cs from soils with the activity concentration of 1×10^3 Bq kg^{-1} (Prister et al. 1991).

Erosion models are formulated to estimate the horizontal mass flux of soil particles through a surface perpendicular to the ground and wind whereas the study of resuspension intensity is concerned with the assessment of the vertical flux of particles (Gillette, Blifford and Fenster 1972, Shao 2008).

8.3.1. Saltation models

Loosmore and Hunt (2000) discussed possible mechanisms of dust resuspension due to mechanical impact on deposited particles. They pointed out resuspension by abrasion or through the direct action of the wind on the surface. Abrasion occurs when the surface is disturbed in some way, either mechanically, as when a vehicle drives across a field, or naturally, through particles saltation. In the presence of saltation, the abrasion becomes the main mechanism for dust resuspension.

Using the measurement results of the movement and drifting of dune sands Bagnold proposed the model for estimation of the mass horizontal flux of saltation

particles F_h (kg m (crosswind)$^{-1}$ s^{-1}) in terms of the friction velocity u_*(m s^{-1})

$$F_h = C_h u_*^3. \tag{8.69}$$

The coefficient of proportionality C_h vary greatly depending on soil and surface characteristics. According to Gillette (1973), the typical value of C_h is about 10^{-1} (kg s^2 m^{-4}). The dependence of the coefficient C_h on a grain diameter d could be presented as (Smith, Whicker and Meyer 1982)

$$C_h = C\left(\frac{d}{\tilde{D}}\right)^{1/2}\frac{\rho}{g}, \tag{8.70}$$

where g is the acceleration of gravity, ρ is the air density, $\tilde{D}$ is the reference grain diameter of 250 μm and C is the empirical constant equal to 1.5, 1.8, or 2.8 for uniform sand, naturally graded sand, and poorly sorted sand, respectively.

This model allows prediction of the saltation flux over a uniform sand bed but does not include a treatment of the suspension flux of fine dust that may be present in the bed. The model is suitable for an application such as a uranium mill tailings pile that is sandy.

Gillette, Blifford, and Fenster (1972) proposed an empirical formula for prediction of the horizontal soil flow for field less than 16,000 ft:

$$F_h = 2\frac{LX}{16{,}500}\left(\frac{\tau_e}{\tau_r}\right)^{3/2}, \tag{8.71}$$

where F_h is the horizontal flux of soil in tons per rod width per hour, L is a field length in feet, X is a soil erodibility function, τ_e is the effective momentum flux, and τ_r is the reference flux. The equation states that the horizontal flux increases linearly with distance downwind in a field due to the effect of «avalanching» loosening of soil due to abrasion from particles originating upwind. Since the momentum flux is related to the surface drag velocity u_* by $\tau = \rho u_*^2$, where ρ is the density of the air, the last term in (8.71) agrees with the u_*^3 dependency in Eq. (8.69).

The effective momentum flux τ_e is the actual momentum flux τ corrected for the surface soil moisture content

$$\tau_e = \tau - \alpha, \tag{8.72}$$

where α is the resistance due to cohesion of the absorbed water films exerted against the wind. It was found to be equal to 6 (ω/ω') (in dyn cm^{-2}), where ω is the amount of water held in the soil, and ω' is the amount of water held by the same soil at a 15-atmoshere percentage. The 15-atmosphere percentage is the upper limit of hygroscopic water and corresponds approximately to the percentage of water at the permanent wilting point of plants (Travis 1975).

The soil erodibility function X is given by

$$X = \frac{aI}{(R_v K_r)^b}, \tag{8.73}$$

where I is the dimensionless soil erodibility index based on the fraction of the soil mass in particles greater than 840 μm (Gillette, Blifford and Fenster (1972), R_v is the amount of vegetative residue (kg m^{-2}), K_r is a surface roughness equivalent (m), a and b are empirical constants. The soil erodibility function expresses that soil is more erodible the less the soil is agglomerated, the less vegetative residue present, and the smaller the surface roughness which tends to trap soil movement.

If the field length dependence could be discarded the formula (8.73) has a form

$$F_h = X\left(\frac{\tau_e}{\tau_r}\right)^{3/2} = X\left(\frac{u_*}{u_{*r}}\right)^3, \tag{8.74}$$

where u_{*r} (cm s^{-1}) is the reference friction velocity for conditions when the formulation for a soil erodibility function was determined. Travis (1975) mentioned that Gillette used a value of 3.31 N m^{-2} for the reference flux τ_r. Accordingly it the reference friction velocity u_{*r} could be estimated to be 1.60 m s^{-1}.

On the base of available experimental data Gillette (1974) proposed a formula for the horizontal saltation flux in the form

$$F_h = C_h u_*^3\left(1 - \frac{u_{*t}}{u_*}\right). \tag{8.75}$$

In this model, the saltation is predicted to occur only above a certain threshold friction velocity u_{*t} when the soil begins to move. When the surface friction velocity approaches the threshold friction velocity from above, the flux F_h tends to zero. The value of C_h was taken to be 6.7.

Kok et al. (2012) analyzed different approaches for the horizontal saltation flux estimations. They showed that the saltation mass flux can be derived from the momentum balance in the saltation layer, that is, that the sum of the horizontal momentum fluxes due to particles and the fluid equals the fluid momentum flux at the top of the saltation layer. The equation for steady state saltation mass flux depends on the particle's hop length L, the average difference between the particle's impact and lift-off speeds Δv, and the threshold friction velocity u_{*t}. Different assumptions about the dependence of L, Δv, and u_{*t} on u_* have resulted in different equations relating F_h to u_*. On the base of this analysis, Kok et al. (2012) proposed a formula for F_h in the form

$$F_h = C_{DK}\frac{\rho_a}{g} u_{*t} u_*^2\left(1 - \frac{u_{*t}^2}{u_*^2}\right), \tag{8.76}$$

where ρ_a is the air density and a dimensionless constant $C_{DK} \approx 5$.

The models of dust emission generated by saltation mechanism are based on the relation between the horizontal saltation flux F_h (e.g. estimated according to formulas (8.69)-(8.76)) and the vertical mass flux of dust at the surface (suspension flux) F_v (kg m^{-2} s^{-1}).

The most used approach to deriving an expression for F_v is to assume that the vertical dust flux is proportional to the horizontal saltation flux (Mills, Dahlman

and Olson 1974)

$$F_v = \alpha \cdot F_h, \tag{8.77}$$

where α is the sandblasting efficiency dependent on the height of the suspended dust measurement and conditions of the soil or tailings. The model provides estimates of saltation and respirable particle flux but not the flux of all particles in suspension.

Mills, Dahlman, and Olson inferred value for α of 10^{-5} m^{-1} for particles 0.4 to 6.0 μm in diameter suspended at 3.75 m above agricultural soil. According to another data, α is on the order of 10^{-5}-10^{-2} m^{-1} (Kok et al. 2012).

As was the case for parameterizations of the saltation mass flux, Kok et al. (2012) picked out main factors which have an effect on a form for the dependence of the vertical dust flux F_v on u_*, namely the average mass of dust aerosols produced by a unit of impacting energy and the mean saltator impact speed. The different parameterization of theses values resulted in formulas proposed by Shao, Raupach, and Findlater (1993)

$$F_v = C_S \rho u_* (u_*^2 - u_{*t}^2) \tag{8.78}$$

and by Kok et al. (2012)

$$F_v = C_F \rho u_{*t} (u_*^2 - u_{*t}^2). \tag{8.79}$$

Gillette (1974) proposed the formula for the suspension flux F_v based on measurements, which were made for particles in the range of diameters from 2 to 20 μm:

$$F_v = C_v \left(\frac{u_*}{u_{*t}}\right)^{\gamma}, \tag{8.80}$$

where $\gamma > 3$ and is high soil specific, C_v is a proportionality constant. The same as in Eq. (8.75) the flux is set to be zero for the condition $u_* < u_{*t}$.

Travis (1975) estimated the constant C_v equals to 2×10^{-9} kg m^{-2} s^{-1} and γ as

$$\gamma = \frac{P}{3} + 3, \tag{8.81}$$

where P is a mass percentage of particles of diameter <20 μm in a given soil.

Using Gillete's data Travis proposed a combined model for estimation of saltation and suspension fluxes. Its important feature is an attempt to include the characteristics of the underlying surface into the model. Taking into account Eqs. (8.74) and (8.75) he obtained an equation for the horizontal flux in the form

$$F_h = X \left(\frac{u_{*e}}{u_{*r}}\right)^2 \left(\frac{u_{*e}}{u_{*r}} - \frac{u_{*t}}{u_{*r}}\right). \tag{8.82}$$

The equation includes an effective friction velocity u_{*e} that accounts for soil moisture and the presence of large roughness elements (large rocks, plants, trees), which may reduce the friction velocity acting on the soil.

An equation for the vertical flux in the model is

$$F_v = F_h \left(\frac{C_v}{C_h u_{*t}^3}\right)^2 \left[\left(\frac{u_*}{u_{*t}}\right)^{P/3} - 1\right]. \tag{8.83}$$

Smith noted some interesting features of this formulation. First, as the mass percentage of particles <20 μm approaches zero, the suspension flux is forced to zero. Second, the suspension flux has been made functionally dependent on the saltation flux F_h.

Gillette and Passi (1988) suggested that the vertical dust flux F_v could be well represented by

$$F_v = C u_*^4 \left[1 - \left(\frac{u_{*t}}{u_*}\right)\right]. \tag{8.84}$$

Using their data of the dust flux measurements Shaw et al. (2008) estimated the values of the formula (8.84) as $C = 1.0 \times 10^{-5}$ kg m^{-6} s^{-3} and $u_{*t} = 0.2$ m s^{-1}.

This approach is used for calculation of the vertical dust flux in a dust transport model DUSTRAN (Allwine et al. 2006) developed in Pacific Northwest National Laboratory. Additionally effects of soil moisture and vegetative cover are taken into account, so a final form for the total dust flux is given as

$$F_v = \alpha C u_*^4 \left[1 - \left(\frac{f_w u_{*t}}{u_*}\right)\right], \tag{8.85}$$

where α is a vegetation mask ranged from zero to one. The soil wetness factor f_w is determined according to

$$f_w = \begin{cases} [1 + 1.2\,(w - w')^{0.68}]^{1/2}, & w > w', \\ 1, & w \le w', \end{cases} \tag{8.86}$$

where w is the gravimetric soil moisture (mass of water/mass of soil;%), and w' is the maximum amount of water that can be absorbed by the soil (%). Fecan, Marticorena, and Bergametti (1999) obtained dependence of w' on the soil's clay content c_s in a percent:

$$w' = 0.17\, c_s + 0.0014\, c_s^2. \tag{8.87}$$

Maticorena and Bergametti (1995) related the vertical suspension flux to the horizontal saltation flux taking into account the value of c_s:

$$F_v = F_h \cdot 0.01 \exp(0.308 c_s - 13.82). \tag{8.88}$$

Several models were developed to relate the vertical suspension flux to the horizontal saltation flux with consideration of particle size distribution. Lu and Shao (1999) derived a model to estimate the dust suspension flux caused by the

saltation of particles of size d_s in the form

$$F_v(d_s) = \frac{C_\alpha g \eta \rho_b}{2\mathrm{P}} \left(0.24 + C_\beta u_* \sqrt{\frac{\rho_p}{\mathrm{P}}}\right) F_h(d_s), \tag{8.89}$$

where C_α and C_β are coefficients, η is dust mass fraction, ρ_b and ρ_p are bulk-soil and soil particle densities, respectively, and P is the plastic pressure of the soil surface. The total dust suspension flux F_v is obtained by the integration of inputs $F_v(d_s)$ over all particle sizes d_s in the range of sand particle diameters.

Shao (2001, 2004) proposed a modified model that considers the two major dust emission mechanisms, namely, saltation bombardment and aggregation disintegration. The formula for the dust suspension flux includes two particle size distributions which are corresponds to two extreme cases: when the soil disturbances by wind is so weak that the breakup of aggregates does not occur, and when all aggregates break up into their fundamental particle sizes. So, the accuracy of the model depends on the availability of high-quality particle size data.

The Shao model predicts the size distribution of emitted dust aerosols p_d on a particle diameter D as

$$p_d(D) = \gamma p_m(D) + (1+\gamma) p_f(D), \tag{8.90}$$

where p_m, and p_f are respectively the particle size distributions of the minimally disturbed soil and the fully disaggregated soil. Shao postulated a weighting factor γ in the form

$$\gamma = \exp\left[-k(u_* - u_{*t})^n\right], \tag{8.91}$$

where k and n are empirical coefficients.

The Shao model predicts that an increase in u_* results in more disaggregated, and hence smaller, dust aerosols. However, Shao et al. (2011) recently found that a constant value of γ (i.e., independent of u_*) produced the best agreement with field measurements.

Cowherd et al. (1985) developed two models for estimating PM10 particle emissions from surfaces with unlimited erosion potential and with a limited reservoir of erodible particles. The decision criterion in choosing between these model types is a value of threshold friction velocity u_{*t}. For $u_{*t} > 0.75$ m s^{-1} a limited reservoir model is recommended, otherwise, an unlimited model must be used. On the whole, a limited reservoir model could be applied for surfaces covered by continuous vegetation or composed of elements too large to be eroded, or of erosion-resistant crusts.

For screening of potential inhalation risks at contaminated soil sites, EPA recommends the PM10 emission model (Cowherd et al. 1985) for a surface with unlimited erosion potential. The equation for particle emissions has the form:

$$E_{10} = 0.036 \times (1 - V) \times ([u]/u_{t-7})^3 \times F(x), \tag{8.92}$$

where E_{10} is the annual-average PM10 emission rate per unit area of contaminated soil (g m^{-2} h^{-1}); V is the fraction of vegetative cover; $[u]$ is the mean annual wind speed (m s^{-1}); $u_{t\text{-}7}$ is the threshold value of wind speed at 7 m (m s^{-1}).

$F(x)$ is a function dependent on the value of $x = 0.886 \times (u_{t-7}/[u])$, where

$$u_{t-7} = (u_{*t} \times F_{adj}/0.4) \times \ln(700\,\text{cm}/z_0), \tag{8.93}$$

u_{*t} is the unadjusted threshold friction velocity (m/s); F_{adj} is the threshold friction velocity adjustment factor.

The function $F(x)$ is approximated using the following equations:

$$f_w = \begin{cases} (6 - x^3)/\pi, & x < 1; \\ -1.3x + 2.89, & 1 \le x < 2; \\ (8x^3 + 12x) \cdot \exp(-x^2), & x \ge 2. \end{cases} \tag{8.94}$$

8.3.2. Non-saltation models

In the absence of saltation, an alternate mechanism for dust resuspension involves the direct removal of dust particles by the wind. On the base of laboratory measurements in wind tunnel flow, Loosmore and Hunt (2000) proposed the approximation form for a long-term steady dust flux in the absence of saltation

$$F_v = 3.6 \cdot 10^{-9} (u_*)^3, \tag{8.95}$$

where F_v is in kg m^{-2} s^{-1}. The authors noted that in this case nonzero resuspension fluxes were observed for all velocities tested in this study. The threshold friction velocity, below which truly no dust is removed, not be determined in the experiments.

In general, the dust fluxes observed in these experiments are small relative to values expected for scenarios with saltation. Loosmore and Hunt estimated that the abrasion model (Eq. (8.75)) with constant β according to Marticorena et al. (1997) gave the dust mass flux ~3000 times larger than the nonabraded steady fluxes (8.95) for u_* much larger than the threshold value. So, the model (8.95) becomes prevailing for u_* very close or below to the threshold value. They concluded that the model (8.95) may give reasonable results for estimations of small fluxes that could pose hazards to human health and the environment, especially for estimation in radionuclide contaminated areas.

Chkhetiami et al. (2012) presented the results of experimental studies and modeling of dust resuspension under weak wind conditions. They obtained that fine mineral dust aerosol resuspension under conditions of weak wind and strong heating of the surface is possible, almost in the absence of saltation processes. For small and moderate values of friction velocity (when u_* is higher than

the threshold value ~0.4-0.5 m s^{-1}), strong convection of the air over the sand layer during hot weather is treated as the main mechanism of dust resuspension compared with saltation processes. The lift of sand and aerosol due to convective turbulence is determined by the thickness δ_T of the convective boundary layer (in which the air temperature falls sharply with height) and by the characteristic convective horizontal velocity u_T at the outer boundary-layer edge. The value of δ_T is determined by temperature drop in a viscous thermal boundary layer δT. The experimental data on the dependence of resuspension intensity on the friction velocity u_* and temperature drop in a thermal boundary layer δT would give strong dependence on u_*. Unfortunately, empirical data are too scarce to construct a possible approximation of such functions. The model of aerosol resuspension from the upper soil layer is proposed for such conditions in the layer $\delta_* < z < \delta_T$, where δ_* is the height of the viscous boundary layer. It was obtained that for small and moderate values of u_* the resuspension intensity increases as δT grows as a power function with positive exponent ranging from 1/2 to 2/3. For stronger winds ($u_* > 0.3$-0.4 m s^{-1}), the u_* dependence of the resuspension intensity changes. As δT grows, the resuspension intensity decreases with negative exponent –0.5. In this case, the model gives the Bagnold's dependence u_*^3. However, for these conditions, the basic mechanism for aerosol resuspension or emission from the soil is the rolling and saltation of large particles pulled out of the viscous boundary layer δ_* due to wind forcing.

Hence, atmospheric transport models for a ground surface area source could be used for estimation of resuspension impact in substantially nonuniform radioactive deposition field at different distances from the source. The emission intensity of a source could be parameterized using the resuspension rate value. The alternative approach is based on the results of dust emission models. In this case, the estimation of mass flux from such a model may be converted into radioactivity flux through the mass loading approach.

CHAPTER 9

STATISTICAL CHARACTERISTICS AND LONG-TERM PREDICTION OF THE ACTIVITY CONCENTRATION OF RADIONUCLIDES IN THE AIR

The input data used in most assessments of the radiological exposure from inhalation, ingestion and external radiation are average values of the activity or mass concentrations of radioactivity in the air, soil, water, and food. But there can be a significant temporal and spatial variability of many factors determining the radioactivity concentrations in the different media. The variability of the atmospheric activity concentration is particularly large because of the fast transport of trace substances in the atmosphere (compared to the transport in water or soil).

For an inhalation dose assessment, it is necessary to have reliable estimations of the average concentration of radioactivity in the atmosphere. An appropriate selection of the period for averaging is important because of the large variability of the activity concentration. Neglecting the fluctuation of the activity concentration can lead to serious errors in the estimates of the inhalation dose rate. Until now, this question is not too well investigated because of the lack of empirical data. Garger et al. (1994) tried to improve this situation by statistical analysis of the measured activity concentrations in the surface boundary layer of the atmosphere. These concentrations were regularly measured at two locations inside the 30 km zone around the Chernobyl Nuclear Power Plant starting in the second half of 1987 until the end of 1991. The object of this analysis is a better understanding of the time dependence of these concentrations and to provide statistical characteristics of these time series.

Daily filter samples of aerosol were taken with high-volume samplers in the towns of Pripyat and Chernobyl, which are located 18 km apart from each other inside the 30 km zone of Chernobyl (Garger 1994). The samplers, designed by SPA «Typhoon», operated at a flow rate of 100,000 m^3 day^{-1}

(1.16 $m^3 s^{-1}$) with a sampling height of about 1.5 m. The filter used was of the Russian type Petryanov cloth FPP-15-1.5 with an area of 1.05 m^2. The exposed filters were pressed into discs and analyzed by γ-spectrometry. On 5-7% of the days of the year it was not possible to obtain data because of various technical problems, but the series of measurements as a whole can still be used for the estimation of basic characteristics of the fluctuations in the activity concentration.

9.1. Statistical characteristics of the ^{137}Cs activity concentration in the air

The daily measurements of the activity concentration of ^{137}Cs in the atmospheric surface boundary layer, made from July 1987 to December 1991 in Pripyat and Chernobyl, are reproduced in Fig. 9.1(*a*-*e*). The straight dotted lines correspond to the annual average of the activity concentration in the cities of Pripyat (see also Table 9.l) and Chernobyl (see also Table 9.2). Please note the different scale: the activity concentrations are generally higher in Pripyat than in Chernobyl.

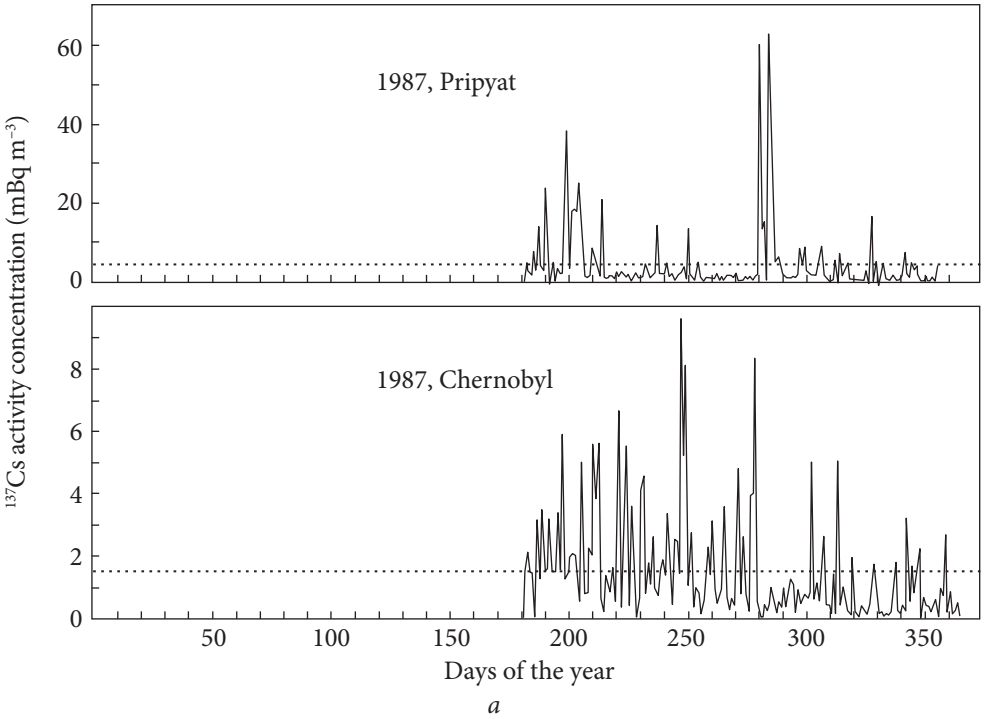

a

Fig. 9.1. ^{137}Cs activity concentration in the surface boundary layer of the atmosphere in the cities of Pripyat and Chernobyl in the period July 1987 — December 1991: *a* – in 1987; *b* – in 1988; *c* – in 1989; *d* – in 1990; *e* – in 1991. Note the different scale: the activity concentrations are generally higher in Pripyat than in Chernobyl (see also pp. 139-140)

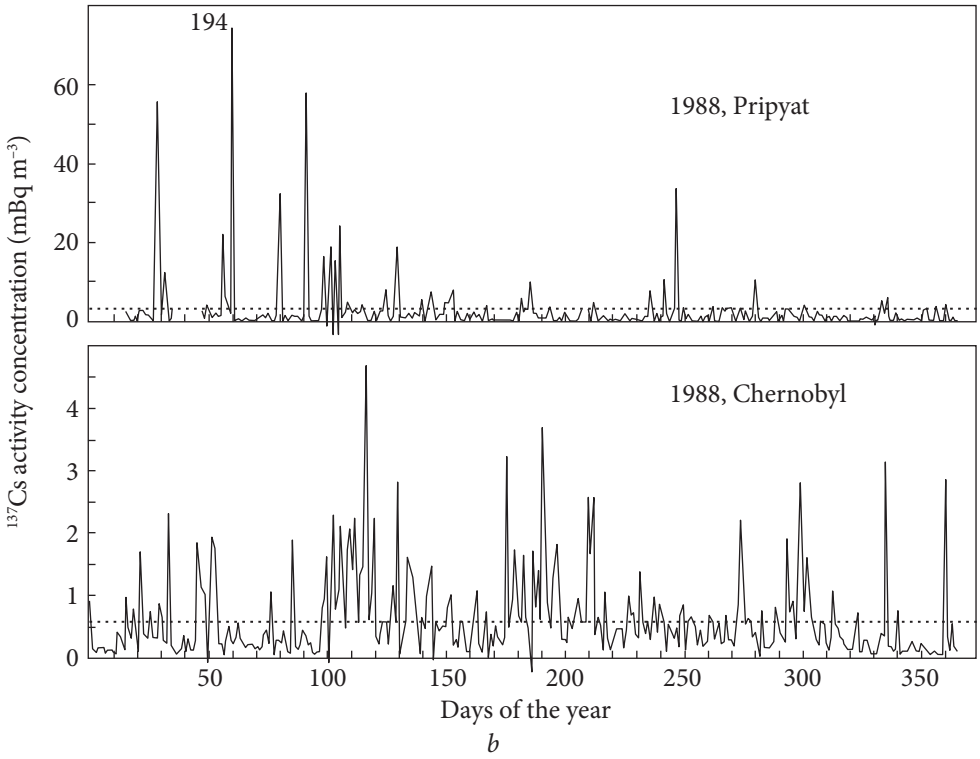

b

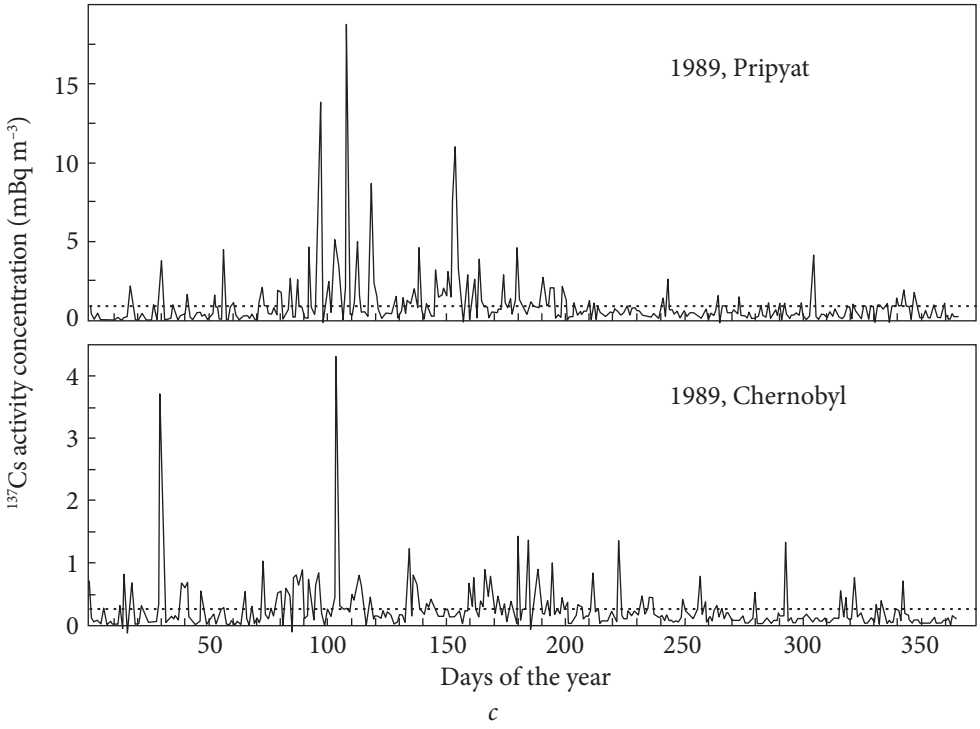

c

Fig. 9.1. *Continued*

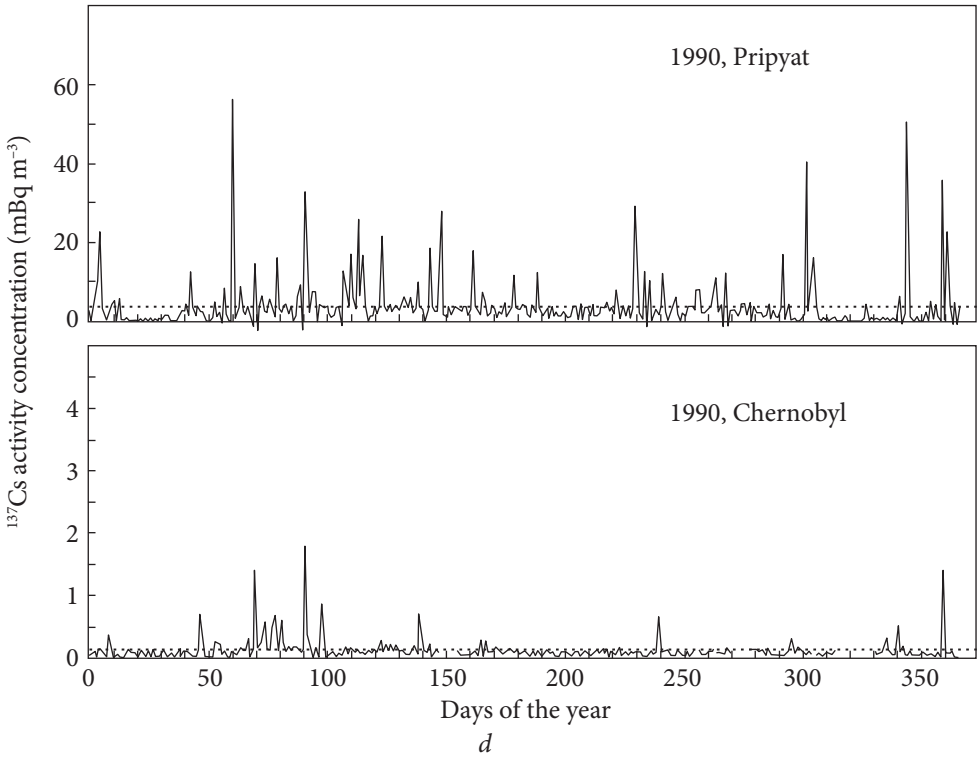

d

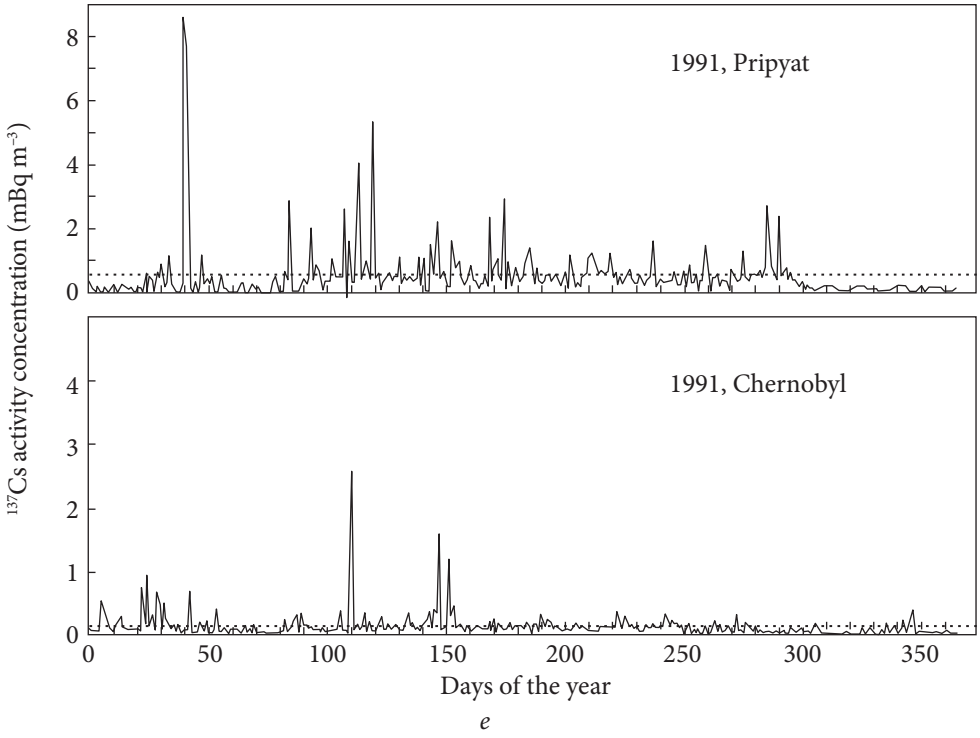

e

Fig. 9.1. *End of Fig. 9.1*

Table 9.1. **Statistical characteristics of distribution functions of the daily average activity concentration of ^{144}Ce and ^{137}Cs in Pripyat**

Statistical characteristics	Nuclide	1987	1988	1989	1990	1991
Number of days with data	^{144}Ce	165	294	223	124	—
	^{137}Cs	184	366	365	365	365
Average activity concentration ($\mu Bq\ m^{-3}$)	^{144}Ce	16283	5841	1334	385	—
	^{137}Cs	4145	2989	935	516	463
Median ($\mu Bq\ m^{-3}$)	^{144}Ce	4214	1324	495	188	—
	^{137}Cs	1616	1075	498	341	320
Standard deviation ($\mu Bq\ m^{-3}$)	^{144}Ce	34829	16265	2727	781	—
	^{137}Cs	8154	11524	1623	762	741
Skewness	^{144}Ce	4.04	6.4	5.21	6.52	—
	^{137}Cs	4.75	13.3	6.38	4.91	6.84
Kurtosis	^{144}Ce	18.8	46.8	34.5	53.1	—
	^{137}Cs	27.7	209.1	54.9	30.4	60.7
Intensity of fluctuation	^{144}Ce	2.14	2.97	2.04	2.03	—
	^{137}Cs	1.97	3.86	1.74	1.48	1.60
Ratio of average activity concentration to median	^{144}Ce	3.93	4.14	2.67	2.05	—
	^{137}Cs	2.56	2.78	1.88	1.51	1.45

Table 9.2. **Statistical characteristics of distribution functions of the daily average activity concentration of ^{144}Ce and ^{137}Cs in Chernobyl**

Statistical characteristics	Nuclide	1987	1988	1989	1990	1991
Number of days with data	^{144}Ce	163	306	240	104	—
	^{137}Cs	184	366	365	365	365
Average activity concentration ($\mu Bq\ m^{-3}$)	^{144}Ce	5216	1233	307	85.6	—
	^{137}Cs	4145	2989	248	117	137
Median ($\mu Bq\ m^{-3}$)	^{144}Ce	2738	629	191	60.6	—
	^{137}Cs	888	370	148	93	96
Standard deviation ($\mu Bq\ m^{-3}$)	^{144}Ce	7346	1989	464	96.0	—
	^{137}Cs	1638	620	357	150	184
Skewness	^{144}Ce	3.20	7.39	6.74	3.64	—
	^{137}Cs	2.27	2.53	7.00	6.77	8.14
Kurtosis	^{144}Ce	13.3	80.2	61.5	17.6	—
	^{137}Cs	6.09	8.59	69.1	60.6	91.5
Intensity of fluctuation	^{144}Ce	1.41	1.61	1.51	1.12	—
	^{137}Cs	1.10	1.08	1.44	1.28	1.34
Ratio of average activity concentration to median	^{144}Ce	1.90	1.96	1.61	1.41	—
	^{137}Cs	1.67	1.54	1.68	1.26	1.43

These examples visually demonstrate the random nature of the deviations from the average of the activity concentration expressing its non-stationary character. The imbalance of the height of positive and negative fluctuations relative to the annual average is obvious; the ratio of the measured maxima of concentration to the annual mean is 10-20 in all the observed years.

Statistical characteristics of the distributions of the activity concentrations of ^{137}Cs and ^{144}Ce are given in Table 9.l (Pripyat) and Table 9.2 (Chernobyl). In addition to the first to a fourth statistical moment of the ^{137}Cs and ^{144}Ce activity distribution, the intensity of the fluctuations (determined as the ratio of the standard deviation to the average concentration) is given. During all years, the intensity of fluctuation exceeded unity and was largest in Pripyat in 1987-1988 when technogenic (i.e. mechanical) activity, including decontamination and reconstruction, was most intense. The strong asymmetry of the distribution of ^{137}Cs and ^{144}Ce activity concentration is reflected by the large ratio of the average concentration to the median and the values of the skewness.

The decrease of the absolute values of the activity concentration with time is demonstrated in Fig. 9.2*a* and *b*. The monthly mean values for both radionuclides, ^{137}Cs and ^{144}Ce, decline by one to two orders of magnitude in these 4 years. The straight lines reflect the radioactive decay of ^{137}Cs or ^{144}Ce, respectively, standardized to the activity concentration in June 1989. At that time the majority of decontamination work in the 30 km zone was finished and resuspension by technogenic (i.e. mechanical) activity became less important. In 1987 and 1988, the years of high efforts in the decontamination of large areas, there is some evidence of the contribution by technogenic resuspension to the atmospheric activity.

The decrease of the atmospheric activity concentration is higher than expected, assuming radioactive decay only, which is clearly illustrated in the ^{137}Cs time series (Fig. 9.2*a*). There must be further processes that are responsible for the reduction of the activity concentration in the air, mechanisms for instance which reduce the source term of resuspension such as vertical migration in soil, run-off with rain or melting water and snow cover. For the second halves of 1987 and 1989, the frequency distributions of the ^{137}Cs atmospheric activity concentration in Pripyat and Chernobyl are given in Fig. 9.3*a* and *b***.** The histograms show very wide distributions of the ^{137}Cs activity concentration in 1987 but very narrow distributions in 1989. This change is especially striking for the city of Pripyat, the closest place to the ChNPP site. Technogenic activity almost ceased by 1989 and Pripyat became a closed city. In contrast, the traffic in Chernobyl city remained an effective additional source of radioactive aerosol.

The description of these empirical distributions by such theoretical functions as the log-normal-, the exponential- or the gamma-distribution was not successful for the ensemble of measurement series in the sense of the χ^2 criterion. The empirical distributions reflect more complex situations than described by the

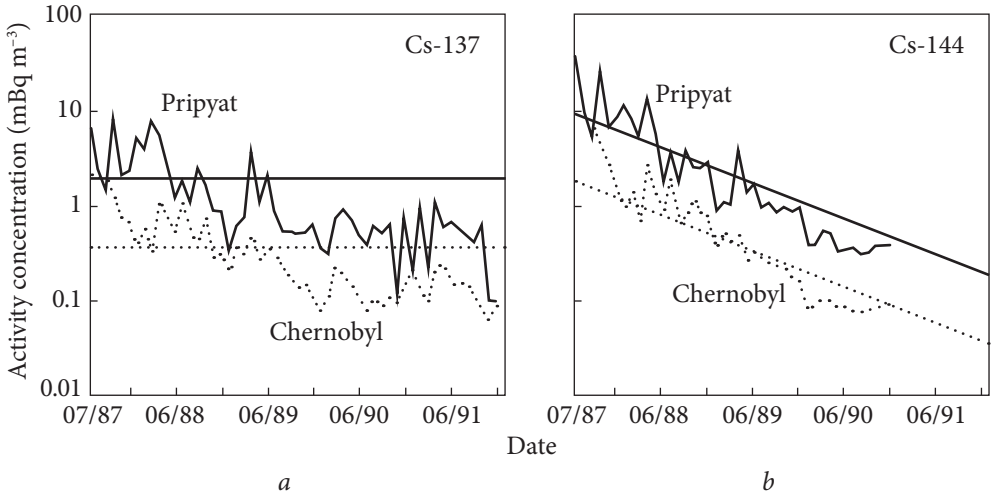

Fig. 9.2. Monthly mean activity concentrations of ^{137}Cs in the surface boundary layer in Pripyat and Chernobyl in the period July 1987 – December 1991 (the straight lines illustrate radioactive decay) (*a*); Monthly mean activity concentrations of ^{144}Ce in the surface boundary layer in Pripyat and Chernobyl in the period July 1987 – December 1991 (the straight lines illustrate radioactive decay) (*b*)

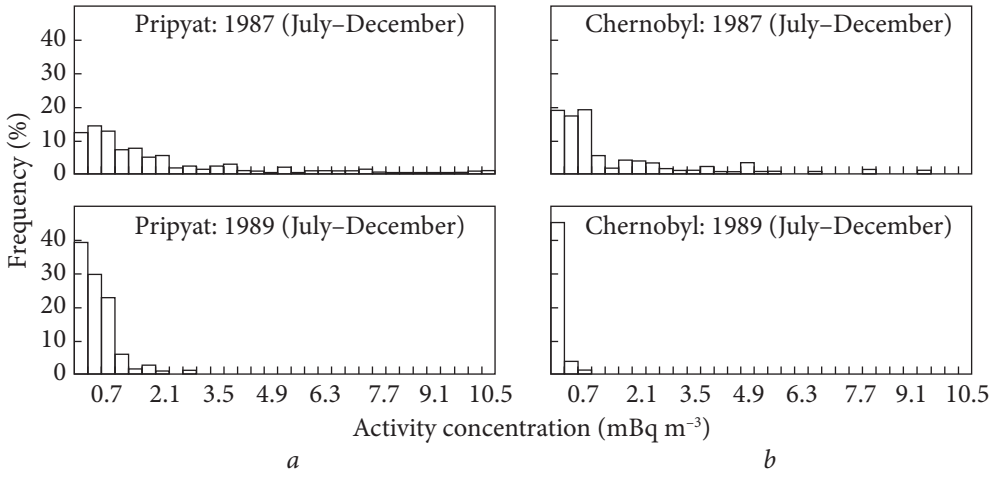

Fig. 9.3. Frequency distributions of the atmospheric activity concentration of ^{137}Cs in the second half of the years 1987 and 1989 in Pripyat (*a*); Frequency distributions of the atmospheric activity concentration of ^{137}Cs in the second half of the years 1987 and 1989 in Chernobyl (*b*)

model distributions. The empirical function of the activity concentration distribution results from the influence of several different processes: local resuspension by wind, transport of radioactive aerosol from distant highly contaminated areas and resuspension by technogenic (mechanical) activity. The superposition

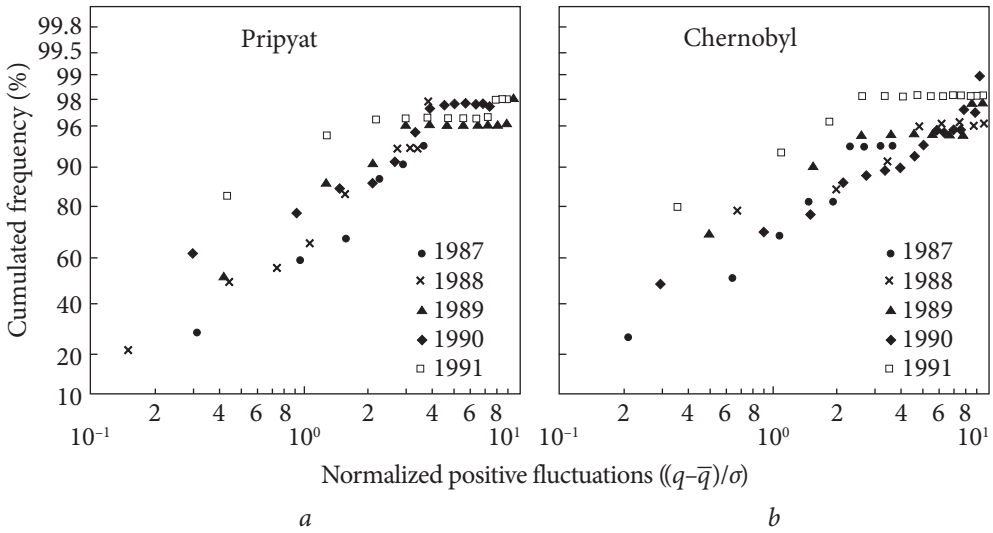

Fig. 9.4. Cumulated frequency distribution of the ratio of those concentrations exceeding the average annual concentration and the standard deviation in a probability plot for the years 1987-1991 in Pripyat (*a*) and Chernobyl (*b*)

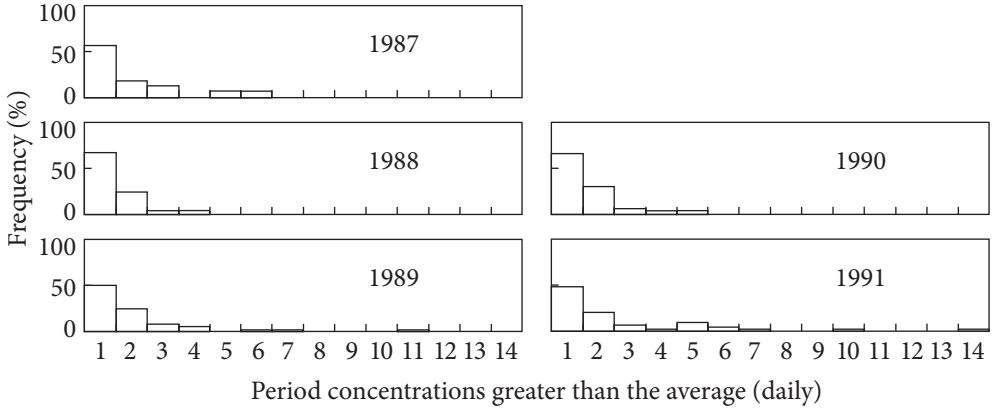

Fig. 9.5. Frequency distributions of periods of the ^{137}Cs activity concentrations greater than the mean in the years 1987-1991 in Pripyat

of these processes gives rise to a complex distribution function which changes with time as the different processes are also changing with time.

For specific periods, however, certain distributions may describe well the empirical data. For example, while no log-normal distribution could be fitted to the empirical distribution in 1987 this became possible in 1988-1990. Bencala and Seinfeld (1976) found a good correlation of the air pollutant concentration distributions with log-normal distributions when concentrations depend strongly on wind speed. The gamma-

distribution better describes the measurement series in Chernobyl as a whole. The quality of the fit improves with time. A distinct change in the shape of the distribution of the activity concentration in the surface layer of the atmosphere could be noticed.

In the following, only concentrations exceeding the average annual concentration (positive fluctuations) are discussed because of their significance on the dose rate and their potential health effects. In Fig. 9.4a and b for Pripyat and Chernobyl the cumulative frequency distribution is given for the ratio of these positive fluctuations and the standard deviation $((q-\overline{q})/\sigma)$ in a probability plot. A log-normal distribution follows a straight line in this kind of plot. While the smaller fluctuations in Fig. 9.4a and b are rather well described by the log-normal distribution (in Pripyat better than in Chernobyl), the very high fluctuations (amplitudes larger than 2-3 times the standard deviation) lie further from a straight line. From year to year, the cumulative distribution is shifted towards lower values. For example, the frequency in Pripyat and Chernobyl of the concentration with relative amplitudes less than or equal to 1 is 60-70% in 1987 but is 92% in 1991. Conversely, the frequency of high concentration decreases with time.

The length of the periods with high activity concentrations in the air could be discussed with the help of Fig. 9.5. For the series of measurements in Pripyat, the histograms show the frequency distribution of the periods with concentrations greater than the mean. The length of the period is measured from the time when the concentration rises above the annual average until it has again fallen below the average value. The fluctuations last from 1 to 14 days; the average period is 2 days. It should be noted that the correlation between the maximum of the concentrations and their duration was about 0.4-0.5 in the first years of measurement (1987 and 1988), it later decreased.

9.2. Dependence of the activity concentration on the averaging period

Finally, we consider the influence of the averaging period on the estimation of the normalized standard deviation of the activity concentration $\sigma(T)/\overline{q}$, where $\overline{q}$ is the annual mean concentration; T is the averaging period; and $\sigma(T) = [\overline{(q(T)-\overline{q})^2}]^{1/2}$.

The normalized standard deviation was calculated for $T \in \{2, 3, 4, 6, 10, 15, 20, 30, 60 \text{ days}\}$ in the years 1987-1991 with the measured air concentrations in Pripyat and Chernobyl. The dependence of $\sigma/\overline{q}$ on T can be expressed by a power function

$$\frac{\sigma(T)}{\overline{q}} \approx T^{-m},$$

with the empirical determined exponent m. Values for the exponent m are given in Table 9.3. There is no significant difference in m for the cities of Pripyat and Chernobyl, the mean value is $m = 0.33 \pm 0.08$.

The above relation can be used to compare different averaging periods T_1 and T_2 (Fig. 9.6):

$$\sigma(T_2) = \sigma(T_1)\left[\frac{T_2}{T_1}\right]^{-m}.$$

We now can estimate the effect of increasing the internal averaging time by sampling 3 (10) days instead of 1 day: the standard deviation will decrease to

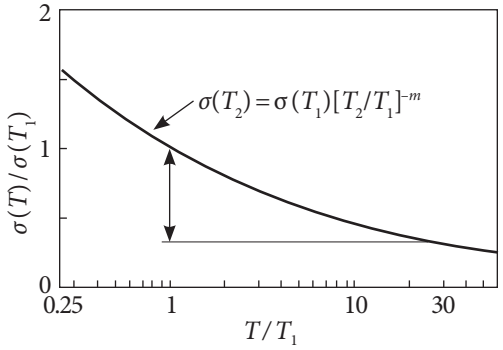

Fig. 9.6. Dependence of the standard deviation of the activity concentration on the observation time ratio

Table 9.3. **The exponent *m* as determined by daily measurements of the activity concentrations in Pripyat and Chernobyl**

Year	Pripyat	Chernobyl
1987	–0.27	–0.27
1988	–0.47	–0.25
1989	–0.25	–0.34
1990	–0.45	–0.37
1991	–0.34	–0.32
Mean	–0.36 ± 0.10	–0.31 ± 0.05

Table 9.4. **The long-period characteristics of the ^{137}Cs activity concentration in the surface layer of the atmosphere in Chernobyl**

Year	Average annual activity concentration q (μBq m^{-3})	Daily average coefficient of variation σ_q/q	Average month coefficient of variation σ_q/q	Exponent m
1986 [a)]	1.96×10^4	5.1	2.0	0.27
1987	1.98×10^3	3.0	1.2	0.27
1987 [b)]	1.4×10^3	1.1	0.48	0.27
1988	570	1.08	0.45	0.25
1989	248	1.44	0.39	0.34
1990	117	1.28	0.39	0.37
1991	137	1.34	0.38	0.32
1992	176	1.84	0.54	0.24
1993	66.5	1.34	0.47	0.30
1994	40.8	1.5	0.53	0.30
Average				0.30 ± 0.05

Note: [a)] Data from June 1 till December 31; [b)] Daily data from July 1 till December 31.

69% (47%) of the daily value. Therefore, the averaging period is of importance in the assessment of activity measurements and the design of a field measurement program.

Hence, the selection of averaging period is important for the estimations of measuring activity and planning of field measurement with a given degree of uncertainty. Besides, the presented formula helps to restore values of the relative standard deviations.

The results presented in Table 9.4 demonstrate differences between coefficients of variation of daily average and monthly average values of the activity concentration in the air. It is well visible, that in 1986 daily average coefficient of variation reached 5, monthly average — 2. Since the second half of 1987, these coefficients have decreased at the average down to 1.5 and 0.5 accordingly, which is necessary to take into account while estimating dose loadings due to inhalation intake.

9.3. Long-term time course of the atmospheric ^{137}Cs activity concentration

In Fig. 9.7 the time course of the activity concentration of ^{137}Cs for a period of May 1986 — October 1994 in Chernobyl and Baryshevka (~150 km from ChNPP) is shown (Garger et al. 1994). The leftmost points represent an initial leap of the activity concentration, related with the arrival of radioactive cloud to these points, which in May has reached approximately by seven orders of magnitude higher than a monthly average value obtained there in 2000-2002. In May-June 1986 a fast decrease of the activity concentration on the average by two orders of magnitude and a slow decrease later were the main tendency.

Bogatov et al. (1990) stated that the initial depositions finally have finished in June 1986 only, and resuspension became a dominant process in the formation of the near-ground air concentration of radioactivity. This statement is rather correct for the territory outside the 30 km ChNPP zone. In the close vicinity of the ChNPP continued releases from the accidental 4th unit could contribute to the measured value of the atmospheric ^{137}Cs activity concentration in that period.

Fig. 9.7 shows clearly, that the amplitude of oscillations of the monthly averaged activity concentration of ^{137}Cs in the air in some cases reached approximately one order of magnitude as in Chernobyl and in Baryshevka during the entire period of measuring.

The above data were determined in main by local and mesoscale processes of radioactive aerosol transport in the atmosphere.

Measuring in Sweden in 1992 and 1993 demonstrated an example of long-range transport of radioactivity lifted in the atmosphere due to resuspension. In Sweden, the atmospheric activity concentration of ^{137}Cs decreased from 1986 till 1991, then later in 1992 and 1993 the influence of the ^{137}Cs transport was noticed in Southern

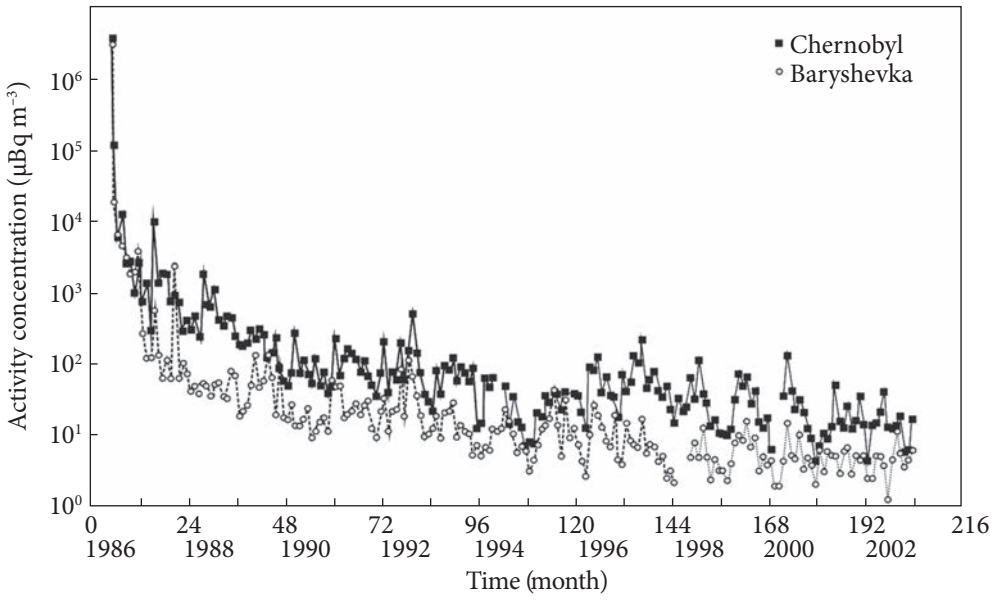

Fig. 9.7. Temporal course of the atmospheric activity concentration of ^{137}Cs in Baryshevka and Chernobyl

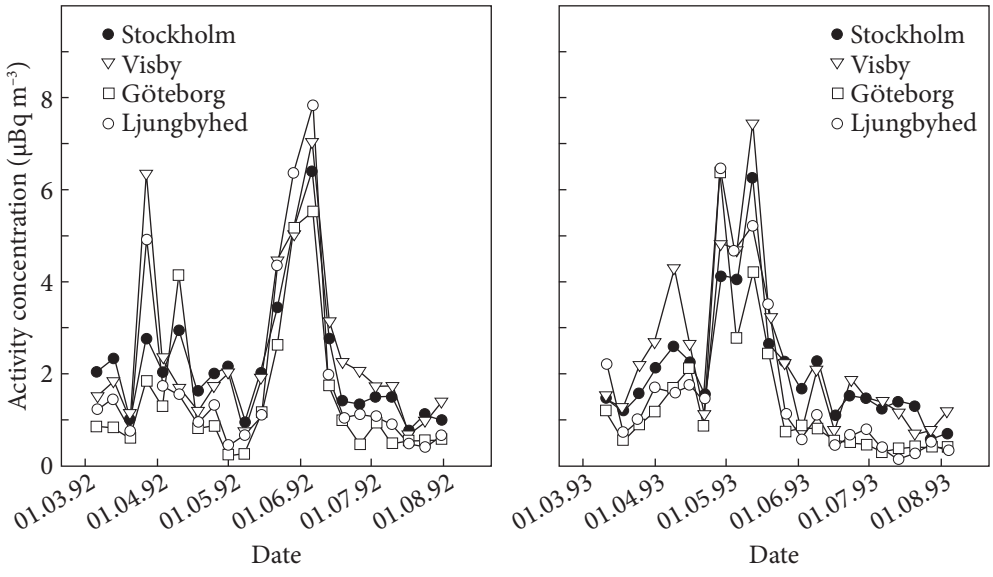

Fig. 9.8. Atmospheric activity concentration of ^{137}Cs in southern Sweden

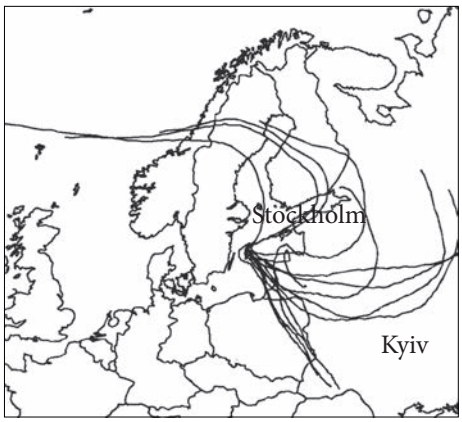

Fig. 9.9. Three day receptor-oriented trajectories calculated at the 950 mbar level for Visby, Sweden during April 26 — May 3 1993, one trajectory every 12th hour

Sweden according to air concentration measurement (Vintersved et al. 1994).

In Fig. 9.8 the weekly averaged activity concentration of ^{137}Cs at four measurement sites during spring 1992 and 1993 are given. As it turned out, some weekly concentrations exceed concentrations over previous or subsequent weeks by 4 times. In Sweden, the phenomena were observed when the activity concentration of ^{137}Cs raised simultaneously on large areas, and in these cases, weather in Northern Europe was determined by anticyclone above the territory of Russia, Ukraine and Belarus. Receptor-oriented air mass trajectories, calculated for these periods (Vintersved et al. 1994), show that the Chernobyl zone could be a possible source of additional air activity. Fig. 9.9 shows an example, when the trajectories were calculated at the level of 950 mbar every twelve hours for one week from April 26 till May 3, 1993.

9.4. Statistical prediction of the ^{137}Cs activity concentration in the surface layer of the atmosphere of the Chernobyl exclusion zone

After the termination of the primary release of radionuclides from the destroyed Chernobyl nuclear reactor into the atmosphere natural wind resuspension of radioactive aerosols formed the atmospheric activity contamination in the Chernobyl exclusion zone (Garger et al. 1998) along with forest fires (Hollander and Garger 1996, Yoschenko et al. 2006, Paatero et al. 2009), emission from gaps of the Chernobyl «Shelter» object (Garger et al. 2006) and re-entrainment due to human activities on contaminated fields, roads, and construction sites. In this context, it is necessary to estimate the resulting inhalation dose, its variation in time and the horizontal redistribution of radioactivity due to the migration of radioactive particles in the 30-km exclusion zone and the surrounding area.

The knowledge of the activity concentration of the dose-relevant radionuclides is required at first for estimation of inhalation dose and related analysis, e.g. the horizontal redistribution of the radionuclides. Since ^{137}Cs is a major radionuclide released from the Chernobyl accident with a relatively long half-life, information of the soil contamination density and long-time series data of its atmospheric concentration have been accumulated for inside and around the exclusion

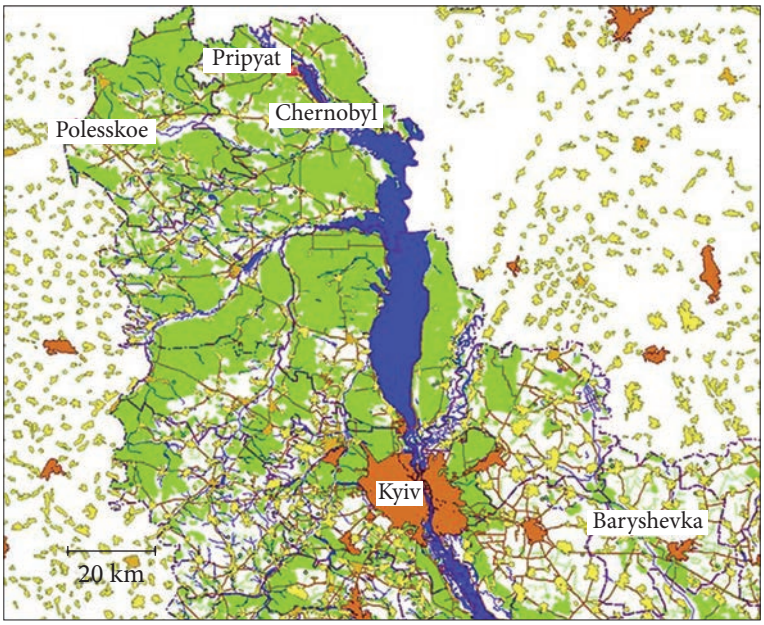

Fig. 9.10. The Ukrainian Polesye region with Kyiv in the center and the location of the five measurement stations

zone. In Garger et al. (1997) prospects and limitations are shown of the approach to predict the activity concentration in the air by using the soil contamination density and the resuspension factor. In particular, Garger et al. (1995) have found that the models based on the resuspension factor does not take into account the fluctuations of the airborne activity concentration, and the predicted values may, therefore, differ from the measured values several orders of magnitude.

In the present Chapter, an alternative statistical approach is presented. It uses the measurement of the ^{137}Cs activity concentration in the air to construct a long-term predictive model. The aims of this Chapter are

1) to report about establishing the model for predicting the ^{137}Cs air activity concentration based on data measured in the town of Pripyat in the period 1987-1991 and

2) to validate the predicted values with measurement data in the same town in the later period 1991-1997.

Filter samples of aerosol were taken at five locations (Table 9.5) in the Ukrainian Polesye region (including Pripyat and locations up to 230 km distance from the Chernobyl nuclear power plant, see Fig. 9.10) from samplers designed by SPA «Typhoon», at a sampling height of about 1.5 m above lawn. One sampler was situated in the town of Pripyat in an evacuated residential area in the middle of a large lawn. It must be noticed that the measurement device was relocated closer

to the nuclear power plant in 1998. In Pripyat, the filters were changed daily, at other places the period of sampling was variable depending on the level of the airborne activity concentration (1-10 d). The exposed filters (Russian type Petryanov cloth FPP-15-15 with an area of 1.05 m^2) were pressed into tablets and analyzed by γ-spectrometry for ^{137}Cs. The γ-spectrometer based on the semi-conductor detector GMX-30190 (relative efficiency 32.5%, energy resolution 1.89 keV on the line 1.33 MeV) and the multichannel buffer Spectrum Master (ORTEC Inc.). Energy and efficiency calibration were performed with the standard source OSGJ No. 13166. The measured values of the ^{137}Cs activity concentration in the air were averaged over consecutive 10 d for Pripyat and consecutive 30 d (monthly average) for the other sites and compiled for further analysis. In Fig. 9.11 the 10-year time series of the ^{137}Cs airborne activity concentration in the town of Pripyat is presented. Table 9.5 shows the collection period of the filter samples at the five sites in the Ukrainian Polesye region.

The Pripyat data demonstrates the significant temporal variation of the airborne ^{137}Cs activity concentration in the aftermath of the Chernobyl accident (Fig. 9.11). Therefore, the time series are considered as the result of dynamic processes that include different components such as trend and low-frequency fluctuations and other stochastic fluctuations.

A first attempt to calculate a long-time prediction from the Pripyat air concentration data was made by Viswanathan et al. (2000). A technique specially adjusted for a high portion of missing data (about 7%) was applied for the calculations based on the least-square power spectrum analysis of Lomb (1976). To proceed further, an approach is applied of consequent selecting the time trends to

Table 9.5. **Collection period of the filter samples and the averaged sample period for the five sites in the Ukrainian Polesye region**

Site	Collection period	Averaged sample period (d)	Source
Kyiv	July 1987 – December 1992 January 1993 – December 2002	30	Garger et al. (1999) Garger et al. (2012)
Baryshevka	July 1987 – August 1994 September 1994 – December 2002	30	Garger, Hoffman and Thiessen (1997) Garger et al. (2012)
Chernobyl	July 1987 – December 1991 January 1992 – December 2002	30	Garger et al. (1994) Garger et al. (2012)
Polesskoe	July 1987 – March 1991	30	Garger et al. (1999)
Pripyat	July 1987 – December 1991 January 1992 – August 2005	10	Garger et al. (1994) Garger et al. (2012)

estimate the single constituents of the variability of the ^{137}Cs activity concentration. It consists of the following three steps:

1) Identification and reduction of a descending trend,

2) Detection of a periodic component and

3) Calculation of the stochastic components for the prediction.

Further analysis is based on the ^{137}Cs time series $c(t)$ collected in Pripyat from 1987 to 1991.

The descending trend of the ^{137}Cs activity concentration without any periodic component was analyzed at first, and the results are shown in this section. The 10-day averages of the ^{137}Cs activity concentration are used to reduce the influence of measuring errors and high-frequency fluctuations. After some empirical dependence functions were tested using regression analysis, the following function was selected as the best one:

$$c_0(t) = a \exp(-t/\tau) + b, \tag{9.1}$$

where $c_0(t)$ is the estimated value of the 10 d averaged ^{137}Cs activity concentration, a and b are empirical parameters, $1/\tau$ is decreasing rate coefficient.

Using the weighted least-squares technique, the coefficients a, τ and b were determined to be $a = 6725$ μBq m^{-3}, $\tau = 300$ d and $b = 346$ μBq m^{-3}.

Then the ^{137}Cs time series of measured $c(t)$ were detrended by dividing by the estimated $c_0(t)$, and a dimensionless time series were obtained that represents the relative fluctuations around a descending trend. For further calculations $u(t) = \log [c(t)/c_0(t)]$ was used (Fig. 9.12).

To obtain a periodic component a method commonly known as the Group Method of Data Handling (GMDH) (Ivachnenko 1975, Ivachnenko et al. 1980) was then applied to $u(t)$ educed above. The GMDH is a set of several algorithms used to solve different problems. It consists of parametric, clusterization, analogs complexing, rebinarization, and probability algorithms. This inductive approach is based on the sorting out of gradually complicated models and selecting the best solution based on an external criterion.

The GMDH algorithms for modeling polyharmonic processes and fields are widely used and work especially well for the short time series with a minimum of *a priori* information on the modeling process. These algorithms rest upon the idea of the inductive self-organization principle and choice of the best model depending on some external discrimination criterion.

During the modeling procedure, the GMDH algorithm involves four heuristics that represent the main features of the GMDH theory:

(1)Collect a set of observations that seems to be relevant to the object.

(2)Divide the observations into two groups. The first will be used to estimate the coefficients of the model while the second will separate the information embedded in the data into either useful or harmful.

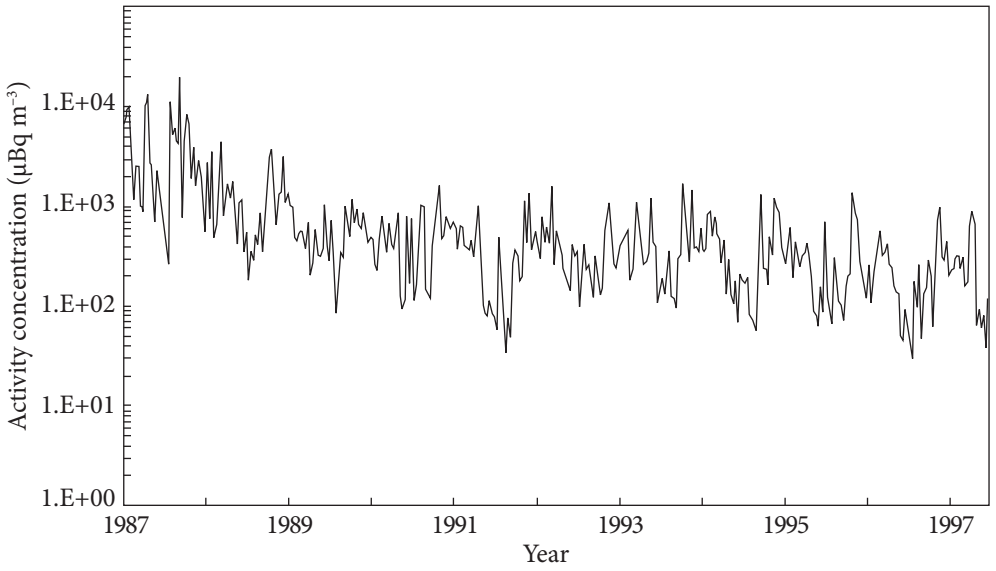

Fig. 9.11. Activity concentration of airborne ^{137}Cs (10-day average) measured in the town of Pripyat. Data until 1991 is from (Garger et al. 1994)

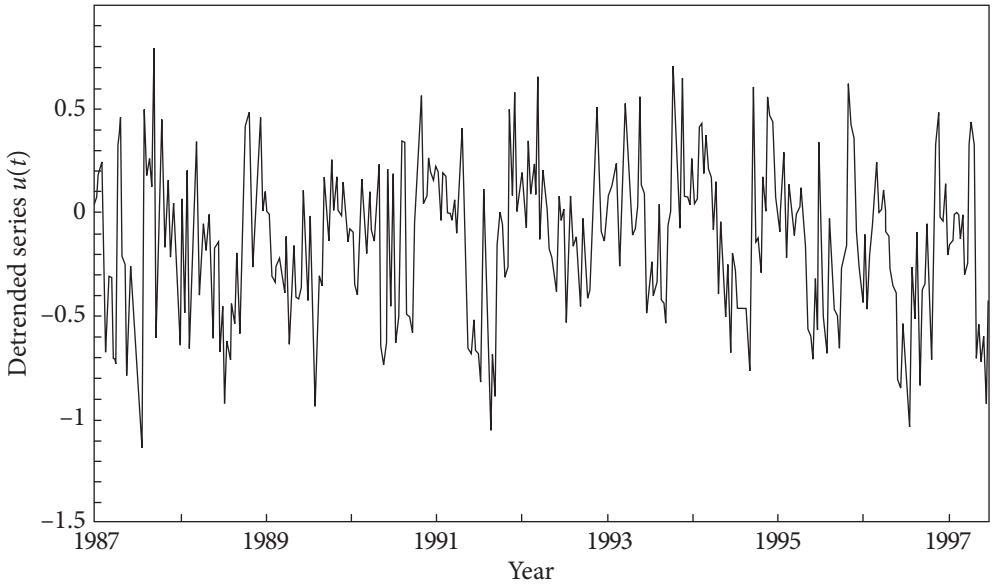

Fig. 9.12. Detrended time series $u(t) = \log[c(t)/c_0(t)]$ of the data presented in Fig. 9.11

(3)Create a set of elementary functions where its complexity will increase through an iterative procedure producing different models.

(4)According to Godel's incompleteness theorem, apply an external criterion to choose the optimal model.

In the change of the activity concentration in the atmospheric surface layer, as well as in most multifactor processes in nature, exact periodicity is absent. Therefore, for the identification of a harmonic trend of the oscillatory process $u(t) = u_n$ and the construction of models for long-term predicting a model structure was introduced in the form of the sum of periodic functions with non-multiple frequencies $\omega_k \neq k\omega_1$, not necessarily related to the period of observation

$$u_n = A_0 + \sum_{k=1}^{m} [A_k \sin(\omega_k n) + B_k \cos(\omega_k n)] + \varepsilon_n,$$
$$0 < \omega_k < \pi, \quad k = 1, 2, ..., m, \tag{9.2}$$

where A_k and B_k are coefficients, minimizing the sum of squares of errors $\sum_{n=1}^{N} \varepsilon_n^2 = \sum_{n=1}^{N} (u_n - u_n^*)^2$, where u_n^* is the computational results of the model, m is the present maximum number of harmonic components, N is a number of 10-day in the examined interval of time.

Unlike the methods of the fast Fourier transform, in this case, the frequencies ω_k are defined from the values of $\cos\omega_1$, $\cos\omega_2$, …, $\cos\omega_m$, determined as roots of the algebraic equation

$$\alpha_0 + \sum_{p=1}^{m-1} \alpha_p \cos(p\omega) = \cos(m\omega) \tag{9.3}$$

with coefficients α_p which must satisfy the system of linear equations

$$\sum_{p=1}^{m-1} \alpha_p (u_{i+p-1} + u_{2m+i-p-1}) + \alpha_m u_{m+i-1} = u_{i-1} + u_{2m+i-1},$$
$$(i = 1, 2, ..., N-2m). \tag{9.4}$$

The GMDH harmonic algorithm employs the following scheme. At first, for each fixed m the harmonic components are computed with frequencies ω_k. The model parameters A_0, A_k, and B_k are estimated for each combination by using the least-squares technique. Then the obtained models are compared using the discrimination criterion. The best model is selected according to the value of the external criterion. The value of the external criterion in GMDH is always calculated on the sample data which has not been used for estimating the model coefficients, so called «test set», unlike the «training set» used for calculating the coefficients

As an external criterion, it was used the criterion of minimizing the mean square error S_B, calculated on the test set $u(t)_B$

$$S_B = \frac{\sqrt{\sum_{i=1}^{N_B} (u_{Bi} - u_{Bi}^*)^2}}{N_B}, \tag{9.5}$$

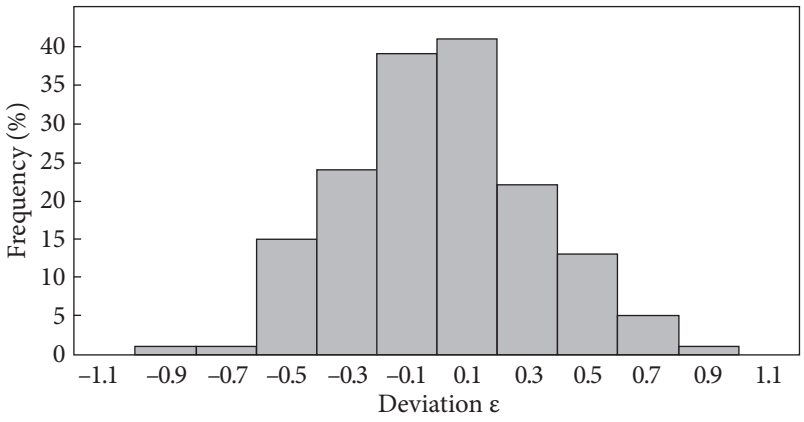

Fig. 9.13. Histogram of the frequency distribution of the deviations $\varepsilon_i = u_i - u_i^*$ for the measurements at Pripyat

including the N_B points of the row explored, not used for estimating the coefficients A_k and B_k in Eq. (9.2) and consisting of about 30% of the total number of available data points N.

The analysis of the deviations $\varepsilon_i = u_i - u_i^*$ showed, that they are poorly correlated and normally distributed (Fig. 9.13). Therefore, $x = \mu_\varepsilon + \sigma_\varepsilon \xi$ was calculated as a stochastic component where μ_ε and σ_ε are mean and standard deviation from $\varepsilon(t)$, and $\xi \sim N(0,1)$ is a random variable following a standard normal distribution. Usually, μ_ε are very close to zero. The length of the sequence x is equal to the number of 10-day periods in the predictive period.

The coefficients of the model obtained using the GMDH based on trigonometric polynomial (Eq. ((9.2)) are represented in Table 9.6.

Table 9.6. **Coefficients of the model computed using the Group Method of Data Handling (GMDH)**

Frequency, radian ω_k	Period, day T_k	Amplitude $\sqrt{A_k^2 + B_k^2}$	Coefficient A_k	Coefficient B_k	Constant term A_0
0.174	362	0.237	–0.048	0.232	–0.112
0.241	261	0.085	–0.083	0.018	
0.329	191	0.045	0.028	–0.036	
0.528	119	0.055	–0.052	0.018	
0.935	67	0.094	0.041	–0.084	
1.272	49	0.036	0.014	–0.033	
1.748	36	0.025	0.012	0.022	
1.935	32	0.022	–0.016	–0.015	
2.594	24	0.034	0.024	0.025	

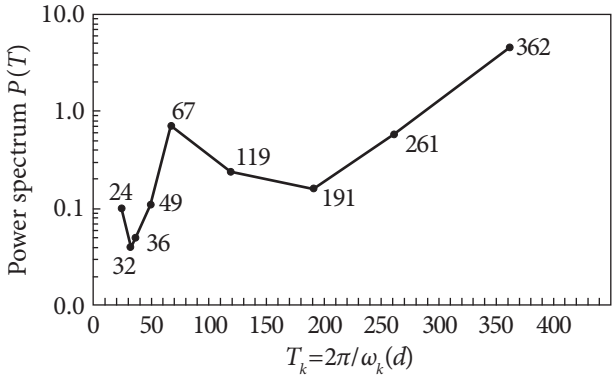

Fig. 9.14. Estimation of a power spectrum $P(T)$ of the time series $u(t)$ of the measurements at Pripyat with GMDH, $T_k=2\pi/\omega_k$ (see text). Number in figure shows T_k in day

Based on the structure of the model, in Fig. 9.14 estimations of the spectral density of the examined row *u(t)* are displayed in a periodogram as the semi-log plot of the function $P(\omega_k)=\frac{N}{2}(A_k^2+B_k^2)$, where $P(\omega_k)$ is a function of the period $T_k=\frac{2\pi}{\omega_k}$. It can be seen that the most relevant contribution to a function in Eq. (9.2) is by annual low-frequency fluctuations with a period of about 360 d (one year). The annual cycle may be induced by the annual increase in the activity concentration of ^{137}Cs in April after the withdrawal of the snow cover. Furthermore, there is another peak at a period approximately equal to 70 d indicating seasonal fluctuations. Long-term recurrent seasonal fluctuations are characterized e.g. by a change of the mean wind speed, reduced surface roughness due to the lack of a vegetation cover and dryness/humidity of the soil surface attributable to the local climate. The cycle of 24 d may be associated with human activity at the «Shelter» site which responds to a particular shift system and the periodicity in the change of the wind direction. Since the method aims to identify hidden periodicities in time series, not all influencing factors or combinations of them may find a clear and unambiguous explanation.

The final expression for a long-term prediction of $c(t)$ of the atmospheric activity concentration of ^{137}Cs can be written as

$$c^*(t)=10^{z(t)}c_0(t). \tag{9.6}$$

Here $c_0(t)$ is a descending exponent fit with the constant term, while $z(t)=u^*(t)+x(t)$ is a random cyclic component, which has the same low-frequency periods of fluctuation, variance and mean value as $u(t)$, with $u^*(t)$ and $x(t)$ calculated above.

9.5. Statistical model of the atmospheric ^{137}Cs activity concentration prognoses and its comparison with measured data

In Fig. 9.15 the experimental data at Pripyat are shown for the whole measurement period from 1987 till 2015. The descending trend of the activity concentration in the air can be matched only by a model using a constant term.

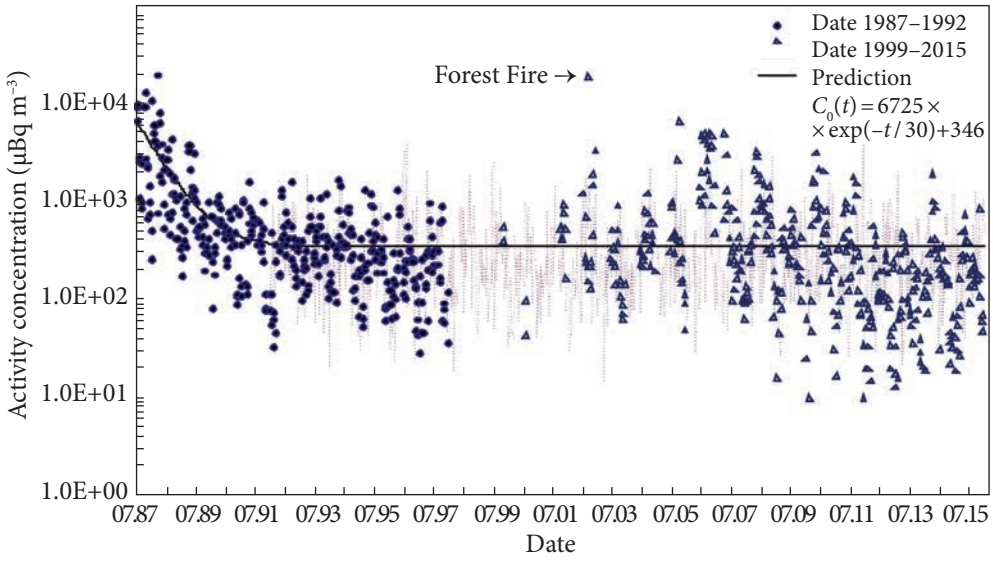

Fig. 9.15. Measured and predicted ^{137}Cs activity concentration for Pripyat until 2015 (10-day average). A large value of measured concentration (indicated with the arrow) was due to forest fires in August - September 2012 (see Chapter 14.3)

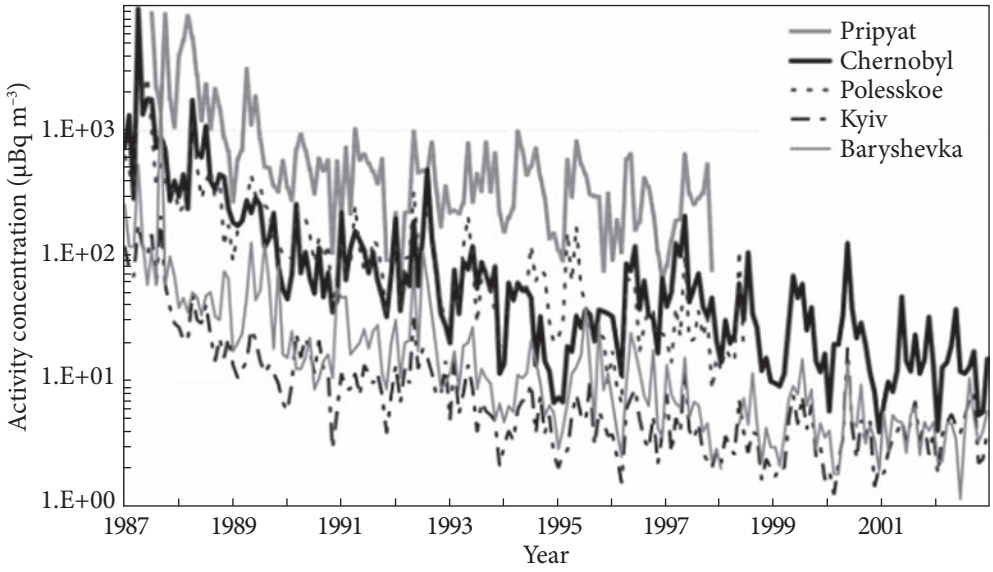

Fig. 9.16. The temporal course of the airborne ^{137}Cs activity concentration at five places in Ukrainian Polesye

Table 9.7. **Correlation coefficients between the different sampling sites from the mean monthly values (139 values) of the activity concentrations of ^{137}Cs in the surface air**

	Kyiv	Baryshevka	Chernobyl	Polesskoe	Pripyat [a]
Kyiv	1.0	0.70	0.71	0.82	0.54
Baryshevka		1.0	0.35	0.34	0.43
Chernobyl			1.0	0.79	0.70
Polesskoe				1.0	0.70
Pripyat					1.0

Note: [a] 128 values.

Finally, the predicted values of the airborne ^{137}Cs activity concentration as shown in Fig. 9.15 were computing using a formula

$$c^*(t) = 10^{z(t)} \cdot [6725 \exp(-t/30) + 346], \tag{9.7}$$

where $c^*(t)$ is the required modeling function.

The model predictions match the observed atmospheric activity concentration of ^{137}Cs pretty well. Two major deviations to the predicted values can be explained by unexpected phenomena: intense forest fires happened in 2002, and a significant release of radionuclides from the Chernobyl Shelter occurred in 2005.

Additionally, the behavior of the model's parameters was studied in dependence on the length of the time series. It was observed that the model parameters began to stabilize when the time series of the ^{137}Cs activity concentration in the air reached a length of about 4.5 y, which corresponds to a time series beginning in 1987 and ending in the middle of 1991. A longer time series could not improve the model significantly and result in a variation of the parameters a and τ of about 1-3%. At the same time, the change in the constant term b did not exceed 10%. This confirms the reliability of the determined parameters of the model, obtained for the 1987-1991 period, and enhances the confidence of its use for long-term prediction, relying on the estimates from the first 4-5 y after the accident.

Furthermore, one is interested in the prediction of the atmospheric activity concentration of ^{137}Cs in different locations close to, but outside the exclusion zone. In Fig. 9.16 the temporal course of the measured activity concentrations of ^{137}Cs at five places in the Ukrainian Polesye is shown. Three of the places (Polesskoe, Kyiv, Baryshevka) are all located between 60 and 230 km away from the Chernobyl nuclear power plant (Fig. 9.10).

It can be seen from Fig. 9.16 that the phase of stabilization of the airborne activity concentration has begun at around 1995 or 1996 for all sites. Table 9.7 shows the coefficients of correlation of the data measured at the five different sites. The measurements show a high positive correlation. Therefore, it is con-

cluded that the atmospheric activity concentration of ^{137}Cs at the five places is influenced by the same synoptic processes (wind speed, soil humidity, snow cover, etc.) and hence a prediction of the airborne activity concentration can be based on the same prediction method using the observations from these sites. However, to formulate such prediction will be the task of a further study.

Hence a model for long-term predicting of the ^{137}Cs activity concentration in the atmospheric surface layer from a limited number of observations in the Pripyat area was developed. The model is based on the identification of individual components of the non-stationary process, such as descending and harmonic trends, and stochastic fluctuations. It takes into account the influence of annual and seasonal variations due to basic meteorological processes.

According to the sampling and measurements performed from 1987 to 1991, the prediction appeared satisfactory both on average value of the atmospheric activity concentration and on values of the amplitudes of fluctuations. It could be shown that the length of the sampling period was sufficient enough for setting up a reliable prediction model.

In general, the magnitude and character of fluctuations of the predicted activity concentration in the air are similar to those that were measured in the Pripyat area from 1991 to 1997 (validation period).

CHAPTER 10

ACTIVITY SIZE DISTRIBUTION OF RADIOACTIVE PARTICLES

10.1. Introduction

After the Chernobyl accident, numerous measurements were made to characterize the primary radioactive atmospheric aerosol in terms of nuclide composition and particle size at several locations in Europe (Jost et al. 1986; Tschiersch and Georgi 1987; Reineking et al. 1987; Horn, Bonka and Maqua 1987). Within the 30-km exclusion zone of the Chernobyl Nuclear Power Plant, only a few measurements were made for the characterization of that primary aerosol (Report of the IEM 1987, Gaziev et al. 1993, Gaziev and Kabanov 1993). At present, it is obvious that the 30-km zone is a permanent source of radioactive aerosol including hot particles due to the high soil contamination. Knowledge of characteristics of the resuspended aerosol will be required for a long time for a more detailed dose assessment and estimation of processes of redistribution of the contamination of the surface soil. In a series of papers, results of the measurements of the resuspended radioactive aerosol of the Chernobyl zone are presented which were obtained in two scientific programs. One was launched by the Hydrometeorological Committee of the USSR, the other (ECP1 1996) by the European Commission. This chapter includes an analysis of the size-resolved airborne activity concentrations of wind-driven resuspension which have been measured since 1986. The analysis of accumulated data has shown, that the accident at the ChNPP has given in formation of a composite disperse system consisting of aerosols of a various physicochemical nature: particles of fuel; particles of dispersed substance; condensation aerosols formed by condensation of radionuclide vapors in a release plume on a surface of aerosol particles and on atmospheric nucleus of condensation; fractal structures — condensation aerosols and conglomerates having in a basis a soot with the volume density, practically of equal to the air density.

In Western and Central Europe observations of radioactive aerosols have begun at once after the accident (Bunzl et al. 1995, Besnus et al. 1997, Livens and Baxter 1988). In July 1986 in the 30-km zone of the ChNPP the aerosol station near Zapolie, located in 14 km to the south from ChNPP, was created by SPA «Typhoon» of Hydrometeorological Committee of the USSR. Measurements of the physicochemical characteristics of secondary wind lift of radioactive aerosol, its dispersion in space and time, secondary contamination the atmospheric surface layer due to various types of sources, including object «Shelter», were begun (Garger 1994, Garger et al. 1998).

Aerosol measurements were made in the surface layer of the atmosphere in the 30-km zone. They were conducted periodically from September 1986 till June 1993 at two sites: Zapolie and Pripyat. The main task was to estimate the time evolution of the particle size distribution of radioactive aerosol. To this end, data of granulometric analysis of soil with attached radionuclides and the time evolution of the general characteristics of the resuspended radioactive aerosol are considered.

10.2. Radionuclide attachment to the soil

Radionuclides deposited in a particulate form on the ground do not remain unchanged with time in concentration and shape in the top soil layer, which is accessible for resuspension. Radionuclides may be remobilized from the aerosol particles and become available for migration. They are transported to deeper soil layers and attach to soil minerals. The concentration in the top soil layer decreases, and the size distribution changes. Because of the different behavior of the radionuclides, the nuclide ratio may change as well (ECP1 1996).

The first measurements at the experimental sites were made during August and September 1986 (Garger 1994). Surface contamination was measured using samples of 15 cm diameter and a depth of 5 cm. Detailed data are presented of twelve locations in the southern part of the 30-km zone with distances to the NPP from 4 to 25 km. At the main experimental site Zapolie, the following mean values were measured: 0.5 MBq m^{-2} of ^{137}Cs contamination and 6.9 MBq m^{-2} of ^{144}Ce contamination. The activity ratio $^{144}Ce/^{137}Cs = 13.8$ is in good agreement with data (Begichev et al. 1990, Bogatov et al. 1990) confirming that this site is representative for the 30-km zone.

According to measured residence half-times in the top soil layer for ^{137}Cs (Bunzl et al. 1995), two cases can be distinguished. In the far-field site in Bavaria, Germany an increase of the residence time from about 0.85 years (two years after deposition) to about 1.65 years (seven years after deposition) was observed, whereas in the near-field site in 6 km distance from the ChNPP a decrease of the residence time was measured: from about 6.8 years (two years after deposition) to about 3.2 years (seven years after deposition). The different behavior was attributed to the different matrix in which ^{137}Cs was fixed. In the near-field site, the major part of ^{137}Cs was deposited

in the form of rather insoluble fuel particles, which need several years for disintegration; in the far-field site ^{137}Cs was transported mainly as condensation aerosol in a more soluble form. Seven years after deposition about 17% of the deposited activity is in both cases still in the top soil layer (0-1 cm) available for resuspension.

Data in Table 10.1 give information on the time evolution of the inventory of ^{137}Cs and ^{144}Ce at the site Zapolie from 1986 to 1993. The detection limit was assumed to be twice the background value, which is 1.9 Bq / sample for ^{137}Cs and 0.12 Bq / sample for ^{144}Ce (soil sample in a 1,000 cm^3 Marinelli beaker). From these data, it follows that the inventory of ^{137}Cs is constant (within the limit of measurement errors), whereas the total activity of ^{144}Ce has decreased.

During the resuspension experiments in Zapolie 1992/1993 soil samples were taken and the activity concentration profiles were determined (Besnus et al. 1997). In the top soil layer, the relatively high variability of the activity concentration was found. About 20% of the deposited activity was still available in the top soil layer (0-1 cm), in the soil layer 0-5 cm about 80% of the total activity was found. There was no significant difference in the activity depth profile observed between the several types of nuclides.

Radionuclides attached to soil particles, but they were not uniformly distributed throughout the soil particle size range. Studies at sites in the UK (Livens

Table 10.1. **Activity inventory of ^{137}Cs and ^{144}Ce in soil at the Zapolie site**

Year	^{137}Cs (MBq m^{-2})	^{144}Ce (MBq m^{-2})	Nuclide ratio
1986	0.50 [a]	6.9 [a]	13.8
1988	0.44 [a]	0.96 [a]	2.18
1991	0.51 ± 0.18	0.08 [b]	0.157
1993	0.53 ± 0.11	0.027 [c]	

Note: [a] value measured after mixing and homogenization of 5 samples according to (Report of the IEM 1987); [b] value measured on single samples (activity close to detection limit); [c] value calculated according ^{144}Ce activity in September 1986.

Table 10.2. **Specific activity in different granulometric soil fractions at Zapolie (Besnus et al. 1997)**

Granulometric size range (μm)	20–10	10–5	5–1.4	<1.4
Median diameter (μm)	20.5	7.2	2.2	0.8
Specific surface (cm^2 g^{-1})	2.215	7.650	12.260	33.790
Specific ^{137}Cs activity (Bq g^{-1})	4.3	16.0	33.0	210
Specific ^{144}Ce activity (Bq g^{-1})	0.42	2.16	3.34	1.46
Nuclide ratio ^{144}Ce/^{137}Cs	0.098	0.135	0.101	0.00695

and Baxter 1988) showed that the radionuclides tend to be concentrated in the finer size fractions of soils. The value of the atmospheric activity concentration depends on the size distribution of soil particles and is closely related to the specific surface areas of the soil fractions. In the finer size fractions with the clay-sized particles (<2 μm) enrichments of ^{137}Cs were measured to be in the range of factor 3 to 35, enrichments of plutonium in the range of factor 1.5 to 40 (Livens and Baxter 1988).

At Zapolie the size distribution of soil particles and the specific activity distribution were measured (Besnus et al. 1997). The Zapolie soil texture consists mainly of silts and fine sand with respectively 33% of particles ranging from 50 to 200 μm and 42% ranging from 2 to 50 μm. The fine volume fraction of soil (< 2 μm) is about 8%. For a particle size larger than 20 μm a linear relationship was found between specific ^{137}Cs activity and size. The high increase in specific activity measured for the smallest particle sizes seems not to depend just on their external surface. Clay minerals with structures provide larger surfaces than the approximation by spheres; fuel particles contribute as well in there. In comparison with ^{144}Ce, a higher proportion in the fine particle fraction was found for ^{137}Cs (see Table 10.2).

According to the presented data, it may be expected that the radioactive loading of airborne particles will follow a unimodal size distribution with the maximum specific activity concentration in the fine particle fraction with $d < 1.4$ μm.

In the summer of 1986, the permanent field site near the village Zapolie was set up, at which various types of samplers could be deployed. The size distributions of radionuclides were measured at this site with the multicascade impactors IK (6 cascades, ≈40 $m^3\,h^{-1}$) and PK (6 cascades, ≈380 $m^3\,h^{-1}$, since 1991). An additional multicascade impactor UP (5 cascades, ≈400 $m^3\,h^{-1}$) was set up in the town Pripyat in the autumn of 1987. The exposed filters were analyzed by γ-spectrometry. The detection limit was assumed to be twice the background value, which is 0.45 Bq / sample for ^{137}Cs and 0.03 Bq / sample for ^{144}Ce (compressed aerosol filter sample). More details of the measurement sites, instruments, and the experiments are given in (Garger et al. 1997).

10.3. Activity distribution of size particles during natural wind-driven resuspension

At two different sites in the 30-km zone differing by soil and the primary deposition, impactor measurements allowed the characterization of the size distribution of the radioactive aerosol. First, the total airborne radioactivity concentrations measured by impactors at Zapolie were compared with data obtained by the Chernobyl high volume sampler «Typhoon», which permanently sampled total suspended particulate. Fig. 10.1 presents the monthly

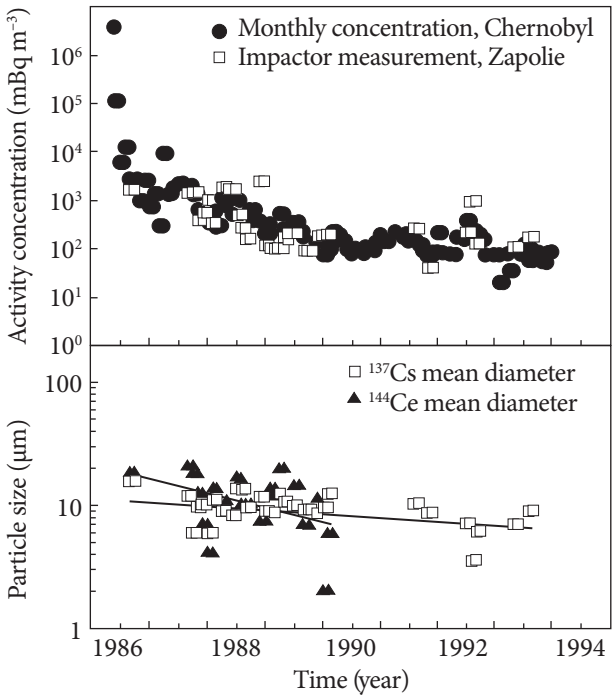

Fig. 10.1. Temporal course of the airborne ^{137}Cs activity concentration and ^{137}Cs, ^{144}Ce mean diameters according to impactor measurements at Zapolie. For comparison the monthly airborne ^{137}Cs activity concentrations at Chernobyl are given. Linear regression of the mean diameter shows a decrease with time

air activity concentration of ^{137}Cs during eight years. In spite of the different sites and methods of measurements, the temporal course of the total air activity concentration of ^{137}Cs at these two sites is similar.

For the retrospective inhalation dose assessment for workers who participated in the Chernobyl accident (liquidators), in general, the assumption is made that the size distribution of the radioactive aerosol has the form of a log-normal distribution. To check this assumption, the first two statistical moments of the measured activity size distributions were calculated.

In Tables 10.3 and 10.4, the total activity concentration of ^{137}Cs and ^{144}Ce and the main parameters of the activity size distributions are given for the measurement periods in 1986—1993. The mean weighted diameter was calculated by the equation

$$\overline{d} = \frac{\sum_j a_j \cdot d_j}{A}, \tag{10.1}$$

where d_j is the mean diameter (in μm); a_j is the activity of the j-th size range of particles and A is the total nuclide activity of a sample. The geometric diameter d_g and the standard deviation σ_g of the experimental data were calculated by using the following expressions (Finlayson and Pitts 1986)

$$\ln d_g = \frac{\sum_j a_j \cdot \ln d_j}{A}, \qquad \ln \sigma_g^2 = \frac{\sum_j a_j \cdot \ln (d_j - \overline{d})}{A}. \tag{10.2}$$

The standard deviation of a log-normal distribution may be calculated by the equation

$$\sigma = \ln \sigma_g. \tag{10.3}$$

The estimation of the standard deviation σ_1 in Table 10.3 was performed according to Eq. (10.3).

Assuming a log-normal size distribution with the median diameter d_m, σ_g may be estimated from the probability plot of the integral radioactivity size distribution and gives a second estimation of the standard deviation (σ_2) in Table 10.3:

$$\sigma_g = \frac{d_{84\%}}{d_m} \quad \text{or} \quad \sigma_g = \frac{d_m}{d_{16\%}}. \tag{10.4}$$

The second estimation (σ_2) could only be determined for a limited number of the experimentally determined activity size distributions. In the cases where both estimates are available, the ratio was calculated. For a log-normal distribution, the ratio must be unity.

For the independent estimation of the median diameter, for example, by numerical integration of the area under the experimental curve of the particle size distribution, it is possible to use the following theoretical ratio between the mean diameter and the median diameter for a log-normal distribution (Finlayson and Pitts 1986)

$$\frac{\overline{d}}{d_m} = e^{\sigma^2/2}. \tag{10.5}$$

In Tables 10.3 and 10.4, the median diameter was calculated by numerical integration of the experimentally determined radioactivity distribution in the coordinates $\frac{\Delta N}{N \cdot \Delta \log d}$ and $\log d$. In Table 10.3 the total airborne activity concentra-

Table 10.3. **General parameters of airborne particle size distributions of ^{137}Cs at Zapolie**

Period of measurement	Total activity concentration (mBq m^{-3})	Mean and median diameters $\overline{d}$, d_m (μm)	σ_1	$\frac{\overline{d}}{d_m}$	$\frac{d_g}{d_m}$	$\frac{\sigma_1}{\sigma_2}$
IK impactor						
17.09–23.09.86	1.64	15.7 (20.9)	2.1	0.75	0.47	
23.09–14.10.86	1.00	16.5 (15.8)	1.4	1.04	0.78	
08.09–26.09.87	1.46	12.0 (11.5)	2.4	1.04	0.39	
30.09–14.10.87	1.43	6.0 (0.78) ($d_m^1 \approx 0.4$ μm, $d_m^2 \approx 17.4$ μm)	1.8	7.7	2.5	
15.10–01.11.87	0.39	9.8 (4.4)	2.0	2.2	1.08	
27.11–14.12.87	0.56	10.2 (4.6)	2.1	2.2	1.09	1.07

Continuation of Table 10.3.

Period of measurement	Total activity concentration (mBq m^{-3})	Mean and median diameters $\overline{d}$, d_m (μm)	σ_1	$\frac{\overline{d}}{d_m}$	$\frac{d_g}{d_m}$	$\frac{\sigma_1}{\sigma_2}$
15.01–07.02.88	1.00	6.0 (2.6)	1.5	2.3	1.04	0.83
12.02–08.03.88	0.33	11.1 (4.6)	2.2	2.4	1.2	
15.03–22.04.88	1.86	9.0 (4.3)	1.8	2.1	1.08	1.15
24.05–24.06.88	1.64	8.4 (0.95)	2.1	8.8	3.0	
27.06–29.07.88	0.52	13.8 (10.0)	2.1	1.4	0.85	1.37
30.07–03.09.88	0.29	13.6 (8.5)	2.1	1.6	0.96	1.42
05.09–30.09.88	0.16	9.8 (4.5)	1.9	2.2	1.4	1.38
09.12.88–09.01.89	2.40	11.9 (2.5) ($d_m^1 \approx 1.7$ μm, $d_m^2 \approx 25.1$ μm)	2.4	4.8	2.0	
16.01–11.02.89	0.12	9.0 (5.0)	1.8	1.8	1.2	
13.02–14.03.89	0.108	8.9 (5.0)	1.8	1.8	1.2	
18.03–18.04.89	0.11	12.4 (7.6)	2.2	1.6	0.89	1.10
03.05–10.06.89	0.16	10.6 (4.4)	1.9	2.4	1.5	1.15
14.06–20.07.89	0.21	10.1 (5.5)	1.9	1.8	1.07	1.40
08.09–17.11.89	0.092	9.2 (5.4)	1.5	1.7	1.1	1.45
17.11–20.12.89	0.176	8.9 (4.8)	1.7	1.8	1.1	1.52
20.12–23.01.90	0.180	9.7 (4.1)	2.0	2.36	1.3	1.60
23.01–01.03.90	0.190	12.4 (12.3) ($d_m^1 \approx 2.2$ μm, $d_m^2 \approx 15.3$ μm)	1.7	1.0	0.65	
20.08–27.08.91	0.260	10.3 (5.3)	2.0	1.94	1.15	1.48
		PK impactor				
04.11–27.11.91	0.040	8.9 (6.8)	2.08	1.3	0.79	
05.07–10.07.92	0.210	11.3 (8.8)	0.7	1.28	0.76	0.49
23.07–30.07.92*	0.944	3.2 (0.28)	0.9	11.4	6.1	
05.08–05.09.92*	0.134	3.6 (0.5)	1.1	12.8	6.8	
08.09–27.09.92	0.109	6.2 (1.7)	1.5	3.6	1.7	0.60
08.05–11.05.93	0.220	7.7 (4.2)	1.6	1.8	1.05	1.07
27.05–01.06.93	0.152	6.5 (4.1)	1.4	1.6	0.90	0.74
01.08–06.08.93	0.164	7.0 (4.3)	1.5	1.6	0.93	0.94
06.08–10.08.93	0.209	14.8 (19.0)	2.2	0.78	0.46	
10.08–19.08.93	0.119	5.6 (2.6)	1.2	2.15	1.2	0.70

* Period with a forest fire.

Table 10.4. **General parameters of airborne particle size distributions of ^{137}Cs and ^{144}Ce at Pripyat**

Period of measurement	Total activity concentration (mBq m^{-3})	Mean and median diameters $\overline{d}$, d_m (μm)	σ_1	$\frac{\overline{d}}{d_m}$	$\frac{d_g}{d_m}$	$\frac{\sigma_1}{\sigma_2}$
		^{137}Cs				
27.09—14.10.87	5.95	4.7 (3.0)	0.88	1.57	1.10	0.96
16.10—01.11.87	*	5.6 (3.1)	0.46	1.81	1.16	0.42
05.11—21.11.87	*	6.2 (0.6)	0.62	10.3	2.8	0.17
01.12—19.12.87	*	10.1 (7.5)	0.44	1.35	1.03	0.24
18.01—07.02.88	7.34	11.6 (9.6)	0.60	1.21	0.92	0.29
12.02—05.03.88	3.00	10.9 (7.6)	0.64	1.43	0.91	0.42
15.03—14.04.88	3.35	10.6 (7.0)	0.65	1.51	0.90	0.43
21.04—17.05.88	1.98	8.6 (5.1)	0.16	1.70	1.02	0.13
23.05—18.06.88	1.78	7.8 (5.7)	0.35	1.40	0.91	0.28
28.06—28.07.88	1.59	7.6 (4.7)	0.49	1.60	0.91	0.40
30.07—02.09.88	1.65	14.7 (14.2)	0.69	1.04	0.73	–
04.09—18.09.88	1.12	6.5 (3.6)	0.52	1.80	1.02	0.40
13.07—07.10.90	*	5.5 (2.5)	0.52	2.20	1.12	0.40
10.10—20.12.90	*	7.6 6.7)	0.05	1.13	0.92	—
15.01—25.01.91	0.30	7.6 (4.9)	0.45	1.55	0.96	0.41
02.07—14.07.92	0.726	7.1 (3.7)	0.56	1.92	0.84	—
08.09—26.09.92	0.479	6.5 (3.1)	0.57	2.10	0.97	0.34
		^{144}Ce				
27.09—14.10.87	23.80	5.0 (3.1)	0.36	1.61	1.13	0.39
16.10—01.11.87	*	5.8 (3.3)	0.46	1.76	1.18	
05.11—21.11.87	*	8.0 (0.65)	0.65	12.3	3.38	
01.12—19.12.87	*	11.0 (8.3)	0.52	1.32	1.08	
18.01—07.02.88	25.50	12.5 (9,7)	0.63	1.29	1.03	
12.02—05.03.88	12.36	11.1 (8.4)	0.57	1.32	1.01	
15.03—14.04.88	10.91	11.6 (8.7)	0.64	1.33	0.91	0.48
21.04—17.05.88	4.29	8.9 (5.6)	0.19	1.60	0.91	0.16
23.05—18.06.88	2.30	9.5 (7.1)	0.22	1.30	1.01	
28.06—28.07.88	3.57	9.8 (7.0)	0.48	1.40	0.90	
30.07—02.09.88	1.74	7.3 (3.8)	0.58	1.92	0.74	
04.09—18.09.88	1.02	7.7 (5.7)	0.40	1.35	0.75	
13.07—07.10.90	*	1.3				
10.10—20.12.90	*	8.8				

* Due to break of electric power, only activity size distribution is available.

tions, the ratios between the mean and median diameters and the ratios between geometric mean and median diameters are documented. In the case of a log-normal distribution, these ratios must be unity. When the experimental distribution had two modes with a well defined gap in between, it was possible to estimate two median diameters. Analysis of Table 10.3 shows that the measured distributions are generally very wide and mostly differ from a log-normal distribution. The statistical parameters of the activity size distributions are more uniform at Pripyat (Table 10.4) compared to the values at Zapolie (Table 10.3).

10.4. A typical form of distribution shapes

Detailed analysis of the radioactivity size distribution has shown that five typical shapes of distributions can be distinguished (see Fig. 10.2). The type (*1*) represents a log-normal distribution with a median diameter between 2-4 μm. The types (*2*), (*3*) and (*5*) have two modes and are together the most frequent distributions with 91% from 88 cases at Zapolie. The medians of these bimodal distributions are in the following diameter ranges: at about 0.5 μm and between 10-20 μm (type *2*), between 1-2 μm and between 10-20 μm (type *3*), at about 4 μm and between 20-30 μm (type *5*). Type (*2*) is a very distinct bimodal distribution with a very large part of inhalable particles. The type (*4*) has a broad maximum in the large particle size range (median at about 10 μm).

The main parameters of the size distribution of type (*4*) were reported to be representative for fuel particles inside the 10-km zone of ChNPP by other authors as well (Report of the IEM 1987, Begichev et al. 1990, Bogatov et al. 1990). However, the size range of particles, the mean and median diameter depend on the transport direction of the primary radioactive clouds. In general, the interval of the median diameter ranges from 5 to 55 μm, the size of the particles does not exceed 100 μm.

The relative frequency of the distribution types measured at Zapolie and Pripyat is given in Table 10.5. In all 88 examined cases the log-normal size distribution of type (*1*) is observed only three times at Zapolie (3%). Type (*5*) was observed in 56% of all cases, type (*2*) in 19%, type (*3*) in 16% cases and type (*4*) in 6% of all cases. In other words, at Zapolie mainly a bimodal radioactive aerosol distribution was observed with a considerable part of respirable and inhalable particles and an important fraction of large particles. Taking this into account, the unimodal distribution which we expected from the soil activity size distribution will not give a correct estimation of the inhalation dose.

At Zapolie the different types of distribution were split up into three groups according to different total ^{137}Cs activity concentrations: a background case, when the total concentration was equal or less than the mean annual value for Chernobyl in 1991 (0.12 mBq m^{-3}), a case with high airborne concentration (equal or

Table 10.5. **Frequency of size distribution types (see Fig. 10.2) in (%) at Zapolie and Pripyat for different ^{137}Cs activity concentration q (mBq m^{-3}) ranges**

Distribution type	*1*	*2*	*3*	*4*	*5*
Zapolie, all	3	19	16	6	56
Zapolie, $q \le 0.12$ mBq m^{-3}	0	29	43	0	29
Zapolie, 0.12 mBq m^{-3} < $< q < 1$ mBq m^{-3}	6	0	6	6	82
Zapolie, $q \ge 1$ mBq m^{-3}	0	50	12.5	12.5	25
Pripyat, all	23	13	3	55	0

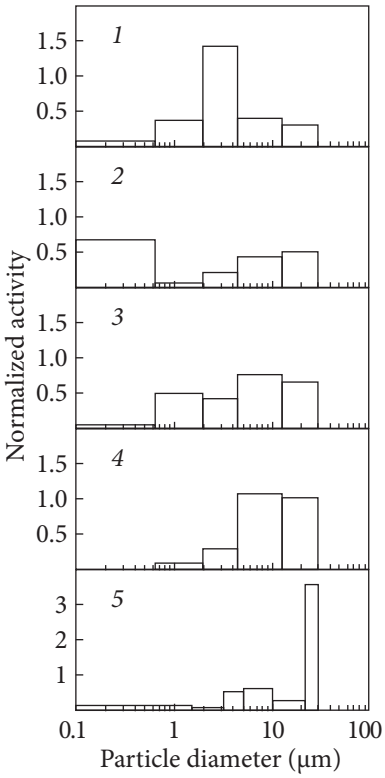

Fig. 10.2. The five most frequent shapes of the activity size distribution in the Chernobyl area. In Zapolie the bimodal types (*2*), (*3*) and (*5*) amount to 91% of all cases; in Pripyat type (*4*)

more than 1.0 mBq m^{-3}) and an intermediate case with airborne concentrations between these values. For the intermediate case, it was found that 82% of the distributions were of type (*5*). For the background conditions, 29% of distributions were of type (*5*). In periods with high airborne concentrations, 50% of distributions were of type (*2*) with a considerable quantity of fine particles.

In distinction to Zapolie, the distribution type (*5*) was not observed at all at Pripyat (see Table 10.5). The distributions of type (*4*) were measured in 55%, type (*1*) in 23%, type (*2*) in 13% and type (*3*) in 3% of all 31 cases. In two other cases, the activity could be detected in only one or two cascades. A unimodal type of activity size distribution is predominant at Pripyat, which is situated close to the very high contaminated area. For ^{137}Cs, the maximum of the mean aerodynamic diameter ranges from 8 μm to 12 μm and the maximum of the median aerodynamic diameter from 5 μm to 10 μm. For ^{144}Ce the maxima are between 8-12.5 μm and 6-10 μm, respectively. In Fig. 10.3, distributions of the three nuclides ^{137}Cs, ^{144}Ce and ^{106}Ru are shown. In spite of small differences, we observe similar types of distributions for all three nuclides. Differences between the mean diameter values are small, too. The radioactive aerosol was generally of fuel origin. A considerable part of fine particles was found in some

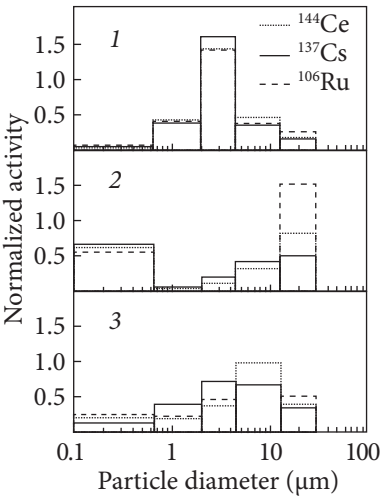

Fig. 10.3. Measured activity size distributions of one sampling period showed at Pripyat the same shape for all three radionuclides considered

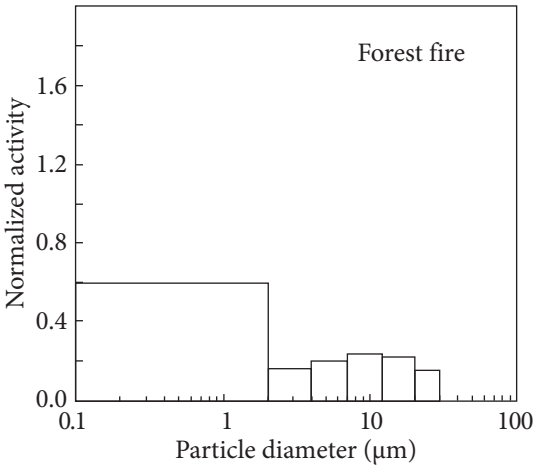

Fig. 10.4. ^{137}Cs activity size distribution measured at Zapolie during a forest fire at about 17 km distance from the burning area

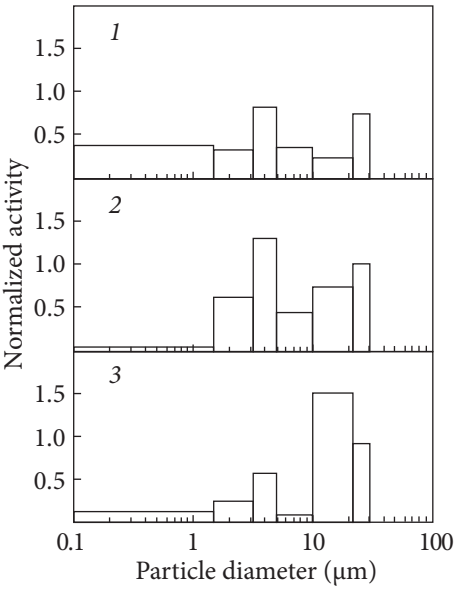

Fig. 10.5. Typical ^{137}Cs activity size distributions as measured in the winter months January and February at the Zapolie site: (*1*) 15.01–07.02.1988; (*2*) 16.01–11.02.1989; (*3*) 23.01–01.03.1990

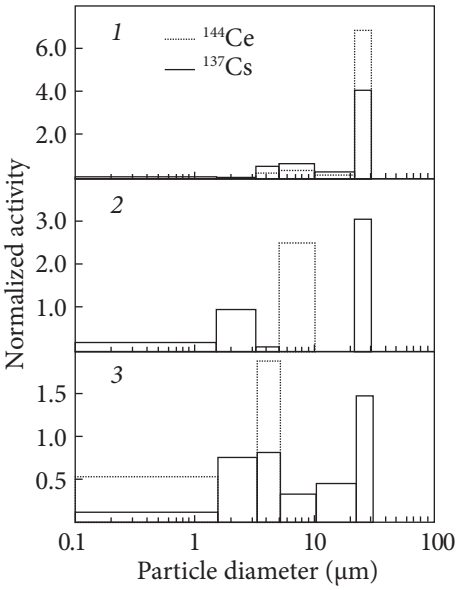

Fig. 10.6. Activity size distributions for the radionuclides ^{137}Cs and ^{144}Ce at Zapolie in an early and in two later sampling period: (*1*) 17.09–23.09.1986; (*2*) 09.12.1988–09.01.1989; (*3*) 20.12.1989–23.01.1990

cases (see Fig. 10.3). At present, the source of these particles near the epicenter of the accident is not clear.

A special case of the radionuclide size distribution was found during two periods of forest fire (23.07-30.07.1992, 05.08-05.09.1992) (Fig. 10.4). The main part of radioactivity was connected to submicron particles with median diameters of 0.28 and 0.5 μm, respectively. These data are consistent with measurements of the volume distribution during forest fire (Hollander and Garger 1996).

Examples of winter measurements (January — February) of the activity size distribution at the Zapolie site are presented in Fig. 10.5. Significant airborne activity concentrations of ^{137}Cs and ^{144}Ce were measured also during snow cover (0.12-1.0 mBq m^{-3}). The main source of the radioactive particles was high contaminated territories where decontamination was performed. A second potential

Table 10.6. **Time evaluation of radionuclide size distributions at Zapolie**

Range (μm)	Nuclide	Relative nuclide activity concentrations (%)							
		1986	1987	1988	1989	1990	1991	1992	1993
$d \geq 10$	^{137}Cs	63.2	34.6	36.6	36.1	49.5	32.8	20.5	27.3
	^{144}Ce	69.5	57.8	37.8	37.1	0.0	—	—	—
	^{106}Ru	22.0	50.0	44.4	—	—	—	—	—
$10 > d > 5$	^{137}Cs	15.5	9.9	12.9	19.0	6.1	22.6	8.4	13.3
	^{144}Ce	14.6	16.4	11.0	43.8	26.5	—	—	—
	^{106}Ru	5.5	0.0	5.9	—	—	—	—	—
$5 > d > 3.2$	^{137}Cs	8.4	8.0	13.8	15.1	13.4	10.2	8.7	11.2
	^{144}Ce	14.6	9.4	5.8	6.6	41.8	—	—	—
	^{106}Ru	25.5	—	4.2	—	—	—	—	—
$d \leq 3.2$	^{137}Cs	13.0	47.6	36.6	29.8	30.8	34.4	60.2	48.2
	^{144}Ce	1.4	16.3	25.4	12.5	31.6	—	—	—
	^{106}Ru	47.0	50.0	45.6	—	—	—	—	—

Table 10.7. **Time evaluation of the radionuclide ratio ^{144}Ce/^{137}Cs for different particle size ranges at Zapolie**

Particle range (μm)	Nuclide ratio ^{144}Ce / ^{137}Cs				
	1986	1987	1988	1989	1990
$d \geq 10$	6.8	1.7	1.6	0.21	—
$10 > d > 5$	10.6	2.0	1.6	1.0	2.0
$5 > d > 3.2$	17.9	1.9	3.3	0.4	2.9
$d \leq 3.2$	6.0	1.9	2.6	0.9	1.0

source was the contaminated forest. In the size distribution, two maxima were observed: at 4 μm and between 10-20 μm particle diameter. In the first case (*1*), we observed also a considerable part of inhalable aerosol.

In Fig. 10.6 the size distributions of the ^{137}Cs and ^{144}Ce activity concentrations are shown together. In 1986, ^{144}Ce was generally observed in the large 20-30 μm particles. In winter 1990, where the source can not be a soil surface, ^{144}Ce is localized in the middle and fine particles. A more probable source is the NPP and the contamination work around it.

Table 10.6 presents the mean annual air activity concentrations of ^{137}Cs, ^{144}Ce and ^{106}Ru size discriminated in four size ranges (the giant particles with $d > 10$ μm, the respirable ones with 10 μm $> d >$ 3.2 μm and the inhalable particles with $d <$ 3.2 μm) for the years 1986-1993. In spite of the averaging process of the data, bimodal annual distributions are retained all the time. However, the proportion of the large particles containing ^{137}Cs was about 60% in autumn 1986 and decreased to about 30% in 1993. The part of the inhalable particles increased to about 50% in the years 1992 and 1993. The radioactivity on the respirable particles fluctuated near 25% of the total ^{137}Cs activity concentration. In the first two years at Zapolie, the part of particles containing ^{144}Ce was considerably higher than the part containing ^{137}Cs. ^{106}Ru was generally attached to the fine and large particles in the years 1986-1988.

From different literature sources related to measurements in the 30-km zone, it follows that a significant part (about 50%) of the isotope ^{137}Cs was of a more stable form. The mean nuclide ratio ^{144}Ce / ^{137}Cs was close to 16, the ratio ^{106}Ru / ^{137}Cs was close to 6 (Bogatov et al. 1990, Begichev et al. 1990, Garger 1994). Numerous measurements in the western countries (Devell et al. 1986, Jozt et al. 1986, Reineking et al. 1987, Horn, Bonka and Maqua 1987, Aoyama 1988, Rulik, Buchina and Malatova 1989) gave nuclide ratios and estimations of median particle diameters. Only the ratio ^{134}Cs / ^{137}Cs agreed with the data obtained in the 30-km zone. The ratio ^{144}Ce / ^{137}Cs differed 2-3 orders of magnitude. This means that the fuel component in the particles measured in western countries is very small. The median diameters ranged in an interval of 0.5-1.0 μm for ^{137}Cs and 1.9-5.0 μm for ^{144}Ce (Ogorodnikov and Pazuhin 2005).

The annual mean ^{144}Ce / ^{137}Cs ratio in the airborne samples is presented in Table 10.7. In 1986, this nuclide ratio was as low as reported by Kuriny et al. (1993). The mean ratio of these nuclides was less than in the soil at Zapolie in 1986, and in 1988 it varied between a factor of 0.7 to 1.5 for the different particle size ranges. This is an indication of a different origin of the measured particles: the advection of particles from different places seems to be an essential factor contributing to the local air concentration.

It can be seen from Table 10.3 and Fig. 10.1 that the first moments of the size distribution function of ^{144}Ce and ^{137}Cs at Zapolie did not transform fast. The

mean in the total measurement period of the mean diameter was 9.7 ± 3.2 μm and of the median diameter, it was 6.1 ± 4.9 μm. A slight decrease with time can be observed. At Pripyat, the mean diameters of ^{144}Ce and ^{137}Cs show no noticeable time dependence (see Table 10.4). The mean in the total measurement period of the mean diameter was 8.5 ± 3.0 μm and of the median diameter it was 5.9 ± 2.8 μm. It is possible to explain the differences by the soil properties of these sites. At Zapolie the mechanical destruction of soil particles, the solubility of ^{137}Cs and the resorption on the smallest particles of soil are processes responsible for the transformation of the radionuclide size distribution with time.

Thus, the analysis of 88 samples has shown that at Zapolie a bimodal distribution of ^{137}Cs was observed in 91% of all cases which was formed by two processes: the local resuspension and the advective transport of radioactive aerosol from high contaminated territories, e.g. from the ChNPP.

However, at Pripyat, which is situated within a highly contaminated area, the shapes of size distributions were representative for local resuspension with only a weak transformation.

The observed variability of the radionuclide size distributions in the air of the 30-km zone makes it difficult to calculate resuspension parameters taking into consideration only local processes (e.g., the estimation of the resuspension factor or the estimation of the airborne activity concentration using the radioactive loading of soil particles).

During the measurement period, the log-normal radionuclide size distribution was observed in only 3% of all cases in Zapolie. Because of the heterogeneously contaminated territory of the 30-km zone, the use of the log-normal size distribution for airborne radionuclides does not seem to be correct for the calculations of the inhalation dose. An estimation of the error of dose calculation assuming a log-normal distribution is strongly suggested.

At Zapolie, the mean air activity concentrations of ^{137}Cs discriminated in four size ranges showed an increasing part of inhalable particles with time since the accident. In 1993 the inhalable fraction was about 48% of the total concentration.

During a forest fire, the activity size distribution was measured at a distance of 17 km from the burning area. The main part of radioactivity was connected to submicrometer particles with median meters in the range 0.28-0.50 μm.

CHAPTER 11

RADIOACTIVE PARTICLES DURING ANTHROPOGENIC ACTIVITY

Anthropogenic activities, such as agricultural soil management (e.g. harrowing, plowing) or automobile traffic (especially on unpaved roads), can significantly enhance the atmospheric soil dust concentration. Radionuclides which are already deposited will get resuspended together with the soil dust. The enhanced resuspension of radionuclides will affect the inhalation dose and the spread of contamination, at least on a local scale. In particular, persons who are involved in the activities or live downwind close to roads and agricultural used land warrant concern.

To investigate the influence of different types of anthropogenic activities on the resuspension process and the secondary contamination, measurements were performed in the 30-km exclusion zone of the Chernobyl Nuclear Power Plant. In this chapter, the results are presented of measurements performed in 1993 during enhanced resuspension due to various anthropogenic activities.

The emphasis in the chapter is on describing the resuspended radioactive particles in terms of the number concentration and their size distribution for estimation of human inhalation dose. The experimental information on the particle size distribution can be used directly, avoiding any general assumptions. Moreover, the shares of the fine and coarse particles can be estimated for modeling the processes of transport and redistribution of contamination. For different anthropogenic activities, this may result in different effective scales for potential effects. The redistribution estimation requires knowledge of the resuspension and the deposition rates. Therefore, the dry deposition velocity was determined experimentally as well in the measurements described below.

11.1. Methods and measurements of data

The resuspension measurements were carried out at the site Zapolie which is located on a large open grass field (see Chapter 2.7). Anthropogenically enhanced resuspension was measured during

different simulated agricultural activities and operations of different trucks. For that purpose, two different soil surfaces free of vegetation were prepared on which several tractor types were driven simulating soil management such as harrowing. The soil surface strips represented fixed line sources. In a typical experiment, the tractor started at one end of the strip, passed the sampler at a certain fixed distance, drove to the other end of the prepared surface and returned. For a certain experiment, the strip was chosen for which the wind trajectories pass the sampling equipment after crossing the prepared surface. Detailed information about the orientation of the strip sources and the positions of the different samplers are given in (ECP1 1996).

The size distribution of radioactive particles was measured by a cascade impactor PK. The mass concentration for the different particle size ranges was determined with a Berner impactor (Berner and Lurzer 1980). The number concentration of airborne particles in the size range 0.6-30 μm was measured by a size-resolved APS (Aerodynamic Particle Sizer) (Blackford, Quant and Sem 1987). The samplers operated close together at a sampling height of 3.0-3.5 m and at a distance of approximately 45 m from the north-eastern dust strip and approximately 120 m from the south-western strip. The vertical profile of the atmospheric nuclide activity concentrations was determined by the installation «Grad», 4 identical filter samplers operating on the heights 1.0, 1.8, 2.5 and 3.5 m (Garger et al. 1997). In addition to air samples, deposited material was collected. The samples were collected on planchettes, which are gauze-covered flat plates. The planchettes were placed near each other at the heights 0.5, 1.0, 1.5 and 2.0 m.

At different parts of the soil strips, the ^{137}Cs inventory of the upper 5 cm soil layer was determined. For the north-east strip, the mean ^{137}Cs contamination and specific activity was 0.31 ± 0.05 MBq m^{-2} and 4.94 ± 0.75 Bq g^{-1}, respectively (the density of the poured soil was adopted to be 1.3 g cm^{-3}); for the south-west strip, they were 0.56 ± 0.06 MBq m^{-2} and 8.85 ± 0.98 Bq g^{-1}, respectively. The number of hot particles per unit area was 27×10^4 m^{-2} (4.2 particles g^{-1}) for the north-east strip and 60.5×10^4 m^{-2} (9.4 particles g^{-1}) for the south-west strip.

In May 1993 15 experiments were performed during anthropogenically enhanced resuspension (see Table 7.3). The first experiment was made during the assembling of equipment of other teams of the project ECP1 (ECP1 1996): dust was raised by scientists and technicians walking near the samplers. Cutting the dry grass of the previous year around the site by a small tractor produced dust as well. Distances varied between 50 and 250 m from the central point of the site. In the following days, soil management with 2 types of tractors (a small MTZ-82 and a big T-150) was simulated in 8 experiments. Two different trucks (a six-wheeled army truck ZIL-131 and a large truck ZIL-130) were driven on the prepared surface strips, simulating traffic on unpaved roads.

During the experiments, soil and meteorological parameters were measured as part of the project ECP1 (ECP1 1996).

Meteorological information was available from the Chernobyl meteorological station as well. The vertical profiles of air temperature and wind velocity were determined for micrometeorological information. The Monin and Obukhov similarity theory of the surface layer of the atmosphere (Zilitinkevich 1979) was used for estimation of the friction velocity and classification of the thermal stability (Slade 1968).

Three of the experiments were performed during neutral thermal conditions (see Table 7.3): on 12.05.93 afternoon and 13.05.93 when the Monin-Obukhov length L was approximately –100 m or less and the standard deviation of the wind direction was between 3° and 12° (at mean wind velocities from 5.0 to 6.8 m s^{-1}). In general, the experiments were performed during slight and moderate unstable thermal conditions (-84 m $\leq L \leq -28$ m) with standard deviations of the wind direction between 9° and 25° at wind velocities from 3.1 to 4.6 m s^{-1}. The mean roughness length was 8-10 cm during all experiments. The soil humidity decreased with time during the experimental period, thus influencing the concentration of resuspended particle mass and activity (see Table 7.3).

11.2. The size distribution of radioactive particles

Results of measurements show that the total airborne radionuclide activity concentrations and deposition rates were increased considerably during anthropogenically enhanced resuspension. Depending on the experimental conditions, the increase was by a factor of several thousand in comparison to the concentrations occurring during wind resuspension at distances about 20-30 m from the dust source and a factor 10-100 at distances of about 100 m or more (ECP1 1996).

The measurements of the number concentrations of hot particles showed an increase of 3 orders of magnitude, reaching 0.7-1.0 hot particles / m^3 with a maximum activity of 1.5-2.0 Bq / particle.

The arithmetic mean, and the median diameter of the size distribution of the ^{137}Cs activity concentration in the air as measured by the PK impactor during the experimental period in May 1993 are given in Table 7.3. If we do not consider the results during assembling of the equipment and wind resuspension, the mean and median diameters of the ^{137}Cs size distributions were very similar in the experiments. The mean value for the 10 experiments was 7.1 ± 1.1 μm for the mean diameter and 4.4 ± 1.5 μm for the median diameter. During assembling of equipment with dust resuspension caused by people walking close to the samplers, a mean diameter of 13.8 μm and a median diameter of 11.0 μm were observed. In the experiment with only wind resuspension from the bare soil of the prepared dust strip, the mean diameter was 5.6 μm and the median 3.0 μm.

Certain typical shapes of the measured size distributions can be distinguished. In Fig. 11.1 the ^{137}Cs size distributions are given in the normalized coordinates

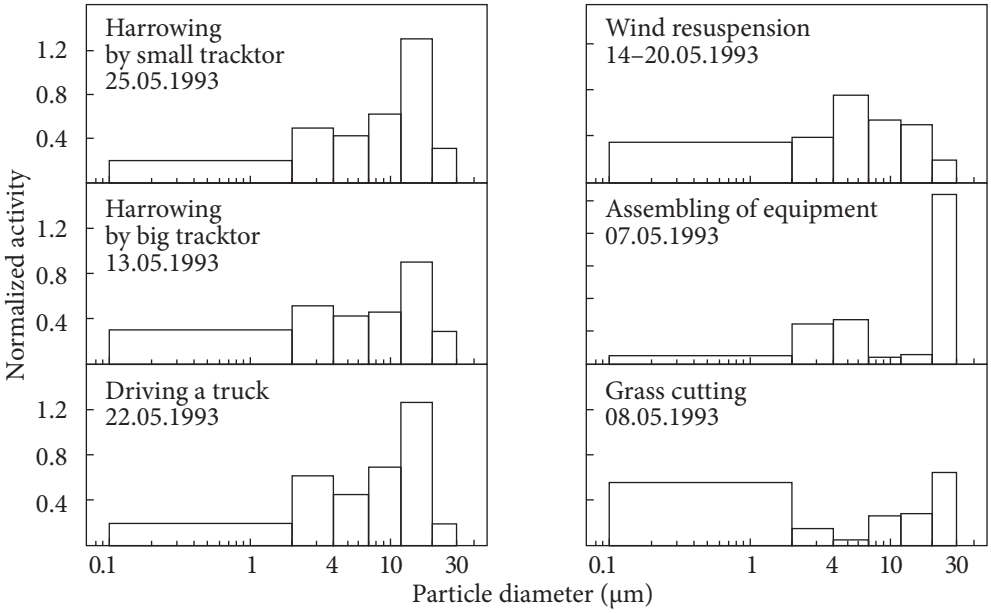

Fig. 11.1. ^{137}Cs activity size distributions in the normalized coordinates $\frac{\Delta c}{c \cdot \Delta \log d}$ and log d, where c is the ^{137}Cs air activity concentration, and d is the aerodynamic particle diameter, during resuspension experiments in May 1993 at Zapolie. The first three distributions are typical for simulated soil management and traffic on unpaved roads. The other distributions are the results of individual experiments

$\frac{\Delta c}{c \cdot \Delta \log d}$ and log d, where c is the air activity concentration of ^{137}Cs and d is the aerodynamic particle diameter. In the experiments with the tractors simulating harrowing and the trucks simulating traffic on the unpaved road, very similar distributions were observed. The two maxima, the first in the range 2-4 μm (which is only weakly developed) and the second in the range 12-20 μm (which is more pronounced) are characteristic. A considerable part of the activity was measured in the fine particle range (0.1-2.0 μm): 33 ± 6% of the total activity. These size distributions are very similar to a certain type of distribution measured at Zapolie during wind-driven conditions (Garger et al. 1998). We may explain these distributions in wind-driven conditions by the large-scale anthropogenic decontamination works close to the ChNPP at a distance of approximately 12-14 km from the sampling site.

Very different shapes of ^{137}Cs activity size distributions were measured during the other experiments. Wind resuspension across the bare soil of the prepared dust strip resulted in a unimodal distribution with the maximum in the size fraction 4-7 μm. During the assembling of equipment, a bimodal distribution was measured with a very high maximum in the range of 20-30 μm and a secondary maximum in the range of 4-7 μm. Grass cutting around the site produced a very

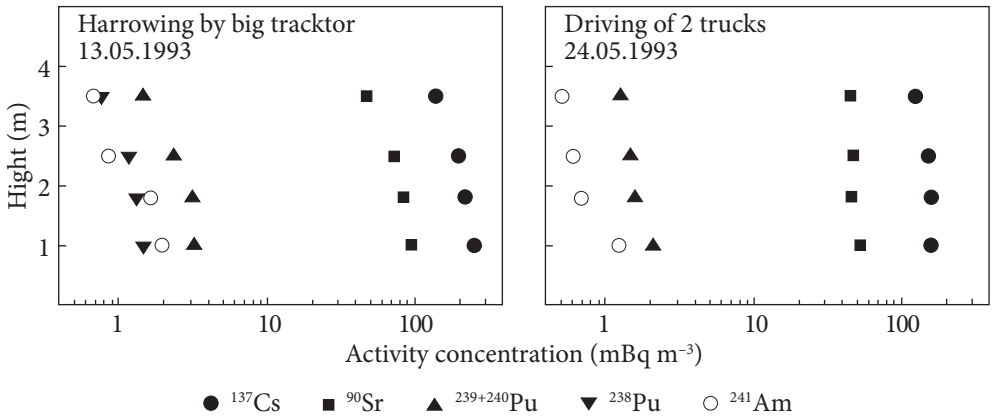

Fig. 11.2. Activity concentration height profile of the radionuclides ^{137}Cs, ^{238}Pu, $^{239+240}$Pu, ^{241}Am and ^{90}Sr at Zapolie during 2 resuspension experiments according to the filter samples of the «Grad» sampler

high proportion of fine particles (0.1-2 μm), but a second maximum as well in the range of 20-30 μm. Comparison of these distributions again with the wind-driven cases (Garger et al. 1998) shows a striking similarity between the «assembling of equipment« distribution and the distribution type measured most frequently at Zapolie during wind resuspension. Local small scale anthropogenic activities seem to influence significantly the particle size distribution.

The total activity concentrations of the radionuclide ^{238}Pu, $^{239+240}$Pu, ^{241}Am, and ^{90}Sr in aerosol particles were determined by filter sampling (with the «Grad» sampler) and radiochemical analysis. The activity of these nuclides was compared to the total activity of ^{137}Cs, which was measured by gamma-spectrometry of the same filters. The vertical profile of the nuclide activity concentrations is given in Fig. 11.2. For the sampling height of 3.5 m (which is also the inlet height of the PK impactor), the mean ratios of the nuclides to ^{137}Cs were calculated to be 0.0103 for $^{239+240}$Pu, 0.00456 for ^{241}Am and 0.352 for ^{90}Sr. Assuming that the activity ratios did not change with different particle size ranges, an estimation was made of the distribution of these radionuclides on different size fractions according to the measured ^{137}Cs size distribution. In Table 11.1 the measured ^{137}Cs activity and the estimated activities of the other nuclides in the different size ranges are given for 2 experiments with heavy anthropogenic activities. The air activity concentrations of the plutonium nuclides were significant concerning inhalation dose and spread of contamination for the fine particle range (0.1-2.0 μm) with 36-40% of the total concentration and the giant particle range (12.0-20.0 μm) with approximately 20% of the total concentration.

The transport behavior of particles in the surface layer of the atmosphere depends on the ratio of the settling velocity of aerosol particles and the friction velocity (Slade 1968, Byzova, Garger and Ivanov 1991). To assess the relevance

of particles in the different particle size ranges for medium-range transport and inhalation, the settling velocity w of aerosol particles was compared to the atmospheric friction velocity u_*. For fine particles with their very small settling velocities, it is well known that they can be transported long distances from fields with agricultural activities. At a soil density of $\rho = 2.3$ g cm^{-3}, the settling velocity in the particle size range 12-20 μm is in the range of 1.1-3.0 cm s^{-1}. The friction velocity during the experiments was $u_* = 43 \pm 0.11$ cm s^{-1}, and the resulting ratio w / u_* was in the range 0.026-0.070. This means that particles with $d \leq 20$ μm may travel distances in the order 1-10 km during these atmospheric stability conditions, which last typically 6-8 h in the summer (Slade 1968, Byzova, Garger and Ivanov 1991). Therefore, during anthropogenically enhanced resuspension, large and giant particles should be taken under consideration for inhalation dose assessment and spread of contamination as well. The possibility of atmospheric dispersion of these particles is an additional argument for the importance of taking into account the coarse particles (Pires do Rio, Amaral and Parezke 1994, Wagenpfeil et al. 1994).

The dependence of the temporal variation of airborne particle number per unit air volume on the particle size was measured by an APS. An episodic injection of a huge number of particles in the atmosphere during anthropogenic activities was observed. In Fig. 11.3 the temporal course of the number concentration on the afternoon of 13 May 1993 is presented after classification in 4 size ranges. In this example, periods of harrowing with a big tractor alternate with break periods in which only wind resuspension happened. The concentration increase in the

Table 11.1. **Distribution of the activity concentrations of $^{239+240}$Pu, ^{241}Am, and ^{90}Sr according to measured ^{137}Cs size distributions and the nuclide ratios of total concentration measurements at Zapolie**

Date of experiment	Size range (μm)	$^{239+240}$Pu (mBq m^{-3})	^{241}Am (mBq m^{-3})	^{90}Sr (mBq m^{-3})	^{137}Cs (mBq m^{-3})
13.05.1993	0.1-2.0	0.481	0.213	16.4	46.7
	2.0-4.0	0.184	0.0816	6.30	17.9
	4.0-7.0	0.123	0.0543	4.19	11.9
	7.0-12.0	0.129	0.0570	4.40	12.5
	12.0-20.0	0.240	0.106	8.20	23.3
	20.0-30.0	0.0591	0.0262	2.02	5.74
24.05.1993	0.1-2.0	0.355	0.157	12.1	34.5
	2.0-4.0	0.172	0.0762	5.88	16.7
	4.0-7.0	0.132	0.0584	4.51	12.8
	7.0-12.0	0.110	0.0488	3.77	10.7
	12.0-20.0	0.187	0.0830	6.41	18.2
	20.0-30.0	0.0388	0.0172	1.33	3.77

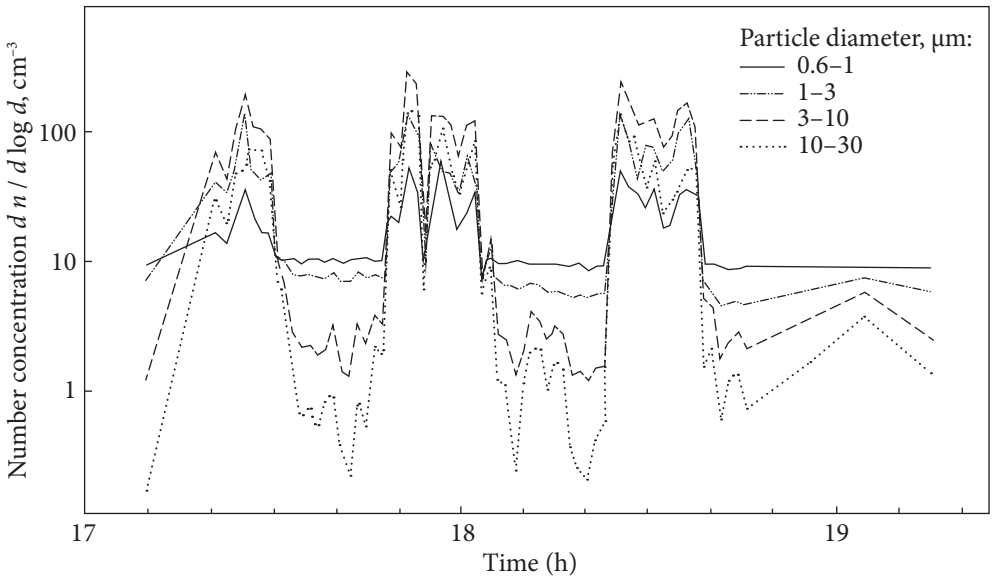

Fig. 11.3. Time record of the normalized particle number concentration in four different size ranges as measured by an Aerodynamic Particle Sizer during the resuspension experiment on 13 May 1993 at Zapolie. The periods of operation of the big tractor can be identified by the periods of increased particle concentrations. The increase of large particles is much higher than the increase of fine particles

periods of soil management is not uniform for all size ranges: the concentration of large particles increases much more than the concentration of fine particles.

In Table 11.2 this observation is quantified. In 4 size ranges parameters of the number concentration are presented, summarizing 3 experimental conditions: periods of soil management, break periods and the total experimental period. For example, if we consider the mean number concentration for the total experimental period, we find the maximum concentration in the large particles range (3-10 μm) and the minimum concentration in the fine particles range (0.6-1.0 μm). This can be explained by the fact that larger adhesive forces are found for the fine particles in comparison to the large ones, preventing the atomizing of the fine soil particles (Zimon 1980, Sehmel 1984).

Averaging over the whole measurement period even blurs this effect, which can be seen by comparing the mean number concentration of the harrowing periods only with the periods without any soil management. The mean concentration of large particles (3-10 μm) is 4 times and of giant particles (10-30 μm) 2 times more than the mean concentration of fine particles (0.6-1.0 μm). Without anthropogenic activity, the relation is the opposite: the concentration of fine particles is three times more the concentration of large particles and 6 times the concentration of giant particles. For giant particles, the coefficient of variation (standard deviation / mean

Table 11.2. **Parameters of number concentration measurements on 13 May 1993, afternoon, by APS during harrowing with the big tractor**

Parameter	Particle size range (μm)			
	0.6–1.0	1–3	3–10	10–30
N_H (cm^{-3})	25.4	59.4	108.8	52.2
N_T (cm^{-3})	15.2	26.0	41.8	20.1
N_B (cm^{-3})	9.37	6.76	3.17	1.63
S_H / N_H	0.449	0.0537	0.520	0.615
S_T / N_T	0.678	1.23	1.47	1.55
S_B / N_B	0.0593	0.194	0.726	1.07
N_H / N_B	2.71	8.79	34.3	32.0
N_T / N_B	1.62	3.85	13.2	12.3
N_{max} / N_{min}	6.79	31.7	259	987

Note: N_H – normalized mean number concentration of particles during the harrowing periods; N_T – normalized mean number concentration of particles during the total experimental period; N_B – normalized mean number concentration of particles during break periods; S_H, S_T, S_B – standard deviation of mean in the respective period; N_{max}, N_{min} – maximum rsp. minimum number concentration of particles during the total experimental period.

Table 11.3. **Mass specific ^{137}Cs activity concentration (mBq g^{-1}) of airborne and soil particles of different particle size ranges during anthropogenically enhanced resuspension in Zapolie; in the last two lines the relation between the concentration in air and soil (the enhancement factor) is given for the measurements in Zapolie and two other sites**

Experiment	<2.0 μm	2–4 μm	4–7 μm	7–16 μm
13 May 1993 big tractor	370	160	74	71
22 May 1993 truck	290	430	220	550
24 May 1993 two trucks	640	340	320	330
25 May 1993 morning, small tractor	180	230	100	270
25 May 1993 afternoon, truck	810	640	145	360
May 1993 Soil (Shinn 1992)	120	38	20	11
	Enhancement factor			
May 1993 Zapolie	3.8 ± 2.2	9.5 ± 4.9	8.6 ± 5.0	28.8 ± 15.7
Nevada Test Site (Shinn 1992)	3.6			
Bikini Atoll	3.9			

concentration) is the largest, and the ratio of the maximum to the minimum concentration (N_{max} / N_{min}) is close to three orders of magnitude. For the fine particles, the coefficient of variation is the smallest, and (N_{max} / N_{min}) is smaller than one order of magnitude. During anthropogenically enhanced resuspension a lot of large particles were created, which must be considered for radiological estimations.

To compare the radioactive loading of the airborne particles with the loading of the soil particles, the mass specific activity concentration of airborne particles was determined. From data of the Berner impactor (mass concentration) and PK impactor (activity concentration), specific concentrations during different experiments were calculated for the particle size ranges $d < 2$ μm, 2 μm ≤ $d < 4$ μm, 4 μm ≤ ≤ $d \leq 7$ μm and 7 μm ≤ $d \leq 16$ μm (Table 11.3). Soil measurements resulted in an empirical equation relating to specific soil activity with particle size (Besnus et al. 1997). In Table 11.3, the specific soil activity concentrations are given for the same particle ranges as for the aerosol measurements. The aerosol measurements showed varying specific activities with the lowest values generally in the range 4-7 μm and the highest values either in the range < 2 μm or in the range 7-16 μm. The specific activity decreased with particle size. In all experiments and all size ranges the airborne specific activity concentration was higher than the concentration in soil.

This enhanced radioactive loading of airborne particles is quantified in Table 11.3 by the enhancement factor, which is the ratio of the mass specific air concentration and the mass specific soil concentration (see Chapter 6).

11.3. Estimation of dry deposition velocity

Deposition measurements were performed in 4 different heights in Zapolie. By the theory of the atmospheric surface layer for stationary conditions, no differences in the deposition rates at the various heights were found. Typical values of dry deposition rates during wind-driven resuspension were 1.9-2.3 μBq m^{-2} s^{-1}.

The total deposition $D(x, y)$ at a position with coordinates (x, y) in the sampling time T is given by

$$D(x, y) = v_d \int_0^T q(x, y, z)\, dt, \tag{11.1}$$

where q is the air activity concentration and v_d is the dry deposition velocity at the sampling height z. By measuring the deposition D and the concentration q during anthropogenic activities, the dry deposition velocity was calculated using Eq. (11.1). In Table 11.4 results are presented using the average deposition to deposition planchettes in the heights 0.5, 1.0, 1.5 and 2.0 m and the average air activity concentrations measured in the heights 1.0 and 1.8 m (ECP1 1996).

The mean deposition velocity of all experiments was 0.026 ± 0.016 m s^{-1}. This mean was calculated under the assumption of a uniform set of observations,

e.g. similar meteorological conditions during the experiments, which explains the large uncertainty. The deposition velocities were measured at a roughness length $z_0 \sim$ 8-10 cm. The results agree with curves of the deposition velocity given by (Sehmel 1984) for particle deposition on various solid surfaces at $z_0 = 10$ cm.

The mean deposition velocity can be used for estimating the mean particle diameter. According to the Stokes law, the mean diameter of a spherical particle moving with a speed of $v_d = 0.026$ m s^{-1} is roughly estimated to be $\overline{d} \approx 19$ μm. We can make the more realistic assumption that the dry deposition velocity v_d is the sum of two independent parts, the settling velocity w and the deposition velocity for adhesive processes bu_*. Then

$$v_d = bu_* + w, \tag{11.2}$$

where $b = 0.01$ for particles with $d > 5$ μm and natural dry grass (Byzova, Garger and Ivanov 1991), leading to a diameter range of $\overline{d} \approx 6.2$-12.6 μm for the range of measured u_* (0.30-0.61 m s^{-1}). This is in agreement with the measured mean diameters in the experiments 11-25 May 1993 presented in Table 11.3, where $\overline{d}$ is in the range 5.6-8.7 μm with the mean at 7.1 μm.

Table 11.4. **Dry deposition velocities during anthropogenic activities at Zapolie; each value refers to the average deposition to four planchettes (at the heights 0.5, 1.0, 1.5 and 2.0 m) and the average aerosol concentration (measured at the heights 1.0 and 1.8 m)**

Date and time	Dry deposition velocity (m s^{-1})	Standard deviation (m s^{-1})
11.05.93, 12:15–14:40	0.036	0.009
11.05.93, 16:15–17:55	0.047	0.021
12.05.93, 11:20–15:00	0.040	0.021
12.05.93, 16:00–18:00	0.063	0.009
13.05.93, 09:40–13:00	0.018	0.007
13.05.93, 17:15–18:40	0.023	0.007
21.05.93, 12:30–16:30	0.009	0.003
22.05.93, 10:00–12:15	0.008	0.004
22.05.93, 12:15–16:20	0.006	0.001
23.05.93, 10:30–13:00	0.021	0.001
24.05.93, 15:30–18:30	0.035	0.005
25.05.93, 11:15–13:10	0.027	0.007
25.05.93, 16:00–17:10	0.033	0.011
Arithmetic mean	0.026 ± 0.016	

Deposition velocities for dry deposition of ^{137}Cs were measured in Goiânia, Brazil, as well (Pires do Ria, Amaral and Paretzke 1994). In the numerous measurements in an urban area during different meteorological conditions, deposition velocities were observed in the range 1-30 cm s^{-1} with the average value of approximately 5-6 cm s^{-1}.

Thus we may see that anthropogenic activities such as soil management or traffic on unpaved roads in contaminated areas increase the resuspension of radionuclides in the surface layer of the atmosphere; the size distributions of atmospheric ^{137}Cs particulate activity during these kinds of enhanced resuspension showed a similar common shape with two maxima, the first in the 2-4 μm range, the second in the 12-20 μm range; in the fine particle size range (0.1-2.0 μm) 33% ± 6% of ^{137}Cs activity was found in the mean of all experiments.

An estimation of the airborne plutonium activity concentrations in two experiments of anthropogenically enhanced resuspension showed a significant part of the activity in the fine particle size range (36-40%) and the large particle range (approximately 20%).

The analysis of the micrometeorological conditions during the experiments showed that particles with d = 12-20 μm are subject to medium range transport during unstable and windy situations. This means that the large particles have to be considered not only on a local scale for inhalation dose assessment and transport of contamination but also on the mesoscale.

Measurement of the number concentrations of particles has shown that means for large particles (3-10 μm) and giant particles (10-30 μm) are, respectively, 4 times and 2 times larger than the mean number concentration of fine particles (0.6-1.0 μm) during periods of soil management. The increase of the mean number concentration in periods of soil management has been a factor of about 40 for large and giant particles, but only a factor of approximately 3 for the fine particles. The variability of the concentration is higher for giant particles. During anthropogenically enhanced resuspension predominantly large particles are injected in the atmospheric surface layer.

The estimated radioactive loading of particles showed an enhancement of resuspended radionuclides compared to soil particles. The highest enhancement factor was found for large particles, the lowest for fine particles.

Dry deposition velocities were estimated for the experiments with anthropogenically enhanced resuspension. The mean value of the dry deposition velocity of ^{137}Cs was 0.026 ± 0.016 m s^{-1}, which is typical for particles with a mean diameter of 6-9 μm.

The different size-resolved measurements of resuspended radioactive particles proved the importance of considering large and giant particles in the assessment of inhalation dose and spread of contamination in mesoscale distances from the source of anthropogenically enhanced resuspension.

CHAPTER 12

FUEL PARTICLES COLLECTED ON AIR FILTERS IN 1987 DURING NATURAL WIND RESUSPENSION, THEIR SOLUBILITY, AND IMPLICATION TO DOSE

12.1. Methods and conditions of the aerosol measurements

After the Chernobyl accident, daily filter samples of aerosol were taken with high-volume samplers of the type SPA «Typhoon» in the town Pripyat located around 4 km to the west from the reactor building.

Four filter units of the type Petryanov FPP-15-1.5 with the dimensions 75 × 35 cm were used. The filter material of the type FP (filter Petryanov) is made by electrostatic formation presenting uniform layers of ultra-thin polymeric fibers (perchlor-vinyl resin) with diameters in the range of 0.1-10 μm (Petryanov et al. 1968). In these measurements, the Petryanov filters had the following properties: fiber diameter 1.5 μm; effectiveness of filtration not less than 99.9% (for particle diameter 0.3 μm); airflow resistance of 1.4-1.8 Pa at the sampling flow rate of 1 cm s^{-1}. All filters were divided into two parts: the first part was measured in 1987 and the second part was kept for future investigations, sealed individually in a rigid box made of polystyrene (PS) and stored in a dry place at room temperature to preserve the sampled nuclear material. Two filters collecting during 12-13 October 1987 and 22-23 November 1987 were selected for our investigations. They showed at the time of sampling high activities especially of radionuclides indicating fuel particles (Wagenpfeil and Tschiersch 2001). The mean airborne radionuclide activity concentrations during the first collection period were 20.8 mBq m^{-3} for ^{137}Cs, 89.3 mBq m^{-3} for ^{144}Ce and 30.5 mBq m^{-3} for ^{106}Ru. During the second period, they were 12.1 mBq m^{-3} for ^{137}Cs, 34.9 mBq m^{-3} for ^{144}Ce and 24.3 mBq m^{-3} for ^{106}Ru.

At the same time the particle size distribution of radioactivity was measured by the impactor UP (5 cascades, flow rate around 400 $m^3\ h^{-1}$). In Garger et al (1997) more detailed information on the technical characteristics of the installations used can be found. These measurements showed differences in the distributions of activities for these two periods. For the first period, the distribution was approximately symmetric. For the second period, the distribution was skewed towards larger particles. For the first period, the median diameter was 3.0 μm and $\log \sigma_g = 0.88$; for the second, the median diameter was 7.5 μm and $\log \sigma_g = 0.44$. The distribution characteristics of the particles for these two observation periods were not identical.

The surface of the filters was preliminary scanned by α-β-radiometer for revealing parts with higher radioactivity. Consequently, in total 7 filter fragments with diameters of about 6.5 cm (the size of the filter holder diameter is about 8 cm) were cut out and labeled. The quantity of hot particles on each filter fragment was determined by autoradiography.

Measurements on the solubility of the fuel particles deposited on the filters were made using static in vitro test systems. Being aware that results from in vitro studies cannot be directly applied to human exposures with reasonable confidence, there are circumstances where they are the only possible approach as was the case in this study. A review and critical analysis of in vitro methods designed to estimate dissolution rates in the respiratory tract and discussions of factors affecting *in vitro* dissolution rates were published in (Ansoborlo et al. 1999). Based on these considerations, a static *in vitro* test system as described in (Eidson and Griffith 1984, Miglio, Muggenburg and Brooks 1977, Gamble 1967) was applied in this study. The filter holders were made from fluorinated polymer (PTFE). Fragments of the Petryanov filters were confined within 2 membrane filters with 0.14 μm pore size, of the type MFA (Dubna, Russia) as a filter sandwich. For the solvent, Gamble's solution was chosen (Gamble 1967). Several lung fluid simulates had been proposed which were designed to approximate the composition of extracellular fluid and are generally called serum ultrafiltrate simulate (SUF), serum lung fluid (SLF), and Gamble's or Ringer's solution. They differ slightly in their composition and all were widely used by different investigators (Eidson and Mewhinney 1983, Dennis, Blauer and Kent 1982, Ansoborlo et al. 1998). The findings of a comparison of different solvent media (Ansoborlo et al. 1998) justify the choice of Gamble's solution as the lung fluid simulate. The filter holders were stood in a horizontal position for 7-28 days in Gamble's solution and at defined time intervals, the solution was analyzed for the radionuclides ^{90}Sr, ^{137}Cs, ^{238}Pu, $^{239+240}Pu$, ^{241}Am, and ^{244}Cm; the most relevant nuclides in respect to dosimetry.

For the measurement of ^{137}Cs on filters and in the solutions, γ-spectrometer based on the semi-conductor detector GMX-30190 (effectiveness 32.5%, energy resolution 1.89 keV on the line 1.33 MeV) and the multi-channel buffer 919 Spectrum Master (Ortec Inc.) was used.

The nuclides ^{238}Pu, $^{239+240}$Pu, ^{241}Am, and ^{244}Cm were separated and concentrated without carriers from aerosol filters and leaching solutions according to (Ageyev, Odintsov and Sajeniouk 2003). Sources for the a-spectrometric measurements were prepared by electrochemical deposition of Pu, Am, and Cm on polished stainless steel discs from a sulfate solution at pH 2.1. The chemical yield of americium and curium (defined with the use of the tracer ^{243}Am) was in the range 50-60%. The yield of plutonium (defined with the use of the tracer ^{236}Pu) was 60-80%. The activities of the radionuclides Pu and Am were measured with the eight-channel α-spectrometer Octete PC (Ortec Inc.) using the siliceous semi-conductor detector of the series Ultra with a detection efficiency of > 25%. The background at 3 MeV is not more than 1 impulse per hour, the energy resolution is 19 keV on the line 5.486 MeV (^{241}Am). The radiometric analysis of ^{90}Sr after the chemical isolation was conducted with the help of the low background 10-channel counter (background 0.45 ± 0.12 imp/min) of the α-β-counter LB 770 PC (Berthold).

12.2. Experimental characteristics of particle solubility

The total activities of the significant radionuclides in the seven individual aerosol filter fragments are presented in Table 12.1. It can be seen that all principal long-lived transuranium radionuclides are present in the aerosol particles. From the composition, it can be concluded that the particles originated from the irradiated fuel, and that the radionuclides are fixed in the matrix of uranium dioxide. Usually, for the description of radionuclide characteristics of different radioactive products of the Chernobyl accident, the fractionating factor (the ratio of a radionuclide activity to the refractory ^{144}Ce actitivity) was used (Ermilov and Ziborov 1993, Dubasov, Savonenkov and Smirnova 1996, Bogatov et al. 1990, Kutkov and Kamarinskaya 1996, Wagevpfeil and Tschiersch 2001). In the present work, the nuclides ^{239}Pu+^{240}Pu were taken as the reference radionuclides, as these plutonium isotopes are products of the ^{238}U(n, γ) ^{239}U$^{-\beta}\rightarrow$ ^{39}Np$^{-\beta}\rightarrow$ ^{239}Pu(n, γ) ^{240}Pu reaction chain and are more solidly connected with the uranium matrix of the hot particles. In Table 12.2 the activity ratio related to that reference is shown. The values are in good agreement with calculated values for the reactor fuel just before the Chernobyl accident (Ageev et al. 1998) which confirms that the investigated aerosol particles represented irradiated fuel at different grades of dispersion.

The mean density ρ of hot particles from samples of the zone close to the ChNPP was found to be equal to 10 ± 0.8 g cm^{-3} (Kutkov and Kamarinskaya 1996). The mean specific activity of $^{239+240}$Pu in the irradiated fuel was 1.3×10^{7} Bq g^{-1} (U_3O_8) or 1.15×10^{7} Bq g^{-1} (UO_2) (Ageev et al. 1998). The assumption used was that particles have a spherical form and the estimated size of the particle equiva-

Table 12.1. **Radionuclide activities in the aerosol filter fragments before the solution experiments (in the year 2000)**

Number of fragment	Sampling date	^{137}Cs Bq / sample	^{90}Sr Bq / sample	$^{239+240}$Pu Bq / sample	^{238}Pu Bq / sample	^{241}Am Bq / sample	^{244}Cu Bq / sample
1	12–13.10.1987	3.6 ± 0.4	2.7 ± 0.2	0.035 ± 0.005	0.016 ± 0.005	0.042 ± 0.008	*
2	12–13.10.1987	2.9 ± 0.5	3.2 ± 0.3	0.065 ± 0.007	0.025 ± 0.004	0.073 ± 0.013	*
3	12–13.10.1987	6.1 ± 0.5	9.6 ± 0.6	0.18 ± 0.01	0.084 ± 0.009	0.21 ± 0.02	0.008 ± 0.002
4	12–13.10.1987	8.0 ± 0.6	9.7 ± 0.5	0.20 ± 0.02	0.075 ± 0.008	0.23 ± 0.02	*
5	12–13.10.1987	28 ± 1	31 ± 1	0.61 ± 0.02	0.38 ± 0.05	0.81 ± 0.05	0.045 ± 0.006
6	22–23.11.1987	6.1 ± 0.4	6.1 ± 0.2	0.11 ± 0.01	0.07 ± 0.01	0.14 ± 0.02	*
7	22–23.11.1987	17 ± 1	21 ± 1	0.43 ± 0.02	0.29 ± 0.04	0.56 ± 0.03	0.034 ± 0.004

Note: *Below detection limit.

lent diameter d_0 is given by the formula:

$$d_0 = 2\left(\frac{3A}{4\pi\rho_p q}\right)^{1/3}, \qquad (12.1)$$

where A is the activity of the particle (Bq) and q is the particle specific activity (Bq g^{-1}). On the seven individual filter fragments, some hot particles and an unknown quantity of small submicron particles of low specific activity were deposited. In the calculations made in this chapter, the activity values of $^{239+240}$Pu from Table 12.1 were used. On the radiographic films, only one single large spot could be found on the fragment number 7. The equivalent diameter of hot particle was calculated according to Eq. (12.1) for each filter fragment. This made it possible to estimate the dissolution rate constant from the next equation (Mercer 1967)

$$m = m_0\left(1-\frac{\alpha_s kt}{3\alpha_v\rho_p d_0}\right)^3, \qquad (12.2)$$

where m_0 is the initial mass of the particle and d_0 is its initial diameter; t is time; s is the particle surface area; $\alpha_s = s/d^2$ is the surface shape factor; $\alpha_v = m/\rho_p d^3$ is the volume shape factor, ρ_p is the particle density; k is the dissolution rate constant.

In Table 12.3, the activity of the radionuclides in the simulated lung fluid solution (SLF) is shown, together with the derived equivalent diameter of the particles. The much lower solubility of activity in fragment 7 (particularly for ^{137}Cs and ^{90}Sr) compared to the other fragments, reflects that the activity in fragment 7 is concentrated in only one hot particle. The large scatter in the activities found in the solution, especially for $^{239+240}$Pu, might be connected with the

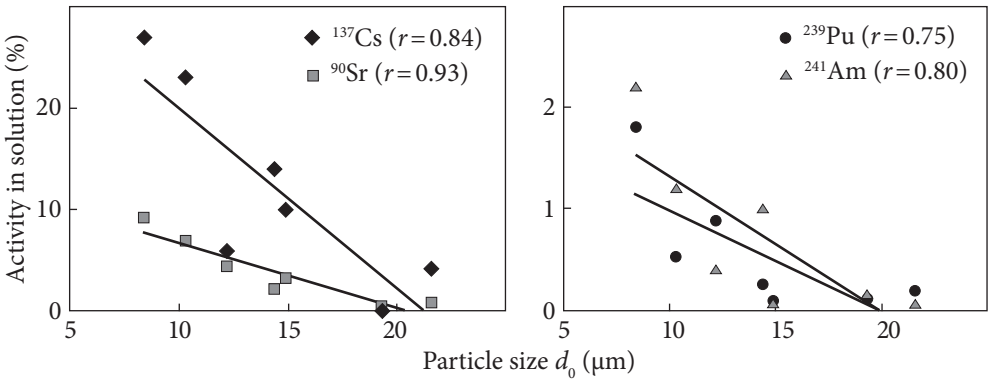

Fig. 12.1. Relationship between particle size d_0 and solubility in simulated lung fluid (SLF) for ^{137}Cs and ^{90}Sr. Time exposure to SLF was 3–4 weeks (see Table 12.3) (*a*); Relationship between particle size d_0 and solubility in simulated lung fluid (SLF) for ^{239}Pu and ^{241}Am. Time exposure to SLF was 3–4 weeks (see Table 12.3) (*b*)

Table 12.2. **Activity ratio of the nuclides ^{137}Cs, ^{90}Sr, ^{238}Pu, ^{241}Am and ^{244}Cu related to the reference activity of $^{239+249}$Pu according to the measurements and calculations for the Chernobyl reactor fuel at the time of the accident**

Value	^{137}Cs / $^{239+240}$Pu	^{90}Sr / $^{239+240}$Pu	^{238}Pu / $^{239+240}$Pu	^{241}Am / $^{239+240}$Pu	^{244}Cu / $^{239+240}$Pu
Mean	52 ± 20	56 ± 9	0.52 ± 0.11	1.22 ± 0.1	0.065 ± 0.011
Calculation	77	65	0.53	1.24	0.08

Table 12.3. **The activity of radionuclides in the solution in % of the total activity**

Number of fragment	Exposition in solution (days)	Equivalent diameter of particle d_0 (μm)	^{137}Cs	^{90}Sr	$^{239+240}$Pu	^{241}Am
1	28	8.4	27	9.2	1.8	2.2
2	28	10.3	23	7.0	0.52	1.2
3	28	14.4	14	2.2	0.25	1.0
4	28	14.9	10	3.2	0.09	0.07
5	25	21.6	4.2	0.8	0.18	0.06
6	21	12.2	5.9	4.4	0.88	0.40
7	21	19.3	0.1	0.41	0.10	0.16
Mean		14.4 ± 4.7	12 ± 9.9	3.9 ± 3.2	0.54 ± 0.62	0.73 ± 0.79

sampling period of the filters of only 1 day in 1987. There were many different secondary sources of radioactive particles in the zone near to the «Shelter» object causing large airborne concentration fluctuations. The relationship between particle size and solubility, expressed as a percentage of the total activity present in the solution, is shown in Fig. 12.la for ^{137}Cs and ^{90}Sr, and in Fig. 12.1b for $^{239+240}$Pu and ^{241}Am. Although there is a considerable scatter in the data, the effect

Table 12.4. **Dissolution characteristics of hot particles**

Number of fragment	$^{239+240}$Pu activity in the solution (%)	Dissolution rate constant $k_s \times 10^{-6}$ (g cm^{-2} d^{-1})	Time for complete dissolution of the particle (years)
1	1.8	5.4	13
2	0.52	1.9	45
3	0.25	1.3	91
4	0.09	0.72	170
5	0.18	1.6	110
6	0.88	5.1	20
7	0.10	0.92	170
Mean		2.4 ± 2.0	

Table 12.5. **Slow solubility rate s_s (assumed to be represented by the measured leaching constants k_1) and inhalation dose coefficients for the radionuclides investigated**

Number of fragment	^{137}Cs		^{90}Sr		$^{239+240}$Pu		^{241}Am	
	$s_s \times 10^{-4}$ (d^{-1})	Dose coefficient (Sv Bq^{-1})	$s_s \times 10^{-4}$ (d^{-1})	Dose coefficient (Sv Bq^{-1})	$s_s \times 10^{-4}$ (d^{-1})	Dose coefficient (Sv Bq^{-1})	$s_s \times 10^{-4}$ (d^{-1})	Dose coefficient (Sv Bq^{-1})
1	112	3.9×10^{-9}	34	1.7×10^{-8}	6.5	7.5×10^{-6}	7.9	7.2×10^{-6}
2	93	3.3×10^{-9}	26	1.6×10^{-8}	1.9	6.0×10^{-6}	4.3	4.9×10^{-6}
3	54	3.0×10^{-9}	7.9	1.5×10^{-8}	0.89	4.0×10^{-6}	3.6	2.9×10^{-6}
4	38	3.2×10^{-9}	12	1.3×10^{-8}	0.32	3.8×10^{-6}	0.25	4.1×10^{-6}
5	17	2.7×10^{-9}	2.9	1.2×10^{-8}	0.64	2.7×10^{-6}	0.24	2.9×10^{-6}
6	22	4.6×10^{-9}	16	1.5×10^{-8}	3.2	3.7×10^{-6}	1.4	5.1×10^{-6}
7	0.36	6.1×10^{-9}	1.5	1.4×10^{-8}	0.36	3.0×10^{-6}	0.57	3.2×10^{-6}
Median	38	3.3×10^{-9}	12	1.3×10^{-8}	0.89	4.0×10^{-6}	1.4	4.3×10^{-6}
ICRP Default 5 μm AMAD	Type F	6.7×10^{-9}	Type M	2.4×10^{-8}	Type M	3.3×10^{-5}	Type M	2.7×10^{-5}
ICRP 14.4 μm AMAD	Type M	3.1×10^{-9}	Type M	1.0×10^{-8}	Type S	4.2×10^{-6}	Type S	4.3×10^{-6}

of decreasing solubility with increasing particle size is clearly demonstrated. The leaching of the radionuclides from the hot particles into the SLF decreases in the order ^{137}Cs > ^{90}Sr >> ^{241}Am > $^{239+240}$Pu.

Table 12.4 presents the shape modified dissolution rate constant $k_s = k\alpha_s/\alpha_v$ as derived from the measured activities of the radionuclides in the solution (Table 12.3). The dissolution rate was assumed to be constant in time, and the time t_∞ when the particle will be completely dissolved was estimated according to (Mercer 1967)

$$t_\infty = 3\alpha_v \rho_p d_0 / \alpha_s k. \tag{12.3}$$

From these data, it can be seen that the solution process for $^{239+240}$Pu will need many years for the dissolution of fuel particles in the size of the order of 10 μm. It was found in (Mercer 1967) however, that the particle to dissolve completely as calculated from Eq. (12.3) from (Garger et al. 2004) is an overestimation. The solubility rate constant can be expected to increase rapidly as the particle size diminishes below about 0.01 μm. From Table 12.4 it follows that the dissolution rate constants of fragments 1 and 6 are about 3-7 times higher than the others and the complete dissolution time is much less as well. The mean equivalent diameter for these particles is 10.3 μm and $k_s = 5.2 \times 10^{-6}$ g cm^{-2} d^{-1}, for the other fragments the mean equivalent diameter is higher (16.1 μm) and the dissolution rate accordingly lower, $k_s = (1.29 \pm 0.48) \times 10^{-6}$ g cm^{-2} d^{-1}.

Experimental estimations of k are discussed in Mercer (1967) and it is concluded that in vivo solubility rate constants for compounds including U_3O_8 and UO_2 dusts in the order of magnitude are approximately 10^{-7} g cm^{-2} d^{-1} which is in agreement with data of Table 12.4. In Bogatov et al. (1990) the dependence of leaching agents and the destruction of matrix-bond radionuclides were discussed and were found to range from 5.7×10^{-6} to 1.6×10^{-4} g cm^{-2} d^{-1} for ^{137}Cs,^{134}Cs, and ^{90}Sr.

The leaching constants k_1 (in d^{-1}) for ^{137}Cs, ^{90}Sr, $^{239+240}$Pu, and ^{241}Am were calculated according to Mercer (1967)

$$dA(t)/dt = -k_1 A(t), \tag{12.4}$$

where $A(t)$ is the activity at time t and k_1 is the leaching constant (Table 12.5).

From these data, it can be seen that the leaching constants for ^{137}Cs and ^{90}Sr are 4-100 times higher than for $^{239+240}$Pu including fragment 7 where the leaching constant for cesium is surprisingly small, and the range of the values is very high. In (Gudihy et al. 1989) leaching constant of about 0.004 day^{-1} for all the analyzed γ-emitting radionuclides was found. In (Kutkov and Kamarinskaya 1996) the leaching constant for the total of all α-emitting nuclides was determined to be 0.005 ± 0.002 day^{-1} and for ^{137}Cs to be 0.002 ± 0.001 day^{-1}. For ^{137}Cs and ^{90}Sr these data are in good agreement with the estimations here, but the leaching constants for $^{239+240}$Pu and ^{241}Am were one to two orders magnitude lower than for the radionuclides presented in (Kutkov and Kamarinskaya 1996).

12.3. Inhalation dose coefficients applying measured solubility parameters

Inhalation dose coefficients for the radionuclides ^{137}Cs, ^{90}Sr, ^{239}Pu, and ^{241}Am were calculated by P. Roth (Garger et al. 2004) applying the IMBA (**I**ntegrated **M**odules for **B**ioassay **A**nalysis) computer code developed by NRPB (Birchall et al. 2003). The program implements the dosimetric model for the human respiratory tract (ICRP 1994), the systemic biokinetic models as described in (ICRP 1990, ICRP 1993) and uses the (ICRP 1983) nuclear decay data to calculate internal doses. The dissolution and absorption to blood of material deposited in the respiratory tract is described in the ICRP model by two components: a rapid component (f_r) with a dissolution rate (s_r) of 100 day^{-1}, and a slow component ($1 - f_r$) with dissolution rates (s_s) of 5×10^{-3} d^{-1} (Type M) and 1×10^{-4} d^{-1} (Type S). The fraction dissolved rapidly (f_r) is assumed to be 1 for Type F, 0.1 for Type M, and 0.001 for Type S material.

In Fig. 12.2, the general dependency of the inhalation dose coefficients on the solubility rate s_s is shown for the radionuclides ^{137}Cs, ^{90}Sr, ^{239}Pu, and ^{241}Am. The fraction dissolved rapidly is assumed to be zero. For ^{137}Cs and ^{90}Sr, the dose coefficients decrease with increasing solubility, whereas they increase for ^{239}Pu and ^{241}Am with increasing solubility. The findings for ^{137}Cs and ^{90}Sr reflect the general behavior of radionuclides where the lung dose is the dominant contributor to the effective dose. In these cases, increasing solubility decreases the lung dose and also the resulting effective dose. On the other hand, for ^{239}Pu and ^{241}Am, liver and red bone marrow contribute similar fractions to the effective dose as the lung. Thus, in these cases, higher absorption to blood and hence transfer to systemic organs more than counterbalances the decrease in lung dose, resulting in increasing effective doses with increasing solubility.

The dependency of the inhalation dose coefficients for these radionuclides on the particle size is shown in Fig. 12.3. Solubility was assumed to be constant here; the values are given in the legend. For particle sizes in the range between 1 and 100 μm, there is a monotonous decrease with increasing size for all four radionuclides. This reflects the different deposition and clearance patterns in the lung for particles of different sizes.

Since solubility generally decreases with particle size, as described in the previous sections, the combined effect on the resulting effective dose is different for these radionuclides. Whereas for ^{137}Cs and ^{90}Sr, increasing particle size and associated decreasing solubility will have opposite effects on the resulting dose coefficients, and hence may partly counterbalance each other, for ^{239}Pu and ^{241}Am larger particles and lower solubility both result in a reduction in the effective dose.

For the particles investigated here, individual inhalation dose coefficients were calculated, applying the particle characteristics as given in Table 12.3 and Table 12.5. Particle sizes were taken from Table 12.3 with an assumed geometric

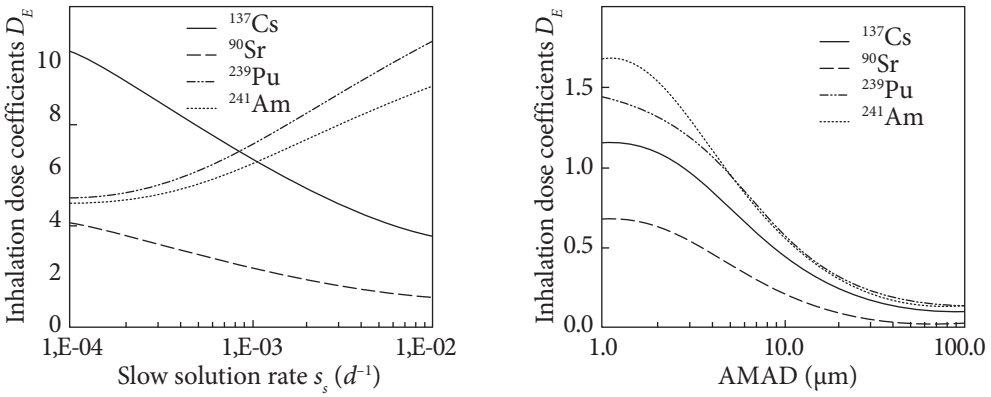

Fig. 12.2. The dependency of the inhalation dose coefficients D_E on the solubility parameter s_s for ^{137}Cs, ^{90}Sr, ^{239}Pu, and ^{241}Am. D_E is 10^{-9} Sv/Bq for ^{137}Cs, 10^{-8} Sv/Bq for ^{90}Sr, and 10^{-6} Sv/Bq for ^{239}Pu and ^{241} Am. Dose coefficients were calculated applying the IMBA computer code (Birchall et al. 2003). The assumed AMAD is 14.4 μm (median values from the measurements see Table 12.5). Assuming f_1-values are 0.1 for ^{137}Cs and ^{90}Sr, 0.00001 for ^{239}Pu and 0.0005 for ^{241}Am. All other parameters are default values from the ICRP lung model (ICRP 1994)

Fig. 12.3. The dependency of the inhalation dose coefficients D_E on the particle size (AMAD) for ^{137}Cs, ^{90}Sr, ^{239}Pu, and ^{241}Am. D_E is 10^{-8} Sv/Bq for ^{137}Cs, 10^{-7} Sv/Bq for ^{90}Sr, and 10^{-5} Sv/Bq for ^{239}Pu and ^{241}Am. Dose coefficients were calculated applying the IMBA computer code (Birchall et al. 2003). Assumed solubility rate s_s is 3.8×10^{-3} d^{-1} for ^{137}Cs, 1.2×10^{-3} d^{-1} for ^{90}Sr, 8.9×10^{-5} day^{-1} for ^{239}Pu, and 1.4×10^{-4} d^{-1} for ^{241}Am (median values from the measurements see Table 12.5). Assuming f_1-values are 0.1 for ^{137}Cs and ^{90}Sr, 0.00001 for ^{239}Pu and 0.0005 for ^{241}Am. All other parameters are default values from the ICRP lung model (ICRP 1994)

standard deviation (σ_g) of 2.5, density was assumed to be 3 g cm^{-3} and a shape factor of 1.5 was assumed. For the physiological parameters, default values for a standard worker were assumed. Dissolution and uptake to blood was described by a single component with the leaching constants as given in Table 12.5 assumed to represent the slow solubility rate s_s. A fraction of the material originally deposited in the lung is transferred to the gastro-intestinal (GI) tract from where it is partially absorbed into the systemic circulation. The respective f_1 values were assumed to be 0.1 for ^{137}Cs and ^{90}Sr, 0.00001 for ^{239}Pu and 0.0005 for ^{241}Am. The thus calculated dose coefficients for the fragments investigated, together with ICRP values, are given in Table 12.5.

For ^{137}Cs, the solubility varies by more than two orders of magnitude whereas the resulting dose coefficients vary roughly within a factor of two (between 2.7×10^{-9} and 6.1×10^{-9} Sv Bq^{-1}). The mean ^{137}Cs dose coefficient for the fuel fragments (for a median solubility factor of 3.8×10^{-4} d^{-1}) is with 3.3×10^{-9} Sv Bq^{-1} very close to the ICRP Type M value for the same AMAD of 14.4 μm (3.1×10^{-9} Sv Bq^{-1}), but only about half of the respective ICRP default value of 6.7×10^{-9} Sv Bq^{-1} (5 μm AMAD; Type F). For

^{90}Sr, the variation in solubility is with a factor of about 20 smaller than for ^{137}Cs. But again, the inhalation dose coefficients for the fragments show a rather small variability with values ranging between 1.2×10^{-8} and 1.7×10^{-8} Sv Bq^{-1}. The mean value of 1.3×10^{-8} Sv Bq^{-1} is again very close to an ICRP type M value for 14.4 μm AMAD with 1.0×10^{-8} Sv Bq^{-1}. The ICRP default value (5 μm AMAD; type M) would again be about double with 2.4×10^{-8} Sv Bq^{-1}.

For both ^{239}Pu and ^{241}Am, the solubility for the different fragments varies by a factor of 20-30. The dose coefficients for ^{239}Pu vary between 2.7×10^{-6} and 7.5×10^{-6} Sv Bq^{-1}. The mean value is 4.0×10^{-6} Sv Bq^{-1} for a median solution rate of 8.9×10^{-5} d^{-1}. This value nearly perfectly matches the ICRP Type S value of 4.2×10^{-6} Sv Bq^{-1} for this size but is about a factor of eight lower than the recommended ICRP default value (5 μm AMAD; type M) of 3.3×10^{-5} Sv Bq^{-1}. The individual values for ^{241}Am range from 2.9×10^{-6} to 7.2×10^{-6} Sv Bq^{-1}. The value for the median solution rate of 1.4×10^{-4} d^{-1} for ^{241}Am is 4.3×10^{-6} Sv Bq^{-1}. Again, there is a perfect match with the ICRP Type S value for this size (also 4.3×10^{-6} Sv Bq^{-1}) but a large difference with respect to the ICRP default value (5 μm AMAD; type M) with 2.7×10^{-5} Sv Bq^{-1}.

The comparison of the experimentally determined dose coefficients with ICRP values (see Table 12.5) indicates that nuclear fuel particles closely resemble type M material characteristics for ^{137}Cs and ^{90}Sr and Type S material characteristics for ^{239}Pu and ^{241}Am. The discrepancies between the dose coefficients as derived from the experimental parameters and the default ICRP values predominantly arise from the differences in solubility, whereas different particle sizes play a minor role.

Hence with the use of initially airborne nuclear fuel material from the Chernobyl accident (which reasonably may be assumed to be preserved on the stored air filters) and the concept of equivalent diameter, the dependence of particle solubility on particle size could be successfully measured and analyzed. The experimental investigations clearly demonstrate the effect of decreasing solubility with increasing particle size as predicted from the theoretical considerations.

The combined effect of increasing particle size with associated decreasing solubility on inhalation dose, however, is different for different radionuclides. For ^{137}Cs and ^{90}Sr, increasing particle size and associated decreasing solubility have opposite effects on the resulting dose coefficients. Decreasing dose with size and increasing doses with lower solubility may partly counterbalance each other for these radionuclides. On the other hand, for ^{239}Pu and ^{241}Am larger particles and associated lower solubility both result in a reduction in the effective dose.

The comparison of the dose coefficients using solubility parameters from *in vitro* measurements with ICRP values indicates that nuclear fuel particles closely resemble type M material characteristics for ^{137}Cs and ^{90}Sr and Type S material characteristics for ^{239}Pu and ^{241}Am. The differences between the dose coefficients (as derived from the experimental parameters) and the default ICRP values pre-

dominantly arise from the differences in solubility, whereas different particle sizes play a minor role.

It can be concluded that whereas for ^{137}Cs and ^{90}Sr the ICRP default inhalation dose coefficients are still in reasonable agreement with the values calculated from *in vitro* experiments, for ^{239}Pu and ^{241}Am the resulting doses (and hence risks) are overestimated when the ICRP default type dose coefficients are applied. This emphasizes again that whenever possible, material-specific parameters should be applied for dose calculations. Although dose coefficients based on *in vitro* experiments may not be transferred straightforward to *in vivo* situations due to the complexity of conditions in the respiratory tract. Nevertheless, there are circumstances where *in vitro* studies are the only possible approach to obtain valuable information on the solubility of inhaled material which is otherwise not available. This was the case in the present study where not enough material was available to conduct *in vivo* studies and where ethical reasons exclude investigations on humans. The results presented here therefore provide novel and valuable information on the solubility of inhaled airborne fuel particles and the resulting radiation doses, particularly when compared to the values obtained with default parameters.

CHAPTER 13

RADIOACTIVE AEROSOLS RELEASED FROM THE «SHELTER» OBJECT

13.1. Introduction

During 30 years of the nuclear accident in Chernobyl, from the accident in 1986 until finishing the New Safe Cofinement construction in 2016, the former unit 4 of the Chernobyl nuclear power plant remained a source of radionuclide emissions into the environment. Soon after the fire in the reactor was stopped in 1986, a containment structure («Shelter») was constructed to prevent any further release of radioactive material (Nosovskiy 2016a, 2016b). The «Shelter» was erected very quickly and has many small and some large openings (up to a few tens of square meters) through which radionuclides can be swept away by the wind and rain (Krasnov et al. 2016). Investigations of the processes occurring in the «Shelter» (e.g., resuspension and deposition of the radioactive indoor dust) and of the characteristics of the released radioactive aerosol (Borovoj 1990, Bogatov et al. 1990, Borovoj 2000, Bogatov 2000, Borovoj and Gagarinskiy 2001) began immediately after the construction of the «Shelter» had been finished. Two types of «Shelter» aerosol particles can be distinguished: aggregates of fine particles from the irradiated fuel (which are usually low in levels of volatile radionuclides) and atmospheric aerosol particulates with attached radionuclides (Bogatov 2000). The contaminated aerosol under the roof space of the «Shelter» is formed by roughly dispersed fuel particles, with an activity median aerodynamic diameter (AMAD) close to 5 μm (Bogatov 2000). Particles redistributed from the surfaces inside the «Shelter» are in the range 6-9 μm AMAD. The total mass of the fuel dust is close to 5,000 kg, from which 100 kg is potentially available for resuspension into the environment. Therefore, the radioactive aerosol still represents one of the potential radiological risks originating from the ChNPP. In particular, during three decades it was one of the

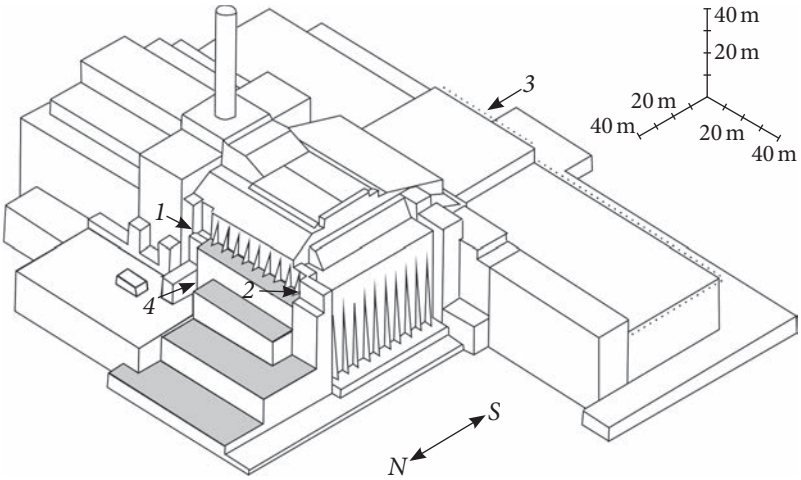

Fig. 13.1. Containment («Shelter») of the former Unit 4 of the Chernobyl nuclear power plant with the main gaps 1-4 where aerosol samplers were deployed

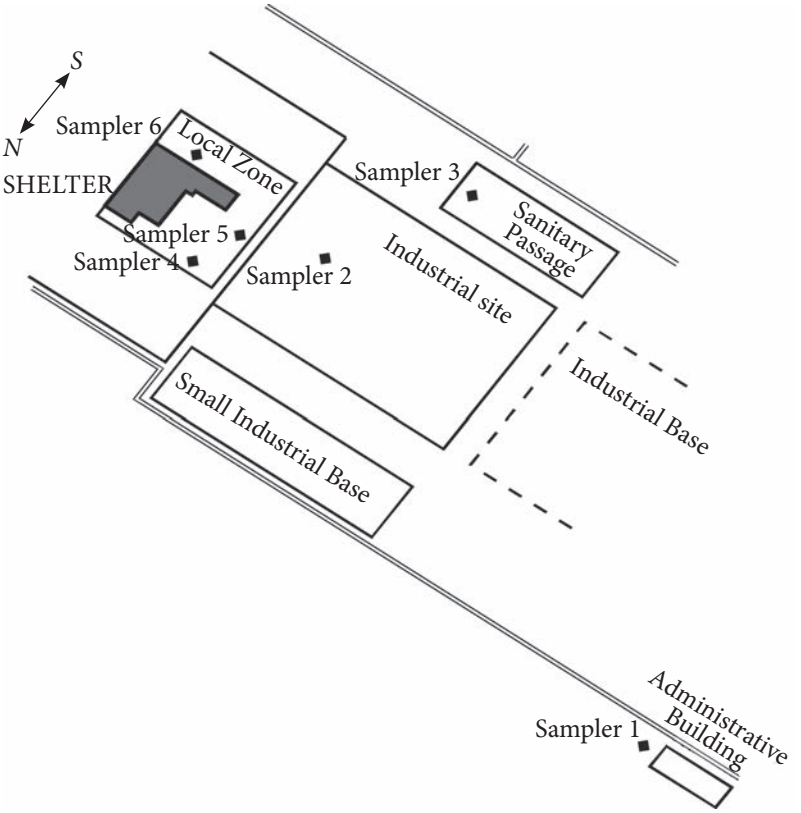

Fig. 13.2. Sketch of the nearest environment of the «Shelter» («Shelter» site) including the location of the aerosol samplers. The following samplers were deployed: «Typhoon» (sampler 1), «Grad» (samplers 2, 4, 5, 6), and SES (sampler 3)

major factors of radioactive exposure of the personnel working on the industrial site and in the local zone of the ChNPP. The most of results presented in this Chapter (Chapters 13.2-13.8) was obtained during studies in 1997-2003 aiming to specify the actual radioactive releases into the surface layer of the atmosphere and to assess the inhalation dose for personnel worked at New Safe Cofinement construction. For that purpose, the atmospheric activity concentration of the relevant radionuclides and their activity size distribution were measured, at the gaps of the «Shelter» (Fig. 13.1), and in the near environment of the «Shelter» (Fig. 13.2). To estimate inhalation doses, the results were used to determine the individual input parameters for the applied standard dose assessment model. The last chapter 13.9 containes data obtained in 2015-2017, i.e. on the last stage of construction of New Safe Confinement with the main aim to transform the Shelter into an environmentally safe system. The completion of the NSC creation made it possible to ensure the safety of the Shelter object and significantly reduced the risk of possible radioactive contamination of the territory as a result of the collapse of unstable building structures of the object.

13.2. Materials and methods

For measurements of the airborne radionuclide activity concentration at the «Shelter» site from 1997 until 2003 places of allocation of sampling sites were chosen. Such monitoring efforts required continuous representative measurements of the concentration field of the radioactive aerosol. The following aerodynamical considerations were made, to identify appropriate locations of the samplers.

Obstacles cause reverse (backward) flows near the surface. Measurements of stream lines of different building models performed in aerodynamic tunnels (Slade 1968) and under natural conditions (Garger, Zhukov and Lukoyanov 1988) have shown that this slipstream area depends on the height and width of buildings. The horizontal dimension of that zone is larger than two heights of the obstacle (Garger, Zhukov and Lukoyanov 1988).

At a distance of two building heights, the height of the slipstream zone is less than the obstacle height. Thus, with the given maximum «Shelter» height of 68 m, for different directions of the flow, shadow lengths of 190-270 m were estimated (Bogatov 2000). From the sketch of the «Shelter» site (Fig. 13.2) it can be seen that the lee part of the industrial site is always in the aerodynamic shadow of the «Shelter» building. The zone around the «Shelter» is characterized by a high turbulence and reverse flow, which means that the air activity concentrations do not vary much within this zone. Three samplers were therefore placed 50-100 m to the north, northwest, and south of the «Shelter», respectively. The fourth sampler was positioned at the south-west side near a personnel road (Fig. 13.2). The filter samples were taken with high-volume samplers «Typhoon», «Grad», and SES for determination of the

activity concentration. For size-segregated sampling, the impactors IBP and Andersen PM10 were used. Sampler characteristics are given in Tables 13.1 and 13.2; more details of the experimental set-up can be found in (Garger and Kashpur 2000).

Several large gaps with areas of 10-90 m^2 (about 200 m^2 in total) were monitored between May 1996 and December 2000. Within the gaps, the samplers were installed as centrally as possible, depending on the availability of fixing possibilities at the building (Fig. 13.1). The total release through a certain gap was estimated using the following equation (Garger et al. 2001):

$$Q_j = q_j \sum_{i=1}^{n} A_i v_i, \tag{13.1}$$

where Q_j (Bq s^{-1}) is the total mean activity flow rate through a gap j, which was divided into n rectangles of area A_i (m^2); v_i (m s^{-1}) is the wind velocity in the center of the rectangles, and q_j (Bq m^{-3}) is the mean activity concentration in the air. While the mean activity concentration q_j was measured typically for a period of 2-4 days, the flow parameters were determined by short-time measurements, daily. To record wind velocities, the portable anemometer AMW-441 (with a velocity range of 0.05-30.0 m s^{-1}) was used.

Details of activity measurements of ^{137}Cs, ^{7}Be, $^{239+240}$Pu and ^{241}Am on the filters and in the leaching solutions are given in Chapter 12.1. More detailed information on the experimental equipment is given in (Garger et al. 2001). Radiochemical analyses were only performed for those size-segregated samples that were high in ^{137}Cs. For those low in the ^{137}Cs, $^{239+240}$Pu and ^{241}Am activity concentrations were below the detection limit. For these nuclides, the mean activity concentrations must, therefore, be considered as upper limits.

Table 13.1. **Integrating aerosol samplers used for monitoring around the «Shelter»**

Sampler name	Flow rate (m^3 h^{-1})	Filter size (m)	Filter material
Typhoon	4,170	1.55 × 0.34	Petryanov
Grad	400	0.77 × 0.34	Petryanov
Andersen PM10	67.8	0.20 × 0.30	Whatman-441
SES	70	0.20 × 0.30	Whatman-441

Table 13.2. **Size-segregating aerosol samplers at the gaps and near the «Shelter», including cut-off diameters of the different stages, and the flow rate through the instrument**

Sampler name	Flow rate (m^3 h^{-1})	Size limits (μm)
Andersen PM10	67.8	4.9, 2.3, 1.4, 0.8, < 0.8
IBP impactor	1.05	29, 14, 5.4, 1.6, 0.56, < 0.56

13.3. Measurements at the gaps: flow rates

The total flow rate of activity through the gaps of the «Shelter» was 274.1 Bq s^{-1}, corresponding to 8.64×10^9 Bq $year^{-1}$. Of the release, 78.5% was due to ^{137}Cs, 21.1% due to ^{90}Sr, and 0.4% due to $^{239+240}$Pu. In Fig. 13.3 the time courses of the activity concentration of ^{137}Cs, ^{241}Am, ^{7}Be, ^{90}Sr, and $^{239+240}$Pu measured with the Andersen PM10 samplers at the vertical southern opening near the «Shelter» roof (gap 3 in Fig. 13.1) are presented. The high correlation of the ^{137}Cs, ^{90}Sr, and ^{241}Am time courses is obvious. A peculiarity in the data is the presence of two periods with very high emissions of radioactive aerosols, i.e., about 100 mBq m^{-3} for ^{137}Cs, 50 mBq m^{-3} for ^{90}Sr, 1.5 mBq m^{-3} for $^{239+240}$Pu, and 0.8 mBq m^{-3} for ^{241}Am. The intensities of the ^{137}Cs and ^{241}Am releases varied by a factor of about 100, those of ^{90}Sr by a factor of 25, and those of $^{239+240}$Pu by a factor of only

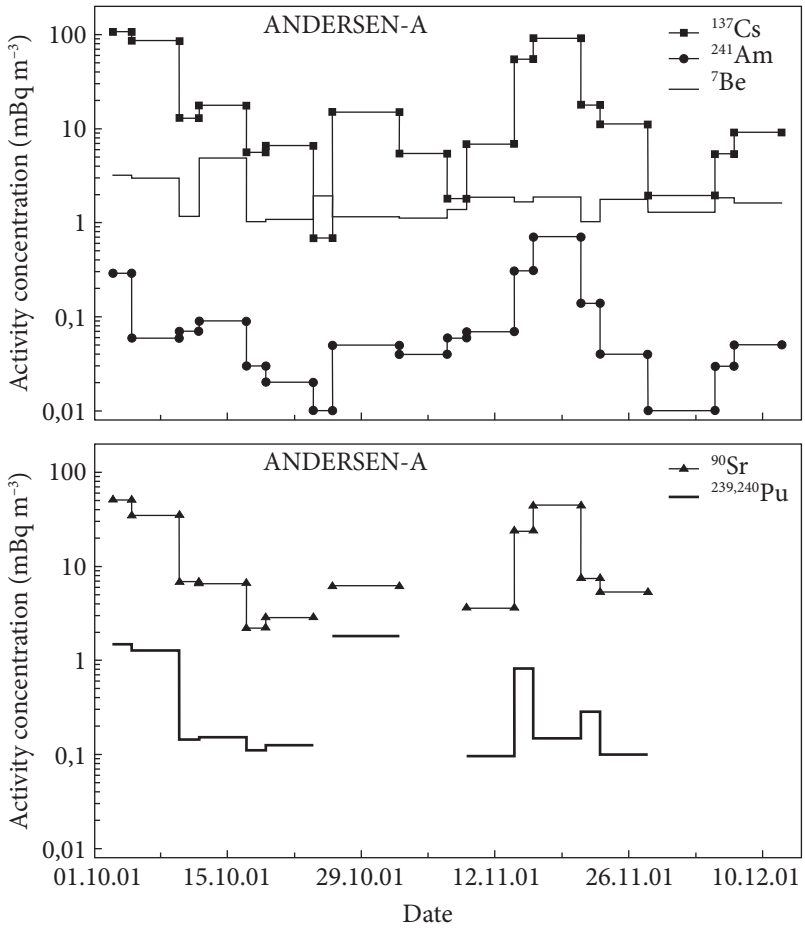

Fig. 13.3. Time records of the ^{137}Cs, ^{90}Sr, ^{241}Am, $^{239+240}$Pu, and ^{7}B activity concentrations in the air flow of the vertical gap 3, at the south wall of the «Shelter», and during the period 03.10.2001-12.12.2001

15. According to (Garger et al. 1994) these concentration fluctuations may be 2-3 times higher for shorter periods than the 2-7 days periods presented in Fig. 13.3. In contrast to that, the ^{7}Be activity concentrations, which originate from sources independent of the «Shelter» release, were rather constant. This emphasizes the high variability of the local source. It must be noted that the Andersen PM10 sampler only collects particles smaller than 10 μm, which could result in an underestimation of the actual releases.

13.4. Measurements at the gaps: size distribution of the released aerosol

The activity size distributions of the particles released at the largest gaps were determined by impactor measurements. In Table 13.3 the major parameters of the particle size distributions obtained for the years 1996, 1997, and 1999 are summarized. The flow of the activity out of the «Shelter» was more than one order of magnitude higher than that into the «Shelter». On average (i.e., weighted by the number of measurements), the measured activity concentrations and their standard deviations were 243 ± 228 mBq m^{-3} for ^{137}Cs, 119 ± 60.3 mBq m^{-3} for ^{90}Sr, 1.83 ± 0.70 m^{3} for $^{239+240}$Pu, and 2.04 ± 1.73 mBq m^{-3} for ^{241}Am. In the period 2001-2003, the significantly lower activity concentrations were determined (Table 13.4). The corresponding mean activity concentrations and their standard deviations were 14.0 ± 10.0 mBq m^{-3} for ^{137}Cs, 3.12

Table 13.3. **Results of size-resolved aerosol measurements performed at the different «Shelter» gaps: activity concentration, the standard deviation σ of *N* samples, AMAD, the geometric standard deviation σ_g in the years 1996, 1997, and 1999, and the related effective dose rate**

Radionuclide measurement period	Activity conc. ±σ(*N*) (mBq m^{-3})	AMAD (μm)	σ_g	Eff. dose rate (nSv h^{-1})	Gap no., impactor type, flow direction
	^{137}Cs				Gap 1, IBP
16.07-28.10.1997	464 ± 625 (6)	2.0 ± 0.5	3.8 ± 1.6	5.47	Out-flow
12.07-16.07.1997	85.8 (1)	1.9	7.1	1.06	In-flow
	^{90}Sr				
02.11-05.11.1996	135 (1)	13.0	2.9	2.84	Out-flow
	$^{239+240}$Pu				
02.11-05.11.1996	2.0 (1)	3.5	5.4	23.7	Out-flow
	^{241}Am				
16.07-28.10.1997	5.1 ± 7.8 (5)	1.7 ± 0.6	4.1 ± 1.1	108	Out-flow

Continuation of Table 13.3.

Radionuclide measurement period	Activity conc. $\pm\sigma(N)$ (mBq m^{-3})	AMAD (μm)	σ_g	Eff. dose rate (nSv h^{-1})	Gap no., impactor type, flow direction
	^{137}Cs				Gap 1, Andersen PM10
09.10-30.10.1997	16.6 ± 22.8 (5)	2.0 ± 0.4	3.3 ± 2.1	0.201	Out-flow
17.10-21.10.1997	3.2 (1)	1.8	1.8	0.0495	In-flow
	^{137}Cs				Gap 4, IBP
18.07-22.07.1997	534 ± 407 (3)	3.0 ± 1.0	6.3 ± 1.2	5.59	Out-flow
22.07-24.07.1997	72.8 (1)	2.5	6.3	0.811	In-flow
	^{90}Sr				
06.11-12.11.1996	184 (1)	3.1	6.8	11.4	Out-flow
	$^{239+240}$Pu				
06.11-12.11.1996	2.6 (1)	15	5.5	18.4	Out-flow
	^{241}Am				
18.07-22.07.1997	3.3 ± 2.1 (3)	1.4 ± 0.6	4.0 ± 2.2	75.2	Out-flow
	^{137}Cs				Gap 3, IBP
17.11-19.11.1999	14.6 (1)	4.1	10.0	0.147	In-flow
19.11-23.11.1999	11.7 (1)	5.6	4.2	0.0963	In-flow
23.11-26.11.1999	45.9 (1)	7.2	8.5	0.361	Half in-flow and half out-flow
26.11-30.11.1999	409.8 (1)	5.1	7.0	3.58	Out-flow
	^{241}Am				
17.11-19.11.1999	0.33 (1)	1.0	7.3	9.74	In-flow
19.11-23.11.1999	0.55 (1)	1.7	6.2	12.6	In-flow
23.11-26.11.1999	0.71 (1)	1.7	6.9	16.7	Half in-flow and half out-flow
26.11-30.11.1999	2.23 (1)	1.05	7.6	65.0	Out-flow
	^{90}Sr				
17.11-30.11.1999	38.8 (1)	4.5	7.5	2.10	Combined samples: in + out-flow
	$^{239+240}$Pu				
17.11-30.11.1999	0.9 (1)	6.0	4.8	7.95	Combined samples: in + out-flow

± 2.57 mBq m^{-3} for ^{90}Sr, 0.095 ± 0.025 mBq m^{-3} for $^{239+240}Pu$, and 0.845 ± 0.515 mBq m^{-3} for ^{241}Am.

Probably, closure of several gaps, which reduced the wind flow through the building, and dust reduction inside the «Shelter» were responsible for the observed decrease.

The median diameter with its geometric standard deviation does not show the same large variability as the atmospheric activity concentration. The mean AMADs for the out-flow during the 1996—1999 period (weighted by the number of measurements) were 2.4 ± 0.8 μm for ^{137}Cs, 1.5 ± 0.2 μm for ^{241}Am and from 3.1 to 13.0 μm for ^{90}Sr, and from 3.5 to 11 μm for $^{239+240}Pu$ (Table 13.3). The corresponding standard deviations s_g were 4.4 ± 1.3, 4.5 ± 1.1, 2.9-7.5, and 4.8-5.5,

Table 13.4. **Results of size-resolved aerosol measurements performed at the different «Shelter» gaps: activity concentration, standard deviation σ of *N* samples, AMAD, geometric standard deviation σ_g in the years 2000-2003, and the related effective dose rate**

Radionuclide measurement period	Activity conc. $\pm\sigma(N)$ (mBq m^{-3})	AMAD (μm)	σ_g	Eff. dose rate (nSv h^{-1})	Gap no., impactor type, flow direction
	^{137}Cs				Gap 3, IBP
18.08-30.08.2000	20.9 ± 13.3 (4)	2.2 ± 0.3	5.9 ± 0.8	0.241	Out-flow
05.10-12.12.2001	33.05 ± 28.0 (4)	6.8 ± 6.9	6.8 ± 2.6	0.256	Out-flow
	^{241}Am				
18.08-30.08.2000	0.33 ± 0.26 (4)	1.0 ± 0.2	4.0 ± 1.5	6.57	Out-flow
05.10-12.12.2001	1.36 ± 1.5 (4)	2.6 ± 1.6	6.6 ± 1.0	20.7	Out-flow
	^{137}Cs				Gap 3, Andersen PM10
04.09-03.12.2002	8.08 ± 5.87 (11)	1.7 ± 0.8	3.5 ± 1.4	0.0999	Out-flow
	^{90}Sr				
01.10-03.10.2002	0.55 (1)	2.0	3.0	0.0391	Out-flow
28.10-31.10.2002	5.69 (1)	2.9	3.2	0.353	Out-flow
	$^{239+240}Pu$				
01.10-03.10.2002	0.07 (1)	2.0	3.3	1.02	Out-flow
28.10-31.10.2002	0.12 (1)	2.0	1.8	2.17	Out-flow
	^{137}Cs				Gap 3, Andersen PM10
02.12-10.12.2003	13.75 ± 1.96 (3)	3.5 ± 0.6	1.8 ± 0.6	0.182	Out-flow
17.10-02.12.2003	1.29 ± 1.0 (3)	2.2 ± 0.3	2.0 ± 0.6	0.0189	In-flow

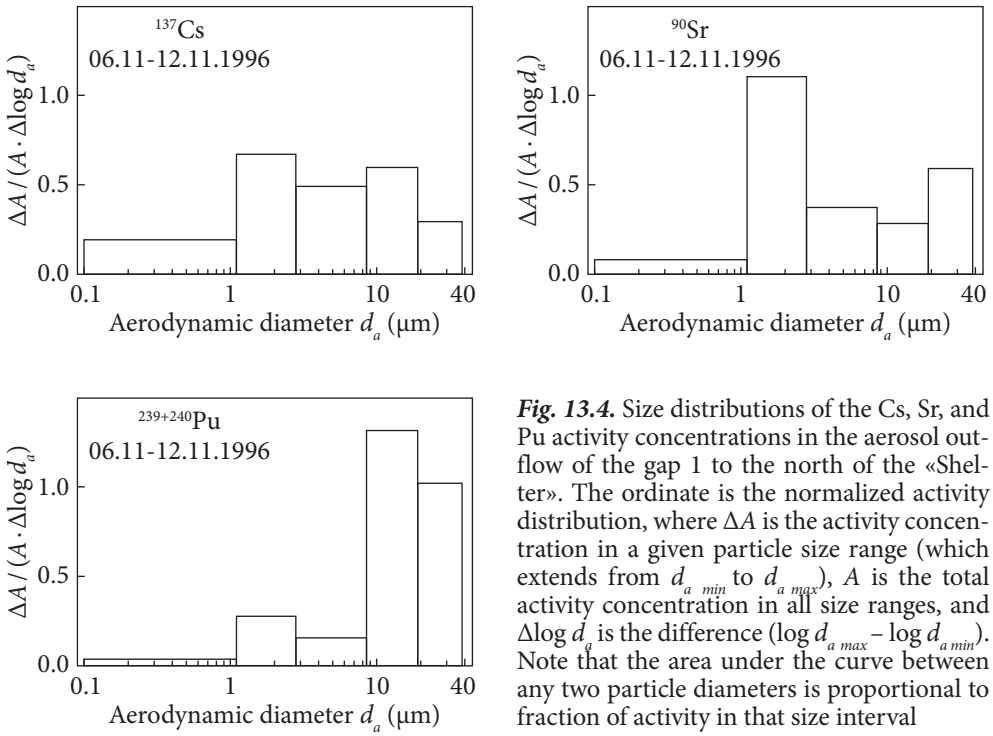

Fig. 13.4. Size distributions of the Cs, Sr, and Pu activity concentrations in the aerosol outflow of the gap 1 to the north of the «Shelter». The ordinate is the normalized activity distribution, where ΔA is the activity concentration in a given particle size range (which extends from $d_{a\ min}$ to $d_{a\ max}$), A is the total activity concentration in all size ranges, and $\Delta \log d_a$ is the difference ($\log d_{a\ max} - \log d_{a\ min}$). Note that the area under the curve between any two particle diameters is proportional to fraction of activity in that size interval

respectively. In the 2000-2003 period, the mean AMAD for ^{137}Cs was 3.0 ± 1.9 μm, and the corresponding standard deviation was $\sigma_g = 4.3 \pm 1.7$ (Table 13.4). In the two series of measurements, the ^{241}Am, ^{90}Sr, and $^{239+240}$Pu AMADs were in the range of 1.0-2.9 μm and σ_g in the range of 1.0-6.6.

Activity size distributions of ^{137}Cs, ^{90}Sr, and $^{239+240}$Pu are presented in Fig. 13.4, measured in the out-going flow of gap 1 at the north side of the «Shelter». The distributions are wide and show two maxima, one in the fine-particle range (at about 2 μm) and one in the coarse-particle range (above 10 μm). In comparison, the activity in the sub-micrometer particle range is low for $^{239+240}$Pu, medium for ^{90}Sr, and high for ^{137}Cs.

13.5. Measurements at the «Shelter» site: activity concentrations

Results of integral radionuclide measurements in the surrounding of the «Shelter» building are given in Fig. 13.5. Depicted are the simultaneous time courses of the ^{137}Cs and $^{239+240}$Pu activity concentrations in the air at two sampling locations. In general, during the total observation period, the higher activity concentrations were measured in the southern vicinity

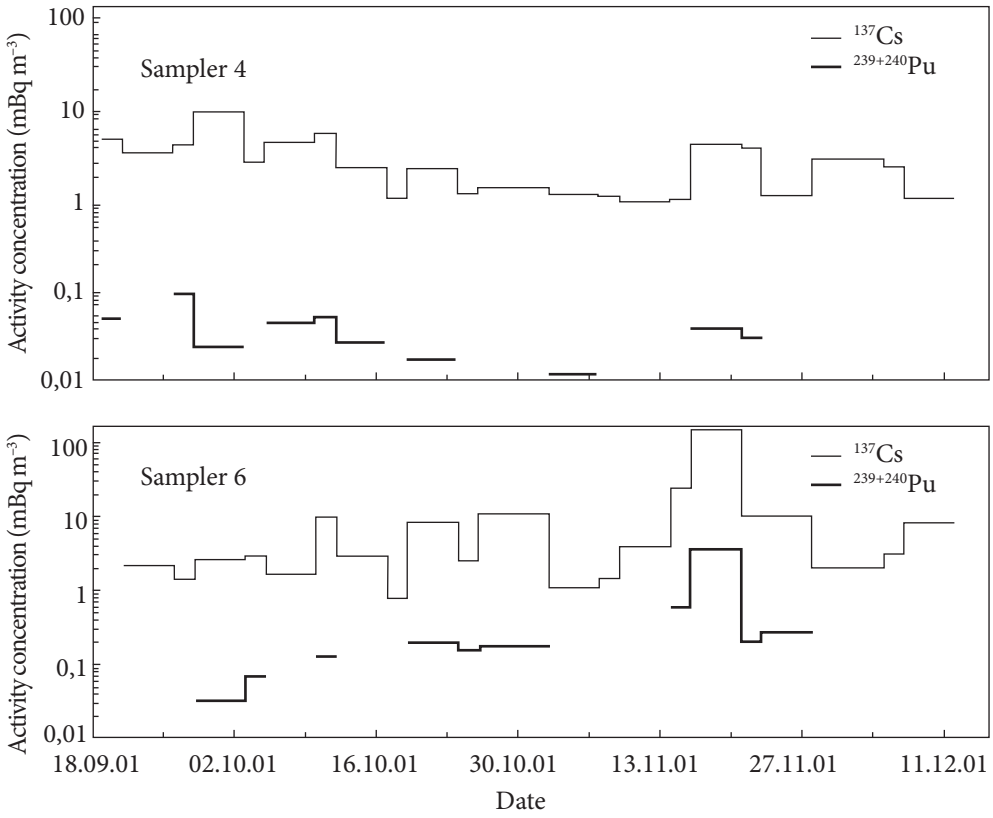

Fig. 13.5. Activity concentrations of ^{137}Cs and $^{238+240}$Pu in the surface layer of the atmosphere in the local zone of the «Shelter» site (samplers 4 and 6) and as a function of time, during the period 19.09.2001-12.12.2001

of the «Shelter» (sampler 6), reaching pronounced maxima in the period 14-23.11.2001 of 142 mBq m^{-3} for ^{137}Cs, 115 mBq m^{-3} for ^{90}Sr, and 3.55 mBq m^{-3} for $^{239+240}$Pu. In the northern vicinity of the «Shelter» (sampler 4), lower activity concentrations were measured that did not exceed 10 mBq m^{-3} for ^{137}Cs and 0.1 mBq m^{-3} for $^{239+240}$Pu, and that showed a much smaller variability in the activity concentrations compared to those measured in the southern vicinity of the «Shelter». About 800 m to the north-west of the «Shelter» (sampler 1 in Fig. 13.2), only small ^{137}Cs activity concentrations of the order of 1.0 mBq m^{-3} were measured. Therefore, sampler 6 can be regarded as situated in the lee of the «Shelter» building during most weather conditions. The data obtained from this sampler can, thus, provide a conservative estimate (i.e., an upper limit) of the exposure of the workers at the «Shelter» site, due to the inhalation of radioactive aerosols.

13.6. The size distribution of the released aerosols

Size-segregated measurements performed with the Andersen PM10 sampler at locations 3, 4, and 6 are presented in Table 13.5. The mean ^{137}Cs activity concentration was 1.74 ± 2.68 mBq m^{-3}. Again, the highest ^{137}Cs activity concentrations were measured in the south of the «Shelter» (sampler 6). The AMAD values ranged from 0.6 to 3.6 μm. Their mean geometric standard deviations ranged from 1.3 to 4.7. During several experiments with increased activity concentration, the measured AMADs were in the sub-micron range. This has to be considered for inhalation dose assessment. The measurements in Pripyat may be taken as background concentrations for the «Shelter» site, as Pripyat is situated 4 km north-west of the «Shelter». Nine series of measurements were performed there using the Andersen PM10 sampler in the 1996-2000 period. The mean activity concentrations were found to be in the range of the lowest concentrations at the «Shelter» site. It is interesting to compare the present mean parameters of the particle size distributions of ^{137}Cs with those measured at Pripyat in 1987-1992 (Garger et al. 1994). Probably due to previous decontamination, less anthropogenic activities, and weathering in general, the atmospheric activity concentration was reduced by one order of magnitude and the AMAD decreased from 5.4 to 1.2 μm (Table 13.5), compared to the earlier values (Garger et al. 1994).

Table 13.5. **Results of size-resolved aerosol measurements performed in the immediate environment of the «Shelter» (Fig. 13.2): ^{137}Cs activity concentration, the standard deviation σ of *N* samples, AMAD, geometric standard deviation σ_g, in the years 1997-2003, and the related effective dose rate**

^{137}Cs measurement period	Activity conc. ± σ(*N*) (mBq m^{-3})	AMAD (μm)	σ_g	Eff. dose rate (pSv h^{-1})	Sampler location (see Fig. 13.2)
10.07-31.07.1997	2.2 ± 1.2 (7)	2.2 ± 1.1	4.3 ± 2.4	25.1	Sampler 4, 50 m north
05.11-15.11.2002	9.95 ± 8.64 (3)	0.7 ± 0.5	3.1 ± 1.7	139	Sampler 6, 50 m south
12.08-30.09.2003	0.97 ± 0.42 (7)	3.6 ± 0.8	4.3 ± 1.3	9.50	Sampler 6, 50 m south
30.09-10.12.2003	0.33 ± 0.17 (10)	2.1 ± 0.3	2.2 ± 0.4	2.57	Sampler 6, 50 m south
30.07-07.12.2002	0.87 ± 0.23 (4)	1.2 ± 0.1	4.7 ± 0.9	12.1	Sampler 3, 200 m south-west
07.08-16.10.2003	0.79 ± 0.20 (7)	2.1 ± 0.6	2.1 ± 0.9	11.3	Act. conc. < 1.0 mBq m^{-3}
07.08-16.10.2003	3.36 ± 2.26 (3)	0.57 ± 0.06	1.3 ± 0.2	30.4	Act. conc. > 1.0 mBq m^{-3}
1987-1992	2.44 ± 2.19 (17)	5.4 ± 3.2	1.7 ± 1.2	21.9	Pripyat, 4 km north-west
1996-2000	0.34 ± 0.18 (9)	1.2 ± 0.1	4.7 ± 1.0	4.57	Pripyat, 4 km north-west

Note: Values measured in the abandoned city of Pripyat are given for comparison.

13.7. Transformation of radionuclide characteristics

In Fig. 13.6 the ^{137}Cs activity size distributions are compared which were determined in the outgoing southern flow from the «Shelter» (a) directly at gap 3 and (b) at a 50 m distance from the south wall of the «Shelter» (sampler 6 in Fig. 8.2). Directly at the «Shelter» gap, the size distributions show one mode in the coarse-particle range, with only a little tailing in the fine-particle rang (below 1 μm). In contrast, the size distributions at a 50 m distance are characterized by a wider range in particle size, with a considerable portion in the fine-particle range, and a second mode that appears at about 1-2 μm. Causes of this observed transformation of the size distribution might be the preferential deposition of the coarse particles in the forward flow from the «Shelter» due to the dependence of the deposition velocity on the particle size, and/or the re-entrainment of contaminated soil by the backward flow at the «Shelter» building. In agreement with our results, measurements inside the «Shelter» (Kuzmina

Table 13.6. **Radionuclide ratios at the southward «Shelter» gap 3 and at a distance of 50 m from the south wall of the «Shelter» (see Fig. 13.1 and 13.2): mean of *N* sampling intervals during different sampling periods**

Measurement location, period (*N*)	$^{137}Cs/^{239+240}Pu$	$^{90}Sr/^{239+240}Pu$	$^{238}Pu/^{239+240}Pu$	$^{241}Am/^{239+240}Pu$	$^{137}Cs/^{90}Sr$
Gap 3, 26.11-30.11.1999 (4)	111	37.3	0.49	0.70	2.96
Gap 3, 18.08-01.09.2000 (4)	149	72.6	0.52	0.97	1.97
Gap 3, 20.09-03.10.2002 (2)	39.2	10.5	0.36	0.38	3.72
Gap 3, 03.10-28.11.2001 (8)	75.5 ± 20.0	35.0 ± 10.9	0.41 ± 0.10	0.33 ± 0.17	2.19 ± 0.18
Sampler 6, 03.10-28.11.2001 (8)	48.5 ± 13.7	40.4 ± 11.9	0.39 ± 0.06	0.35 ± 0.20	1.21 ± 0.09
Gap 3, 20.08-12.12.2003 (20)	139 ± 51	49 ± 13.7	045 ± 0.04	1.03 ± 0.38	2.78 ± 0.42
Sampler 6, 27.08-26.09.2003 (7)	119 ± 93	34.3 ± 32.6	0.46 ± 0.07	1.49 ± 1.41	5.8 ± 4.3
Pripyat 1987 (ICRP, 1983)	52 ± 20	56 ± 9	0.52 ± 0.11	1.22 ± 0.10	0.93
«Shelter» 1997 (Garger et al. 2004)	77	65	0.53	1.24	1.18

Note: Literature data for Pripyat and the «Shelter» premises are given for comparison.

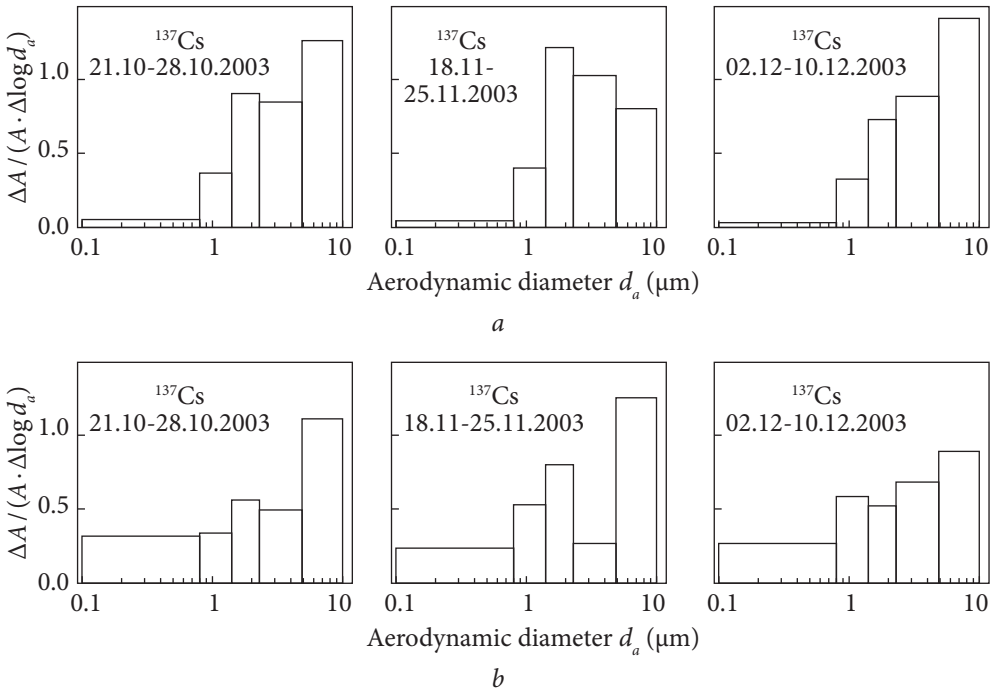

Fig. 13.6. Size distribution of the normalized ^{137}Cs activity concentration A: *a* — in the aerosol out-flow of gap 3 (south of the «Shelter» in Fig. 13.1); *b* — 50 m south of the «Shelter» (sampler 6 in Fig. 13.2)

1994, Kuzmina and Tokarevskii 1996) have shown that the main contribution to the activity deposited onto the indoor surfaces of the building are due to particles characterized by sizes in the range of 1-5 and 5-10 μm, respectively. In indoor air samples, the main activity concentration (about 60%) falls into the range 1-5 μm. The observed transformation of the particle size distribution with distance may be accompanied by a change in the radionuclide composition of the aerosol involved. In Table 13.6, radionuclide ratios measured at the large vertical gap 3 of the machine-hall (Fig. 13.1) and at a distance of 50 m from the south wall of the «Shelter» (sampler 6 in Fig. 13.2) are given. In the periods 2001 and 2003 when samplers were operated at both locations, the ratios generally match each other within their limits of uncertainty. In general, the variability of the ratios was small, with the ^{90}Sr/$^{238+240}$Pu (change from 10.5 to 72.6) and ^{137}Cs/$^{238+240}$Pu ratios (change from 39.2 to 149) being exceptions. These differences were connected with a change of the flow direction and working activities inside the «Shelter» premises. Compared with literature data (Garger et al. 2004, Garger et al. 1998), the activity concentrations at the gap measured in the present work show higher ^{137}Cs/^{90}Sr ratios.

13.8. Assessment of inhalation dose

Effective dose rates were calculated by Garger et al. (2006) for all sampling periods as discussed in Chapter 12.3. Experimental data on the Chernobyl aerosol (e.g., on the solubility) were utilized instead of model default values, if available. Individual activity concentrations, median particle sizes, and geometric standard deviations of the particle size distributions were taken from Tables 13.3-13.5. The resulting individual effective dose rates were tabulated (Tables 13.-.5) and summarized in Tables 13.7 and 13.8.

At the «Shelter» gaps, mean total effective dose rates of 97.5 nSv h^{-1} were calculated for the period 1996-1999. The main dose contribution resulted from ^{241}Am, while ^{137}Cs contributed only about 3% to the total inhalation dose. The reduced emissions observed in the period 2000-2003 resulted in a dose rate decrease of more than one order of magnitude, for most radionuclides. Because dose rate from ^{241}Am decreased only by a factor of 5, a mean total effective dose rate of 15.6 nSv h^{-1} was determined in the period 2000-2003 (Table 13.7).

Table 13.7. **The weighted mean of individually calculated effective dose rates (nSv h^{-1}) from inhalation at the «Shelter» gaps**

Period	^{137}Cs	^{90}Sr	$^{239+240}$Pu	^{241}Am	Total
1996-1999	2.70	5.46	16.7	72.6	97.5
2000-2003	0.149	0.196	1.60	13.7	15.6

Note: for the 1996-1999 period data were taken from Table 13.3; for the 2000-2003 period from Table 13.4.

Table 13.8. **The weighted mean of individually calculated effective dose rates (nSv h^{-1}) from inhalation in the close environment of the «Shelter»**

Period	^{137}Cs	^{90}Sr	$^{239+240}$Pu	^{241}Am	Total
1997	0.0251				
2002-2003	0.0214				
14.11-23.11.2001					
d = 0.5 μm, σ_g = 2.46	1.87	10.3	69.4	25.6	107
d = 1 μm, σ_g = 2.47	1.87	9.4	61.3	23.0	95.6
d = 5 μm, σ_g = 2.50	1.33	5.55	43.0	13.2	63.1

Note: for the years 1997 and 2002-2003, data were taken from Table 13.5. For the single sampling interval with increased integral activity concentration (sampler 6, Fig. 13.4), dose rates were calculated for three different particle size distributions.

In the vicinity of the «Shelter», it was only possible to analyze ^{137}Cs distribution characteristics (Table 13.5), because the activities were generally much lower there compared to those at the «Shelter» gaps. The resulting calculated dose rates were on average about two orders of magnitude lower than directly at the gaps, in the early period. The reduced emissions in 2002—2003 led to a minor dose rate reduction and to a ^{137}Cs dose rate which was about a factor 7 smaller than directly at the gaps, for that period. The integral measurements performed in the «Shelter» vicinity (Fig. 13.5) may be used for the dose assessment of the rest of the radionuclides considered. A literature data for Pripyat and the «Shelter» premises (Table 13.8) are used for very conservative (i.e., an upper limit for the effective dose rate from inhalation) estimation for the single period of high airborne activity concentrations in the lee of the «Shelter» (sampler 6). For this estimate, dose rate calculations were performed for three different realistic particle size distributions. As a result, total effective dose rates of up to 107 nSv h^{-1} were calculated, which are comparable to those calculated at the gaps (Table 13.8).

The main contribution to inhalation dose results from the nuclide $^{239+240}$Pu. However, the data are shown in Fig. 13.5 suggest the mean total effective inhalation dose rate, if averaged over time, to be two orders of magnitude lower, confirming the result found for ^{137}Cs.

Effective dose rates due to inhalation in the range of 100 nSv h^{-1} as determined at the gaps or during some periods in the «Shelter» vicinity would result in additional doses that are not negligible for any construction workers of New Safe Cofinement. Assuming an annual working time of 1,710 h (standard working time in the European Union and Ukraine) the inhalation dose rate would sum up to about 0.2 mSv year^{-1}. This dose rate would not be in conflict with any legal regulations of radiation exposure at work places, but must be taken into consideration if assessing the total radiation exposure in the case of any potential external exposure.

Measurements at the containment building of the destroyed Chernobyl reactor and in the immediate environment have demonstrated that the reactor remains are a source of airborne radionuclides even many years after the accident. The mean activity concentration in the aerosol measured directly at the gaps was about 240 mBq m^{-3} with an activity median aerodynamic diameter (AMAD) of 2.4 μm for ^{137}Cs, 120 mBq m^{-3} with an AMAD in the range 3.1-13 μm for ^{90}Sr, 1.8 mBq m^{-3} with an AMAD in the range 3.5-11 μm for $^{239+240}$Pu, and 2.0 mBq m^{-3} with an AMAD of 1.5 μm for ^{241}Am. In the near environment, the mean ^{137}Cs activity concentration in the aerosol form was 2.2 mBq m^{-3} with an AMAD of 2.2 μm. Activity concentrations at the «Shelter» gaps and within the «Shelter» site were measured to be significantly higher than those in the city of Pripyat, at a distance of 4 km from the site of the «Shelter».

13.9. Aerosol contamination in the near area of the Chernobyl NPP during the building of New Safe Confinement

During the construction of the New Safe Confinement, the level of surface air pollution in the near Chernobyl NPP zone was largely determined by the influence of intensive construction work both at the facility itself and in the area around it (deinstallation of building structures, construction of the western and eastern walls of the NSC enclosing loop, moving the NSC to its normal position, etc.). According to Lagunenko et al. (2017) unorganized release of the sum of long-lived beta-emitting aerosols (including ^{137}Cs, ^{90}Sr + ^{90}Y, ^{241}Pu isotopes) from the Shelter object in the period from 2008 to 2016 decreased from about 570 MBq in 2008 to 150 MBq in 2016. But in some years there was an increase in annual emissions, in particular in 2011 due to the installation of a new ventilation stack, in 2013 — as consequences of the dismantling of the old VT-2 ventilation stack, and in 2016 — due to the dismantling of building structures during construction of the NSC enclosing perimeter. Compared with

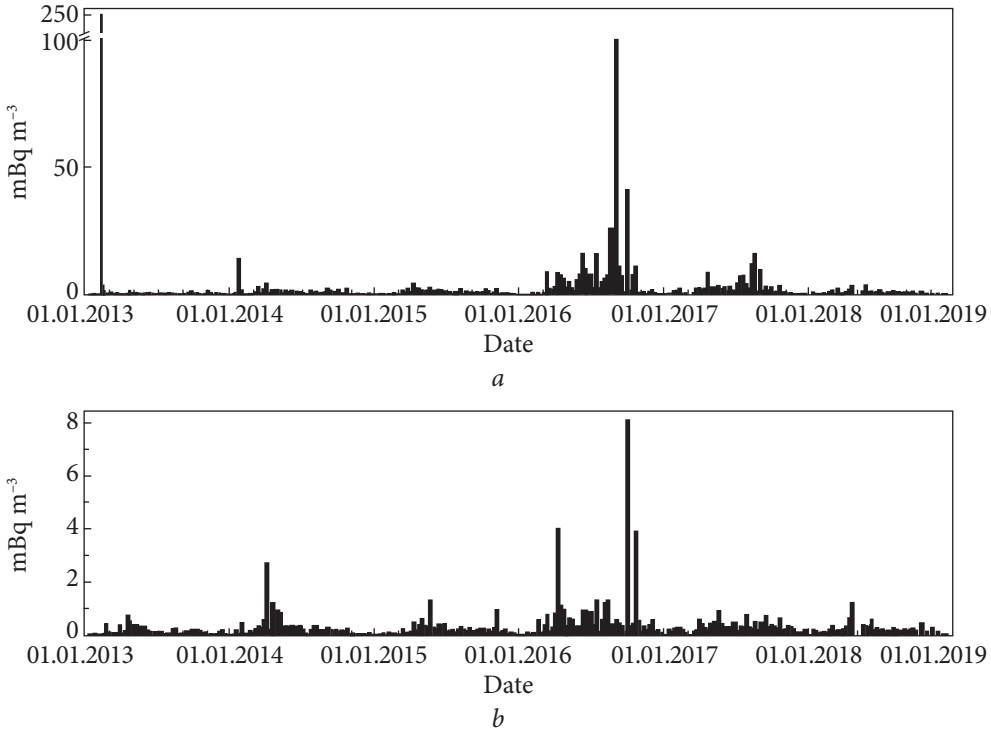

Fig. 13.7. ^{137}Cs volume activity in the atmospheric surface layer near the Shelter object in the period from 2013 to 2018: *a* — measurement with sampler 3, *b* — measurement with sampler 1 (their places are shown in Fig. 13.2)

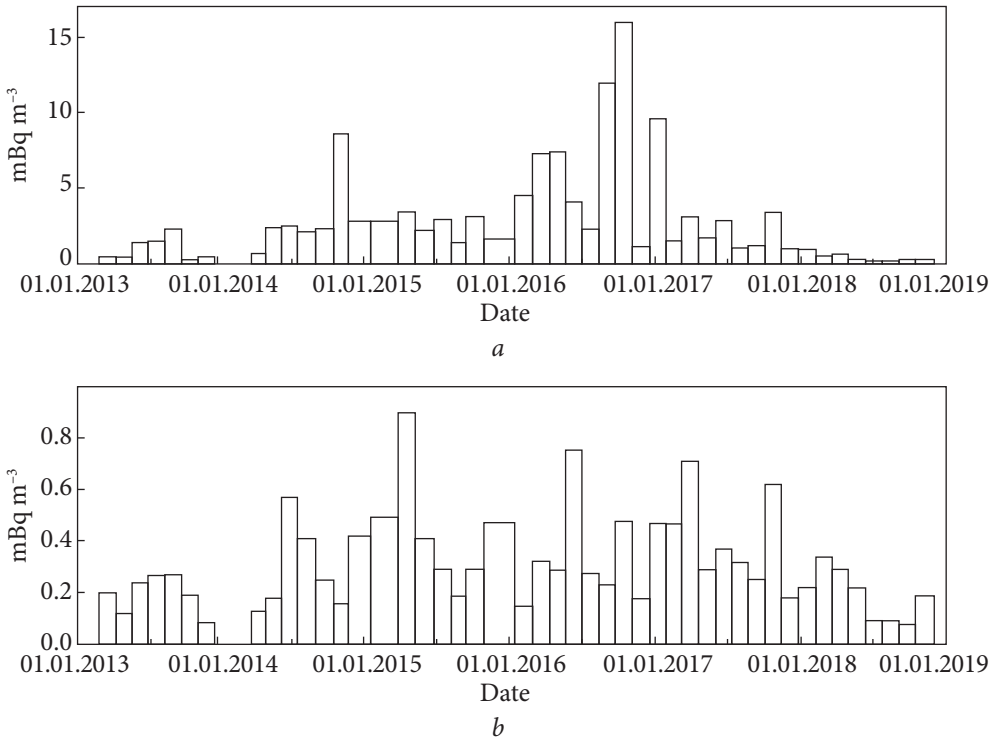

Fig. 13.8. The same as in Fig.13.7 but measurement data are shown separately for 2017 (after moving New Safe Confinement into its final position)

the measurement data carried out in the late 1990 — early 2000 (chapter 13.3) emissions from the Shelter decreased by more than one order of magnitude. At the same time, the mean AMAD of aerosol particles released from the Shelter object, determined by the activity of ^{137}Cs in the spring of 2015, ranged from 1.5 to 2.1 μm with an average value of 1.9 μm. Thus, during this period it remained almost the same as before (Tables 13.3 and 13.4). Later, in the second half of 2015 and 2016, the AMAD increased due to work carried out at the «Shelter» facility. In particular, in the fall of 2015, AMAD of aerosol particles, determined by 137Cs activity, was in the range 1.6-10.3 μm with an average value of 7.5 μm (Lagunenko et al. 2017).

Measurements of the air volume activity in the near-ground layer of the atmosphere in the near zone of the «Shelter» object using stationary aerosol samplers (Fig. 13.2) carried out during the last years showed a gradual decrease in ^{137}Cs activity up to 2013-2015 compared with previous periods (Chapter 13.5) (Shynkarenko et al. 2016). However, in 2016-2017, a substantial (almost by the order) increase of the air volume activity was registered compared with 2013-2015 due to operations on dismantle of the roof and quipment, excavation works that

reveal surface soils strongly polluted during the accident and other techo-genic activity in the ChNPP industrial site (Garger et al. 2017).

Figures 13.7 and 13.8 show data on the ^{137}Cs volume activity in the atmospheric surface layer near the Shelter object for two measurement points. Sharp increases in the volume activity during the period of construction work before moving New Safe Confinement into its final position were noted. After the movement completed at the end of November 2016, there was a significant decrease in radioactive air pollution at the Chernobyl NPP industrial site. Due to the decrease in emissions of radinuclides from the 4th Chernobyl NPP unit into the atmosphere, the main source of the formation of the concentration level of cesium-137 activity in the near-ground air even in the near zone of the power plant during this period is natural radionuclide resuspension from the contaminated territory of the exclusion zone.

CHAPTER 14

RADIONUCLIDE EMISSION DUE TO FOREST FIRES AT RADIOACTIVELY CONTAMINATED TERRITORY AROUND THE CHERNOBYL NUCLEAR POWER PLANT

14.1. General characteristic of forest fires in radioactively contaminated regions

The highly contaminated territories of Ukraine, Belarus, and Russia after the Chernobyl accident remain potential sources of radioactive contamination due to forest fires there. The radionuclides in the vegetation and soil would be emitted to the atmosphere during vegetation fires, which could lead to serious environmental damage. Radioactive emissions from contaminated wildfires could represent a risk for firefighters. Besides populations are affected by radioactive smoke particles transported over long distances.

The main source is the Chernobyl exclusion zone (ChEZ) with an area of 2,600 km^2. The forests covered 53% of the area before the disaster. After 1986 economic activity stopped and the forest area extended. Now about 38% of the territory is Scots pine forests, 30% broadleaf forests, and the other 32% is deforested and former agriculture areas. However, there was no active forest and fire management after the accident. Scots pine stands became overstocked and stressed, predisposing them to attack by insects and diseases. The lack of fire management allowed the vegetation to overgrow, creating conditions favorable for fires to ignite and spread (Hao et al. 2009). Forest inventory data shows 15,300 hectares (ha) of forests in ChEZ are damaged, including 5,300 ha damaged by pests that are now very fire prone (Hohl et al. 2012).

The accumulation of understory vegetation and downed trees over the past 20 years has increased the probability of crown fires. Large, intense crown fires often create highly buoyant smoke plumes which penetrate the free troposphere and undergo long-range transport (Hao et al. 2009).

As a result, there is an increasing frequency of fires in the region. For example, MODIS (Moderate Resolution Imaging

Spectroradiometer) satellite showed 54 fires in contaminated areas in 2010 and more than 300 in other areas (Evangeliou et al. 2014).

The radionuclides ^{137}Cs, ^{90}Sr, ^{238}Pu, and $^{239+240}$Pu are concentrated mostly in the top layer of soil in the forests and grasslands in ChEZ (Yoschenko et al. 2006a). The radioactivity of litter is higher than that in live foliage, bark, or live grasses.

14.2. The largest wildland fires in the radioactive contaminated regions after the Chernobyl accident

According to Goldammer et al. (2015), from 1993 to 2013 more than 1,250 wildland fires of different type and intensity occurred in the ChEZ. Approximately 55% of the fires occurred in former agricultural lands. An additional 33% occurred in forested land. Although these fires consumed only 3,300 ha of vegetation, larger fires have occurred in the region. The strongest fire on a total area of 17,000 ha of agricultural and forest land (including crown fire over an area of 5,000 ha) occurred in August 1992 over two weeks, and hundreds of firefighters were involved to extinguish it. Separate combustion sources were developed in different parts of ChEZ, including the most polluted central part. Additionally, 1,200 ha of forest were burnt in the Belarusian part of the Chernobyl exclusion zone (Dusha-Gudym 2005).

In the period from 1992 until 1994, about 200 forest fires were counted in this area. According to Sukhoruchkin and Marchenko (1996), this destroyed 2.4-3.9 thousand ha of forests and 1.9-2.6 thousand ha of meadow ecosystems.

After 1992 on the most territories contaminated by radionuclides the ratio of forest and non-forest lands burnt by fires changed appreciably. In 1993-2001 a total of 770 wildfires in the ChEZ of Ukraine affected 2,482 ha (4.4% forest, > 95% abandoned lands and agricultural estates). In the period 1993-2000 186 wildfires occurred in the closed zone of Belarus and affected an area of 3,136 ha, including 1,458 ha of forest (46.5%) (Dusha-Gudym 2005).

Besides forest fires within the Chernobyl exclusion zone, some large contaminated regions in Ukraine, Belarus, and Russia during some hot and dry years were substantial sources of secondary air contamination both in these territories and within the ChEZ itself.

In 1992 outside the exclusion zone fires covered 870 ha of forest lands in Gomel and Mogilev regions (Belarus). In the Bryansk region (Russia) the area of radioactive fires was less than 200 ha. As a result of the fires, ^{137}Cs radionuclides were lifted and transported by the smoke to the territory of Russia in May and August 1992 (Dusha-Gudym 2005).

In 2002 several regions of the Russian Federation were characterized by a hard situation. In the last years, 1,015 fires were recorded in the Bryansk region. The forest land area burnt by fires made up 1986 ha (Dusha-Gudym 2005).

In 2001-2002 forest fires of different scales influenced a radiation situation in the Chernobyl exclusion zone (Garger et al. 2004). In Fig. 14.1 one may see the development of forest fires in two large territories of the mesoscale in the north of Volyn and Rivne regions of Ukraine (photos 1 and 2), and a large smoked territory in Zhytomyr, Kyiv and Chernihiv regions of Ukraine (photo 3).

The long-range transport of smoke plumes produced by fires in the ChEZ was observed by the U.S. National Oceanic and Atmospheric Administration's (NOAA) Advanced Very High-Resolution Radiometer (AVHRR) satellite on May 8, 2003 (Fig. 14.2). The satellite image showed that the smoke plumes of a spring fire in the ChEZ reached Kyiv.

Fig. 14.3 shows the spatial distribution of fires and smoke in Ukraine and neighboring countries on April 16, 2006. Smoke plumes originating from active fires south of Kyiv traveled north about 100 km.

The long-range transport of Chernobyl's smoke plumes not only was observed by the satellites but also may be detected by the ground radioisotope monitoring stations in Sweden. During the 1972-1985 period, the monthly ^{137}Cs levels peaked in May, which were caused by the nuclear test fallout in the stratosphere (Kulan 2006). However, during the 1987-2000 period, the ^{137}Cs levels peaked in April and October, which coincided with the periods of most intense burning in the ChEZ. The resuspension of mineral dust in Chernobyl may also have contributed to the elevated ^{137}Cs levels (Kulan 2006).

Lujaniene et al. (2006) presented results of the air activity measurements in Vilnius, Lithuania made after the Chernobyl accident. A considerable ^{137}Cs activity concentration in the atmosphere was registered on 31 August - 1 September 1992 (up to 300 μBq m^{-3}) and on 6-7 September (190 μBq m^{-3}) during extensive forest fires in the 30-km exclusion zone. In 1996 the maximum activity concentration of ^{137}Cs was observed in April. The mean monthly activity concentration was 25.9 μBq m^{-3}, but in two days samples, it increased up to 253 μBq m^{-3} (09 April 1996). Another event of transport of products of forest fires was registered 6-9 September 2002 after an extensive fire in the forests and peat-bogs of Belarus (up to 200 μBq m^{-3}). The measurements carried out on aerosol samples collected in Vilnius in 1995-2003 indicated the presence of alpha emitting radionuclides. The activity concentrations of $^{239+240}$Pu and ^{241}Am ranged from 1 to 500 and from 0.3 to 500 nBq m^{-3}, respectively.

Several events in 2002 redistributed and transported ^{137}Cs over Europe (Evangeliou et al. 2015). These fires were so serious that peat bogs also burned, followed by forests, causing massive smoke emissions that persisted for nearly 2 months, sometimes reducing visibility to below 60 m. These fires resulted in significant exposures of smoke to major population centers such as Kyiv and Moscow. The highest release occurred at the end of July, with ^{137}Cs fallout reaching Sweden, Finland, and Central Europe.

The picture No. 1 of 20.08.2002, 18:36. It shows several forest fires in Rivne region, Ukraine. Wind direction: from August 19 till August 21 the direction changed from north to south through east direction.

The picture No. 2 of 01.09.2002, 16:49. The smoke loops from forest fires in Rivne and Zhytomyr regions near Slavutych (Ukraine) are clearly visible. Direction of a wind: South-West.

The picture No. 3 of 06.09.2002, 08:43. On the territory of Zhytomyr, Kyiv and Chernihiv regions (Ukraine) and Belarus a strong smoke-screen is observed. Direction of a wind: West-Southwest.

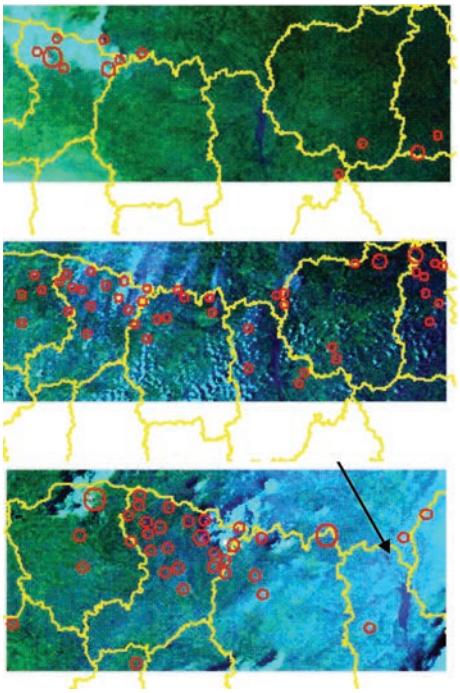

Fig. 14.1. Development of forest fires in Ukrainian and Belarusian Polesye

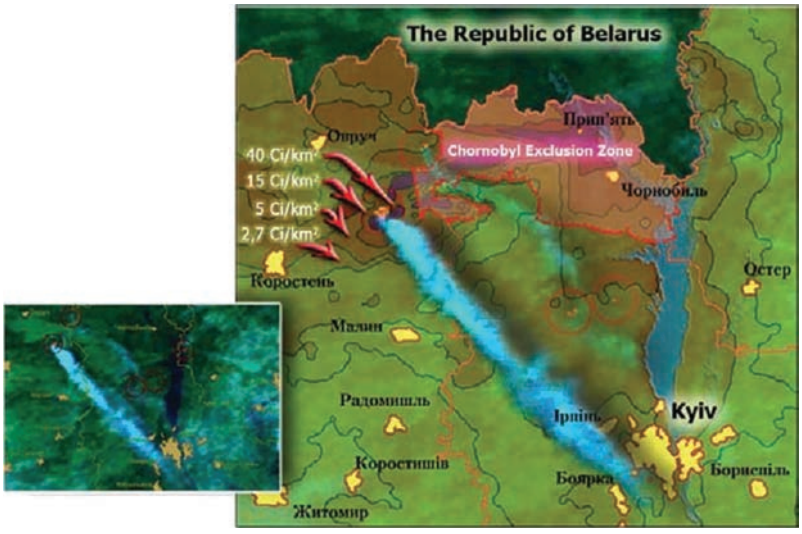

Fig. 14.2. Wildland fires in western Ukraine near the Chernobyl exclusion zone at territories with different ^{137}Cs contamination density (1 Ci km^{-2} = 37 kBq m^{-2}) and smoke plume toward Kyiv, May 8, 2003 (from Goldammer et al. 2015)

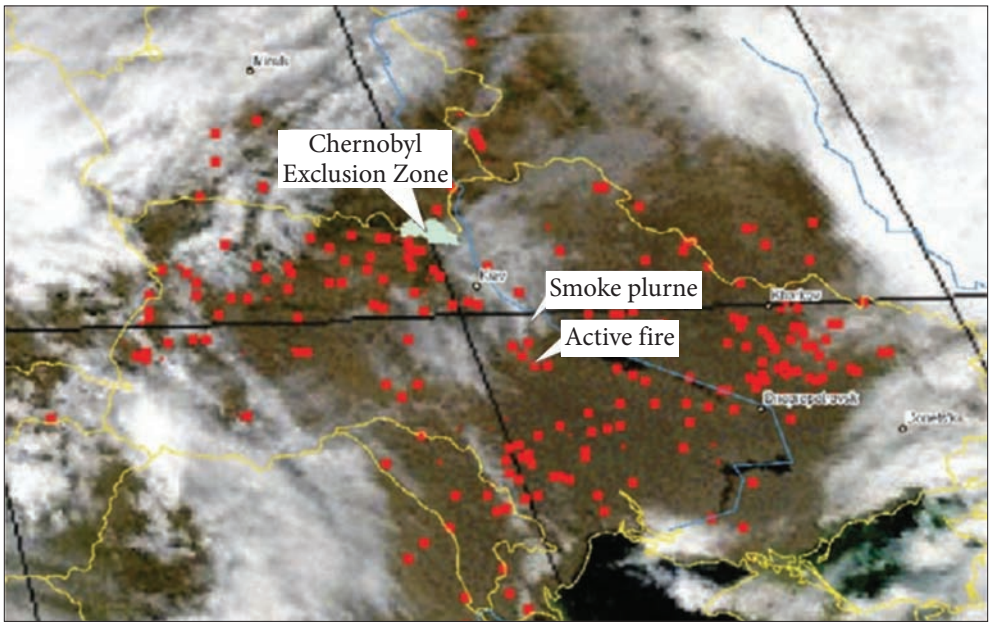

Fig. 14.3. The MODIS satellite image of fire locations (red dots) and smoke in Ukraine and its neighboring countries, April 16, 2006 (from Goldammer et al. 2015)

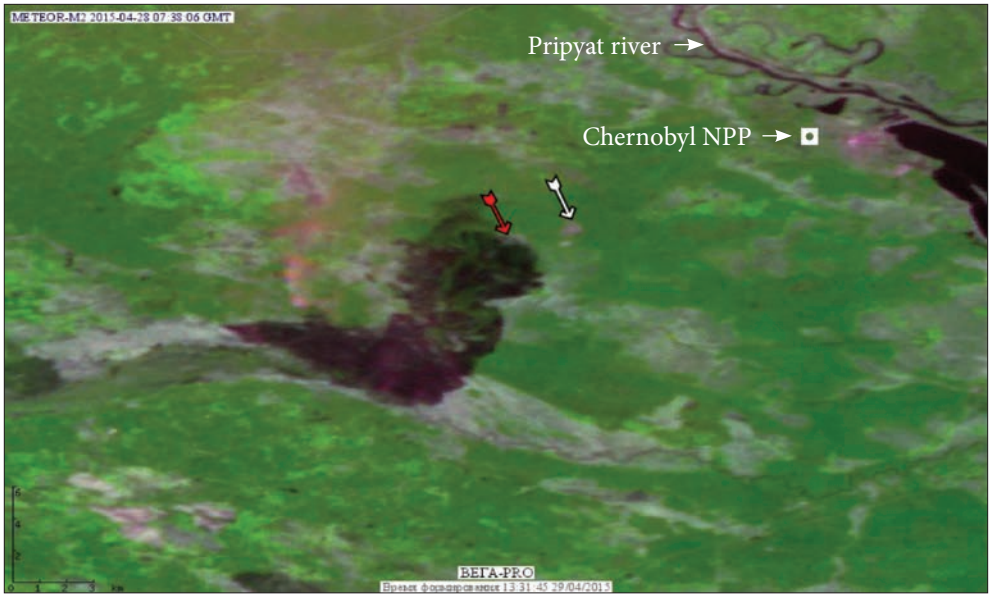

Fig. 14.4. Fire area on 28 April 2015 (07:37 GMT). The fire has spread close to the Radioactive Waste Disposal Point (red arrow). A distance to another RWDP (white arrow) is about 1 km. The data of Meteor M 2 satellite (http:/vega.smislab.ru))

Fires in 2008 were of lower intensity and frequency. However, some took place inside highly contaminated regions, injecting a significant plume into the atmosphere. In March 2008, ^{137}Cs covered Belarus and a large part of Russia, and another event in August distributed ^{137}Cs more locally (Evangeliou et al. 2015).

Paatero et al. (2009) reported about two biomass burning events in 2006 in western Russia. The deposition of ^{137}Cs in these areas has been estimated to be mostly 2-10 kBq m^{-2} with limited areas of higher values, 10-40 kBq m^{-2}. During the spring smoke episode, the ^{137}Cs activity concentration in the air in Helsinki increased by a factor of 10 (up to 13 μBq m^{-3}) compared to values just before the episode due to a long-range radionuclides atmospheric transport. Simultaneously there was an increase of the same order of magnitude in the concentrations of PM10. The increase in the PM10 concentration is related to soot emissions from the fires, in other words, the incomplete combustion of organic material. The summer episode was less severe even though these times there were wildfires close to the Finnish-Russian border. During the summer smoke episode, the ^{137}Cs activity concentration in the air increased by a factor of 5 compared to values just before the episode. Based on the measurement data obtained they concluded that from the radiological point of view the exposure to the increased radionuclide activity concentration was insignificant compared to health hazards due to the increased concentration of aerosol particles and their chemical components.

Wildfires in 2010 affected several countries of Southern Europe, including the Balkan countries, Turkey, and southern Italy. The same raging forest fires affected; 3,900 ha locally in the fallout zone from the 1986 disaster (Evangeliou et al. 2015).

On 26 April 2015 at 23.30 (local time) a massive fire started in the Chernobyl exclusion zone (Evangeliou et al. 2016, Kashparov et al. 2015). The next morning (April 27) at 07.30 the fire was partially stabilized and the fire-fighters focused on only two areas of 4.2 and 4.0 ha. However, the fire spread to neighboring areas due to the prevailing strong winds. During the night of April 27 to 28, 2015, the fire spread to areas close to the Radioactive Waste Disposal Point (RWDP) and burned around 10% of the grassland area at the western of the RWDP (Fig. 14.4). On April 29 and 30, 2015, the attempts to stop the fires in the ChEZ did not succeed. Fire brigades from Chernobyl and Kyiv region supported extinguishing attempts and the last 70 ha were suppressed on May 2, 2015.

It was found that the grass fire covered 6,250 ha of meadows, the forest ground and crown fires — 2,737 and 1,140 ha, respectively. The maximum density of contamination in the areas of the ground forest fire in Lubyanka Forestry reached by ^{137}Cs — 1,040, ^{90}Sr — 368, $^{238+240}$Pu — 11.4 and ^{241}Am — 14.4 kBq m^{-2} (Kashparov et al. 2015).

Another less intensive fire episode took place in August 2015. About 32 ha were initially burned in the ChEZ on August 8. The fires started at three locations in the Ivankov district. As of 07.00 on August 9, the fires had been reportedly localized

and fire-fighters continued to extinguish the burning of dry grass and forest. The same fire affected another forested area, known as Chernobylskaya Pushcha. The fire spread through several abandoned villages located in the unconditional (mandatory) resettlement zones of the ChEZ and ended on August 11 (Evangeliou et al. 2016).

14.3. Measurements of air contamination caused by forest fires within the Chernobyl exclusion zone

Hollander and Garger (1996) reported about measurements of the air activity concentration of ^{137}Cs in 28-31 July, 1992, when a large forest fire happened in the Chernobyl exclusion zone. The fire enveloped 1,300 ha of forest and besides 2,300 ha of a grass cover. The estimations show that at the fire of such scale the emission of combustion products in the atmosphere may reach a height of 2-3 km. Also, combustion products are involved within such plume in long-range transport on distances about hundreds of kilometers. The measuring of the atmospheric ^{137}Cs activity concentration was carried out in Zapolie, the area with grass cover in 17 km to the northeast of the fire. In months before the fire, the atmospheric activity concentration of ^{137}Cs was 0.2-0.5 mBq m^{-3}. The fire has increased the radioactivity concentration by 10 times and it has reached 2.1 mBq m^{-3}.

Garger et al. (2004) presented the measurement results of the radioactive contamination of air at the industrial site of the Chernobyl nuclear power plant for two periods: 1) in August 2001, and 2) in August - September 2002. They reported that in the period of forest fires of different scales in 2001-2002 the activity concentration of ^{137}Cs increased by 200-700 times in the Chernobyl NPP area (see Fig. 9.15, in which the activity concentration measured in Pripyat is shown). In the surface layer of the atmosphere, the particles of smoke with AMAD less than 1 μm predominated.

On August 16, 2001 there was a fire of forest area located at a distance of 2 km from the Chernobyl NPP in a westerly direction on the territory of a sufficiently high level of radioactive contamination of the soil (10^6-10^7 Bq kg^{-1}). The fire has covered an area of no more than 10 ha.

The values of the activity concentration of aerosols in the atmospheric boundary layer during the active phase of a fire (burning of litter, shrubs, dead trees, abandoned buildings) amounted to 69 mBq m^{-3} in 16 August at a distance of 500 m from the source, and 293 mBq m^{-3} in 17 August at a distance of 50 m from the source. On the stage of smoldering in 21 August, 2001 the aerosols activity concentration was obtained to be about 25 mBq m^{-3} at a distance of 5 m from the source. Even during the smoldering phase, the activity concentration in the air at the Chernobyl NPP industrial site has increased by two orders of magnitude compared with the background values equal to 0.1-0.2 mBq m^{-3}.

In all phases of fire on 16-23 August 2001, the maximum number of particles with aerodynamic diameters in the range of 0.5-1.0 μm was observed. The activ-

ity size distribution of ^{137}Cs particles during the active phase of the fire on 16 and 17 August, 2001 differ slightly in shape from each other. The median diameters and the standard deviations for a lognormal distribution were found to be $d_m = 1.4$ μm, $\sigma_g = 1.4$ and $d_m = 1.5$ μm, $\sigma_g = 1.1$, respectively. In contrast, in a phase of smoldering the median diameter of radioactive particles was found to be 0.37 μm and the standard deviation of 2.49. In other words, most of them belonged to the submicron size particles and the distribution width was considerably wider than in the days of active forest burning. Similar characteristics were observed in 1992 in Zapolie at a distance of 19 km from the fire near Burakovka village in the 30-km zone (Garger et al. 1998), where the median diameter of aerosol particles in the period of the fire 23.07-30.07.1992 was found equal to 0.28 μm.

In the period from 29 August to 03 September, 2001, as a result of severe forest fires outside of the Chernobyl exclusion zone (in Belarus and the north-eastern part of Zhytomyr region of Ukraine) in the vicinity of Chernobyl NPP there was heavy smokiness. According to the measurement data, the maximum value of the activity concentration of aerosols in the atmospheric surface layer of 187 MBq m^{-3} was observed on 02-03 September 2002. During this period, the number of fine smoke aerosol particles increased 12-20 times that can be attributed to the transfer of smoke particles from Belarus. The distributions of counting aerosol concentration on the particle size during the fire in 2001 and the heavy smokiness in 2002 have differences caused partly by different distances (from 50 meters to tens of kilometers) between the aerosol sampling points and the fire places. So, in 2001 a share of particulate matter with an aerodynamic diameter in the range of $0.5 < d \leq 1.0$ μm was 77.9%, and in 2002 — 92.7%, i.e. in 2002 aerosol particles with large diameters deposited from the atmosphere on the ground before reaching the territory of the ChNPP industrial site.

According to the measurement results, the activity concentration of aerosols in the atmospheric boundary layer during the wildfires was determined mainly by ^{137}Cs (in August 2001 — 98.2% of the total activity, in September 2002 — 97.2%).

Preliminary dose estimation of internal exposure showed that a dose of internal exposure of personnel during the smokiness was about 0.0092 mSv.

Kashparov et al. (2015) presented results of measurements in the period of a forest fire in April 2015. Within a smoke zone the atmospheric activity concentration was 0.77 mBq m^{-3} of ^{137}Cs and 0.35 mBq m^{-3} of ^{90}Sr on 27 April in Stechanka village, 7.6 mBq m^{-3} of ^{137}Cs and 10 mBq m^{-3} of ^{90}Sr on 28 April in Staraya Krasnica village, and 1.4 mBq m^{-3} of ^{137}Cs and 0.71 mBq m^{-3} of ^{90}Sr on 29 April in Lubyanka village. When extinguishing meadow and forest fires the total committed effective dose of firefighters from Chernobyl radionuclides does not exceed 42 μSv. During forest fires, more than half of the expected effective dose of internal radiation may be caused by inhalation of ^{90}Sr. During grassland fires, the inhalation intake of ^{90}Sr, $^{238\text{-}241}$Pu, and ^{241}Am can give approximately equal

contributions in the expected effective dose of internal radiation of firefighters. The contribution of beta-emitting ^{241}Pu in the formation of the expected effective dose of internal exposure of personnel is commensurate with the contribution of each of the alpha-emitting radionuclides of plutonium ($^{238, 239,240}$Pu).

14.4. Wildland fire experiments in radioactively contaminated territories

Kashparov et al. (2000) reported results of measurements of radioactive aerosol characteristics (emission parameters, distribution within the experimental site, dispersal composition, deposition parameters) during the controlled burning of forest and meadow ecosystems on two experimental sites: 1) the site of 100×200 m size vegetated with pine forest and contaminated mainly by ^{137}Cs at 1.1±0.2 MBq m^{-2}, 2) the site of 50×140 m with dry grass from previous year, ^{137}Cs inventory of grass per unit area was 550±30 Bq m^{-2}. At these sites, the ^{137}Cs background airborne activity concentration was 0.5-1.5 and 3 mBq m^{-3} respectively.

In the active phase of a fire, the airborne activity concentrations of radionuclides increase by several orders of magnitude relative to the background value. The airborne activity concentration of ^{137}Cs in the lower layer of the atmosphere varied within the range 10-100 mBq m^{-3}. After the active phase, in the period of smoldering, the activity concentration was 5-20 mBq m^{-3} and, in the post-fire period, one day later, 2-5 mBq m^{-3}. Thus, the emission factor (an analog of the resuspension factor for wind resuspension process) for the fire active phase and the period of smoldering can be estimated to be in the range 10^{-7}-10^{-8} m^{-1}, while the value of the emission rate had a 10^{-10} s^{-1} order of magnitude at a deposition velocity of 1-2 cm s^{-1}.

During active and smoldering phases of the experiment, the airborne concentration of aerosol particles larger than 10 μm doubled at 100 m from the source, and the airborne concentration of particles smaller than 10 μm increased by 20-700 times compared to natural background levels. In the post-accident period, the airborne concentration of fine particles (smaller than 10 μm) exceeded background values by 3-30 times. The number of large particles decreases with time from the beginning of the fire and with increasing distance from the source. At a distance 15 m from the source the share of large aerosol particles with size > 8.5 μm in the ^{137}Cs total activity concentration in the lower air layer was obtained as 46% and the share of small particles with size <2.8 μm was 37%. At a distance of 150 m, the shares were obtained to be 20% and 69% accordingly.

The additional terrestrial contamination due to a forest fire can be estimated as a value in the range 10^{-4}-10^{-5} of its background value, so even for the most unfavorable conditions, radionuclide emission during forest fires will not provide a significant contribution to terrestrial contamination.

During the grassland fire, the mean value of airborne ^{137}Cs aerosol activity concentration in the lower air layer was 19.2 Bq m^{-3} at an average emission factor of 1.6×10^{-7} m^{-1}.

According to the obtained data at ^{137}Cs contaminated experimental sites, the doses to firemen as a result of staying 1 h near a fire area were assessed about 1.5 μSv. The firemen inhalation doses were estimated to be less than 1% of the total doses and can be ignored (for cases without contamination with transuranium α-emitting radionuclides). Lately (Kashparov et. al 2015) clarified this conclusion when estimating radiation doses to firefighters during the fire on April 26-27, 2015 in the ChEZ. They showed that it is valid for fires on the purely condensation traces of the radioactive fallout of cesium-137 (outside the exclusion zone). For the territory of the exclusion zone, on the fuel traces of depositions, the contribution of internal exposure into the total excected effective dose of firefighters is larger. However, even at maximum levels of the territory contamination with ^{90}Sr, $^{238\text{-}241}$Pu, and ^{241}Am, the effective dose from external exposure for firefighters will exceed the expected doses from internal exposure. According to estimates for the fire in 2015, the total expected effective dose of firefighters during one fireline hour did not exceed 0.64 μSv in case of external exposure and 0.37 μSv in case of internal exposure in the most contaminated forest areas.

Studies on wildland fire emission (Kashparov et al. 2000) had been performed outside the Chernobyl exclusion zone giving only data on the nuclide ^{137}Cs. In Yoschenko et al. (2006a) the focus of the investigation was on the potential impact of the radionuclides ^{90}Sr, ^{238}Pu and $^{239+240}$Pu, besides ^{137}Cs. Controlled burning of experimental plots of forest or grassland in the Chernobyl exclusion zone has been carried out to estimate the parameters of radionuclide emission, transport and deposition during forest and grassland fires and to evaluate the working conditions of firemen.

The active experiments were performed on two grassland sites (3,600 m^2 and 5,400 m^2 area) and one forest site (8,770 m^2 area). Both grassland fires were carried out within the same experimental area near the former village Chistogalovka, at a distance of approximately 3 km west of the Chernobyl reactor site. The forest site is located 5 km of the Chernobyl reactor close to the former village Novoshepelichi. It is a cultivated pine forest surrounded by grassland. At three chosen sites the background values of the airborne activity concentration were 2.1-4.6 mBq m^{-3} for ^{137}Cs, 0.8-4.4 mBq m^{-3} for ^{90}Sr, 1.5-8.3 μBq m^{-3} for ^{238}Pu, and 2.9-22 μBq m^{-3} for $^{239+240}$Pu.

During the grassland fires, the airborne activity concentrations of ^{137}Cs and ^{90}Sr reached values of several Bq m^{-3} near the source of release and decreased with the distance. The activity concentration of plutonium was generally 3 orders of magnitude lower and an increase with the distance was observed in site #1. In site #2,

rather constant values were measured at greater distances after an initial decrease.

During the forest fire experiment, an increase of several orders of magnitude of the airborne radionuclide activity concentration was observed in the territory near the fire area. But, in general, one order of magnitude lower activity concentrations for ^{137}Cs and ^{90}Sr were measured in comparison to the grassland fires. After an initial decrease in concentration over long distances a rather constant airborne concentration was observed for all nuclides. At the furthest sampling site, the concentration increased again.

During the grassland fires, the emission factor K of ^{137}Cs and ^{90}Sr was determined to range from 10^{-6} to 10^{-5} m^{-1}, and K of the plutonium nuclides to range from 10^{-7} to 10^{-6} m^{-1}, if K is related to the burning biomass. If the contamination density includes the soil contamination as well, the calculated emission factors will be of 2 orders of magnitude lower.

During the forest fire, the emission factor of all radionuclides was in the range 10^{-7}-10^{-6} m^{-1} if they were related to the biomass contamination, and 10^{-8}-10^{-7} m^{-1} if they were related to the total contamination. In general, they were lower than those during the grassland fires, probably because of the absence of understorey in the forest.

Thus, only a relatively small fraction of the total areal contamination is available for re-entry into the atmosphere caused by the fires.

The additional contamination is low, even in the near vicinity of the burning plots; e.g., for plot #1, the additional contamination density of the grass after the fire would be about 1% ^{90}Sr, 1% ^{137}Cs, 7% ^{238}Pu and 7% $^{239+240}$Pu of the contamination density before the fire if all newly deposited material is fixed on the grass. **Thus, the wildland fires in the Chernobyl exclusion zone do not lead to a significant redistribution of contamination on the scale of the whole zone.** However, if vegetation was grown next to a site with burning biomass on uncontaminated soil the new vegetation could be contaminated with about 1 kBq kg^{-1} ^{90}Sr, 500 Bq kg^{-1} ^{137}Cs, 0.1 Bq kg^{-1} ^{238}Pu and 0.2 Bq kg^{-1} $^{239+240}$Pu in close vicinity of fire territory. So, for decontaminated areas inside the zone, the secondary contamination by fire events might be a problem for areas at a distance up to several hundreds meters from the burned territory.

According to data obtained in Yoschenko et al. (2006a), the dose of the external irradiation from soil and vegetation, a significant contribution to the total dose can be provided by the inhalation intake of the plutonium radioisotopes and their progenies. In some conditions, this contribution can reach half of the total dose. At the same time, taking into account the sharp decrease of the airborne radionuclide activity concentration with the distance from the source of release, they stated that the inhalation component of the total dose (as well as the external irradiation from radionuclides in air) is not important for the personnel of the exclusion zone which is not involved in the fire fighting.

Formation and transformation of aerosol particles carrying the radionuclides were studied during the forest fire experiment in a highly contaminated Briansk region, Russia in August 1993 (pine forest burning on 0.2 ha area) (Lujaniene et al., 1997). According to obtained data forest fires were responsible for the generation of a great amount of submicron (0.2 μm) aerosol carriers of ^{137}Cs. In aerosol samples collected during this active fire experiment, about 80% of submicron aerosol particles of ^{137}Cs of 0.1-0.4 μm contributed to the total aerosol (Lujaniene, Aninkevicius and Lujanas 2009). The formation mechanism of submicron ^{137}Cs particles can be attributed to the evaporation, condensation on nuclei available in the atmosphere and their further coagulation. These results agree well with experiments carried out in different laboratories. It was shown that about 95% of fine particles formed during the combustion of contaminated biomass had a size of 0.1-0.4 μm (Grebenkov et al. 2002). Natural burning experiments with the burning of fir needles indicated the formation of aerosol particles of ^{137}Cs in the range of 0.62-0.72 μm below 600-700 °C (Ogorodnikov 2002). Simultaneously, the fraction of large particles with AMAD of 10-14 μm was formed due to the underburning of needles.

14.5. Modeling of secondary air contamination caused by forest fires

As can be seen from the previous section, wildland fires may result in additional contamination of the air both near the fire territory and over long distances, including long-range atmospheric transport of fine aerosol. Therefore, different types of models of emission, following atmospheric transport and deposition of fire products are developed for the local area around the fire (up to 10 km) and mesoscale and long-range atmospheric transport. The main features of the radionuclide atmospheric transport models for different spatial and temporal scales are determined primarily by the nature of the diffusion processes of pollutants in the atmosphere, and they are similar for both models of emissions from point sources (e.g., from an NPP stack) and for the re-suspension models during forest fires. The main problem for models of forest fires is the correct description of the radioactive aerosol source parameters (duration and area of the fire, emission intensity for the different phases of the fire, the initial raising height of smoke plume, the activity size distribution of radioactive particles). Therefore, in general, the model of atmospheric transport of smoke particles must be a part of a more general model of wildland fire evolution (Grishin 1992; Mandel, Beezley and Kochanski 2011). Using several simplifying assumptions, a subtask of assessment of radioactive contamination of the atmosphere by combustion products can be singled out of the general picture describing the development of the fire and its consequences. Then this problem can be solved by relatively simple methods. The price for such simplification is the introduction into used models several constants whose values have to be determined empirically.

14.5.1. Radionuclide emission fraction during forest fires

One of the main problems of radionuclide atmospheric transport models due to forest fires is the parameterization of the emission fraction of radionuclide after a fire event, namely the fraction that will be emitted compared to what is present on the ground or in the biomass. Evidence from laboratory experiments and field studies are quite contradictory.

Amiro et al. (1996) conducted field and laboratory burns to determine the fate of I, Cs and Cl in biomass tires. Straw and wood were combusted with temperatures varying from 160 to l,000° C, representing the normal range of field fire temperatures. The loss to the atmosphere increased with fire temperature and during a typical field fire, 80-90% of the I and Cl, and 40-70% of the Cs was lost to the atmosphere. The remainder was left behind in the ash and was soluble.

Horrill et al. (1995) performed experiments for heather burning and found that 10-40% of ^{137}Cs would be emitted after heather fires depending again on the temperature (12% after a cool burning and 39% after a hot burning).

Beyond biomass, ^{137}Cs is accumulated in the top-soil layer. Evangeliou et al. (2014) noted that it presents a low boiling point (669 °C) and it is lost in the smoke even when located in the soil through volatilization. Paliouris et al. (1995) showed that the redistribution from the soil is more than 20% in North American boreal forests.

Wotawa et al. (2006) demonstrated that ^{137}Cs deposited world-wide from past nuclear testing is reinjected into the atmosphere due to forest fires to a significant extent and on a large scale, and is subsequently transported across great distances. The whole boreal burning activity emits and redistributes about 1% of all ^{137}Cs available within the burnt region or about 10% of the ^{137}Cs fraction presumably available in the biomass (assuming that the biomass stores 10% of the total ^{137}Cs).

Evangeliou et al. (2014) used a relatively conservative emission fraction of ^{137}Cs (40% of what is deposited will be re-emitted) in their modeling of possible consequences of radioactive materials redistribution over Europe for different forest fires scenarios. In another work, they team used values 20% of the deposited amount of the labile radionuclides (^{137}Cs, ^{90}Sr) and 10% of the refractory ones (^{238}Pu, ^{239}Pu, ^{240}Pu, and ^{241}Am) (Evangeliou et al. 2016).

The first estimation of the emission fraction on the base of environmental measurements data in the Chernobyl exclusion zone was made by M. Talerko after a forest fire near village Burakovka in July 1992 (Hollander and Garger, 1996, 6-6, 8-3). Using data of the ^{137}Cs atmospheric activity concentration measurements near the fire territory and results of soil activity measurements after the fire it was obtained from solving an inverse problem of radionuclide atmospheric transport that about 3-5% of total ^{137}Cs amount in soil and vegetation raised in the air under forest fires.

A similar value was obtained by Yoschenko et al. (2006a) who reported that this fraction was obtained to be 4% after measuring budgets in the fire experiments in the Chernobyl exclusion zone.

14.5.2. Near-range radionuclide atmospheric transport modeling during forest fire experiments

A model of aerosol emission, following atmospheric transport and deposition during a forest fire developed by M. Talerko, has been applied in (Kashparov, 2000) to clarify the measurement results obtained in the course of the controlled fire experiments (see Chapter 14.4). The model is based on the approach proposed in (Talerko 1990). The model describes two possible scenarios of wildfires: formation of the convective plume over a fire area and non-convective diffusion regime of aerosol particles dispersion in the atmosphere. It was concluded that the process of admixture transport in the atmosphere, in this specific case, could be described by a superposition of the above-mentioned processes. The main contribution to the field of aerosol activity concentrations at a distance of 10 m is provided by non-convective transport. In intermediate zones (10-110 m) the non-convective transport still gives a comparable contribution, while at larger distances the contribution of convective transport is much higher (Fig. 14.5).

Estimates of the additional terrestrial contamination by activity redistribution caused by fire have demonstrated that it is very small at all distances from the source. Maximum deposition, according to the above calculations, should be observed at 1,500-2,000 m distance — it is approximately 110 Bq m^{-2}. The additional terrestrial contamination due to a forest fire can be estimated to be in the

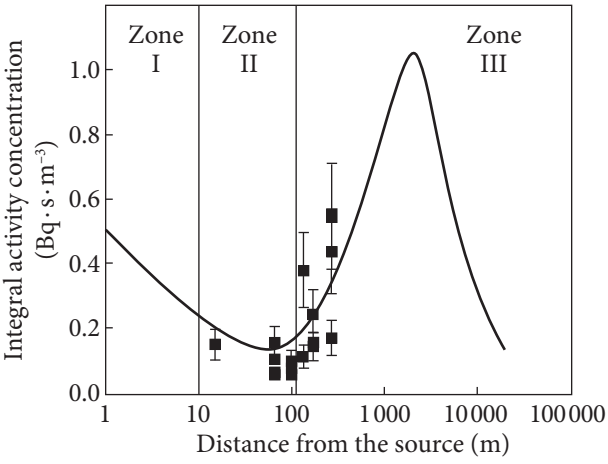

Fig. 14.5. Integral airborne ^{137}Cs activity concentration ($kBq \cdot s \cdot m^{-3}$) on the downwind axis (active burning phase) (Kashparov 2000). The solid line represents the relationship obtained in the calculations by the superposition of the convective and non-convective modes of admixture transport in the atmosphere. Three zones of deposition are indicated: I — non-convection flux deposition zone, 0-10 m; II — intermediate zone, 10-110 m; III — convection flux deposition zone, >110 m. The solid line is calculation result; observed values combined with their uncertainty range

range 10^{-4}-10^{-5} of its background value. At 20 km from the fire source, the deposition is several tenths Bq m^{-2} and can be neglected even on territory contaminated only with global fallout.

Yoschenko et al. (2006b) used experimental results obtained in Yoschenko et al. (2006a) for verification of the model presented in Kashparov (2000). They complete the model with equations for calculation of an initial air temperature in a plume above a fire area and an initial plume radius.

Compared experimental data and model calculation of the airborne activity concentration and the deposition density they concluded that the developed model satisfactorily describes the studied process.

The model predicts that during the grassland fires the radionuclide fraction from the fuel material (litter and grass) emitted into the atmosphere can be estimated as follows: ^{137}Cs and ^{90}Sr — up to some ‰; Pu — up to 1‰. During the forest fires, up to 3-4% of ^{137}Cs and ^{90}Sr and up to 1% of the Pu isotopes can be released from the forest litter.

14.5.3. Modeling of consequences of mesoscale and long-range atmospheric transport of radionuclides during forest fires

Several works were made on modeling the consequences of forest fires in the Chernobyl exclusion zone during the last years. They may be classified in two main areas: 1) assessment of the consequences of real forest fires (secondary atmospheric pollution, redistribution of deposition density, radiation doses of firefighters and the ChEZ personnel and population outside the ChEZ); 2) modeling using different possible wildland fire scenarios for developing optimal strategy of fire-fighting and minimizing their impact on environment and people health.

Evangeliou et al. (2016) carried out modeling of the radioactive contamination after fires that started in the ChEZ on April 26th (ended 7 days after) and August 8th (ended 4 days after) 2015. The estimated total area affected by fires in spring 2015 was 10,882 ha and in August 2015 was 5,867 ha. Simulation of the atmospheric transport and deposition of the radioactive plume released by the forest fires using an atmospheric dispersion model showed that the release from the continuous burning of the ChEZ was transported to Western Russia, then to the north and reached southern Finland and Sweden and subsequently Latvia and Lithuania. In parallel, radionuclides were also transported to the east, and smaller amounts to the south, i.e., towards the Black Sea. The aforementioned circulation only describes the more labile radionuclides ^{137}Cs and ^{90}Sr. The refractory transuranium elements were deposited closer to the source due to the larger particle size.

According to the results of the modeling of radionuclides transport released from the fires in August 2015, the plume was immediately transported to the east

during the first four days. Thereafter, the fallout burden was divided into three parts — one part to Russia and Belarus, another part of the plume was transported across Poland, Northern Germany, and Denmark and ended in a big anticyclone that covered whole Scandinavia. Finally, a third part of the smaller intensity moved southwards affecting the Balkan region, the Aegean Sea and Turkey. The simulated activity concentrations were of a similar magnitude as for the spring fires for ^{137}Cs and ^{90}Sr, but ^{238}Pu, ^{239}Pu, ^{240}Pu, and ^{241}Am concentrations were substantially lower.

Evangeliou et al. (2015) simulated fires in Ukraine and Belarus for the years 2002, 2008, and 2010. MODIS satellite imagery recorded 185 fires in 2002, 50 in 2008, and 54 in 2010 that burned 473, 125, and 137 ha, respectively. The coupled model LMDZORINCA was used in the simulations consisting of the aerosol module INCA (INteractions between Chemistry and Aerosols), the general circulation model LMDz (Laboratoire de Meteorologie Dynamique), and the global vegetation model ORCHIDEE. The model accounts for emission, transport, photochemical transformations, and dry and wet scavenging of chemical species and aerosols. The fire incidents were simulated using the zoom version for Europe, achieving a horizontal resolution of $0.51° \times 0.45°$ for 19 vertical levels.

According to modeling results, the highest exposure to the radioactive cloud from 2002, 2008, and 2010 fires occurred over Central Europe, with the annual average air activity concentration of ^{137}Cs ranging from 17 to 120 mBq m^{-3}.

Several studies have presented calculation results of possible consequences of forest fires in the Chernobyl exclusion zone and neighboring contaminated territories for different scenarios, including worst case scenarios.

Hohl et al. (2012) assessed the health implications of a potentially catastrophic wildfire in the Ukrainian part of the exclusion zone on populations living and working beyond the ChEZ. As a worst case scenario, it is assumed that a fire would completely consume the biomass of pine forests and former agricultural lands and release approximately 4×10^{14} Bq of radioactive material into the atmosphere.

The complete analysis consists of four linked submodels: a source model, a transport model, an exposure model, and a cancer risk model. The radionuclides atmospheric transport is calculated using a Gaussian plume model. The atmospheric discharge is treated as a point source, and the wind was assumed to blow towards Kyiv throughout the fire event. Estimates of radionuclide releases, transport, exposures, and doses are based on conservative assumptions and consequently are likely to overestimate potential exposures to members of the general public during an actual wildfire event.

Estimated activity concentrations of ^{137}Cs in the near-ground air after a catastrophic wildfire were obtained to be 12 mBq m^{-3} at a distance of 30 km from a ChEZ center and 1.9 mBq m^{-3} at a distance of 100 km. An additional ^{137}Cs deposition density due to a fire at these distances was estimated as 240 kBq m^{-2} and 38 kBq m^{-2} accordingly.

A screening model using conservative assumptions was used to estimate exposure through plume immersion and plume inhalation during the fire itself and resuspension inhalation and ground exposure in the year following the fire. The estimated exposure of populations 30 or more kilometers from the source of the fire through these three pathways (22 mSv) is below the critical thresholds that would require evacuations. Since the estimated total ingestion doses to a child (1 y) and adult were found to exceed acceptable levels, a restriction of intake of contaminated vegetation, meat, and milk indefinitely would be recommended.

At 100 km (i.e., the approximate distance to Kyiv), the adult exposure through pathways other than ingestion during the first year after the event was obtained to be 3.5 mSv. Ingestion is responsible for an additional 5.9 mSv during that first year. For children, the equivalent values are 1.6 mSv and 5.5 mSv.

Evangeliou et al. (2014) studied the consequences of different forest fires on the redistribution of ^{137}Cs. They used three different scenarios of forest fires: (a) minor fires that cover 10% of the forests in Ukraine, Belarus, and Russia, which can be extinguished by humans, (b) intermediate fires that affect 50% of the same forests, and (c) a worst case scenario, in which the entire area is affected by fires. The temporal variability of these fires has been adopted for the fires of 2010 that were the most severe events of the last decade. The coupled model LMDZORINCA was used in the simulations.

The range of the ^{137}Cs activity concentrations in the atmospheric aerosol in the first scenario is only significant mostly for the local areas around the contaminated forests when concentrations are in the range of few tens of mBq m^{-3}. This is not the case in the most intense scenarios, where the plumes reach North Europe and Central Russia with maximum concentrations up to three orders of magnitude higher.

Activity concentrations of ^{137}Cs during a fire in two last scenarios could reach to an order of 10 Bq m^{-3} in Belarus (to the north of the Chernobyl exclusion zone). The estimates showed that 1 to 90 kBq m^{-2} can be re-deposited over Europe in one fire year affecting an area of several million inhabitants.

According to Evangeliou et al. (2014) estimates, significant amounts of ^{137}Cs can be transferred to largely populated centers, especially in Central and East Europe. They concluded that large fire events in contaminated forests may not imply a «major nuclear event», such as those of Chernobyl and Fukushima, but they can be classified as «accident with local or wider consequences», or even as a «serious accident», according to the predicted emissions of ^{137}Cs.

On the base of obtained results of atmospheric transport modeling, Evangeliou et al. (2014) estimated the number of excess lifetime cancer incidents to be between 20 and 240 for the global population, of which 10-170 may be fatal. These numbers are far lower than the obtained cancer cases after Chernobyl, but somehow comparable to those obtained from the deposition exposure to the

Chernobyl-remaining ^{137}Cs over Europe and the total exposure after Fukushima. It's necessary to note that these estimations have been obtained under assumptions that seem to be too extreme, so they may be treated as very conservative.

In 2018 the European computer decision support system RODOS (Ievdin et al. 2017) was implemented in the exclusion zone. The system has been developed for assessing, presenting and evaluating the consequences of nuclear and radiation emergencies. The RODOS version adapted for conditions of the Chornobyl EZ was used for modeling consequences of forest fires in the contaminated territories. The first attempt with using the RODOS in the ChEZ was reported in Bogorad et al. (2016) for the forest fire that happened in June 2015. The main feature of this work was the joint using both the RODOS system for on-line forecast of radiological situation outside the ChEZ and the mobile radiological laboratory RanidSONNI operating in the Ukrainian State Scientific and Technical Center for Nuclear and Radiation Safety (SSTC NRS). Measurements of gamma-dose and the air contamination made in Kyiv in the period of this fire showed no significant changes in a radiological situation outside the ChEZ.

In June 2018 several areas of grass and forest of a total square about 15 hectares were burned on the territory of the 10-kilometer zone of the Chernobyl NPP. As a result of meteorological conditions during the fire, the activity could be transported to the southern direction, including Kyiv. Using the mobile radiological laboratory RanidSONNI of SSTC NRS the air sampling was made in one of the points of prognostic maxima of near-surface air activity concentration chosen on the base of on-line modeling with RODOS (Bogorad et al. 2018). The detailed results of radionuclide atmospheric transport both in the ChEZ and for distances to Kyiv caused by this fire were presented in Talerko et al. (2019) obtained with using of a modeling complex of the ISP NPP, which includes a mesoscale weather forecast model WRF, model of convective plume formation over the fire area, and the Lagrangian-Eulerian diffusion radionuclide atmospheric transport model LEDI. According to calculations, the maximum value of the ^{137}Cs activity in the surface air in Kyiv in some periods of the fire could reach values of about 1 mBq m^{-3}, in Chernobyl — about 10 mBq m^{-3}. The overall results are in agreement with the measurements of the cesium-137 activity in the air carried out by the network of ASKRO posts of the SSE «Ecocenter», as well as air sampling data of SSTC NRS.

Hence as a result of forest fires in the Chernobyl exclusion zone in past years a short-term (during few days) increase of the ^{137}Cs activity concentration up to 3 orders of magnitude was measured compared with the values in the other periods. During the last large fire in 2015, the daily average activity concentration of ^{137}Cs reached short-term (for 1 day) the values up to 8 mBq m^{-3}, which does not exceed the value of ^{137}Cs reference level of the activity concentration in the air for the ChEZ (10 mBq m^{-3}). Thus, even within the ChEZ, an increase in air contamination due to the forest fires does not result in the formation of the personnel doses exceeding

the established standards. At the same time, estimates indicate that within the fire zone and in the vicinity of the burning area the radionuclide activity concentration in the air can be much greater. Therefore, special attention should be paid to control doses to personnel, which is involved in the fire extinguishing, due to the inhalation of radioactive aerosols resulting from burning trees and grass.

During forest fires in the Chernobyl exclusion zone, an increase in the activity concentration in the air outside of the ChEZ is much smaller and does not lead to a significant increase in the dose of the population of Ukraine and Belarus. The same conclusion can be drawn about the forest fires that may occur outside of the ChEZ near settlements because the quantities of radioactive contamination of forest areas are much less compared to the ChEZ.

However, the problem of assessing the forest fires danger in the contaminated territories in Ukraine and Belarus remains relevant, since up to now forest fires are a source of an additional increase in the activity concentration of radionuclides in the air. Each event of a forest fire in ChEZ attracts the attention of the media and the population living near the ChEZ, including the residents of Kyiv and other major cities. In the case of particularly large and prolonged fires, radioactive aerosols can spread over long distances outside Ukraine, including the countries of Western Europe. It is, therefore, necessary to have a reliable means for rapid assessment and prediction of atmospheric transport of radioactive aerosols rising into the air as a result of forest fires. To date, the main problem that requires further research is the development of methods for operational determining the parameters of the forest fire territory as an area non-stationary source of radioactive aerosols. Among them are the following:

1. Rapid assessment and prediction of the territory size covered by a forest fire, including the temporal dynamics of the spread of the fire front. In general, this is necessary to use special surface fire spread models for the calculation of fire spread over the area taking into account the properties of the area and weather conditions. However, these models require detailed information on the characteristics of the forest, which is not always available. A feature of forest fires in the ChEZ is their relatively small areas (up to several thousand hectares) and duration (up to several days) compared to large-scale fires in Siberia (Russia) or California (USA). Therefore, for practical calculations of air pollution due to the forest fire it's advisable to consider the fire area as a short-term constant area source of radionuclides emission in the atmosphere. These values can be set either according to the observations, either by expert estimates.

2. Estimations of the value of the radionuclide emission fraction during forest fires differ considerably - from a few percents to 70% according to reviewed experimental and modeling works. The most valid are the results of field experiments and model estimates of the radionuclide emission fraction, carried out for the fires in the ChEZ, which give values 3-5% of ^{137}Cs and ^{90}Sr and up to 1% of the Pu isotopes.

Conditions of experiments for biomass burning, for which estimates are obtained from 20% and above, as a rule, don't fully correspond to the real conditions of the wood burning in a forest fire. Besides, it's necessary to note that in the second year after the deposition the bulk of radionuclides migrates to the forest litter and soil. As a result, the proportion of radionuclides that could potentially be raised to the atmosphere from forest fires, in their total stock in the contaminated area is steadily decreasing over time. Thus, the model estimates of the effects of forest fires on the territory of Ukraine and neighboring countries, obtained using the emission fraction value of 10% or more, can be considered as very conservative.

3. Effective height of the smoke plume lifting over a forest fire. Its value is determined primarily by the ratio between the kinetic energy of the rising airflow (determined by the intensity of heat release in the fire zone) and the wind kinetic energy (Byram 1959).

4. The distribution of particulate matter formed during burning in size. The large particles (more than 20 microns) that are formed in a fire, deposited near the burning territory up to 100 meters). Ignoring this factor in the simulation could lead to an overestimation of the long-range transport of radionuclides, and simultaneously to an underestimation of the value of the additional deposition in the near (up to 100-1000 m) fire zone.

Clarification of these parameters values and methods for their reliable estimate will enable to improve models of atmospheric transport of radioactive aerosols rising into the air as a result of forest fires, for a variety of spatial scales.

CHAPTER 15

ATMOSPHERIC RESUSPENSION OF RADIONUCLIDES DUE TO EXTREME METEOROLOGICAL CONDITIONS

Secondary pollution of the atmosphere due to the rise of radionuclides from the earth's surface can occur not only due to the resuspension at low and moderate wind speeds but also in extreme weather events, which include dust storms, tornadoes, squalls. Despite the relatively short duration of such phenomena, their contribution to the overall balance of the flux of dust and related radionuclides from the earth's surface in the atmosphere can be considerable.

15.1. Long-range transport of the global radionuclide depositions resuspended during dust storms

Dust storms are a natural phenomenon under the conditions of (1) strong wind, (2) cyclone movement and (3) a dry, loose and bare sandy soil. They occur frequently in deserts and surrounding areas and many arid and semiarid agricultural regions. Based on its reduction of the visibility in air, dust storms are conventionally classified as dust haze, blowing dust, dust storm and dust devil, with corresponding visibilities of about 10 km, 1-10 km, 0.5-1 km, and <0.5 km, respectively (Wang et al. 2006).

There are various sources of radionuclides of artificial origin with different resuspension intensity worldwide, including territories contaminated after the Chernobyl and Fukushima nuclear accidents, nuclear weapon tests, and waste from the nuclear industry. Resuspended radionuclides may affect in the close area of these sources as well as on the regional scale. The largest source of the ^{137}Cs is the global depositions from atmospheric nuclear weapons testing in the 1950s and 1960s. As a rule, this source has low emission intensity under normal meteorological conditions. But long-distance effects of resuspension during dust storm events could be observed in different continents.

For example, in Asia, a considerable amount of soil dust is lifted into the troposphere in spring by frequent strong winds and sand storms result in events called as *Yellow Sand* in Korea and *Kosa* in Japan (Choi et al. 2006). *Yellow Sand* events are originated from the deserts in northern China and loess deposits around the Huanghe river basin by the cyclone passage with cold front and westerly to north-westerly of 30-50 knots in the upper layer (Choi et al. 2001).

The numbers of days of Asian dust in a year observed in Seoul during the 1986-2005 period varied from 0 (in 1986) to 27 days (including 24 d in spring) in 2001, in average 8.4 d a year (including 7.4 d a year in spring) (Chun et al. 2008). According to Kido et al. (2012), the number of *Yellow Sand* days in Japan exceeded 400 days in 2000, 2001, 2002, 2006 and 2010 (these values were calculated as the sum of yellow-sand phenomena days over 61 observation points in Japan).

Igarashi et al. (2009) pointed out the important role of the large-scale Aeolian dust such as *Yellow Sand* and *Kosa* as the carrier of the anthropogenic radionuclides since the early 1990s after the stratospheric fallout caused by the atmospheric nuclear tests became negligible.

Choi et al. (2006) observe maximum activity concentrations of 0.580 μBq m^{-3} for ^{239}Pu and 0.404 μBq m^{-3} for ^{240}Pu during the *Yellow Sand* event. It was suggested that the atmospheric resuspension of soil particles from China strongly contributes to Pu deposition in Korea and Japan through *Yellow Sand* events. The $^{239+240}Pu$ activity concentration in aerosols is calculated as much as 1.34 mBq g^{-1}.

Akata et al. (2007) measured ^{137}Cs depositions in Rokkasho, Aomori, Japan from March 2000 to March 2006. The annual ^{137}Cs deposition from 2001 to 2005 was obtained 0.04-0.69 Bq m^{-2} with a mean value of 0.27 Bq m^{-2}. They concluded that the ^{137}Cs deposition peaks, especially the high peaks, were coincident with the Asian dust events, although there were no-coincident cases. The highest peak (29.7 mBq m^{-2} d^{-1}) of ^{137}Cs deposition was observed during 7-25 March 2002. The backward trajectory analysis for the periods 17-21 March 2002, 11-12 March 2004 and 21-22 April 2005, which were coincident with the Asian dust events, showed that the high ^{137}Cs deposition flux observed in Rokkasho was caused by Asian dust from northeastern China and southern Mongolia regions.

Fujiwara et al. (2007) confirmed this conclusion and noted that in these territories in China and Mongolia there are no known nuclear test sites or nuclear facilities. The source area for the dust associated with the March 2002 sandstorms is typically covered by grassland and shrubs, and only a small part of the area is desert. The results of soil sampling within the area where dust raising events were observed in northeastern China in March 2002 resulted in the value of ^{137}Cs inventories in the range 176-3710 Bq m^{-2}. This suggests that the ^{137}Cs originated from global fallout caused by past atmospheric nuclear testing. Activities of ^{137}Cs in the surface layer (0-2 cm) of the sampled soils were in the range 5.5-86 mBq g^{-1}. They concluded that the ^{137}Cs deposited by past nuclear tests have settled and accumulated mainly on

the surface soil of the grassland. The massive sandstorms of March 2002 and the accompanying prodigious release of ^{137}Cs-bearing soil particles were the result of wind erosion by seasonal strong winds on the grasslands whose vegetation cover had been greatly reduced by drought. They suggested that desertification on the East Asian continent in response to recent climate change will result in an increase in ^{137}Cs-bearing soil particles in the atmosphere, and their subsequent re-deposition.

Fukuyama and Fujiwara (2008) estimated the relative contribution of Asian dust (*Kosa*) transported from the East Asian continent and locally suspended dust near monitoring sites in Japan to the total ^{137}Cs deposition. Deposition of ^{137}Cs from a single Asian dust event during 30 March- 06 April 2007 in Tsukuba, Japan was estimated equals to 62.3 mBq m^{-2} and accounted for 67% of the total ^{137}Cs deposition during the entire monitoring period. This result suggested that most ^{137}Cs deposition in spring is derived from Asian dust events. Moreover, a high specific activity concentration of ^{137}Cs (81.8 mBq g^{-1}) was also observed at this time. As ^{137}Cs is preferentially adsorbed onto the fine fraction (e.g., clay-sized particle) in the soil, ^{137}Cs specific activity might be high in deposits of Asian dust because of the high content of fine-grained mineral particles in this dust.

Analysis of the ^{90}Sr and ^{137}Cs monthly deposition time series in Tsukuba gave reasons to suggest that due possibly to the anthropogenic and/or climatic change the vigorous Aeolian dust source influencing Japan would be shifting from the conventional arid area to the desert-steppe zone during the 2000s (Igarashi et al. 2009).

Dust particles blown into the atmosphere in desert regions of Mongolia and China can be transported as far away as in Russia (Primorskii Krai, including the city of Vladivostok) (Kondratiev and Skalyga 2011) and the west coast of the United States and southern British Columbia, Canada (McKendry et al. 2001).

On 22 February 2004, a huge dust event occurred in the south of Europe, primarily in France. Huge quantities of dust were deposited: values were so high that instruments became unusable. Using atmospheric transport modeling, Menut, Masson, and Bessagnet (2009) showed that these dust aerosols came from the Sahara Desert, North Africa. They quantified the origin and percentage of dust originating from different possible sources of radioactivity. Of particular interest was the contribution of ^{137}Cs activity concentrations in Europe from «Gerboise» sites, where former French nuclear tests in the 1960s were performed. Simulations showed that the majority (80%) of the dust was coming from eastern Maghreb (territory of Algeria, Tunisia, and Libya), but only 0.7% of the African emissions were from Gerboise, leading to 1-5% of the activity concentrations recorded in the south of France for the day of the peak.

Prezerakos, Paliatsos, and Koukouletsos (2010) described the phenomenon of colored rain over the South Balkans and, in particular, over Greece. Such was the case on 4th April, 1988, when significant synoptic-scale subsidence occurred over Italy and towards Greece. Analysis of such cases revealed that two days before the

occurrence of the colored rain or the dust deposits over Greece a sand storm appeared over the north-western the Sahara Desert. Makrogiannis et al. (1990) noted the observed dust was relatively more radioactive than the common Greek dust or sand found in the area. Papastefanou and Manolopoulou (1989) reported the long-lived fission product radionuclides such as ^{137}Cs, ^{134}Cs, ^{144}Ce, ^{l06}Ru, and ^{125}Sb were identified in dust originating from the Sahara Desert which was precipitated with the rain to produce colored rain over Thessaloniki, Northern Greece, on 4-5 April 1988. All these radionuclides were due to the Chernobyl reactor accident which occurred two years before. Caesium-137 activity reached 1,000 Bq kg^{-1}, resulting in a deposition of 3.03 Bq m^{-2}. Twelve years after a colored rain event originating from the Sahara Desert occurred on April 9, 2000 at Thessaloniki (Papastefanou et al. 2001). Cesium-137 of Chernobyl origin remained 14 years after the Chernobyl accident, reaching 26.6 Bq kg^{-1} in the colored rain dust.

The colored rain and/or dust deposits occur also in other European countries which are further north than Greece, for example, United Kingdom (File 1986), Spain (Rodriguez et al. 2001), and generally Europe (Stuut, Smalley and O'Hara-Dhand 2009).

Hamadneh et al. (2015) reported that dust storms are very common in the Middle East region (Syria, Iraq, Jordan, and Saudi Arabia). They investigated the huge dust storm which occurred in the Middle East in May 2012 and have found that dust storms carry an appreciable amount of radioactivity. ^{137}Cs was detected in all of the dust samples and its activity concentration in these samples is about one order of magnitude larger than its activity concentration in the local soil: the mean value is (±SD) 17.0 ± 2.0 Bq kg^{-1} in the dust compared to 2.3 ± 1.6 Bq kg^{-1} in soil. The increased activity concentration of ^{137}Cs in the dust is attributed to particle size effects as suggested by several studies which found that ^{137}Cs activity concentrations are larger in the finer size fractions of the soil.

15.2. Meso-scale transport of the radionuclides resuspended during dust storms

15.2.1. Wind transport of contaminated sediments from lake Karachay during spring 1967

Territories radioactively contaminated as a result of accidents at radiation hazardous facilities (nuclear power plants, plants for the processing of irradiated nuclear fuel and radioactive waste) are a source of re-entrainment of radioactive aerosols in the environment. In contrast to the resuspension of radionuclides of the global fallout from nuclear weapons tests, such areas with a high density of surface contamination can contaminate the surrounding areas both on a local scale and on a regional scale due to long-range transport. In

these territories, the consequences of radionuclides resuspension in the event of extreme weather conditions may be considered as a serious radiation incident. One of these was the atmospheric transport of radioactive silt from Lake Karachay in 1967.

The production association (PA) «Mayak», located in the Chelyabinsk Region, Russia, was the first nuclear installation in the former Soviet Union and had the task of producing weapons' grade plutonium. As a consequence of deliberate actions in the period 1949-1956, 2.7 million curies of liquid radioactive waste were discharged to the Techa River. Besides it, two large incidents have happened there: 1) the Kyshtym accident: releases due to an explosion in a high-level radioactive waste tank (1957); and 2) wind transport of contaminated sediments from Lake Karachay (1967). This caused contamination of a considerable area of land.

Since October 1951, PA «Mayak» began to use Lake Karachay as a repository for intermediate-level waste. About 1.85×10^{19} Bq (500 million Ci) of beta-radioactive nuclides were put into Karachay during all period of its exploitation. Now Karachay contains approximately 4.4×10^{18} Bq (120 million Ci) of radionuclides, among them about 40% ^{90}Sr+^{90}Y and 60% ^{137}Cs. Radionuclides are distributed as follows: 7% in water, 41% in loams of the bed and 52% in mobile bottom sediments. So, the main part of the activity, accumulated in Karachay, is concentrated in mobile bottom sediments, where specific activities of ^{90}Sr and ^{137}Cs are as large as 3.7×10^{10}-7.4×10^{10} Bq kg^{-1} (Merkushkin 2000).

Between 1963 and 1964, measures were taken to reduce the reservoir area, to prevent the migration of radionuclides into ground water. However, the years from 1962 to 1966 were dry, and the water level in Lake Karachay fell, and uncovering about 5 ha of the shore line and lake bed (JNREG 1997). In 1967 a winter with little snow followed by exceptionally dry weather. Early spring was dry, with strong gusty winds. As a result, during the period from April 10 to May 15, 1967, some 22 TBq (600 Ci) of ^{137}Cs associated with the fine particles of silt sediments were resuspended by the wind and dispersed within an area surrounding the site. We should also note that Aarkrog et al. (2000) estimated the total inventory in 1967 of ^{137}Cs as 220 TBq that is a factor of ten higher than the official reported Russian estimation value.

Most of the fallout was deposited near Lake Karachay, i.e. within the enterprise site area. Due to the influence of winds from different directions, the contamination density distribution in the affected territory was uneven, and the boundaries of the affected area showed a complex configuration. About 1800 km^2 lay within the 3.7 kBq m^{-2} boundaries for ^{90}Sr, or 11 kBq m^{-2} for ^{137}Cs, and the contamination reached a distance of 50-75 km from the »Mayak» PA site (Fig. 15.1). The fallout occurred largely to the north-east and east of the enterprise, partially overlapping the central parts of the EURT region (East Ural Radioactive Trace due to the Kyshtym accident in 1957). A central-axial trace with contami-

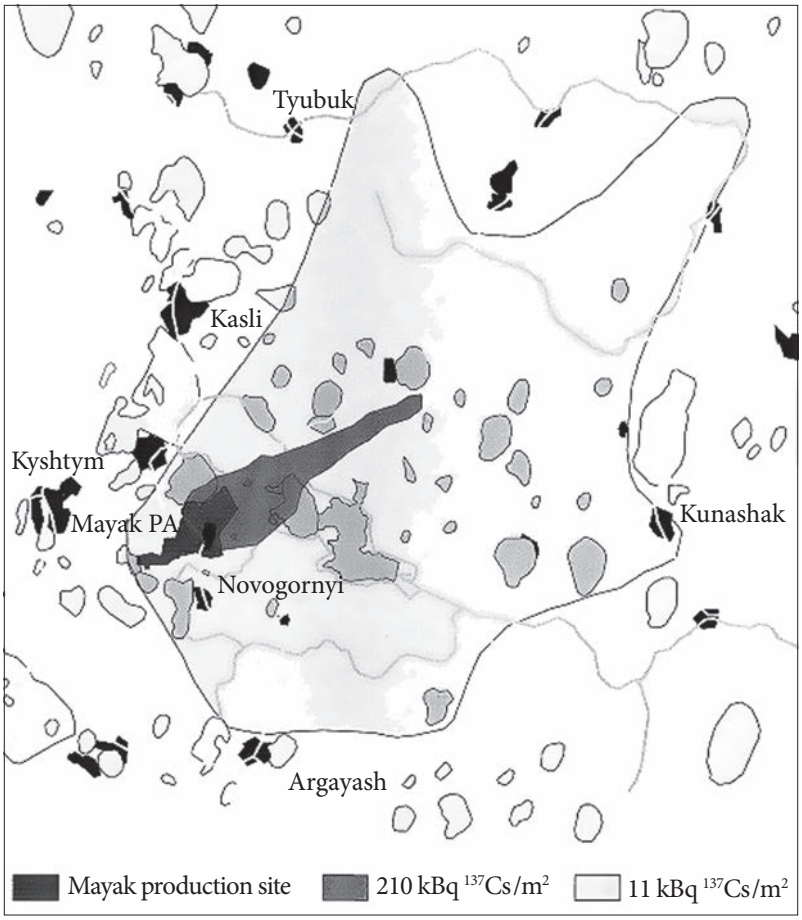

Fig. 15.1. ^{137}Cs deposition density after the lake Karachay incident (from JNREG 1997)

nation levels greater than 74 kBq m^{-2} for ^{90}Sr and 210 kBq m^{-2} for ^{137}Cs was identified, with a maximum density of 260 kBq m^{-2} ^{90}Sr. Beyond the site boundary the length of this trace was 15 km and a width 1.5-3 km (JNREG 1997).

The radionuclide composition of the fallout in the affected region was dominated by ^{137}Cs (48% of the total activity), ^{90}Sr + ^{90}Y (34%) and ^{144}Ce + ^{144}Pr (18%).

Radioactive substances deposited as dust particles. The study of fractional composition of the dust collected from the plants found that 50% of the mass accounts for the fraction of 10-50 μm; 11.2% at 1-10 μ dust fraction, including 1.5% of silt fraction <1 μm (Prister et al. 2016).

The radiation and radiological consequences of the incident are assumed to have been minimal: the increase in the gamma-radiation dose rate at inhabited locations did not exceed 4-7 mR h^{-1} during the initial period, and decreased with

an effective half-life of about 2-3 months (JNREG 1997). Radioactive surface contamination of agricultural produce led to maximum internal doses to the public within the first year which are less than a few percents of the admissible dose (i.e. 6% of the whole body dose). The radiation conditions subsequently improved considerably, and the background levels were attained 2-3 years after the incidence.

15.2.2. Dust storms on the territories of Ukraine and Belarus contaminated after the Chernobyl accident

Dust storms are natural phenomena, which in a short time can lead to the territorial re-distribution of radioactive material deposited to the ground after the accident of the 4th unit of the Chernobyl nuclear power plant in 1986.

According to (Lipinskiy, Osadchiy and Babichenko 2006), dust storms were observed on the territory of the Kyiv region, although their frequency is much less than for the southern part of Ukraine. In particular, a strong dust storm observed in the Kyiv region on 16-17 February 1969 (about 20 hours duration, surface wind speed of 20-28 m s^{-1}).

In the first years after the Chernobyl accident, a sharp increase in aerosol concentrations in the 30-kilometer Chernobyl exclusion zone was observed several times due to strong winds. Derevets et al. (1996) noted that during a dust storm at the end of April 1987 the ^{137}Cs activity concentration increase of order and reached the value 370 Bq m^{-3}.

Three weeks later, during a dust storm on 16-19 May 1987, a disperse composition of aerosol was measured (Ogorodnikov 2011). Wind resuspension and the formation of dust clouds occur in dry weather and wind speeds more than 10-15 m s^{-1}. The aerosol particle size distributions in the near ground (1.0-1.5 m) and high-altitude (150-300 m) layers were found similar. Measurements of radioactive substances concentration were not carried out in this study.

Two months later (24 July 1987) there was a dust storm in the exclusion zone (Meshalkin et al. 1992). It was noted that the visibility dropped to 7-10 m, the concentration of radioactive aerosols at the monitoring site ORU-750 has increased by two orders of magnitude. This site is located half a kilometer to the south of the «Shelter» object.

Israel (1990) characterized the dust storm in the exclusion zone observed on 28-29 July 1988. Under an average wind speed of 12-15 m s^{-1} the daily averaged activity concentration of $^{239, 240}Pu$ in the Pripyat city reached 1.5×10^{-4} Bq m^{-3}. It is 10-15 times higher than the year averaged value for 1988.

Ogorodnikov (2011) examined the meteorological situation at the dust storm during 5-7 September 1992 on the territory of Ukraine and Belarus polluted after the Chernobyl accident in 1986. The emergence and development of the dust storm was due to the passage of the cyclone near the exclusion zone, which origi-

nated on September 4 over the Balkans. Maximal middle wind speed in Chernobyl and Pripyat was 10-12 m s^{-1}.

During the dust storm, the activity concentrations of radioactive aerosols in the Chernobyl exclusion zone increased in 10-100 times. In particular, at the monitoring sites ORU-750, BNS (3 km east of the Chernobyl NPP) and OVD-2 (in the Pripyat city) before and after the dust storm the ^{137}Cs activity concentration was observed in the range 0.005-0.01 Bq m^{-3}. During the dust storm, the contents of aerosols at all three sites have increased sharply. At the ORU-750 monitoring site on 6 September from 14 to 17 hours, the average activity concentration was about 0.2 Bq m^{-3}, increased approximately 20-fold. This value was the highest in 1992 among all 24 aerosol monitoring points in the exclusion zone. On the same day, in the sample taken at the OVD-2 monitoring site from 12 h to 16 h 20 min, the ^{137}Cs activity concentration was close to 0.1 Bq m^{-3}, i.e. it increased by about 100 times. Both samples, obtained during the midday hours, were taken in the period of maximum wind speeds. In the evening the wind dropped somewhat and, as a result, the atmospheric activity concentration of aerosols decreased. In another sample taken at the OVD-2 site from 16 h 20 min to 19 h 30 min, the activity concentration decreased to 0.007 Bq m^{-3}. Nevertheless, it was an order of magnitude higher to «background» levels.

On September 6-7 at the ORU-750 during 21 h (17 h - 14 h) and at the BNS during 23 h (14 hr 20 min - 13 h 20 min) sampling were taken. Since both samples were taken in the period of the dust storm decay, especially at night time, the ^{137}Cs activity concentrations were not as high as at noon on 6 September. At the ORU-750 site, the ^{137}Cs activity concentration was 0.005 Bq m^{-3} and 0.017 Bq m^{-3} at the BNS site.

On September 7 a sample with short exposure time was selected in Chernobyl during the period of 11 h -12 h 40 min. At this time here and in Pripyat the high average wind was again with speed reaches 8-9 m s^{-1}. As a result, the ^{137}Cs activity concentration was about 0.002 Bq m^{-3} and was an order of magnitude higher than the average value observed in Chernobyl in April-October 1992.

Important and interesting data on radioactive aerosols in August and September 1992 outside of the Chernobyl exclusion zone were obtained at several meteorological stations in Ukraine (Oster, Shchors), Belarus (Gomel, Minsk, Mogilev, Mozyr) and in Lithuania (Vilnius) (Ogorodnikov 2011).

In Oster and Shchors, located in the Chernihiv region, the daily averaged activity concentration of the mixture of β-emitting nuclides during a dust storm in September 1992 increased in Oster up to 1.2 mBq m^{-3} and in Shchors — up to 0.9 mBq m^{-3}, i.e. about 5 times as compared with the «background» values.

A jump of radioactive aerosols concentration during the dust storm became apparent most clearly in Minsk and Mozyr. Here the «peak» values were 6-7 times higher than the average for August. After the dust storm (in the second and third decade of September) the values of the concentration of a mixture of β-emitting nuclides were again about the same as in August. In Mozyr during the dust storm,

the mass aerosols content has increased sharply: it increased from an average «background» value of 0.02-0.03 mg m^{-3} to 0.2 mg m^{-3}.

In Mogilev and Gomel on 5-7 September the activity concentration of radioactive substances in the atmosphere has increased in comparison with the average for August is 1.5-3 times, i.e. less than in Minsk and Mozyr. However, the increase of the mass concentration of aerosols was observed clearly. Especially dustiness of the atmosphere increased sharply in Gomel: from 0.02-0.03 to 0.4 mg m^{-3}.

Radiation effects of the dust storm have appeared at large distances from the exclusion zone also. In August and September 1992 in Vilnius (Lithuania) two ^{137}Cs concentration peaks were registered (Lujaniene, Aninkevicius, Lujanas 2009). The former was on 31 August — 1 September and reached 300 μBq m^{-3}, and the latter — on 6-7 September with a maximum of 190 μBq m^{-3}, which are 2-3 orders of magnitude higher than background values this period. Based on the analysis of air masses movement trajectories during the dust storm Ogorodnikov (2011) concluded that the sharp rise of the concentration of radioactive cesium in Vilnius was not due to the fire on 7 September but the arrival of dust aerosols from northern Ukraine and eastern Belarus contaminated by the Chernobyl accident products.

According to Ogorodnikov (2011) even in the territories with a high contamination density, such as the ChNPP industrial site, hardly dust storms can lead to the ^{137}Cs activity concentration in the air exceeding the maximum permissible level for the population. However, for plutonium, such excess is possible because of more strict standards for it. For example, on 6 September 1992 at the ORU-750 site the activity concentration of $^{239, 240}Pu$ was 1.1 mBq m^{-3}, which practically coincides with the maximum permissible level for the population.

According to the meteorological station in Chernobyl data, there were no dust storms in the exclusion zone after 1992 (Ogorodnikov 2011). It is not due to climate change only but also caused by the gradual reforestation of the zone. The number of days in which the wind gusts were recorded more than 15 m s^{-1} is small too. During the period 2006-2009 such situations were observed only nine times. Therefore, the risk of significant resuspension due to dust storms and additional radioactive pollution in ChEZ and surrounding areas decreases with time, although it can not be excluded.

15.3. Radionuclides re-entrainment due to tornado over nuclear installations, radioactive facilities, and contaminated territories

Tornado belongs to the most dangerous natural phenomenon that causes huge catastrophic destruction. The radiological consequences of air pollution as a result of the passage of the tornado over the objects that contain radioactive materials or radioactively contaminated territories have not yet been

fixed. However, the possibility of such situations is not excluded. In many studies on the long-term safety analysis of radioactive facilities the possible scenarios of radiological impacts of a tornado passing over the industrial sites are considered.

Weber and Hunter (1996) reviewed models developed by Pepper (1975) and Haynes and Taylor (1983) for estimating consequences of a tornado strike at the Savanna River Site (SRS) facility. A scenario of a breach in radionuclide storage containers following atmospheric dispersion of radionuclides has been considered.

Pepper's model accounts for the uptake of radionuclides by the tornado vortex and mixing material throughout the parent thunderstorm, followed by conventional dispersion from advection, turbulent diffusion, and wet deposition. Haynes and Taylor assumed heavy rain following the tornado for 10 min, following by a lighter rain for another 10 min, then no rain for the period when the material is transported downwind.

On the base of a more complete understanding of the tornado vortex, Weber and Hunter proposed a revised model for use at SRS. The main feature of the model is taking into account thunderstorm downdrafts in mesoscale circulations accompanying tornadoes. Winds associated with a tornado cause immediate, complete entrainment of the radionuclides into the tornado vortex. Thereafter, the radioactive particles are lifted to the base of a counter-clockwise rotating column of air known as a «mesocyclone». The mesocyclone is located adjacent to a substantial persistent downdraft, which can eventually carry the elevated particles back toward the surface. The mesocyclone forms the radionuclides volume source for following dispersion calculation using a simple Gaussian model.

The problem of the additional air pollution due to the rise of radioactive dust during the passage of a tornado in the Chernobyl exclusion zone has not yet been investigated. However, the model estimates of the possible effects of the tornado on individual radiation hazardous objects in ChEZ were conducted, including the object «Shelter», the Vektor radioactive waste storage facility and the cooling pond of the Chernobyl nuclear power plant.

According to Bryuhan, Lyakhov and Pogrebnyak (1989), the ChEZ is located in an area of high tornado risk. During the period from 1969 to 2012 7 tornadoes were recorded in the Kyiv region. Taking into account recent observations, a probability of a tornado in the Kyiv region within 1000 km^2 area can be estimated to be 1.5×10^{-2} per year, and within the ChEZ — 6×10^{-3} per year. The most intense among observed in the Kyiv region was a tornado on 18 August 1969, which was assigned to be the F3 category according to the Fujita scale.

After the Chernobyl accident, a few calculations of possible secondary air pollution as a result of the removal of radioactive dust from the «Shelter» object with a tornado was carried out. They are differ by approaches to the description of the tornado, as well as methods of modeling the further diffusion of radioactive dust after the tornado dissipation. Among these works are the following:

1. Beskorovajnyj et al. (1994) assumed that the dust which has been taken from the «Shelter» is carried by a tornado virtually without deposition at a distance of about 20 km, after which the tornado ends. Further, the atmospheric diffusion of radionuclides was calculated using the Gaussian model. With the estimation of the total release from the «Shelter» equals to 4.8×10^{16} Bq, it was found that in the area of the tornado dissipation the ground deposition density can exceed 185 MBq m^{-2}. It was concluded that due to a tornado propagation to the territory of Belarus a contamination of nearby areas may exceed pollution during the Chernobyl accident in 1986.

2. In Assessment (2004) under the analysis of the possible consequences of the destruction of the «Shelter» by a tornado, it was assumed that all fuel dust (500 kg) is lifted to the tornado base in a mesocyclone parent cloud at an altitude of about 1000 m for 1 min and further moves in a compact form in the cloud with a mesocyclone. The resulting radioactive cloud moves over the atmospheric boundary layer. 90% of the dust in the parent cloud is washed out by rainfall after the tornado and mesocyclone collapse, and the rest of the fuel dust rises over the troposphere and independently disperses after the collapse of the parent cloud.

Under the adopted assumptions the radioactive fallout zone area is 16 km^2, the trace length is 10 km and a trace width is about 1.5 km. The central part of the radioactive fallout zone is located at a distance of 15-45 km from the «Shelter». The mass deposition density has been estimated to be 28 mg m^{-2}.

3. In Assessment (2004), Bogorad et al. (2006) the results of calculations of the fuel dust transport in the near and distant zone of the Chernobyl nuclear power plant are shown using the atmospheric transport models CALPUFF and meteorological data obtained using a numerical regional weather forecast model MM5 with assumptions on the radionuclides removal from the Shelter mentioned above. For numerical simulation the weather conditions related to a tornado formation on 11 June 2001 in the Zhytomyr region, Ukraine were chosen. The maximum value near the source of contamination was found to be 2.5 mg m^{-2} of fuel dust, and the estimated density of the fuel dust deposition at a distance of 100 km from the «Shelter» is about 0.001 mg m^{-2}.

Rybalka et al. (2013) analyzed the consequences of a tornado passing over the Vector facility site for long-term storage and disposal of radioactive waste in the Chernobyl exclusion zone. They estimated that about 0.2% of the radioactive waste total activity may be drawn into the funnel of a tornado. For disposal of radioactive waste with the estimated activity of 2.5×10^{16} Bq at the Vector site, the dose of potential exposure near the site has been calculated. At a distance of 12 km from the site, it was estimated as 6.9 mSv per year exceeding the criteria of the admissible dose of 1 mSv per year.

The cooling pond (CP) of the Chernobyl nuclear power plant is an artificially created technological water reservoir. The main purpose of this man-made structure is the water cooling of the nuclear power plant reactors. The cooling pond was

commissioned when the 1st unit of the ChNPP started work in 1976. After the last unit of the ChNPP stopped work in 2000 the volume of industrial water use from the cooling pond has declined significantly. At present, the cooling pond is:

- a source of water supply for industrial water supply systems and fire fighting systems;
- environmental object, a safe state of which is achieved by maintaining the water level at the nominal design level for the purpose limiting of radionuclides transport contained in silt after the accident at Unit 4.

The main technical characteristics of the cooling pond are:

- the length of the cooling pond along the axis is 11.5 km;
- average width is 2.2 km;
- the length of the coastline is 25 km;
- the area of the water surface is 22.9 square kilometers;
- the average depth is 6.6 m;
- the useful volume is 151.2 million cubic meters.

The cooling pond is constantly losing water, which flows (infiltrates) into the Pripyat River through the dam wall. The water surface of the cooling pond is seven meters above the Pripyat River, which results in such a large water leakage.

Now in Ukraine, a National Program of the Chernobyl NPP decommissioning and transforming the object «Shelter» into an ecologically safe system is adopted. Within the framework of a Program, the ChNPP cooling pond decommissioning is foreseen. The outcome of the cooling pond decommissioning will partial drainage of the cooling pond, i.e. bringing the territory occupied by the water body to its natural state, determined by the water level in the Pripyat River.

Talerko and Garger (2013) evaluated the effects of a possible rise of radioactive aerosols in the air from the dried part of the cooling pond bottom caused by a tornado passing over it, including transboundary atmospheric transport of radionuclides to the territory of neighboring countries.

According to (Explanatory 2012), while the planned lowering of the water level in the CP at 7 m approximately 14.8 km^2 of 21.7 km^2 water surface to be drained. An assessment of radioactivity stock in this area is about 61.5 TBq ^{137}Cs, 10.95 TBq ^{90}Sr and 0.11 TBq of plutonium. Thus, the average density of radioactive contamination of this territory is $D_{Cs} = 4.16 \times 10^6$ Bq m^{-2} for ^{137}Cs, $D_{Sr} = 7.40 \times 10^5$ Bq m^{-2} for ^{90}Sr and $D_{Pu} = 7.43 \times 10^3$ Bq m^{-2} for Pu. At the specified lowering the water level in the CP a strip of drained territory will be formed along the shoreline of width about $L_{dry} = 750$ m.

Talerko and Garger performed calculations using a set of models, including the conceptual model of a tornado of Weber and Hunter (1996), the mesoscale atmospheric diffusion model of pollutant transport LEDI and dosimetric models. At that, some values of tornado parameters used in Weber and Hunter (1996) have been replaced according data from Decree (2002) and climate data for Ukraine (Table 15.1).

A tornado model is based on the following assumptions:

1. Radioactive dust which captured from the earth's surface by a tornado with a path width W_p (Table 15.1) over a given area, rises in the vortex funnel up to the height of a parent cumulonimbus cloud base H_{ng}. It is assumed that the mixing of air of a vortex with the ambient atmosphere is absent. The height of a tornado-generating cumulonimbus cloud base H_{ng} was assumed to be 1,000 m (Romov et al. 1987). The characteristic value of vertical airflow speed in the vortex is taken equal to $W_{up} = 20$ m s^{-1} (Weber and Hunter 1996). Then the time of the radioactive particles ascent from the earth surface into the cumulonimbus cloud is $t_{up} = H_{ng} / W_{up} = 50$ s.

2. The horizontal speed of the tornado movement U_p is assumed to be equals to the speed of the parent cloud movement (Romov et al. 1987), which, in turn, is determined by the wind speed at the height of the cloud base H_{ng} (relevant data from Table 15.1 are not used).

3. It is assumed that the radioactivity lifted by a tornado from the ground surface, is transported by an upward vortex into a parent cloud mesocyclone having a cylindrical shape with a diameter of 1,000 m and a height $H_{cloud} = 1{,}000$ m above the cloud base (Weber and Hunter 1996). Due to strong vertical air updrafts and turbulence, the rapid mixing of radioactive particles in a mesocyclone occurs. The characteristic time of this process can be estimated equals to $t_{upcloud} = H_{cloud} / W_{up} = 50$ s. As a result, a cloud of radioactive pollutants is formed in the atmosphere with the same size as a mesocyclone.

4. The model takes into account the availability of compensatory downward air flows adjacent to the tornado funnel. It is assumed that a radioactive cloud formed in mesocyclone descends to the ground with a vertical velocity equal $W_{down} = 10$ m s^{-1} and the horizontal speed equal to the speed of movement of the parent cloud.

5. At the time when the lower edge of the cloud reaches the ground, the downdrafts stop. The characteristic time during which the dust particles can fall from the cloud top to the ground can be estimated equal $t_{down} = (H_{ng} + H_{cloud}) / W_{down} = 200$ sec-

Table 15.1. **Estimated parameters of a tornado on the Chernobyl NPP site (Decree 2002)**

Parameter	Parameter value	
Fujita category of a possible tornado, k_p	F3.0	F1.5
Probability of exceeding	1×10^{-6}	1×10^{-5}
Maximum rotational speed in the tornado funnel, V_p, m s^{-1}	81	50
Horizontal speed of the tornado, U_p, m s^{-1}	20.3	12.6
Pressure differential between the centre and the periphery of the tornado funnel, ΔP_p, hPa	81	31.0
The path length of the tornado, L_p, km	28.6	5.0
The pass width of the tornado, W_p, km	0.29	0.05

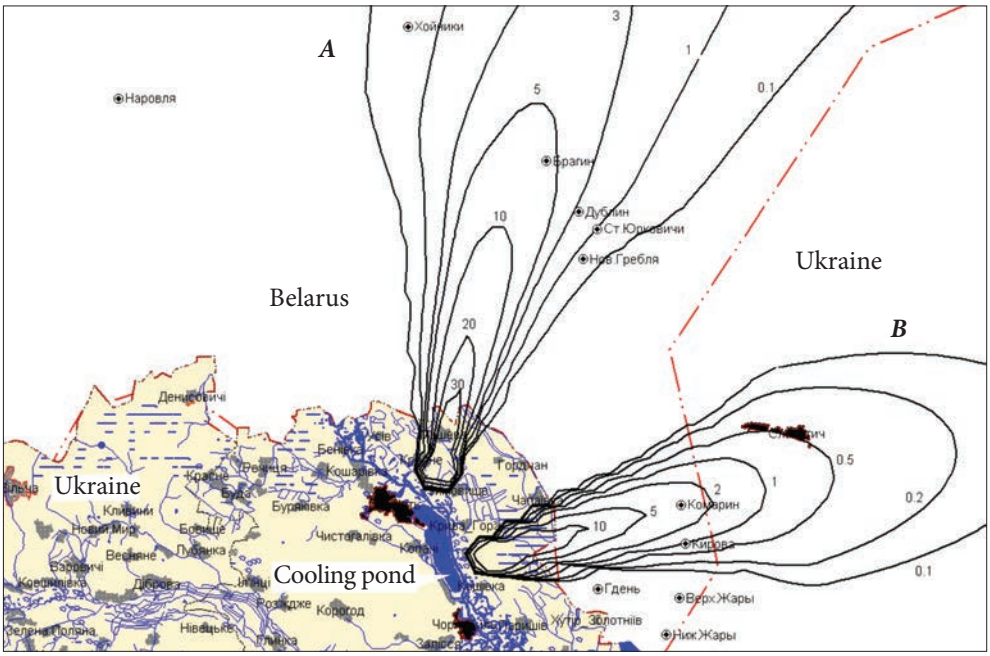

Fig. 15.2. Calculated fields of ^{137}Cs deposition density (kBq m^{-2}) as a result of the passage of the radioactive clouds formed due to tornado events over the ChNPP cooling pond (for two different meteorological scenarios ***A*** and ***B***)

onds. Total time of dust particles spent in a tornado will be $t = t_{up} + t_{upcloud} + t_{down} = 300$ seconds. As a result, in the point at a distance of $s = U_p * t$ from the initial one a volume source of radioactive pollutant is formed with a diameter of 1000 m and with a constant activity over height in the layer 0-1,000 m. For the concerned case of dust lifting from the area source the initial point is regarded as a point in which tornado leaves the contaminated area, i.e., a pollutant inflow into a tornado funnel stops.

Further transport of radioactive pollutant is calculated due to advection and turbulent mixing in the atmospheric boundary layer using a mesoscale atmospheric transport model LEDI (Talerko, Garger and Klyuchnikov 2010). A formed volume source of radioactive pollutant is determined for calculation with the LEDI model as follows:

a) Its initial coordinates are assumed to be equal to coordinates of the point where a downdraft of a cumulonimbus cloud reaches the earth surface (it is determined by the above-numbered list, item 5).

b) A pollutant concentration distribution is assumed to be Gaussian in the direction perpendicular to the transport direction, with a cross-wind standard deviation equals $\sigma_y = 232$ m. The latter value is chosen according to the recommendations (Pasquill and Smith 1983), which provides agreement with a specified diameter of a cylindrical source 1,000 m.

c) According to the LEDI model, a distribution of a pollutant concentration in the cloud over height is calculated by numerical solution of the turbulent diffusion equation. It enables, in contrast to (Weber and Hunter 1996), to set directly a uniform distribution of activity in the layer 0-1,000 m as an initial condition for the LEDI model.

The LEDI model calculates fields of the radionuclide activity concentration in the air, the deposition density on the underlying surface, as well as associated external and internal (due to inhalation of radionuclides) exposure doses.

In further analysis three scenarios were considered under which radionuclides rise takes place from the dried parts of the ChNPP cooling pond due to a tornado and then after the tornado collapse their atmospheric transport to: A) the north (the territory of Belarus); B) the east (the territory of Belarus) and C) the north-east (the territory of Russia).

The activity raised by a tornado vortex of intensity F3 from the CP drained part was assessed as 13.9 TBq ^{137}Cs, 2.47 TBq ^{90}Sr, 0.0248 TBq Pu. Depending on the chosen meteorological scenario a maximal additional density deposition on the territory of Belarus (in Polesye State Radiation Ecological Reserve) was assessed as 35 kBq m^{-2} ^{137}Cs, 6 kBq m^{-2} ^{90}Sr and 60 Bq m^{-2} Pu, whereas in the nearest settlements of Belarus and Russia — 5-9 kBq m^{-2} ^{137}Cs, 1.0-1.7 kBq m^{-2} ^{90}Sr and 10-17 Bq m^{-2} Pu, i.e. it doesn't exceed 1-2% of the actual one (Fig. 15.2).

The radiation dose to the people of Belarus will not exceed 1 μSv, Russia — 10^{-2} μSv. Thus, in the event of a tornado over the ChNPP cooling pond a conservative estimation of total dose for residents of nearby towns of Belarus 3 orders of magnitude, and Russia 5 orders of magnitude less than the limit of effective dose for the population of 1 mSv per year established by the standards of radiation safety in these countries.

In conclusion, we note that people of nearby settlements of Belarus and Russia can obtain the same radiation dose in the case of a F3 category tornado passage over the territory of the Chernobyl exclusion zone with an average density of soil contamination equals to 1,700 kBq m^{-2} ^{137}Cs, 300 kBq m^{-2} ^{90}Sr and 3 kBq m^{-2} Pu. Actual contamination of large part of the Chernobyl exclusion zone in Ukraine and Polesye reserve in Belarus considerably exceeds these values.

Hence, the safety analysis showed that a tornado passage over the CP will not result in an unacceptable dose to individuals in Belarus and Russia. Based on these results one can conclude almost insignificant influence of the effects of the CP drainage on the possible cross-border atmospheric transport of radionuclides, as well as the associated consequences for Belarus and Russian population health.

The radionuclide emission caused by extreme meteorological conditions takes place during relatively short periods (from a dozen minutes for tornadoes to several days for dust storms). But due to the high intensity of soil mass rise into the atmosphere during such events they may result in additional contamina-

tion of the air at different scales including the long-range atmospheric transport. Around the world, the measured ^{137}Cs deposition appears to be the result of resuspension by wind uplift of soil particles contaminated by past nuclear testing. In many countries, this additional contamination may be caused by not only local resuspension but be a result of particles wind uplift during large dust storms, followed by transport and re-deposition, from contaminated distant areas. So, these events may imply on the radiological situation on a global scale. In some cases, extreme meteorological events must be regarded as situations of special importance, when they are taking place over territories with relatively high radioactive contamination density (for example, contaminated after nuclear emergencies). In these cases, a careful analysis using models of radionuclide migration in the environment is needed to assess the potential danger of the object at different distances from it for any possible meteorological scenarios.

REFERENCES

Aakrog A., Botter-Jensen L., Chen Q.J. et al. Environmental Radioactivity in Denmark in 1986. Denmark, R-549, Riso National Laboratory Report. Riso: Roskilde. 1988. 272 p.

Aarkrog A., Simmonds J., Strand P. et al. Radiological Assessment of Past, Present and Potential Sources to Environmental Contamination in the Southern Urals and Strategies for Remedial Measures(SUCON). Riso-R-1243(EN), Riso National Laboratory: Roskilde, Denmark, 2000. 72 p.

Ageev V.A., Vyrichek S.L., Klyuchnikov A.A. et al. Estimate of ^{242m}Am content in fuel from the No. 4 unit of the Chernobyl nuclear power plant. Atomic Energy. 1998. Vol. 84, No. 4. pp. 278-282.

Ageev V.A., Odintsov O.O., Sajeniouk A.D. Routine radiochemical method determination of ^{90}Sr, ^{238}Pu, $^{239+240}$Pu, ^{241}Am and ^{244}Cm in the different environmental samples. Book of Abstracts. *VI Int. Conf. on Methods and Applications of Radioanalytical Chemistry-MARC-VI.* (April 7-11. Kailua-Kona, 2003.) HI, 2003. pp. 64-65.

Akata N., Hasegawa H., Kawabata H. et al. Deposition of ^{137}Cs in Rokkasho, Japan and its relation to Asian dust. *J. Environ. Radioactiv*. 2007. Vol. 95, No. 1. pp.1-9.

Algazin A.I., Demin V.F., Gordeev K.I. et al. Radiation impact of nuclear weapon tests at the Semipalatinsk test site on the Altai region population. *Int. Sympos. of the Environmental Impact of Radiactive Releases.* (May 8-12. Vienna, Austria, 1995.) pp.1-13.

Allwine K.J., Rutz F.C., Shaw W.J. et al. DUSTRAN 1.0 User's Guide: A GIS-Based Atmospheric Dust Dispersion Modeling System, Technical Report PNNL-16055, Pacific Northwest National Laboratory: Richland, WA, 2006. 140 p.

Amiro B.D., Sheppard S.C., Johnston F.L. et al. Burning radionuclide question: What happens to iodine, cesium and chlorine in biomass fires. *Sci. Total Environ*. 1996, Vol.187. pp. 93-103.

Anokhova T.P., Krivtsova I.L. Labor conditions and safety measures for people involved in growing agricultural crops on territories contaminated by radioactive materials. In: Problems of Agricultural Radiology. Kyiv: Ukrainian Research Institute of Agricultural Radioecology, 1991. pp. 205-213. [in Russian]

Ansoborlo E., Guilmette R.A., Hoover M.D. et al. Application of *in vitro* dissolutions testes to different uranium compounds and comparison with *in vivo* data. *Radiat. Prot. Dosim*. 1998. Vol.79. pp. 33-37.

Ansoborlo E., Henge-Napoli M.H., Chazel V. et al. Review and critical analysis of available *in vitro* tests. *Health Phys*. 1999. Vol. 77 No. 6. pp. 638-645.

Anspaugh L.R., Phelps P.L. Resuspension element status report: VI. Results and data analysis. In: The Dynamics of Plutonium in Desert Environments; eds. Dunaway P.B., White M.G., USAEC Report NVO-142, Nevada Operations Office, NYIS, 1974. pp. 55-81.

Anspaugh L.R., Shinn J.H., Phelps P.L., Kennedy N.C. Resuspension and redistribution of plutonium in soils. *Health Phys*. 1975. Vol. 29. pp. 571-582.

Anspaugh L.R., Simon S.L., Gordeev K.I. et al. Movement of radionuclides in terrestrial ecosystems by physical processes. *Health Phys*. 2002. Vol. 82. pp. 669-679.

Aoyama M. Evidence of stratospheric fallout of caesium isotopes from Chernobyl accident. *Geophys. Res. Lett*. 1988. Vol. 4. pp. 327-330.

Assessment of the radiological consequences of the loss of integrity (Research report). SIP-I-SC-21-310-SAR-005-01, 2004. 80 p. [in Russian]

Bagnold R.A. The physics of blown sand and desert dunes. Springer, 1974. 265 p.

Barenblatt G.I. On the motion of suspended particles in a turbulent flow holding semi-infinite space or planar channel of finite depth. *Appl. Math. and Mech*. 1953. Vol. 17. pp. 261-274 [in Russian]

Bartzis J., Erhardt J., French S. et al. RODOS: decision support for nuclear emergencies. In: Zanakis H., Doukidis G., Zopounidis C. Decision Making: Recent Developments and Worldwide Applications, Springer Science & Business Media, 2013. pp. 381-396.

Bechtel SAIC 2006. Inhalation Exposure Input Parameters for the Biosphere Model, ANL-MGR-MD-000001, Rev. 04, Bechtel SAIC Co.: Las Vegas, NV, 2006. 118 p.

Beck H.L. Environmental gamma radiation from deposited fission products, 1960-1964. *Health Phys*. 1966. Vol.12. pp. 313-322.

Begichev S.N., Borovoy A.A., Burlakov E.V. et al. Fuel of 4 unit reactor of the Chernobyl NPp. Moscow: Kurchatov Institute of Atomic Energy, 1990, 21 p. (Preprint IAE-5268/3).

Belyaev S.P., Makhonko K.P., Mashkov S.T. Gauze cone for mass measurements of the radioactive dust concentration in the atmosphere. *Trudy IPG*. 1967. No. 8. pp. 123-129. [in Russian]

Belyaev S.P., Surnin V.A. Estimates of radioactive dust resuspension in Chernobyl in June 1986. *Trudy IEM*. 1991. Vol. 20, No.153. pp.133-140. [in Russian]

Bencala K.E., Seinfeld J.H. On frequency distributions of air pollutant concentrations. *Atmos. Envir*. 1976. Vol.10. pp. 941-950.

Berlyand M.E. Modern problems of atmospheric diffusion and air pollution, Leningrad: Hydrometeoizdat, 1975. 448 p. [in Russian]

Berner A., Lurzer C. Mass size distributions of traffic aerosol at Vienna. *J. Phys. Chem*. 1980. Vol. 84. pp. 2079-2083.

Beskorovajnyj V.P., Kotovich V.V., Molodykh V.G. et al. Radiation Consequences of Collapse of Structural Elements of the Sarcophagus. *Sarcophagus Safety '94*, The State of the Chernobyl Nuclear Power Plant Unit 4. *Proceedings of Int. Sympos.* (March 14-18, Zeleny Mys, Chernobyl, Ukraine. 1994). [in Russian]

Besnus F., Peres J.M., Guillou P. et al. Contamination characteristics of podzols from districts of Ukraine, Belarus and Russia strongly affected by the Chernobyl accident. In: The radiological consequences of the Chernobyl accident; eds. Karaoglou A. et al., Report EUR 16544 EN, Luxembourg: Office for Official Publications of the European Communities, 1997. pp. 205-208.

Beyeler W.E., Hareland W.A., Durán F.A. et al. Residual Radioactive Contamination from Decommissioning, Parameter Analysis. NUREG/CR-5512, Vol. 3. Washington, DC: U.S. Nuclear Regulatory Commission, Office of Nuclear Regulatory Research, 1999. 210 p.

BIOMOVS II. Atmospheric resuspension of radionuclides: Model testing using Chernobyl data, BIOMOVS II Technical Report No. 11, Stockholm: Swedish Radiation Protection Institute, 1996. 26 p.

Birchall A., Puncher M., James A.C. et al. IMBA-EXPERT: Internal dosimetry made simple. *Radiat Prot. Dosim*. 2003. Vol.105. pp. 421-424.

Blackford D., Quant F., Sem G. An improved aerodynamic particle size analyzer. *Proceedings of Fine Particle Society Annual Meeting,* Boston, MA, July 1987.

Bogatov S.A. Estimation of inventory and identification of the dust pollution properties in the roof space of the «Shelter». Chernobyl: ISTC «Ukrytiye», National Academy of Sciences of Ukraine, 2000, 16 p. (Preprint. ISTC «Ukrytiye», National Academy of Sciences of Ukraine; 00-2). [in Russian]

Bogatov S.A., Borovoy A.A., Dubasov U.V., Lomonosov V.V. Form and characteristics of the fuel emission for the accident of Chernobyl NPp. *Atomic Energy*. 1990. Vol. 69. pp. 36-40. [in Russian]

Bogorad V.I., Belov Ya.Yu., Kyrylenko Yu.O. et al. Forecast of a fire consequences in the Exclusion Zone of Chornobyl Nuclear Power Plant: combination of instruments of the mobile laboratory RanidSONNI and computer technologies of the DSS RODOS. *Yaderna ta radiaciyna bezpeka*. 2018. No. 3. 79. pp.10-15. [in Ukrainian]

Bogorad V.I., Litvinskaya T.V., Shevchenko I.A., Dybach O.M., Slepchenko O.Yu. Radiation consequences of a fire in the Exclusion Zone of Chornobyl Nuclear Power Plant. *Yaderna ta radiaciyna bezpeka*. 2016. No. 1, 69. pp. 64-68. [in Ukrainian]

Bogorad V.I., Zheleznyak M.I., Kovalets I.V. et al. Quantitative assessment of radioactive fallout caused by the potential destruction of the New Safe Confinement under the influence tornado class F 3.0. *Yadernaya i radiacionnaya bezopasnost*. 2006. No 1. pp. 28-34. [in Russian]

Bondarenko O.A., Garger E.K., Giriy V.A. et al. The spatial and temporal course of concentration and deposition of radionuclides in the 30 km zone of the Chernobyl nuclear power plant, In: Radiation Aspects of the Chernobyl Accident; ed. Izrael Y.A. *Proceedings of the 1st All-Union Conference «Radiation aspects of the Chernobyl accident»,* June 1988, Vol. 1. St. Petersburg: Hydrometeoizdat, 1993. [in Russian]

Borovoi A.A., Gagarinskii A.Yu. Emission of radionuclides from the destroyed unit of the Chernobyl Nuclear Power Plant. *Atomic Energy*. 2001. Vol. 90. pp. 153-161.

Borovoy A.A. Inside and outside Sarcophagus. *Priroda*. 1990. Vol.11. pp. 83-90. [in Russian]

Borovoy A.A. Release of nuclear fuel and fission products from the reactor of the 4th block of Chernobyl NPP during the accident (Review). Chernobyl: ISTC «Ukrytiye», National Academy of Sciences of Ukraine, 2000, 15 p. (Preprint. ISTC «Ukrytiye», National Academy of Sciences of Ukraine; 00-10). [in Russian]

Braaten D.A., Show R.H., Paw U.K.T. Particle detachment in turbulent boundary layers. AEROSOLS: Formation and Reactivity, *2nd Int. Aerosol Conf.,* Berlin, 1986. pp. 370-373.

Braaten D.A., Show R.H., Paw U.K.T. Coherent turbulent structures and particle detachment in boundary layer flows. *J. Aerosol Sci*. 1988. Vol.19. pp. 1183-1186.

Braaten D.A., Show R.H., Paw U.K.T. Particle resuspension in a turbulent boundary layer. *J. Aerosol Sci*. 1990. Vol. 21. pp. 613-628.

Briggs G.A. Plume Rise Predictions, Lectures on Air Pollution and Environmental Impact Analyses, Workshop Proceedings, Oct. 3, 1975. Boston, MA: American Meteorology Society, 1975. pp. 59-111.

Bryuhan F.F., Lyakhov M.E., Pogrebnyak V.N. Tornado dangerous areas in the USSR and placement of nuclear power plants. *Izvestiya Akademii Nauk, Seriya Geograficheskaya*. 1989. No.1. pp. 40-48. [in Russian]

Buikov M.V. A boundary condition for the equation of turbulent diffusion on the underlying surface. *Meteorology and Gidrology*. 1990. No. 9. pp. 52-56.

Buikov M.V. Turbulent transport of radioactive pollutant in view of the processes of resuspension and dry deposition. *Izvestiya, Academy of Sciences, USSR: Physics of the atmosphere and ocean*, 1993. Vol. 29, No. 2. pp. 202-207. [in Russian]

Bunzl K., Hötzl H., Winkler R. Spruce pollen as a source of increased radiocaesium concentrations in air. *Naturwissenschaften*. 1993. Vol. 80. pp. 173-174.

Bunzl K., Schimmack W., Krouglov S.V., Alexakhin R.M. Changes with time in the migration of radiocesium in the soil, as observed near Chernobyl and in Germany, 1986-1994. *Sci. Total Environ*. 1995. Vol. 175. pp. 49-56.

Byram G.M. Combustion of forest fuels. In: Forest fire: control and use; ed. K.P. Davis. New York: McGraw-Hill, 1959. pp. 61-89.

Byzova N.L., Garger E.K., Ivanov V.N. Experimental investigations of atmospheric diffusion and calculations of pollution dispersion. Leningrad: Gidrometeoizdat, 1991. 280 p. [in Russian]

Byzova N.L., Ivanov V.N., Garger E.K. Turbulence in the boundary layer of the atmosphere. Leningrad: Gidrometeoizdat, 1989. 264 p. [in Russian]

Chamberlain A.C. Radioactive aerosols. Cambridge: Cambridge University Press, 1991. 256 p.

Chepil W.S. Properties of soil which influence wind erosion, 4, State of dry aggregate structure. *Soil Sci*. 1951. Vol.72. pp. 387-401.

Chepil W.S. Transport by wind: Transport of soil and snow by wind. *Agric. Meteorol*. 1965. Vol. 6. pp. 123-132.

Chepil W.S., Woodruff N.P. Sedimentary Characteristics of Dust Storms: II Visibility and Dust Concentration. *Am. J. Sci*. 1957. Vol. 255. pp. 104-114.

Chkhetiani O.G., Gledzer E.B., Artamonova M.S., Iordanskii M.A. Dust resuspension under weak wind conditions: direct observations and model. *Atmos. Chem. Phys.* 2012. Vol. 12. pp. 5147-5162.

Choi J.C., Lee M., Chun Y. et al. Chemical composition and source signature of spring aerosol in Seoul, Korea. *J. Geophys. Res*. 2001. Vol.106. pp. 18067-18074.

Choi M.S., Lee D.-S., Choi J.C., et al. $^{239+240}$Pu concentration and isotope ratio (^{240}Pu/^{239}Pu) in aerosols during high dust (*Yellow Sand*) period, Korea. *Sci. Total Environ*. 2006. Vol. 370. pp. 262-270.

Chun Y., Cho H.K., Chung H.S., Lee M. Historical records of Asian dust events (*hwangsa*) in Korea. *B. Am. Meteorol. Soc.* 2008. Vol. 89. pp. 823-827.

Clausnitzer H., Singer M.J. Intensive land preparation emits respirable dust. *California Agriculture*. 1997. Vol. 51. pp. 27-30.

Cleaver J. W., Yates B. Mechanism of detachment of colloidal particles from a flat substrate in a turbulent flow. *J. Colloid Interface Sci*. 1973. Vol. 44. pp. 464-473.

Cowherd C., Muleski G.E., Englehart P.J., Gillette D.A. Rapid Assessment of Exposure to Particulate Emissions from Surface Contamination Sites, EPA/600/8-85/002, Washington, DC: Midwest Research Institute, 20460, 1985. 160 p.

Csanady G.T. Turbulent diffusion in the environment. Dordrecht: D. Reidel Publ. Comp., 1973. 250 p.

Decree of Construction Committee of Ukraine No. 64 from 21.10.2002 «Basic regulatory requirements and computational properties of tornadoes in the Chernobyl site». [in Russian]

Dennis N.A., Blauer H.M., Kent J.E. Dissolution fractions and half-times of single source yellowcake in simulated lung fluids. *Health Phys*. 1982. Vol. 42. pp. 469-477.

Derevets V.V., Ivanov J.P., Kazakov S.B., Sukhoruchkin A.K. Radiation state of the environment in the Chernobyl exclusion zone. IV *Int. scientific and engineering conf. «Chernobyl-94»:* Collection of reports. (Chernobyl, 1996). Vol. 1. pp. 4-20. [in Russian]

Devell L., Tovedal H., Bergstrom U. et al. Initial observations of fallout from the reactor accident at Chernobyl. *Nature*. 1986. Vol. 321. pp. 192-193.

Dubasov Yu.V., Savonenkov V.D., Smirnova E.A. Ordering of radioactive products of the Chernobyl NPP disaster. *Radiochemistry*. 1996. Vol. 38, No. 2. pp. 101-116. [in Russian]

Dusha-Gudym S.I. Transport of Radioactive Materials by Wildland fires in the Chernobyl Accident Zone: How to Address the Problem, *International Forest Fire News (IFFN)*, 2005. Vol. 32. pp. 119-125.

ECP1 Contamination of surfaces by resuspended material. Final Report EUR 16527, 1996.

Eidson A.F., Griffith Jr. W.C. Techniques for yellow cake dissolution studies *in vitro* and their use in bioassay interpretation. *Health Physics*. 1984. Vol. 46, No. 1. pp. 151-163.

Eidson A.F., Mewhinney J.A. *In vitro* dissolution of respirable aerosols of industrial uranium and plutonium mixed-oxide nuclear fuels. *Health Phys*. 1983. Vol. 45, No. 6. pp.1023-1037.

Ermilov A.P., Ziborov A.M. Radionuclide ratios in the fuel component of fallouts in the near Chernobyl NPP zone. *Radiation and risk*. 1993. Vol. 3. pp. 134-138.

Evangeliou N., Balkanski Y., Cozic A. et al. Wildfires in Chernobyl-contaminated forests and risks to the population and the environment: A new nuclear disaster about to happen. *Environ. Int.* 2014. Vol. 73. pp. 346-358.

Evangeliou N., Balkanski Y., Cozic A., et al. Fire evolution in the radioactive forests of Ukraine and Belarus: future risks for the population and the environment. *Ecol. Monogr.* 2015. Vol. 85(1). pp. 49-72.

Evangeliou N., Zibtsev S., Myroniuk V. et al. Resuspension and atmospheric transport of radionuclides due to wildfires near the Chernobyl Nuclear Power Plant in 2015: An impact assessment. Scientific Reports, 2016. Vol. 6. | DOI: 10.1038/srep26062, 2016.

Explanatory note to the technical solution «On the determination of critical events that must be considered in the development of project documentation for the decommissioning of the cooling pond of the Chernobyl NPP and radiological criteria requirements for end-state territory», 2012. 7 p. [in Ukrainian]

Fairchild C.I., Tillery M.I. Wind tunnel measurements of the resuspension of ideal particles. *Atmos. Environ.* 1982. Vol.16. pp. 229-238.

Fecan F., Marticorena B., Bergametti G. Parametrization of the increase of the aeolian erosion threshold wind friction velocity due to soil moisture for arid and semi -arid areas. *Ann. Geophys-Atm. Hydr.* 1999. Vol.17. pp. 149-157.

Feher I., Zombori P. Behaviour of airborne ^{131}I and ^{137}Cs radioaerosols. *Austrian-Italian-Hungarian Radiation Protection Sympos. Radiation Protection in neighbouring countries in Central* Europe. (28-30 April 1993, Obergirgl / Tyrol, Austria) . Proceedings, Vol. 1. pp. 19-22.

File R.F. Dust deposit in England on 9 November 1984. *Weather*. 1986. Vol. 41. pp. 191-195.

Finlayson-Pitts B.J., Pitts J.N. Atmospheric Chemistry: Fundamentals and Experimental Techniques. New York: John Wiley & Sons, 1986.

Frank G., Kashparov V., Protsak V., Tschiersch J. Comparison measurements of a Russian standard aerosol impactor wirh several Western standard aerosol insruments. *J. Aerosol Sci*. 1996. Vol. 27. pp. 477-486.

Fujiwara H., Fukuyama T., Shirato, Y. et al. Deposition of atmospheric ^{137}Cs in Japan associated with the Asian dust event of March 2002. *Sci. Total Environ*. 2007. Vol. 384, No. 1-3. pp. 306-315.

Fukuyama T., Fujiwara H. Contribution of Asian dust to atmospheric deposition of radioactive cesium (^{137}Cs). *Sci. Total Environ*. 2008. Vol. 405, No. 1-3. pp. 389-395.

Gamble J.L. Chemical anatomy: physiology and pathology of extracellular fluid. Boston: Harvard University Press, 1967. 107 p.

Garger E.K. Experimental evaluation of certain factors of similarity formulas for Lagrangian turbulence characteristics in the surface layer of the atmosphere. *Izvestiya, Academy of Sciences, USSR: Physics of the atmosphere and ocean.* 1982. Vol. 18, No. 8. pp. 783-796. [in Russian]

Garger E.K. Air concentrations of radionuclides in the vicinity of Chernobyl and effects of resuspension. *J. Aerosol Sci*. 1994. Vol. 25. pp. 745-753.

Garger E.K. The emission intensity and the dry deposition velocity of radioactive aerosols in agricultural works. *Agroecological magazine*. 2001. No. 1. pp. 12-15. [in Russian]

Garger E.K. Reentrainment of radioactive aerosol in the surface layer of the atmosphere. Chornobyl: Institute for the Safety Problems of Nuclear Power Plants, 2008. 192 p. [in Russian]

Garger E.K. To calculate local, mesoscale and regional effects of secondary air pollution. Scientific report «Wind lifting and carrying over radionuclides in the around failure of the Chernobyl NPP», SPA»Typhoon», Obninsk: Institute Experimental Meteorology, 1987. 156 p. [in Russian]

Garger E.K., Anspaugh R.L.R., Shinn J.H., Hoffman F.O. A test of resuspension-factor models against Chernobyl data. *Proceedings of an international symposium on environmental impact of radioactive releases* organized by the IAEA, Vienna, 1995. pp. 369-376.

Garger E.K., Gavrilov V.P. Secondary pollution of 30 km zone of the Chernobyl nuclear power plant and the surrounding area due to radionuclides resuspension. *Atomic Energy*. 1992. Vol.72. pp. 588-593. [in Russian]

Garger E.K., Gavrilov V.P., Zhukov G.P. Estimation of the secondary contamination by resuspension within the 30 km zone of the Chernobyl Nuclear Power Plant and its comparison with measured data. In: Precipitation Scavenging and Atmospheric-Surface Exchange; eds. Schwartz S.E., Slinn W.G.N. *Proceedings of the Fifth Int. Conf.* (15-19 July 1991, Richland, WA). Washington, DC: Hemisphere Publishing, 1992, Vol. 3. pp. 1592-1603.

Garger E.K., Hoffman F.O., Miller C.W. Model testing using Chernobyl data. III. Atmospheric resuspension of radionuclides in Ukrainian regions impacted by Chernobyl fallout. *Health Physics*. 1996. Vol. 70. pp. 18-24.

Garger E.K., Hoffman F.O., Thiessen K.M. Uncertainty of the long-term resuspension factor. *Atmos. Environ*. 1997. Vol. 31. pp. 1647-1656.

Garger E.K., Hoffman F.O., Thiessen K.M. et al. Test of existing mathematical models for atmospheric resuspension of radionuclides. *J. Environ. Radioactiv*. 1999. Vol. 42. pp. 157-175.

Garger E.K., Kashpur V.A. Assessment of the secondary radioactive contamination of the environment associated with the transport of radionuclides due to forest fires. Development of recommendations to minimize the harmful impact of ionizing radiation on the body of fire fighters, Report of Institute of Radioecology UAAS, 1995. [in Russian]

Garger E.K., Kashpur V.A. Investigation of the object «Ukrytie» as a radioactive aerosol source in the surface layer of the atmosphere. Regulation of the control of radioactive aerosol releases from the object «Ukrytie». Report of IAB UAAS, 2000, Vols. 1-3. [in Russian]

Garger E.K., Kashpur V.A., Belov G. et al. Measurement of resuspended aerosol in the Chernobyl area. Part I: Discussion of instrumentation and estimation of measurement uncertainty. *Radiat. Environ. Biophys.* 1997. Vol. 36. pp. 139-148.

Garger E.K., Kashpur V.A., Gurgula B.I. et al. Statistical characteristics of the activity concentration in the surface layer of the atmosphere in the 30-km zone of Chernobyl. *J. Aerosol Sci*. 1994. Vol. 25, No. 5. pp.767-777.

Garger E.K., Kashpur V.A., Korneev A.A., Kurochkin A.A. Results of studies of radioactive aerosols release from the «Shelter» object. *Problems of Chernobyl*. 2002. Vol.10, No. 2. pp. 60-71. [in Russian]

Garger E.K., Kashpur V.A., Li W.B., Tschiersch J. Radioactive aerosols released from the Chernobyl Shelter into the immediate environment. *Radiat. Environ. Biophys*. 2006. Vol. 45. pp. 105-114.

Garger E.K., Kashpur V.A., Paretzke H.G., Tschiersch J. Measurement of resuspended aerosol in the Chernobyl area. Part II: Size distribution of radioactive particles. *Radiat. Environ. Biophys*. 1998. Vol. 36. pp. 275-283.

Garger E.K., Kashpur V.A., Sazhenyuk A.D. et al. Aerosol characteristics of disorganized releases from the «Shelter» object. *Problems of Nuclear Power Plants' Safety and of Chernobyl*. 2004. Vol. 1. pp. 125-135. [in Russian]

Garger E.K., Kashpur V.A., Skoryak G.G. et al. Aerosol radioactivity and disperse structure at the Chernobyl NPP during the period of forest fires. *Agroecol. J.* 2004. Vol. 3. pp. 6-12. [in Russian]

Garger E.K., Kuzmenko Yu.I., Sickinger S., Tschiersch J. Prediction of the ^{137}Cs activity concentration in the atmospheric surface layer of the Chernobyl exclusion zone. *J. Environ. Radioactiv*. 2012. Vol. 110. pp. 53-58.

Garger E.K., Paretzke H.G., Tschiersch J. Measurement of resuspended aerosol in the Chernobyl area. Part III: size distribution and dry deposition velocity of radioactive particles during anthropogenic enhanced resuspension. *Radiat. Environ. Biophys*. 1998. Vol. 37. pp. 201-208.

Garger E.K., Sazhenyuk A.D., Odintzov A.A. et al. Solubility of airborn radioactive fuel particles from the Chernobyl reactor and implication to dose. *Radiat. Environ. Biophys*. 2004. Vol. 43. pp. 43-49.

Garger E.K., Shynkarenko V.K., Kashpur V.O. et al. Assessment of aerosol radiation environment in short-range region of ChNPP during building of the New Safe Confinement. *Problems of Nuclear Power Plants' Safety and of Chernobyl*. 2017. Vol. 29. pp.78-84.

Garger E.K., Zhukov G.P., Lukoyanov N.F. Study of pollutant dispersion from low sources in the presence of a single obstacle. *Trudy IEM*. 1988. Vol. 46, No. 136. pp. 106-114. [in Russian]

Garger E.K., Zhukov G.P., Sedunov Yu.S. Estimation of radionuclides resuspension parameters in the Chernobyl nuclear power plant area. *Meteorology and Hydrology*. 1990. No. 1. pp. 5-10. [in Russian]

Garland J.A. Some recent studies of the resuspension of deposited material from soil and grass. In: Precipitation scavenging, dry deposition and resuspension; eds. Pruppacher H.R., Semonin R.G., Slinn W.G.N. Elsevier: Amsterdam, 1983, Vol. 2. pp. 1087-1097.

Garland J.A. Resuspension of particulate material from grass. Experimental programme 1979-1980, AERE-R10106. London: HMSO, 1982. 30 p.

Garland J.A. Resuspension of particulate matter from grass and soil, AERE-R9452. London: HMSO, 1979. 30 p.

Garland J.A., Pattenden N.J., Playford K. Resuspension following Chernobyl, In: Modelling of resuspension, seasonality and losses during food processing, First Report of the VAMP Terrestrial Working Group, Vienna, Austria: *Int. Atomic Energy Agency,* IAEA-TEC-DOC-647, 1992. pp. 9-34.

Garland J.A., Pomeroy I.R. Resuspension of fall-out material following the Chernobyl accident. *J. Aerosol Science*. 1994. Vol. 25, No. 5. pp. 793-806.

Gavrilov V.P., Gormatyuk Yu. Dispersion of a pollutant from stationary sources in the atmospheric surface layer. *Meteorologiya and Gidrologiya*. 1989. No. 2. pp. 37-47.

Gaziev J.I., Kabanov Y.I. Study of contamination of the surface layer of the atmosphere by «hot» particles and inhalation fraction of the aerosol component of products of the accident on the Chernobyl NPp. In: Radiation Aspects of the Chernobyl Accident; ed. Izrael Yu.A. *Proceedings of the 1st All-Union Conf.* (June 1988 Obninsk). Sankt-Petersburg: Gidrometeoizdat, 1993. Vol.1. pp. 104-107. [in Russian]

Gaziev J.I., Nazarov L.E., Lachikhin A.V., Valetova N.K. Investigation of physics characteristics of the radioactive gas-aerosol products of the accident of Chernobyl NPP and estimations of power of technogenic emission of these products in the atmosphere, In: Radiation Aspects of the Chernobyl Accident; ed. Izrael Yu.A. *Proceedings of the 1st All-Union Conf.*, (June 1988, Obninsk). Sankt-Petersburg: Gidrometeoizdat, 1993. Vol.1. pp. 98-103. [in Russian]

Gillette D.A. On the production of soil wind erosion aerosols having the potential for long range transport. Special Issue of Journal de Recherches Atmospheriques on the Nice Symposium on the Chemistry of Sea-Air Particulate Exchange Processes. Nice, France, Oct. 1973.

Gillette D.A. On the production on soil wind erosion aerosols having the potential for long range transport. *Atmos. Res.* 1974. Vol.8, No. 3/4. pp. 735-744.

Gillette D.A. Production of Fine Dust by Wind Erosion of Soil: Effect of Wind and Soil Texture. *Proceedings of the Atmospheric-Surface Exchange of Particulate and Gaseous Pollutants.* Richland, 1976. pp. 591-609.

Gillette D.A., Blifford Jr I.H., Fenster Ch.R. Measurements of aerosol size distributions and vertical fluxes of aerosols on land subject to wind erosion. *J. Appl. Meteorol*. 1972. Vol.11. pp. 977-987.

Gillette D., Passi R. Modeling dust emission caused by wind erosion. *J. Geophys. Res*. 1988. Vol.93. pp. 14233-14242.

Gillies J.A., Etyemezian V., Kuhns H. et al. Effect of vehicle characteristics on unpaved road dust emissions. *Atmospheric Env*. 2005. Vol.39. pp. 2341-2347.

Goldammer J.G., Kashparov V., Zibtsev S., Robinson S. Best practices to combat wildfires in contaminated areas and recommendations on firemen safety under fires on the radioactive contaminated territories. Freiburg - Basel - Kyiv: Global Fire Monitoring Center (GFMC), 2015. 59 p. [in Russian]

Grebenkov A., Baxter L.L., Fogh C.L. et al. Formation and release of radioactive aerosols during combustion of contaminated biomass. In: *Proceedings of Int. Conf. on Radioactivity in the Environment,* (1-5 September 2002, Monaco). pp. 493-496.

Grishin A.M. Mathematical modeling of forest fires and new ways of fire-fighting. Novosibirsk: Nauka, 1992. 408 p.

Gudihy R.G., Finch G.L., Newton G.J. et al. Characteristics of Radioactive Particles Released from the Chernobyl Nuclear Reactor. *Environ. Sci. Technology*. 1989. Vol. 23. pp. 89-95.

Gudiksen P.H., Lindeken C.L., Gatrousis C., Anspaugh L.R. USAEC Rept. UCRL-51242. Livermore, CA: Lawrence Livermore Laboratory, 1972.

Gudiksen P.H., Lindeken C.L., Meadows J.W., Hamby K.O. USAEC Rept. UCRL-51333. Livermore, CA: Lawrence Livermore Laboratory, 1973.

Hall D., Reed J. The time dependence of the resuspension of particles. *J. Aerosol Sci.* 1989. Vol. 20. pp. 839-842.

Hamadneh H.S., Ababneh Z.Q., Hamasha K.M., Ababneh A.M. The radioactivity of seasonal dust storms in the Middle East: the May 2012 case study in Jordan. *J. Environ. Radioactiv*. 2015. Vol.140. pp. 65-69.

Hamilton E.I. Concentration of uranium in air from contrasted natural environments. *Health Phys*. 1970. Vol. 19. pp. 511-520.

Hao W.M., Bondarenko O.O., Zibtsev S., Hutton D. Vegetation fires, smoke emissions, and dispersion of radionuclides in the Chernobyl Exclusion Zone, In: Wildland Fires and Air Pollution; eds. Bytnerowicz A. et al. Developments in Environmental Science. Vol. 8. DOI:10.1016/S1474-8177(08)00012-0, 2009. pp. 265-275.

Harada K.H., Niisoe T., Imanaka M., Takahashi T. Radiation dose rates now and in the future for residents neighboring restricted areas of the Fukushima Daiichi Nuclear Power Plant. *PNAS.* 2014. Vol.111. pp. E914-E923.

Hatano Y., Hatano N. Formula for the resuspension factor and estimation of the date of surface contamination. *J. Atmos. Environ*. 2003. Vol. 37. pp. 3475-3480.

Haynes H.R., Taylor D.H. Estimating doses from tornado winds. DPST-82-982, E. I. du Pond de Nemours & Co., Aiken, SC, 1983. 33 p.

Healy J.W. A Proposed Interium Standard for Plutonium in Soils, USAEC Report LA-5483-MS, Los Alamos Scientific Laboratory, NTIS, 1974. 100 p.

Healy J.W. Review of resuspension models, In: Transuranic Elements in the Environment; ed. Hanson W.C., DOE/TIC-22800, U.S. Department of Energy, 1980. pp. 209-235.

Healy J.W., Fuquay J.J. Wind Pickup of Radioactive Particles from the Ground, In: *Proceedings of the Second United Nations Int. Conf. on the Peaceful Uses of Atomic Energy.* Geneva, New York: United Nations, 1958, pp. 291-295.

Hoetzl H., Rosner G., Wincler R. Long-term behaviour of Chernobyl fallout in air and precipitation. *J. Environ. Radioactiv.* 1989. Vol.10. pp. 157-171.

Hoetzl H., Rosner G., Wincler R. Sources of present Chernobyl derived caesium concentrations in surface air and deposition samples. *Sci. Total Environ*. 1992. Vol.119. pp. 231-242.

Hohl A., Niccolai A., Oliver C. et al. The human health effects of radioactive smoke from a catastrophic wildfire in the Chernobyl Exclusion Zone: A worst case scenario. *J. Earth Bioresources and Life Quality.* 2012. Vol.1. pp. 1-34.

Hollander W. Resuspension factors of ^{137}Cs in Hannover after the Chernobyl accident. *J. Aerosol Sci*. 1994. Vol. 25. pp. 789-792.

Hollander W., Dunkhorst W., Pohlmann G. A sampler for total suspended particulates with size resolution and high sampling efficiency for large particles. *Part. Syst. Charact*. 1989. Vol. 6. pp. 74- 80.

Hollander W., Garger E. Contamination of surfaces by resuspended material. Experimental collaboration project No. 1, Final report. EUR 16527. Luxembourg: Office for Official Publications of the European Communities, 1996. 149 p.

Homann S.G., Aluzzi F. HotSpot. Health Physics Codes. Version 3.0. User's Guide, LLNL-SM-636474, National Atmospheric Release Advisory Center Lawrence Livermore National Laboratory: Livermore, CA, 2013. 160 p.

Horn H-G., Bonka H., Maqua M. Measured particle bound activity size distribution, deposition velocity, and activity concentration in rainwater after the Chernobyl accident. *J. Aerosol Sci*. 1987. Vol.18. pp. 681-684.

Horrill A.D., Kennedy V.H., Paterson I.S., McGowan G.M. The effect of heather burning on the transfer of radiocaesium to smoke and the solubility of radiocaesium associated with different types of heather ash. *J. Environ. Radioactiv*. 1995. Vol. 29. pp. 1-10.

Huang C.H. A theory of dispersion in turbulent shear flow. *Atmos. Environ*. 1979. Vol.13, No. 4. pp. 453-463.

IAEA (Internation Atomic Energy Agency). Handbook of Parameter Values for the Prediction of Radionuclide Transfer in Terrestrial and Freshwater Environments. Technical Reports Series No. 472, Vienna: International Atomic Energy Agency, 2010.

ICRP. *Radionuclide Transformations - Energy and Intensity of Emissions*, Ann. ICRP 11-13, ICRP Publication 38, 1983.

ICRP. Age-dependent Doses to Members of the Public from Intake of Radionuclides. Part 1. Ann. ICRP 20 (2), ICRP Publication 56, 1990.

ICRP. Age-dependent Doses to Members of the Public from Intake of Radionuclides. Part 2. Ingestion Dose Coefficients, Ann. ICRP 23 (3-4), ICRP Publication 67, 1993.

ICRP. Human Respiratory Tract Model for Radiological Protection. Ann. ICRP 24 (1-3), ICRP Publication 66, 1994.

Ievdin I., Trybushnui D., Landman C.J. Rodos User's Guide. Karlsruhe Institute of Technology (KIT). 2017. 111 p.

Igarashi Y., Inomata Y., Aoyama M. et al. Possible change in Asian dust source suggested by atmospheric anthropogenic radionuclides during the 2000s. *Atmos. Environ*. 2009. Vol. 43. pp. 2971-2980.

Ishizuka M., Mikami M., Tanaka T.Y. et al. Use of a size-resolved 1-D resuspension scheme to evaluate resuspended radioactive material associated with mineral dust particles from the ground surface. *J. Environ. Radioactiv*. 2017. Vol. 166. pp. 436-448.

Ivakhnenko A.G. Long-term forecasting and management of complex systems. Kyiv: Tehnika, 1975. [in Russian]

Ivakhnenko A.G., Koppa Yu.V., Stepashko V.S. et al. *The handbook on typical software programs for modeling: ed.* Ivakhnenko A.G. Kyiv: Tehnika, 1980. 184 p. [in Russian]

Izrael Yu.A. Chernobyl: radioactive pollution of the environment, Leningrad: Hydrometeoizdat, 1990.

Izrael Yu.A., De Cort M., Jones A.R. et al. The atlas of caesium-137 contamination of Europe after the Chernobyl accident. In: The Radiological Consequences of the Chernobyl Accident; eds. Karaoglou A., Desmet G., Kelly G.N. et al. *Proceedings of the First Int. Conf.* (March 1996, Minsk, Belarus), EUR 16544. pp. 1-10.

Jacob P., Roth P., Golikov V. et al. Exposures from external radiation and from inhalation of resuspended material. In: The Radiological Consequences of the Chernobyl Accident; eds. Karaoglou A., Desmet G., Kelly G.N. et al. *Proceedings of the First Int. Conf.* (March 1996, Minsk, Belarus), EUR 16544. pp. 251-260.

JNREG. Sources contributing to radioactive contamination of the Techa river and areas surrounding the «Mayak» production association, Urals, Russia (1997). Programme on Investigations of Possible Impacts of the «Mayak» PA Activities on Radioactive Contamination of the Barents and Kara Seas, Joint Norwegian-Russian Expert Group for Investigation of Radioactive Contamination in the Northern Areas, Osteras, 1997. 134 p.

Johnson T.C., Gillette D.A., Schwiesow R.L. Fate dust particles from unpaved roads under various atmospherics conditions, In: Precipitation Scavenging and Atmosphere - Surface Exchange, Hemisphere Publishing Corporation, 1992, Vol. 2. The Semonin volume: Atmosphere — Surface Exchange Processes. pp. 933-945.

Jost D.T., Gäggeler H.W., Baltensperger U. et al. Chernobyl fallout in size-fractionated aerosol. *Nature*. 1986. Vol. 324. pp. 22-23.

Kashparov V., Levchuk S., Khomutynyn I., Morozova V. Chernobyl: 30 Years of Radioactive Contamination Legacy. Report of Ukrainian Institute of Agricultural Radiology of National University of Life and Environmental Sciences of Ukraine, Kyiv, 2016. 59 p.

Kashparov V.A., Lundin S.M., Kadygrib A.M. et al. Forest fires in the territory contaminated as a result of the Chernobyl accident: radioactive aerosol resuspension and exposure of fire-fighters. *J. Environ. Radioactiv.* 2000. Vol. 51. pp. 281-298.

Kashparov V.A., Lundin S.M., Khomutinin Yu.V. et al. Soil contamination with ^{90}Sr in the near zone of the Chernobyl accident. *J. Environ. Radioactiv.* 2001. Vol. 56. pp. 285-298.

Kashparov V.A., Zhurba M.A., Kireev S.I. et al. Evaluation of expected exposure doses for fire-fighting participants in the Chernobyl exclusion zone in April 2015. *Yaderna Fizyka ta Energetyka*. 2015. Vol.16. pp. 399-407 [in Russian]

Kido H., Fujiwara H., Jamsran U., Endo A. The simulation of long-range transport of ^{137}Cs from East Asia to Japan in 2002 and 2006. *J. Environ. Radioactiv*. 2012. Vol. 103. pp. 7-14.

Kind R.J. One-dimensional aeolian suspension abobe beds of loose paricles — a new concentration-profile equation. *Atmos. Environ.* 1992. Vol. 26A. pp. 927-931.

Kok J.F., Parteli E.J.R., Michaels T.I., Karam D.B. The physics of wind-blown sand and dust. *Rept. Prog. Phys*. 2012. Vol. 75, No. 10. pp. 106-901.

Kondratiev I.I., Skalyga O.R. Atmospheric transboundary transport of cesium-137 with terrigenous dust from Asian deserts to the southern Far East. *Geogr. Nat. Resour*. 2011. Vol. 32, No. 2. pp. 126-131.

Kozlov A.S., Ankilov A.N., Baklanov A.M. et al. Investigations of mechanical processes of the submicron aerosol generation. *Atmos. Ocean. Opt*. 2000. Vol. 13. pp. 664-666.

Krasnov V.O., Nosovskyi A.V., Rudko V.M., Shcherbin V.M. *Shelter: 30 Years after the Accident.* Chornobyl: Institute for Safety Problems of NPP, National Academy of Sciences of Ukraine, 2016. 512 p. [in Ukrainian]

Krey P.W., Hardy E.P. Plutonium in soil around the Rocky Flats Plant, USAEC Rept., HASL-235, 1970.

Kulan A. Seasonal ^{7}Be and ^{137}Cs activities in surface air before and after the Chernobyl event. *J. Environ. Radioactiv.* 2006. Vol. 90. pp. 140-150.

Kumazawa S. Reappraisal of predictive models for resuspension. *J. Progress in Nuclear Science and Technology*. 2014. Vol. 4. pp. 875-878.

Kuriny V., Ivanov Y., Kashparov V. et al. Particle-associated Chernobyl fall-out in the local and intermediate zones. *Ann. Nucl. Energy*. 1993. Vol. 20. pp. 415-420.

Kutkov V.A., Kamarinskaya O.I. *In vitro* Solubility of Chernobyl Nuclear Fuel Aerosol With Respect to Collective Behaviour of Its Radionuclides. IRPA 9 International Congress on Radiation Protection, Vol. 2, 1996. pp. 445-447.

Kuzmina I.E. Experimental studies of disperse composition of aerosols of the «Shelter» object. IA9700098, Chernobyl: ISTC «Shelter», 1994. pp. 124-128. [in Russian]

Kuzmina I.E., Tokarevskiy V.V. Aerosol particles dispersed phase «Shelter». *Problems of the Chornobyl exclusion zone*. 1996. Vol. 4. pp. 141-150. [in Russian]

Kuznetsova I.N., Shakina N.P., Ivanova A.R. Episodes of radioactivity increase in the near-ground air in Russia. *Int. Conf. «The radioactivity in nuclear explosions and accidents»* (24-26 April 2000, Moscow), *Proceedings*. Vol. 1. pp. 507-516. [in Russian]

Lagunenko A.S., Khan V.E., Kalinovskiy A.K. et al. Control of releases of radioactive aerosols from Object «Ukryttya» in 2015-2016. *Problems of Nuclear Power Plants Safety and of Chernobyl*. 2017. Vol. 29. pp. 69-77. [in Russian]

Lassey K.R. The possible importance of short-term exposure to resuspended radionuclides. *Health Phys*. 1980. Vol.38, No. 5. pp. 749-761.

Lebedeff S.A., Hameed S. Steady-state solution of the semi-empirical diffusion equation for area sources. *J. Appl. Meteor*. 1975. Vol. 14. pp. 546-549.

Lem P.N., Behar J.V., Buck F.N. Resuspension of plutonium from contaminated land surfaces: meteorological factors. EPA-600/4-77-037, Las-Vegas, NV, 89114, 1977. 36 p.

Linsley G.S. Resuspension of the Transuranium Elements: A Review of Existing Data. Harwell, UK: National Radiological Protection Board, 1978.

Lipinskiy V.M., Osadchiy V.I., Babichenko V.M. Natural meteorological phenomena in Ukraine over the past twenty years (1986-2005), Kyiv: Nika-Center, 2006. [in Ukrainian]

Livens F.R., Baxter M.S. Particle size and radionuclide levels in some West Cumbrian soils. *Sci. Total Env*. 1988. Vol. 70. pp. 1-17.

Lomb N.R. Least-squary frequency analysis of unequally spaced data. *Astrophys. Space Sci*. 1976. Vol. 39. pp. 447-462.

Loosmore G.A. Evaluation and development of models for resuspension of aerosols at short times after deposition. *Atmos. Environ.* 2003. Vol. 37. pp. 639-647.

Loosmore G.A., Hunt J.R. Dust resuspension without saltation. *J. Geophys. Res*. 2000. Vol. 105 (D16). pp. 20663-20672.

Loshchilov N.A., Kashparov V.A., Yudin E.B. et al. Inhalation of radionuclides during farming on the territory contaminated during Chernobyl accident. In: Problems of Agricultural Radiology, Ukrainian Research Institute of Agricultural Radioecology, Kyiv, Ukraine, 1991. pp. 197-205. [in Russian]

Lu H., Shao Y. A new model for dust emission by saltation bombardment. *J. Geophys. Res*. 1999. Vol. 104. pp. 16827-16842.

Lujaniene G., Aninkevicius V., Lujanas V. Artificial radionuclides in the atmosphere over Lithuania. *J. Environ. Radioactiv.* 2009. Vol. 100. pp. 108-119.

Lujaniene G., Ogorodnikov B., Budyka A. et al. An investigation of changes in radionuclide carrier properties. *J. Environ. Radioactiv*. 1997. Vol. 35, No. 1. pp. 71-90.

Lujaniene G., Jbapolaite J., Remeikis V. et al. Cesium, americium and plutonium isotopes in ground level air of Vilnius. *Czechoslovak Journal of Physics.* 2006. Vol. 56 (D). P. D55-D61.

Lukoyanov N.F., Naydenov A.B., Meshkova V.G. Assessment of ^{137}Cs contamination of near-surface atmosphere and its distribution in the soil and the atmosphere above a cultivated field, *Trudy IEM.*, Vol. 57, No. 159. pp. 37-50. [in Russian]

Magnoni M. *A* theoretical approach to the re-suspension factor, EPJ Web of Conferences 24**,** 05008, 2012, DOI: 10.1051/epjconf 20122405008.

Makhonko K.P. Return flow of dust, which has settled on the ground, back into the atmosphere. *Izv. Akad. Nauk SSSR. FAO.* 1979. Vol. 15, No. 5. pp. 568-570.

Makhonko K. P. On the effective velocity of the dust resuspension from the underlying surface. *Meteorology and Hydrology*. 1981. No. 2. pp. 105-107. [in Russian]

Makhonko K.P. Radionuclide deflation effects in a contaminated locality with intermittent and steady-state discharges into the atmosphere. *Atomic Energy*. 1984. Vol. 56, No. 1. pp. 52-55.

Makhonko K.P. Effective rate of wind pickup of dust from the ground. *Meteorologiya i Gidrologiya*. 1984. No. 2. pp. 105-107.

Makhonko K.P. Wind pickup of dust from grass-covered ground. *Meteorology and Hydrology*. 1986. No. 10. pp. 61-65. [in Russian]

Makhonko K.P. Wind uplift of radioactive dust from the ground. *Atomic Energy*. 1992. Vol.72, No. 5. pp. 465-472.

Makhonko K.P. Evaluation of changes with time of the cesium-137 resuspension factor from the ground after the Chernobyl accident. In: Radiation aspects of the Chernobyl accident; ed. Izrael Yu.A. Vol. 1. St. Petersburg: Gidrometeoizdat, 1993. pp. 289-294. [in Russian]

Makhonko K.P. Wind pick-up of radioactive dust from the earth surface. Obninsk: NPO Typhoon, 2008. 428 p. [in Russian]

Makhonko K.P., Robotnova F.A. Resuspension and radioactive fallout from soil surface and particulate contamination of vegetative cover. *Pure Appl. Geophys*. 1982. Vol. 120. pp. 54-66.

Makrogiannis T., Flocas A., Ramos N., Karipidis A. A case of dust fall and coloured rain in the Greek area. *Riv. Meteorol. Aeronau*. 1990. Vol. 50, No. 1-2. pp. 65-74.

Mandel J., Beezley J.D., Kochanski A.K. Coupled atmosphere-wildland fire modeling with WRF 3.3 and SFIRE 2011. *Geosci. Model Dev*. 2011. Vol. 4. pp. 591-610.

Marple V.A., Liu D.Y.H. Characteristics of laminar jet impactors. *Environ. Sci. Technol.* 1974. Vol. 8. pp. 648-654.

Marticorena B., Bergametti G. Modeling the atmospheric dust cycle. 1. Design of a soil-derived emission scheme. *J. Geophys. Res*. 1995. Vol. 100. pp. 16415-16430.

Marticorena B., Bergametti G., Aumont B. et al. Modeling the atmospheric dust cycle. 2. Simulation of Saharan dust sources. *J. Geophys. Res*. 1997. Vol.102 (D4). pp. 4387-4404.

Matthias-Maser S., Jaenicke R. Examination of atmospheric bioaerosol particles with radii > 0.2 μm. *J. Aerosol Science*. 1994. Vol. 25. pp. 1605-1613.

Mauro J., Anspaugh L., Barton R., Meldrum A. Status report on resuspension issues at the Nevada test site, Vienna, Virginia 22182, National Institute for Occupational Safety and Health, NTS Resuspension Issues Status, 2015.

Maxwell R.M., Anspaugh L.R. An improved model for prediction of resuspension. *J. Health Physics*. 2011. Vol.101, No. 6. pp. 722-730.

McKendry I.G., Hacker J.P., Stull R. et al. Long-range transport of Asian dust to the Lower Fraser Valley, British Columbia, Canada. *J. Geophys. Res*. 2001. Vol. 106. pp. 18361-18370.

Menut L., Masson O., Bessagnet B. Contribution of Saharan dust on radionuclide aerosol activity levels in Europe. The 21-22 February 2004 case study. *J. Geophys. Res*. 2009. Vol. 114. pp. D16202.

Mercer T.T. On the role of particle size in the dissolution of lung burdens. *Health Physics*. 1967. Vol.13. pp. 1211-1221.

Merkushkin A.O. Karachay Lake is the storage of the radioactive wastes under open sky. International Youth Nuclear Congress 2000: Youth, Future, Nuclear. *Proceedings and Multimedia Presentation,* 2000. http://www.iaea.org/inis/collection/NCLCollectionStore/_Public/33/011/33011239.pdf.

Meshalkin G.S., Arkhipov N.P., Arkhipov A.N. et al. Water and wind migration of radionuclides in the territory of the Chernobyl exclusion zone. In: *Proceedings of 3rd All-Union scientific and technical conference on the basis of liquidation of the Chernobyl accident consequences,* Chernobyl, 1992. Vol. 2. pp. 225-235. [in Russian]

Miglio J.J., Muggenburg B.A., Brooks A.L. A rapid method for determining the relative solubility of plutonium aerosols. *Health Physics*. 1977. Vol. 33. pp. 449-457.

Mills M.T., Dahlman R., Olson J.S. Ground level air concentrations of dust particles downwind from a tailings area during a typical windstorm. USAEC Report ORNL/TM-4375, Oak-Ridge National Laboratory, NTIS: Oak-Ridge, TN, 1974.

Monin A.S. The atmospheric boundary layer. *A. Rev. Fluid Mech*. 1970. Vol. 2. pp. 225-247.

Monin A.S., Yaglom A.M. Statistical Fluid Mechanics: Mechanics of Turbulence. Vol. 1. Cambridge: MIT Press, 1970. 769 p.

Nair S.K., Miller C.W., Thiessen K.M. et al. Modeling the resuspension of radionuclides in Ukrainian regions impacted by Chernobyl fallout. *Health Physics*. 1997. Vol.72. pp. 77-85.

Naydenov A.V., Lukoyanov N.F. Experimental evaluation of vertical flow and radioactive dust resuspension intensity over contaminated cultivated field, *Trudy IEM*, 1994, Vol. 57, No. 159. pp. 17-27. [in Russian]

NCRP. Recommended Screening Limits for Contaminated Surface Soil and Review of Factors Relevant to Site-Specific Studies, Report No. 129, Bethesda, Md, 1999.

Newman J.E., Abel M.D., Harrison P.R., Yost K.J. Wind as Related to Critical Flushing Speed Versus Reflotation Speed by High-Volume Sampler Particulate Loading, *Proceedings of the Atmosphere-Surface Exchange of Particulate and Gaseous Pollutants-1974 Symposium*, Richland, WA, September 4-6, 1974, ERDA Symposium series, CONF-740921, National Technical Information Service: Springfield, VA, 1976. pp. 466-496.

Nicholson K.W. A review of particle resuspension. *Atmos. Environ*. 1988. Vol. 12. pp. 2639-2651.

Nicholson K.W. Wind tunnel measurements on the resuspension of particulate material. *Atmos. Environ.* 1993. Vol. 27A. pp. 181-188.

Nicholson K.W., Branson J.R. Factors affecting resuspension by road traffic. *Sci. Total Environ.* 1990. Vol. 93. pp. 349-358.

Nicholson K.W., Branson J.R., Geiss P., Cannell R.J. The effects of vehicle activity on particle resuspension. *J. Aerosol Science*. 1989. Vol.20, No. 8. pp. 1425-1428.

Nicholson K.W., Garland J.A., Branson J.R. *The resuspension of particulate material.* A summary report. Oxon, UK: AEA Environment and Energy Harwell Laboratory, 1993.

Nimmatoori P., Kumar A. Development and evaluation of a ground-level area source analytical dispersion model to predict particulate matter concentration for different particle sizes. *J. Aerosol Sci*. 2013. Vol. 66. pp. 139-149.

Noren O. Dust concentrations during operations with farm machines. MI 49085-9659, American Society of Agricultural Engineers St. Joseph, Paper 85-1055, 1985.

Nosovskyi A.V. The experience of construction of a protective shelter over the Chernobyl NPP Unit 4, which had a design accident: a view in 30 years. *Nuclear and Radiation Safety*. 2016. No. 1 (69). pp. 3-13.

Nosovskyi A.V. What to do next with the Chernobyl NPP Unit 4? On the 30th Anniversary of the Shelter. *Nuclear and Radiation Safety.* 2016. No. 4 (72). pp. 45-51.

Obruchev V.A. A role and value of a dust in the nature. *Proceedings of Academy of Sciences the USSR, series of Geographic*. 1951. No. 3. pp.15-26. [in Russian]

Ogorodnikov B.I. Dust storm in the territory of Ukraine and Belarus contaminated with radionuclides after the Chernobyl accident. *Meteorology and Hydrology*. 2011. No. 9. pp. 64-77. [in Russian]

Ogorodnikov B.I. Influence of high temperatures on behaviour of ^{137}Cs in the environment In: *Proceedings of Int. Science Workshop on Radioecology of Chernobyl Zone* (18-19 September 2002, Slavutych, Ukraine). pp. 45-46 [in Russian]

Ogorodnikov B.I., Pazukhin E.M. Radioactive aerosols of the «Shelter» object (Review). Part 4.1. Sources and generation of radioactive aerosols in 1986. Chernobyl: ISTC «Ukrytiye», National Academy of Sciences of Ukraine, 2005, 32 p. (Preprint. ISTC «Ukrytiye», National Academy of Sciences of Ukraine; 05-2). [in Russian]

Oksza-Chosimovski G.V. *Resuspension models Review*, Report ORP. lv-76-11, Environmental Protection Agency, NTIS, 1976.

Oksza-Chocimovski G.V. *Generalized Model of the Time-Dependent Weathering Half-Life of the Resuspension Factor*, EPA Technical Note ORP/LV-77-4, Las Vegas, Nevada 89114, 1977.

Onikul R.L., Khurshudyan L.G. On the question of the dust distribution from its land area sources. *Trugy GGO*. 1983. Vol. 467. pp. 27-36. [in Russian]

Paatero J., Vesterbacka K., Makkonen U. et al. Resuspension of radionuclides into the atmosphere due to forest fires. *J. Radioanal. Nucl. Chem.* 2009. Vol. 282. pp. 473-476.

Paliouris G., Taylor H.W., Wein R.W. et al. Fire as an agent in redistributing fallout ^{137}Cs in the Canadian boreal forest. *Sci. Total. Environ*. 1995. Vol. 160/161. pp. 153-166.

Papastefanou C., Manolopoulou M. The radioactivity of coloured rain in Thessaloniki, Greece. *Sci. Total Environ*. 1989. Vol. 80, No. 2-3. pp. 225-227.

Papastefanou C., Manolopoulou M., Stoulos S. et al. Coloured rain dust from Sahara Desert is still radioactive. *J. Environ. Radioactiv*. 2001. Vol. 55, No. 1. pp. 109-112.

Pasquill F. The Estimation of Dispersion of Windborne Material. *Meteorology*. 1961. Vol. 90. pp. 33-49.

Pasquill F., Smith F.B. Atmospheric diffusion. NewYork: Halsted Press, 1983. 437 p.

Pepper D.W. Dispersion of small particles in a tornado, DP-1387, E. I. du Pond de Nemours & Co., Savannah River Laboratory, Aiken, SC, 1975.

Petryanov I.V., Kozlov V.I., Basmanov P.I., Ogorodnikov B.I. PF Fibrous Filtering Materials. Moscow: Znaniye, 1968. 75 p. [in Russian]

Pires do Rio M.A., Amaral E.C.S., Paretzke H.G. The resuspension and redeposition of ^{137}Cs in an urban area: the experience after the Goiania accident». *J. Aerosol Sci*. 1994. Vol. 25. pp. 821-831.

Prezerakos N.G., Paliatsos A.G., Koukouletsos K.V. Diagnosis of the Relationship between Dust Storms over the Sahara Desert and Dust Deposit or Coloured Rain in the South Balkans. *Advances in Meteorology,* 2010, Article ID 760546, 14 p.

Prister B.S., Kliuchnikov A.A., Baryakhtar V.G. et al. The safety problems of the nuclear power. The lessons of Chernobyl, Chernobyl: Institute for Safety Problems of NPP, 2016. 356 p. [in Russian]

Prister B.S., Omelyanenko N.P., Perepelyatnikova L.B., Lavrovsky A.B. Wind-erosion processes and particularities of the development of optimal, complex measures for soil protection within the zone of radionuclide contamination In: Problems of Agricultural Radiology. Kyiv: Ukrainian Research Institute of Agricultural Radioecology, 1991. pp. 64-74. [in Russian]

Ranade M.B. Adhestion and removal of fine particles on surfaces. *Aerosol Sci. Technol*. 1987. Vol. 7. pp. 161-176.

Reeks M.W., Reed J., Hall D. On the resuspension of small particles by a turbulent flow. *J. Phys. D: Appl. Phys*. 1988. Vol. 21. pp. 574-589.

Reineking A., Becker K.H., Porstendorfer J., Wicke A. Air activity concentrations and particle size distributions of the Chernobyl aerosol. *Radiat. Prot. Dosim*. 1987. Vol. 19. pp. 159-163.

Report of the IEM (Institute of Experimental Meteorology «Typhoon»). Resuspension and diffusion of radionuclides in the area of the Chernobyl accident. Obninsk, 1987. 156 p. [in Russian]

Rodriguez S., Querol X., Alastuey A. et al. Saharan dust contributions to PM10 and TSP levels in Southern and Eastern Spain. *Atmos. Environ*. 2001. Vol. 35, No. 14. pp. 2433-2447.

Romov A.I., Shishkin N.S., Sosnovskaya R.P., Zheleznyak O.M. Tornadoes in Ukraine on 30 May 1985. *Meteorology and hydrology*. 1987. No. 2. pp. 27-36. [in Russian]

Rosner G., Winkler R. Long-term variation (1986-1998) of post - Chernobyl ^{90}Sr,^{137}Cs, ^{238}Pu and ^{239,240}Pu concentrations in air, depositions to ground, resuspension factors and resuspension rates in south Germany. *Sci. Total Environ.* 2001. Vol. 273. pp. 11-25.

RSC Kurchatov Institute. Impact of the «Shelter» object on the environment (release of radioactive aerosols), Report, Moscow, 1990 [in Russian]

Rulik P., Bucina I., Malatova I. Aerosol particle size distribution in dependence on the type of radionuclide after the Chernobyl accident and in the NPP effluents In: *The radioecology of natural and artificial radionuclides; ed.* Feldt W., *Proceedings XVth Regional Congress of IRPA (*Visby, Sweden, 10-14 September 1989). pp. 102-107.

Rybalka N., Mykolaichuk O., Alekseeva Z. et al. *Scenarios of radiological impacts in the long-term safety analysis of radioactive waste disposal at the Vector Site located in the Chernobyl exclusion zone*, EUROSAFE Forum, 4-5 November 2013, Cologne, Germany.

Sedlet J., Golchert N.W., Duffy T.L. USAEC Rept. ANL-8007. Argonne, Il : Argonne National Laboratory, 1973.

Sehmel G.A. Complexities of particle deposition and re-entrainment in turbulent pipe flow. *Aerosol Sci.* 1971. Vol. 2. pp. 63-72.

Sehmel G.A. Deposition and Resuspension In: Atmospheric Science and Power Production; ed. Randerson D, DOE / TIC-27601 (DE 84005177), US Department of Energy Technical Information Service: Springfield, VA, 1984, Vol. 12. pp. 533-572.

Sehmel G.A. Particle resuspension: a review. *Atmos. Environ.* 1980. Vol. 22. pp. 2639-2651.

Sehmel G.A. Deposition and Resuspension: Atmospheric Science and Power Production, DOE/TIC-27601 (DE 84005177), 1984, Chap. 12. pp. 533-572.

Sehmel G.A., Orgill M.M. Resuspension source change at Rocky Flats, Battelle Pacific Northwest Laboratories Annual Report for 1973 to the U.S.A.E.C., Division of Biomedical and Environmental Reserch, Part 3, Atmospheric Sciences — BNWL- Pt.3, UC-11, Richland, WA, 1974. pp. 212-214.

Shao Y. A model for mineral dust emission. *J. Geophys. Res*. 2001. Vol. 106 (D17). pp. 20239-20254.

Shao Y.P. Simplification of a dust emission scheme and comparison with data. *J. Geophys. Res*. 2004. Vol. 109. pp. D10202.

Shao Y. Physics and Modelling of Wind Erosion. Springer. 2008. 452 p.

Shao Y., Ishizuka M., Mikami M., Leys J.F. Parameterization of size-resolved dust emission and validation with measurements. *J. Geophys. Res*. 2011. Vol. 116. pp. D08203.

Shao Y., Raupach M.R., Findlater P.A. The effect of saltation bombardment on the entrainment of dust by wind. *J. Geophys. Res*. 1993. Vol. 98. pp. 12719-12726.

Shaw W.J., Allwine K.J., Fritz B.G. et al. An evaluation of the wind erosion module in DUSTRAN. *Atmos. Environ*. 2008. Vol. 42. pp. 1907-1921.

Shinn J.H. Enhancement factors for resuspended aerosol radioactivity: effects of topsoil disturbance. In: *Proceedings of the Fifth Int. Conf. on Precipitation Scavenging and Atmosphere-*

Surface Exhange Processes; eds. Schwarz S.E., Slinn W.G.N. Washington and Philadelphia: Hemisphere Publishing Corp., 1992. pp. 1183-1193.

Shinn J.H. Studies of plutonium aerosol resuspension at the time of the Maralinga clean-up. Report UCRL-ID-155063, Livermore, CA. 2002.

Shinn J.H., Homan D.N., Gay D.D. Plutonium aerosol fluxes and pulmonary exposure rates during resuspension from bare soils near a chemical separation facility. Vol. 2 *Proceeding of the Fourth Int. Conf.* (29 November - 3 December 1982, Santa Monica, California). pp. 1131-1143.

Shinn J.H., Kennedy N.C., Koval J.S. et al. Observations of dust flux in the surface layer for sready and nonsteady cases. In: Atmospheric-Surface Exchange of Particulate and Gaseous Pollutants, 1974, ERDA Symposium Series, Richland, WA, 3-6 September, CONF-740921, NTIS, 1976. pp. 625-637.

Shynkarenko V.K., Kashpur V.O., Skorjak G.G., Kalinovsky A.K. Assessment of aerosol radiation situation on industrial platform ChNPP during work on building a new safe confinement. *Problems of Nuclear Power Plants' Safety and of Chernobyl*. 2016. Vol. 27. pp. 58-66. [in Russian]

Silver J.D., Lindeken C.L., Meadows J.W. et al. USAEC Rept. UCRL-51547, Lawrence Livermore Laboratory: Livermore, CA, 1974.

Skitovich V.I., Budyka A.K., Ogorodnikov V.I. Results of two-year observations of radioactive particles dimensions within the CNPP 30-km zone. In: Radiation aspects of the Chernobyl accident; ed. Izrael Y.A. *Proceedings of the 1st All-Union Conference «Radiation aspects of the Chernobyl accident»*. June 1988. St. Petersburg: Hydrometeoizdat, 1993, Vol. 1. pp. 115-121. [in Russian]

Slade D.H. Meteorology and atomic energy. TID-24190, Oak Ridge: US Atomic Energy Commission, Division of Technical Information, 1968.

Slinn W.G.N. Formulation and a solution of the diffusion-deposition-resuspension problem. *Atmos. Environ*. 1976. Vol. 10. pp. 763-768.

Slinn W.G.N. Parametrizations for resuspension and for wet and dry deposition of particles and gases for use in radiation dose calculations. *Nucl. Saf*. 1978. Vol. 19, No. 2. pp. 205-219.

Smirnov V.V., Novitski M.A. Mesoscale traneport of dust stream. *J. Aerosol Sci*. 1998. Vol. 29, No. 1. pp. 725-726.

Smith J.G., Simmonds J.R. The Methodology for Assessing the Radiological Consequences of Routine Releases of Radionuclides to the Environment Used in PC-CREAM 08, ISBN 978-0-85951- 651-8, Health Protection Agency, HPA-RPD-058, 2009.

Smith R.J. Dispersion of odors from ground level agricultural sources. *J. Agr. Eng. Res.* 1993. Vol. 54. pp. 187-200.

Smith W.J., Whicker F.W., Meyer H.R. Review and categorization of saltation, suspension, and resuspension models. *Nucl. Safety*. 1982. Vol. 23. pp. 685-699.

Straka H. Pollen und Porenkunde. Sttuttgart: Gustav Fisher Verlag. 1975. 238 p.

Stuut J.B., Smalley I., O'Hara-Dhand K. Aeolian dust in Europe: African sources and European deposits. *Quatern. Int*. 2009. Vol.198, No. 1-2. pp. 234-245.

Sukhoruchkin A.K., Marchenko V.I. Radiation condition of aerial environment. *Bulletin of ecological condition of the exclusion zone.* 1996. No. 1 (6). pp. 22-37. [in Ukrainian]

Takahara S., Iijima M., Shimada K. et al. Method for estimating the dose distribution of people to be returned in long-term contaminated areas. *Int. Experts' Meeting on Radiation Protection after the 1F accident: Promoting Confidence and Understanding* (17-21 February 2014, Vienna, Austria).

Talerko N.N. Calculation of radioactive admixture ascent from Chernobyl NPP accidental unit. *Meteorology and Hydrology.* 1990. No. 10. pp. 39-46.

Talerko N.N., Garger E.K. Prognostic assessment of radionuclides transboundary transport due to a tornado over the Chernobyl NPP cooling pond. *Problems of Nuclear Power Plants' Safety and of Chernobyl*. 2013. Vol. 20. pp. 85-93. [in Russian]

Talerko N.N., Garger E.K., Klyuchnikov A.A. Prediction of the consequences of accidental releases from nuclear power plants with the help of the mesoscale atmospheric transport model LEDI. *Dopovidi Nacionalnoyi academiyi nauk Ukrainy*. 2010. Issue 12. pp. 74-79. [in Russian]

Talerko M.M., Lev T.D., Kireev S.I., Kashpur V.O., Kuzmenko G.G. Evaluation of radioactive air contamination due to a forest fire within the Exclusion zone on 5-8 June 2018. *Nuclear Power and the Environment*. 2019. Vol. 2, No. 14. pp. 47-58.

Tikhomirov F.A., Shcheglov A.I., Mamikhin S.V., Sidorov V.P. Consequences of radioactive pollution of forests near Chernobyl NPp. In: Chernobyl-88. *Proceedings of 1st All-Union Scientific and Technical Conf. on the Chernobyl Accident,* 1989. Vol. 3. pp. 99-115. [in Russian]

Travis J.R. A Model for Predicting the Redistribution of Particuiate Contaminants from Soil Surfaces, LA-6035-MS Informal Report UC-11 1975. Los Alamos, CA: University of California, 1975.

Tschiersch J., Frank G., Hillmann U. et al. Deposition of radionuclides, their subsequent relocation in the environment and resulting implications. Final Report Directorate General Science, Research and Development, EUR 16604 EN. Luxembourg: Office for Official Publications of the European Communities: 1995.

Tschiersch J., Georgi B. Chernobyl fallout size distribution in urban areas. *J. Aerosol Sci*. 1987. Vol. 18. pp. 689-692.

USAEC, Reactor Safety Study — An Assessment of Accident Risks in US Commercial Nuclear Power Plants, Draft Report WASH-1400, Appendix VI, Washington, D.C., 1974.

USAEC, Reactor Safety Study — An Assessment of Accident Risks in US Commercial Nuclear Power Plants, Final Report WASH-1400, Appendix VI, Washington, D.C., 1975.

USSR State Committee on the Utilization of Atomic Energy «The Accident at the Chernobyl NPP and its Consequences», IAEA Post Review Meeting, Vienna, 25-29 August 1986.

Vintersved I. Intercomparison of large stationary air samplers. In: Nordic radioecology. The transfer of radionuclides through Nordic ecosystems to man; ed. Dahlgaard H. Amsterdam: Elsevier, 1994. pp. 385-405.

Vintersved I., Arntsing R., Bjurman B. et al. Resuspension of radioactive caesium from Chernobyl accident. In: The Chernobyl fallout in Sweden; ed. Moberg L. Stockholm: Swedish Radiation Protection Institute, 1991. pp. 85-106.

Vintersved I., Nylen T., Genborg A. et al. ECP-1 Contamination of Surface by Resuspendend Material, Report of FOA, Sundbyberg, 1994.

Viswanathan G.M., Buldyrev S.V., Garger E.K. et al. Quantifying nonstationary radioactivity concentration fluctuations near Chernobyl: A complete statistical description. *Physical Review E*. 2000. Vol. 62, No. 3. pp. 4389-4392.

Vozzhennikov O.I., Nesterov A.B. On the transfer of pollutants in the atmosphere due to the resuspension from the underlying surface. *Meteorology and Hydrology*. 1988. No. 11. pp. 63-70. [in Russian]

Wagenpfeil F., Hartl T., Tschiersch J. Size-fractionating sampler for giant particles. *J. Aerosol Sci*. 1994. Vol. 25. pp. 111-112.

Wagenpheil F., Tschiersch J. Resuspension of coarse fuel particles in the Chernobyl area. *J. Environ. Radioactiv*. 2001. Vol. 52. pp. 5-16.

Walsh C. Calculation of resuspension doses for emergency response, Chilton, NRPB-W1, NRPB, 2002.

Wang X., Oenema O., Hoogmoed W. B. et al. Dust storm erosion and its impact on soil carbon and nitrogen losses in northern China. *Catena*. 2006. Vol. 66. pp. 221-227.

Weber A.H., Hunter C.H. Estimating Dispersion from a Tornado Vortex and Mesocyclone. WSRC-TR-94-0386, Westinghouse Savannah River Company, 1996. 33 p.

Wen H.Y., Kasper G. On the kinetics of particles re-entrainment from surfaces. *J. Aerosol Sci*. 1989. Vol. 20. pp. 483-498.

Wotawa G., De Geer L.-E., Becker A. et al. Inter- and intra-continental transport of radioactive cesium released by boreal forest fires. *Geophys. Res. Lett*. 2006. Vol. 33. P. L12806.

Yablokov M.Yu., Andronova A.V. A model of take-off processes of desert sand aerosols in windless conditions. *J. Aeros. Sci*. 1997. Vol. 28. pp. 563-564.

Yamauchi M. Secondary wind transport of radioactive materials after the Fukushima accident. *J. Earth Planets Space*. 2012. Vol. 64. pp. e1-e4.

Yoschenko V.I., Kashparov V.A., Protsak V.P. et al. Resuspension and redistribution of radionuclides during grassland and forest fires in the Chernobyl exclusion zone: Part I. Fire experiments. *J. Environ. Radioactiv.* 2006a. Vol. 86. pp. 143-163.

Yoschenko V.I., Kashparov V.A., Levchuk S.E. et al. Resuspension and redistribution of radionuclides during grassland and forest fires in the Chernobyl exclusion zone: Part II. Modeling the transport processes. *J. Environ. Radioactiv.* 2006b. Vol. 86. pp. 260-278.

Zhuang Y. A semianalytical solution to a diffusion-deposition-resuspension model of local contamination. *J. Appl. Meteorol*. 1998. Vol. 37. pp. 332-334.

Zilinitkevich S.S. Dynamics of the atmospheric boundary layer, Leningrad: Gidrometeoizdat. 1970. 292 p. [in Russian]

Zimon A.D. Adhesion of Dust and Powder. Plenum Press, 1980. 438 p.

Ziskind G., Fichman M., Gutfinger C. Adhesion moment model for estimating particle detachment from a surface. *J. Aerosol Sci*. 1997. Vol. 28. pp. 623-634.

Ziskind G., Fichman M., Gutfinger C. Resuspension of particulaes from surfaces to turbulent flows — Review and analysis. *J. Aerosol Sci*. 1995. Vol. 26. pp. 613-644.

CONTENTS

PREFACE 5

INTRODUCTION. Re-Entrainment of Radioactive Aerosols as a Process of Redistribution of Surface Contamination 7

CHAPTER 1

BASIC DESCRIPTION OF RESUSPENSION PROCESSES OF AEROSOL PARTICLES

1.1. Aerosol emission from soil 11

1.2 Theoretical and experimental studies of resuspension mechanisms under laboratory and natural conditions 14

1.3. Study of submicron aerosol generation (emission or release) 18

CHAPTER 2

SOURCES OF SECONDARY CONTAMINATION, MEASUREMENT CONDITIONS, AND SAMPLER INSTALLATION IN THE CONTAMINATED TERRITORY AFTER THE CHERNOBYL ACCIDENT

2.1. General description of resuspension conditions in the Chernobyl exclusion zone 20

2.2. Combustion of contaminated wood 22

2.3. Re-entrainment by traffic 24

2.4. Radioactivity entrainment during forest fires 28

2.5. Radioactive pollen 28

2.6. Radioactive aerosol from the object «Shelter» 30

2.7. Sampling locations 30

2.8. Sampler installations 35

2.9. Inter-comparison of integrating aerosol samplers 38

2.10. Inter-comparison of size differentiating aerosol samplers 41

CHAPTER 3

EXPERIMENTAL ESTIMATIONS OF THE RESUSPENSION FACTOR

3.1. Definition of the resuspension factor 44
3.2. Uncertainty of the resuspension factor measurements 45
3.3. The evaluation of the resuspension factor for homogeneous and stationary conditions 46
3.4. Resuspension factor in the Chernobyl exclusion zone 49
3.5. Dependence of the resuspension factor from the fractional composition of soil particles 52
3.6. Time variability of resuspension factor 55
3.7. Comparison of the resuspension factor values 56

CHAPTER 4

EMPIRICAL MODELS OF THE RESUSPENSION FACTOR

4.1. Time-variable models of the resuspension factor 58
4.2. Dependence of the resuspension factor on soil characteristics and meteorological parameters 67

CHAPTER 5

A TEST OF EXISTING EMPIRICAL MODELS OF THE RESUSPENSION FACTOR AND ESTIMATION OF THEIR UNCERTAINTY

5.1. Introduction 71
5.2. Participating modelers 73
5.3. Types of models used 73
5.4. Comparison of model predictions with empirical data 75
5.4.1. Annual data 75
5.4.2. Monthly data 80
5.4.3. A single period of measurements in Kyiv and Zapolie 80
5.5. Discussion 82
5.6. Additional data for the testing the resuspension factor models 82
5.7. Limits of model applications 85

CHAPTER 6

MASS LOADING

6.1. General information 87
6.2. Enhancement factor 91

CHAPTER 7

RESUSPENSION RATE

7.1. Definition of the resuspension rate 93

7.2. The theoretical basis of methods of matter vertical flow measurement 95

7.3. Models of the resuspension rate 96

7.4. The estimation of the resuspension rate in the 30-km Chernobyl zone based on Monin-Obukhov theory 97

7.5. Use of the semi-empirical equation of turbulent diffusion for estimations of the resuspension characteristics 103

7.6. Emission of the radioactive dust from the polluted territory during anthropogenic activities 106

CHAPTER 8

MODELING OF ATMOSPHERIC TRANSPORT OF RESUSPENDED MATERIAL

8.1. General classification of resuspension-diffusion-deposition models 111

8.2. Modeling of resuspension from an area surface source 113

8.2.1. Modifications of the plume model for calculation of atmospheric transport of resuspended material 114

8.2.2. Modeling of atmospheric transport and deposition of resuspended material using analytic solutions of the turbulent diffusion equation 117

8.2.3. Low boundary condition for the equation of turbulent diffusion of resuspended material 126

8.3. Models for horizontal and vertical fluxes of aerosols 129

8.3.1. Saltation models 129

8.3.2. Non-saltation models 135

CHAPTER 9

STATISTICAL CHARACTERISTICS AND LONG-TERM PREDICTION OF THE ACTIVITY CONCENTRATION OF RADIONUCLIDES IN THE AIR

9.1. Statistical characteristics of the ^{137}Cs activity concentration in the air 138

9.2. Dependence of the activity concentration on the averaging period 145

9.3. Long-term time course of the atmospheric ^{137}Cs activity concentration 147

9.4. Statistical prediction of the ^{137}Cs activity concentration in the surface layer of the atmosphere of the Chernobyl exclusion zone 149

9.5. Statistical model of the atmospheric ^{137}Cs activity concentration prognoses and its comparison with measured data 156

CHAPTER 10

ACTIVITY SIZE DISTRIBUTION OF RADIOACTIVE PARTICLES

10.1. Introduction 160

10.2. Radionuclide attachment to the soil 161

10.3. Activity distribution of size particles during natural wind-driven resuspension 163

10.4. A typical form of distribution shapes 168

CHAPTER 11

RADIOACTIVE PARTICLES DURING ANTHROPOGENIC ACTIVITY

11.1. Methods and measurements of data 174

11.2. The size distribution of radioactive particles 176

11.3. Estimation of dry deposition velocity 182

CHAPTER 12

FUEL PARTICLES COLLECTED ON AIR FILTERS IN 1987 DURING NATURAL WIND RESUSPENSION, THEIR SOLUBILITY, AND IMPLICATION TO DOSE

12.1. Methods and conditions of the aerosol measurements 185

12.2. Experimental characteristics of particle solubility 187

12.3. Inhalation dose coefficients applying measured solubility parameters 192

CHAPTER 13

RADIOACTIVE AEROSOLS RELEASED FROM THE «SHELTER» OBJECT

13.1. Introduction 196

13.2. Materials and methods 198

13.3. Measurements at the gaps: flow rates 200

13.4. Measurements at the gaps: size distribution of the released aerosol 201

13.5. Measurements at the «Shelter» site: activity concentrations 204

13.6. The size distribution of the released aerosols 206

13.7. Transformation of radionuclide characteristics 207

13.8. Assessment of inhalation dose 209

13.9. Aerosol contamination in the near area of the Chernobyl NPP during the building of New Safe Confinement 211

CHAPTER 14

RADIONUCLIDE EMISSION DUE TO FOREST FIRES AT RADIOACTIVELY CONTAMINATED TERRITORY AROUND THE CHERNOBYL NUCLEAR POWER PLANT

14.1. General characteristic of forest fires in radioactively contaminated regions 214

14.2. The largest wildland fires in the radioactive contaminated regions after the Chernobyl accident 215

14.3. Measurements of air contamination caused by forest fires within the Chernobyl exclusion zone 220

14.4. Wildland fire experiments in radioactively contaminated territories 222

14.5. Modeling of secondary air contamination caused by forest fires 225

14.5.1. Radionuclide emission fraction during forest fires 226

14.5.2. Near-range radionuclide atmospheric transport modeling during forest fire experiments 227

14.5.3. Modeling of consequences of mesoscale and long-range atmospheric transport of radionuclides during forest fires 228

CHAPTER 15

ATMOSPHERIC RESUSPENSION OF RADIONUCLIDES DUE TO EXTREME METEOROLOGICAL CONDITIONS

15.1. Long-range transport of the global radionuclide depositions resuspended during dust storms 234

15.2. Meso-scale transport of the radionuclides resuspended during dust storms 237

15.2.1. Wind transport of contaminated sediments from Lake Karachay during spring 1967 237

15.2.2. Dust storms on the territories of Ukraine and Belarus contaminated after the Chernobyl accident 240

15.3. Radionuclides re-entrainment due to tornado over nuclear installations, radioactive facilities, and contaminated territories 242

REFERENCES 250

Монографію присвячено дослідженню процесів вторинного підйому радіоактивного аерозолю в атмосферу із забруднених поверхонь у локальному та мезомасштабі (природний вітровий підйом (ресуспензія), сільськогосподарські роботи, лісові пожежі, пилові бурі, торнадо). Викладено експериментальний матеріал, отриманий під час оперативних заходів з мінімізації наслідків аварії на Чорнобильській АЕС, здійснених переважно у 30-кілометровій Чорнобильській зоні відчуження з травня 1986 р. донині. Результати отримано за допомогою радіаційного та метеорологічного моніторингу, польових експериментів, методів фізичного і математичного моделювання, статистичних методів обробки й аналізу даних. Систематизовано результати вимірювань інтегральних характеристик процесу ресуспензії радіоактивних частинок, їхні статистичні характеристики та параметри функції розподілу об'ємної активності за розміром частинок за різних метеорологічних умов у приземному шарі атмосфери. Надано результати вимірювань «гарячих» аерозольних частинок на проммайданчику ЧАЕС у післяаварійний період. Узагальнено дані щодо коефіцієнту й інтенсивності ресуспензії; верифіковано методи розрахунку її основних інтегральних параметрів. Розглянуто основні підходи до моделювання повторного надходження радіонуклідів в атмосферу й подальшого просторово-часового перерозподілу. Викладено результати верифікації моделей ресуспензії на основі результатів вимірювань у зоні відчуження.

Книга розрахована на спеціалістів у галузі радіоекології, охорони навколишнього середовища, фізики атмосфери, метеорології, радіаційної та екологічної безпеки.

Наукове видання

НАЦІОНАЛЬНА АКАДЕМІЯ НАУК УКРАЇНИ
ІНСТИТУТ ПРОБЛЕМ БЕЗПЕКИ
АТОМНИХ ЕЛЕКТРОСТАНЦІЙ НАН УКРАЇНИ

ГАРГЕР Євген Костянтинович
НОСОВСЬКИЙ Анатолій Володимирович
ТАЛЕРКО Микола Миколайович

ВТОРИННЕ РАДІОАКТИВНЕ ЗАБРУДНЕННЯ АТМОСФЕРИ НА ПРОМІЖНІЙ ТА ПІЗНІЙ ФАЗАХ РАДІАЦІЙНОЇ АВАРІЇ

Англійською мовою

Редактор-коректор *В.К. Рего*

Художнє оформлення *Є.О. Ільницького*

Технічне редагування *Т.М. Шендерович*

Комп'ютерна верстка *Н.О. Кучеренко*

Підп. до друку 06.07.2020. Формат 70 × 100/16.
Гарн. Minion Pro. Ум. друк. арк. 22,26. Обл.-вид. арк. 22,93.
Тираж 200 прим. Зам. № 6001.

Видавець і виготовлювач Видавничий дім "Академперіодика" НАН України
01004, Київ, вул. Терещенківська, 4

Свідоцтво про внесення до Державного реєстру суб'єктів
видавничої справи серії ДК № 544 від 27.07.2001 р.